ISDN 1039-3218

Port Phillip Bay Integrated Model: Final Report

Alexander Murray and John Parslow
CSIRO Division of Marine Research
GPO Box 1538, Hobart 7001

Technical Report No.44

Port Phillip Bay Environmental Study
CSIRO Environmental Projects Office
Canberra, ACT, Australia

GPO Box 1666, Canberra, ACT 2601, Australia

September 1997

EXECUTIVE SUMMARY

An integrated model of nutrient cycling and impacts has been developed as Task G8/9 of the Port Phillip Bay Environmental Study (PPBES). The model development and analysis has been undertaken to provide a synthesis of scientific understanding of the Bay ecosystem arising from the Study, and a predictive tool to support future management of nutrient loads to the Bay (Chapter 1).

The ecological model structure has been based on an extensive review of similar models (Chapter 2). The final model structure is moderately complex, incorporating some 16 state variables in both water-column and sediment (Chapter 3). These variables represent pools of nutrients, phytoplankton and zooplankton, detritus, and benthic plants and animals. Nitrogen is the key limiting nutrient in Port Phillip Bay, and is used as the core model currency, but the model also tracks phosphate, oxygen and silicate. Model equations describe the exchanges of nitrogen (and other nutrients) among pools arising from processes as photosynthesis, grazing, mortality and remineralization.

The process formulation is derived from the literature or developed using observations from Port Phillip Bay and elsewhere. Choices between alternative formulae have been made after careful analysis of their effects on the behaviour of the model. The model is unusual in its recognition of the importance of water column – benthic coupling and in its recognition of different functional components within trophic levels. The model pays particular attention to sediment biogeochemistry, which plays a critical role in mediating the impacts of nutrient loads into Port Phillip Bay.

A priori estimates of model parameters were based on an extensive literature survey, and refined using data from process experiments carried out as part of the PPBES (Chapter 4).

The ecological model is based on an efficient and accurate physical transport model for Port Phillip Bay developed under Task P8B. The transport model (and the underlying hydrodynamic model) have been run over the period 1990 to 1995, using time series of observations of tide, wind, rainfall, evaporation and runoff, and calibrated against physical observations over the same period. Time series of forcing data for the integrated model were prepared in the form of nutrient and sediment loads for the same period, based on observations and empirical catchment models for the principal sources (Chapter 5).

Considerable effort has been devoted to analysis of the behaviour of the full numerical model, and its dependence on process formulation and parameter values. Analysis of simplified models which ignore spatial and temporal variation has proved particularly valuable (Chapter 6). This qualitative analysis has highlighted the importance of the formulation of zooplankton mortality, and changes in denitrification efficiency, in controlling the predicted response of the Bay to changes in nutrient load.

The PPBES has generated a complex and comprehensive data set, including underway nutrient and chlorophyll distributions, and point measurements of fluxes, at two week to monthly intervals over two years. This has provided an exacting test-bed for model calibration, and required some innovation in model-data comparison. Model calibration has been conducted in a hierarchical manner, starting with Bay-wide annual average pools and fluxes, and proceeding to increasing spatial and temporal resolution (Chapter 7).

The calibrated model reproduces the observed Bay-wide annual average pools and fluxes within observation errors. The 59 box structure of the transport model was designed to resolve the principle spatial gradients in the Bay, ranging from nutrient enriched coastal waters near the principal sources, to the nutrient-limited waters of the Bay centre, and the exchange zone over the Sands. The calibrated model reproduces these regional differences well, and appears to resolve some of the observed local gradients within regions. The model also reproduces satisfactorily the transients associated with Yarra run-off events in the northeastern Bay, and winter inputs of ammonia from Werribee. The model does not reproduce well an observed decline in chlorophyll in the Bay centre from 1993 to 1994, which was associated with a decline in nutrient loads and runoff in 1994. Nitrate concentrations are also under-predicted, but since most DIN is in the form of ammonium, total DIN concentrations match observations reasonably well.

A key result that has emerged from field observations and model calibration is the role of silicate limitation in limiting diatom blooms off Werribee. The Yarra River is the principal source of silicate, which undergoes large fluctuations in concentration throughout the Bay in response to changes in load, diatom uptake, and release from sediments.

The model has been used to examine a range of possible nutrient loading scenarios (Chapter 8). The key result emerging from these model experiments has been the identification of a maximum assimilative capacity for nitrogen loads to the Bay. The flushing time for Port Phillip Bay is long (ca 1 year), and most of the current nitrogen load is removed by denitrification in the sediment. However, both observations and sediment biogeochemistry models suggest that denitrification efficiency decreases at high sediment respiration rates. It follows that there is a maximum denitrification capacity for the Bay, which model and observations suggest is two to three times current loads. If this capacity is exceeded, nitrogen accumulates until export to Bass Strait matches the external load, at which point the Bay is severely eutrophied. This result is quite robust (given that the representation of sediment biogeochemistry is correct), and is supported by both full model simulations and simplified model analysis.

The factors responsible for the very high denitrification efficiencies observed in Port Phillip Bay, and their dynamical response to changes in organic loadings to the sediment, are not well understood, and deserve further study. The PPBES found unexpectedly high levels of microphytobenthos production in Port Phillip Bay.

While microphytobenthos uptake of ammonia could theoretically increase denitrification efficiency, the observations do not support it. Microbial processes concentrated at interfaces, especially the walls of burrows created by benthic infauna, could also increase denitrification efficiency.

Under conditions of increased nitrogen load or decreased denitrification efficiency, silicate limitation is predicted to become more common, increasing the likelihood of dinoflagellate blooms. Other scenarios presented in Chapter 8 include the effects of a three degree Celsius warming (marginal), and the effects of an increase in benthic filter-feeder biomass, which is predicted to reduce phytoplankton biomass.

Model development has been made possible through the contribution of data and ideas from all PPBES participants. The model may be further used and developed as part of ongoing monitoring and management programs in Port Phillip Bay.

TABLE OF CONTENTS

Page No.

LIST OF TABLES

LIST OF FIGURES

1 INTRODUCTION

Port Phillip Bay is a large (1950 km^2), semi-enclosed Bay in southeast Australia. The Bay has one of the most populated catchments in Australia: the city of Melbourne and the industrial port of Geelong are located within the catchment. The Bay is used for recreation, shipping, commercial fishing, aquaculture, and includes natural habitats of high quality. The Bay is also subject to loadings of nutrients and toxicants from several major point sources (the Werribee Treatment Plant, the Yarra River, and the Patterson-Mordialloc system), and from a large number of minor creeks and drains. The Bay is a vital resource for the state of Victoria and its state of health is a matter of great public interest.

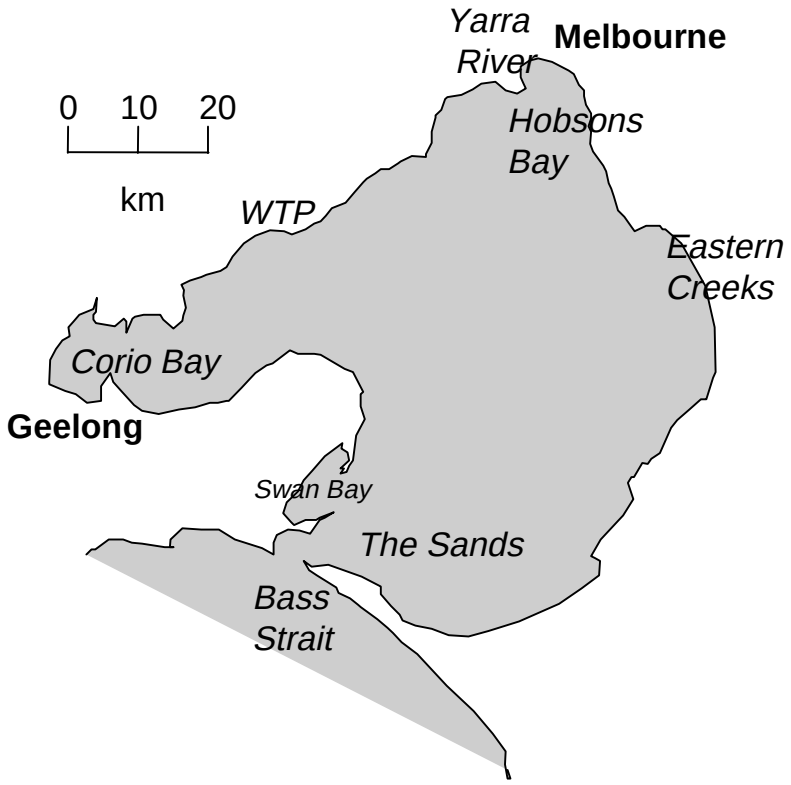

Figure 1.1 Port Phillip Bay with principal nutrient sources

An intensive environmental study of the Bay was conducted from 1992 to 1996. This study, known as the Port Phillip Bay Environmental Study (PPBES) was designed and managed by CSIRO on behalf of Melbourne Water. Individual tasks were subcontracted to numerous agencies, state, national and international. The study was designed and implemented as a coordinated investigation of physics, nutrient cycling, toxicants and ecology of the Bay (CSIRO 1992). The overall objectives of the Study were to assess the environmental health of the Bay, to study and understand the impact of current loadings

of nutrients and toxicants, and to provide a scientific basis for future management of the catchment loads.

An account of the overall study findings and recommendations is given in the Study Final Report (Harris *et al*. 1996). This Technical Report constitutes the final report of the Integrated Modelling Task (Task G8/9). The original Study design identified two broad roles for modelling within the Study. Models would provide a conceptual framework for synthesis and integration of the data sets and process knowledge provided by the diverse field surveys and experiments which made up the major part of the Study. They would also provide a basis for hindcasting / predicting the impacts of past and future management actions on the environmental health of the Bay, allowing the development and analysis of management strategies and scenarios. In this role, models serve as a focus for the interface between environmental studies and management. These two objectives were originally assigned to two Tasks, G8 and G9 respectively, but these were then combined into one integrated Task, G8/9.

During the design phase of the Study, CSIRO undertook extensive consultation with managers and user agencies, in order to identify key management issues and concerns. This process was continued in the early phase of the modelling Task through a modelling workshop held in 1992, attended by representatives of user agencies and scientists with key expertise. This workshop, and subsequent development and analysis of models of Port Phillip Bay, have been based on the Adaptive Environmental Assessment and Management (AEAM) approach described by Holling (1978). The conceptual design and scoping of these models has involved a series of choices (eg. the level of component and process resolution, the selection of state variables, the formulation of process sub-models, and the time and space scales to be resolved). Using the AEAM approach, these choices have been assessed in terms of the need to link management actions to system outputs of value or concern to users.

The management actions of primary concern to the managers are those affecting the loadings of sediments, nutrients and toxicants at the Bay boundaries, either through major point sources such as the WTP, the Yarra River, and major creeks, or through distributed inputs (minor creeks and drains, groundwater, shipping and atmospheric deposition). The impacts of dredging are also of interest. The Port Phillip Bay Environmental Study was not charged with addressing processes in catchments which control loadings to the Bay. This means that management actions in the catchments can be addressed only by making assumptions about their effects on loads at the Bay edge. It is desirable in the long term that the models developed for the Bay be linked with catchment models, to provide an “end-to-end” management support system. (In practice, as described in Chapter 4, the Study has been forced to develop simple empirical catchment models in order to interpolate the generally sparse data on loads.)

Models have the advantage (or disadvantage, depending on your point of view) that they force us to be specific and generally quantitative about both hypotheses and objectives. We cannot develop an ecosystem model of Port Phillip Bay which has “environmental health of the Bay” as an output variable. In the initial Study design and in later meetings and workshops, the Study has worked with managers to specify environmental health in terms of properties which a model can at least potentially predict as output variables.

We can distinguish two classes of these output or indicator variables. One class consists of properties of direct concern to managers or the public. The modelling workshop identified the following list of variables of this type:

- Water column dissolved oxygen, turbidity, foams, oil slicks;
- Sediment grain size, organic content, anoxia;
- Toxic or nuisance algal blooms;
- Valued benthic communities such as seagrass, wetlands, reefs;
- Valued species such as mammals, birds, and general biodiversity;
- Abundance of commercial and recreational finfish and shellfish;
- Contamination of seafoods.

It was recognised at the time that not all of these indicators might be amenable to modelling.

The second class of indicator variables consists of water column and sediment properties which, while not necessarily directly valued or even noticed by the public, reflect changes in system state which can affect valued components. These are generally related to water quality and sediment quality criteria, and include nutrient and toxicant concentrations, phytoplankton biomass, and bio-irrigation levels. The distinction between these two classes of indicators corresponds roughly to the distinction between Environmental Quality Objectives and Environmental Quality Standards (Orr *et al*. 1990). It has been recognised for some time that it would be desirable to manage for objectives based on the variables of direct concern. However, it is easier for regulatory purposes to manage on the basis of water and sediment quality standards, and this is the current situation for Port Phillip Bay.

The “integrated” models developed in the Study and described in this report are nutrient cycling models, involving tight coupling among physics and biogeochemical processes. They are essentially water and sediment quality models. Some ecological indicator variables such as seagrass and macroalgae are included explicitly in these models. Other ecological indicators can be addressed indirectly, by considering separately their response to predicted changes in water and sediment quality.

The time and space scales addressed by the models presented here have also been based on management concerns and needs. Managers were concerned about the long-term impacts of nutrient and toxicant loads to the Bay, and asked the study to address future loading scenarios extending out as far as 50 years. The flushing time of the Bay is about 1 year, but there is the potential for sediment and benthic components to respond to changes in loadings on much longer time scales. Models extending over these time frames need to address the broad spatial gradients within the Bay. Managers are also concerned about dispersal and fate of loadings near point inputs, especially the WTP, over short time and space scales. To provide the flexibility to cope with this range of time and space scales, it was decided to base the integrated models on a physical transport model with flexible spatial resolution. This transport model is connected to the

hydrodynamic model via a particle-tracking module, in a manner described in more detail in Walker (1997b).

The models and analyses presented here have been developed over a period of 4 years, in close collaboration with the rest of the Study. The modellers have attended all Technical Group meetings since the Study began, and participated in the discussion and analysis of field results, and field study design. Conversely, the modellers have had the opportunity to present initial design concepts and results to the rest of the Technical Group and other scientists, and to incorporate feedback into subsequent model development. This arrangement has worked well, and the models and results reported here should be regarded as a product of the Study Team (although the authors of course accept responsibility for any failings).

This Technical Report does not set out to reproduce the development of the models and understanding over the 4 years of the Study, interesting as this has been for the participants. Rather, it describes our current understanding of the Bay as represented in the models and analyses at the end of the Study, and their implications for future management of the Bay.

A modelling exercise of this kind is not of course carried out *de novo*. We have drawn on a long history of ecological models of marine ecosystems in general, and coastal eutrophication in particular. This background is briefly reviewed in Chapter 2.

A detailed description of the final model variables, processes and parameters is given in Chapter 3, and a discussion of model parameters and their *a priori* values is given in Chapter 4. In Chapter 6, we present a series of qualitative analyses of model behaviour, using a variety of mathematical and conceptual approaches. We believe the understanding of model behaviour derived in this chapter is critical to the success of the study.

The full simulation model requires the prescription of physical forcing and loadings with adequate spatial and temporal resolution. The derivation and nature of the data used to drive the model are described in Chapter 5. In Chapter 7, we present the comparison of model predictions and observations for the period of the Study, including the procedures used to tune model parameters which are poorly constrained by the data, and our attempts to assess the effects of unresolved uncertainty in key parameters. The understanding and integration of observations and processes in Port Phillip Bay is represented in Chapters 6 and 7. Finally, in Chapter 8, we present some of the broad implications for management, and a preliminary discussion of the use of the model to address specific management scenarios.

2 MODELLING NUTRIENT CYCLES IN COASTAL MARINE ECOSYSTEMS: A REVIEW

Marine ecosystem modelling has a long and interesting history. One of the earliest models of population interactions was in part developed to describe the changes in fish populations during reduced fishing in World War I (Volterra 1926). Similarly one of the first applications of computers to ecological modelling was for the North Atlantic ecosystem (Riley *et al*. 1949). It is rare now for a major ecosystem study not to include some modelling component (Beer 1983). Modelling in Australian waters include models of Westernport Bay (Shapiro 1975), the Peel-Harvey system (Hodgkin *et al*. 1980), Sydney deepwater sewage outflows (Tong and Cathers 1991) and Western Australian coastal waters (Hodgkin and Birch 1982, Lord 1994, Lord and Hillman 1995). Port Phillip Bay has itself been the subject of previous water quality modelling (Williams 1978), but little has been done between that early work and the present Port Phillip Bay Environmental Study.

However, this is not to say that model formulation and application has become a routine or automatic exercise. The benefits of ecological modelling have been questioned right from the start and are still a subject of some controversy (Thompson 1937, Hedgpeth 1977). Natural ecosystems are complex hierarchical systems with many nested levels of complexity. It is impossible to represent all these levels in detail. In any model, we must choose an appropriate level of description and use approximate or empirical relationships to substitute for processes hidden below that level. In the end, such choices are a matter of judgement, and we can judge their effectiveness only in hindsight, in terms of the insight, understanding and/or predictive power derived from the resulting model. However, we need not make such judgements blind: we can draw on the experience of others. This brief review summarises recent experience with models of nutrient cycling and eutrophication in aquatic ecosystems, and coastal marine ecosystems in particular, and the lessons for the Port Phillip Bay model.

The threat of eutrophication has been a key motivation for attempts to understand and model nutrient cycling in aquatic ecosystems where anthropogenic loads of nutrients have led to algal blooms and anoxia. Other modelling studies have sought to address the causes of contrasting seasonal patterns in oceanic ecosystems (Evans and Parslow 1985), the natural processes underlying fish production, and the global biogeochemical cycles controlling the response to modern fossil fuel releases. While the objectives have differed, many of the model processes and issues are shared across these studies. There have been several other, more complete, reviews of marine ecological modelling. Platt et al. (1981) reviewed, for UNESCO, a series of different techniques involved in oceanic modelling. GESAMP (1991) reviewed models for the International Atomic Energy Authority, with particular emphasis on transport and accumulation of radionucleotides. McGlade and Price (1993) consider the problems of management in the particularly tricky example of the post-war Gulf in which political and economic considerations have to be explicitly considered in ecosystem management. Numerous books consider modelling techniques with applied examples; an example with a strong aquatic bias is that of Jorgensen (1993). Other books deal with the techniques of ecological modelling at a much more abstract mathematical level (eg. May 1981, Murray 1993). These sources have all been used in writing this chapter.

We can distinguish a number of broad traditions across these different areas of modelling. There has been a scientific tradition focused more on understanding ecological or physiological processes, and their role in system behaviour. There has been a very applied stream of water quality engineering, concerned with the immediate impacts of wastewater treatment and discharge, and often based on strong models of physical transport. There have also been a number of more empirical approaches to prediction and/or management of system properties, exemplified by the Vollenweider approach to lakes (1975). In some recent studies, a productive synthesis of these approaches is emerging. We think the Port Phillip Bay Environmental Study is a case in point.

2.1 Conceptual models

Most ecosystem models, especially biogeochemical models, describe the system as a series of functional compartments, connected by flows of energy and/or matter. There are models that describe the behaviour of individual organisms, but these tend to be focused at higher trophic levels or on specific processes. The simplest description of a biological system is the flow diagram that shows the compartments and flows. Examples can be found in almost any textbook; for example, Raymont (1980) shows flow diagrams ranging in scale from photosynthetic processes in a cell to global ocean nutrient cycles. It is possible to produce qualitative descriptions of this kind for systems where we have little specific quantitative data. A conceptualised Port Phillip Bay food web was reproduced in the Port Phillip Bay status review (Skyring *et al*. 1992).

An energy or nutrient budget is essentially the same flow diagram with the magnitude of pools and fluxes indicated in appropriate units. Again, an example can be found in the Port Phillip Bay status review (Skyring *et al*. 1992). Budgets provide a useful quantitative description of the mean or observed state of the system, but do not provide insight into the processes controlling fluxes, and cannot predict the response of the system to perturbation. It is generally not true that these diagrams are simply statements of the facts, as both fluxes and pools are derived using implicit models that may not be formally expressible. In some cases, missing fluxes can be estimated using inverse modelling (Vezina and Platt 1987, Jackson and Eldridge 1992).

In order to predict the response of the system to changes in forcing, it is necessary to have some underlying theory relating pools and fluxes. A simple example of an empirical rule of this kind is the assertion that production is reduced at each trophic level to 10% of the value at the preceding level (Parsons *et al*. 1984). This rule makes it possible to estimate flows of energy to different trophic levels, and to see how production changes with changes in input. Examples of steady state analyses of this kind are given by Taylor and Joint (1990) and Ducklow (1991) for production in the microbial loop. These models, sometimes known as network models (Ducklow 1991), are useful in cases like the microbial loop where throughput is subject to debate, and are also used in estimating the accumulation of toxins. These models are generally linear, and the sensitivity of model predictions to assumptions about inputs and transfer efficiencies can be easily investigated.

Dynamical models are required where the system state changes over time, either autonomously or in response to external forcing, and it is important to understand and

predict these changes. In general, dynamical models describe the state of the system at any one time by a set of state variables, and prescribe the rate of change of these state variables as a function of the current system state and external environmental forcing. In the case of biogeochemical models, the state variables generally represent the content of a set of functional compartments measured in a chosen "currency" such as nitrogen, phosphorus or carbon, and their rate of change is described in terms of the processes controlling sources, sinks and transfers of the modelled element. A direct comparison is generally possible between a flow or budget description and the structure of a dynamical model of this kind.

In the next section, we describe in some detail the typical structure and content of dynamical models of nutrient cycling. There are a variety of techniques for studying the behaviour and properties of dynamical models. For very simple models, it may be possible to produce exact analytical time varying solutions, but most biogeochemical models are sufficiently complex and non-linear that this is not feasible. Most modellers now rely heavily on computer simulation and numerical solutions. Modern computers are powerful enough to allow rapid and accurate solution of very complex models. However, it is still difficult using numerical techniques to explore fully the dependence of model predictions on model assumptions and parameter values.

An intermediate approach is to use techniques to simplify the model, and derive analytical solutions for the simplified version. It is customary to look for steady-state solutions of the model. This may be justified because part or all of the system spends much of the time close to steady-state, especially if it responds on much faster time scales than changes in the external forcing. This approach was used by Evans and Parslow (1985) to understanding the factors controlling seasonal cycles in plankton communities. Klepper (1995) calculated steady-state responses of a system subject to changing external forcing and obtained annual averages in good agreement with a computationally intensive dynamic model. In Chapter 6, we apply this technique to the analysis of nutrient cycling in central Port Phillip Bay where a steady-state approximation appears to be appropriate. A steady-state analysis of a dynamical model yields a set of relationships analogous to a steady-state pool-flux model, except that the relationships between pools and fluxes are generally non-linear, and incorporate the processes and parameters of the dynamical model.

Much simpler empirical models have been developed and applied to nutrient cycling and eutrophication. For example, the Vollenweider (1975) models predict the chlorophyll levels in lakes in response to phosphorus loading. These models have a strong empirical basis, but also incorporate simple compartment - flow ideas. These models have been generalised to apply to nitrogen loadings in estuaries (Monbet 1992).

2.2 Dynamic process models

At the core of most eutrophication or biogeochemical aquatic models is the interaction between the limiting nutrient and plant biomass. The concentration of available nutrient, and the plant biomass (measured as nutrient content), arguably constitute the simplest possible state variable description. The model will then predict the rate of uptake of the available nutrient, and corresponding increase in plant biomass, based on the plant's physiological response to nutrient concentration and other environmental variables (eg.

light availability). The model must also prescribe the rate of loss of plant biomass, and the rate of supply of available nutrient, either through external load or internal recycling. In simple models of this kind, the rate of loss of plant biomass can depend only on plant biomass itself (and possibly nutrient availability and external environmental forcing). In open ocean models, and in coastal systems where plankton production dominates, the plant biomass represents phytoplankton concentration.

Systems in which nutrient availability determines phytoplankton biomass and production are said to be bottom-up controlled. Eutrophic systems may fall into this category, and many models of eutrophication have been developed in this way (eg. Aksnes *et al*. 1995, Stigebrandt and Wulf 1987). An alternative hypothesis is that phytoplankton can be controlled top-down by grazing, or at least that explicit inclusion of grazers is necessary to obtain the correct dynamical response of the system. There is a large family of models in which grazers (in planktonic systems, herbivorous zooplankton) are included as a third component (state variable). These models include a term explicitly prescribing the loss of phytoplankton to grazing, and the consequent increase in zooplankton biomass, in terms of phytoplankton and zooplankton abundance.

If we accept that grazing is an important process, which should be included explicitly, then the minimum state variable description specifies nutrient, phytoplankton and zooplankton concentrations (the so-called NPZ models). These models are already capable of a complex repertoire of dynamical behaviours. When the supply of nutrients is strongly limiting, these models tend to display stable behaviour and approach steady-state solutions. However, in the presence of excess nutrient, NPZ models tend to produce cycles, whose amplitude may increase over time, depending on the exact formulation of the grazing and mortality terms. This has been referred to as the paradox of destabilization by enrichment (Rosenzweig 1971). Typical P-Z models belong to the family of Lotka-Volterra predator-prey models and an account of this family can be found in a number of classic texts (eg. May 1981). There has been considerable debate as to whether such models provide an appropriate explanation for population oscillations in nature (eg. Gilpin 1973).

Plankton oscillations have been reported (McCauley and Murdoch 1987), but it is more commonly observed that the plankton blooms that follow environmental perturbations are strongly damped. In certain ocean regions, high levels of macronutrients are observed along with low stable levels of phytoplankton. There has been considerable debate as to whether this phenomenon is due to top-down grazing control by zooplankton, or bottom-up control by micronutrients such as iron.

It is still an open question as to whether the more complex NPZ models are better suited to modelling impacts of nutrient loading in coastal waters. One can argue that these models are capable of pathological behaviour under high nutrient loads, and therefore more care must be taken in their formulation and parameterisation. On the other hand, NP models may not represent low nutrient situations or transient responses well. We have chosen to explicitly include grazers in the Port Phillip Bay model, partly because much of the Bay has an oligotrophic to mesotrophic character. The issues of grazing responses and stability are discussed in more detail in Chapters 3 and 5.

While the NP or NPZ models form a core description, most models include additional processes and state variables. We can separate these into several categories of issues: trophic complexity, nutrient recycling, benthic communities, and multiple currencies. In addition, models differ widely according to the degree of spatial resolution and complexity represented.

2.2.1 Trophic complexity

Trophic complexity involves two aspects: the number of trophic levels represented, and the number of functional components represented within each trophic level.

We have dealt above with the question as to whether herbivorous zooplankton and their grazing on phytoplankton should be represented explicitly in the model. If they are included, we then of course must consider how to represent zooplankton losses due to predation. If we want to model predation explicitly, we should include the carnivore trophic level, and by extrapolation, the trophic level above that. This has been referred to as the problem of trophic closure. The literature includes numerous examples of NP models: (eg. Aksnes *et al*. (1995), Stigebrandt and Wulf (1987), Tett *et al*. (1986), Tett (1987), Yangi *et al*. (1995)); and NPZ models: (eg. Fasham *et al*. (1990), Chapelle *et al*. (1994), Andersen and Nival (1988), Evans and Parslow (1985), Steele and Henderson (1992), Frost (1987)); but fewer models which explicitly include carnivores: (Radford (1993), Kremer and Nixon (1978)). The latter models are highly detailed and tend to include higher trophic levels for their intrinsic value, not because they are essential to understand nutrient and phytoplankton dynamics.

We have not included higher trophic levels in the Port Phillip Bay model, as we do not think this would increase the model's ability to predict water quality, and we do not have sufficient data to model carnivorous zooplankton or fish. The formulation of the mortality / predation term for the grazers does affect the model behaviour and this is discussed further in the next Chapter.

Trophic levels themselves often lump organisms of very different sizes, life history strategies, feeding methods, etc. An argument can always be made to further subdivide each trophic level into different functional components. Once one decides to separate phytoplankton into different components, there may be strong logical arguments to split grazers as well.

Phytoplankton communities can be subdivided based on a range of functional attributes. The model of Kremer and Nixon (1978) includes two different phytoplankton communities marked by different nutrient requirements and optimum temperatures. The ERSEM model (Radford 1993) and that of Aksnes *et al*. (1995) separate diatoms and flagellates by the diatom requirement for Si. In general few models split phytoplankton by size. The model of Fasham *et al*. (1990) which includes bacteria does not split phytoplankton. Likewise the model of Moloney *et al*. (1986) which contains a detailed model of the microbial loop does not contain separate phytoplankton size classes. On the other hand, Moloney and Field (1991) have developed generic phytoplankton-zooplankton models having a spectrum of size classes. Separation into size classes is more common in steady state models (eg. Taylor and Joint 1990, Murray and Eldridge 1994).

It is a common observation that different water masses support different phytoplankton size classes (Odate and Maita 1988) and that size structure varies with time of year (Nielsen and Richardson 1989) and state of eutrophication (Larsson and Hagstrom 1982). Tamsalu and Ennet (1995) do split their phytoplankton model into four size classes but appear to have little supporting data. The field program in Port Phillip Bay did separate phytoplankton into three size classes, and the data show quite different dynamical behaviour for the different size classes (Beardall *et al*. 1996). The data are consistent with a general observation that small phytoplankton appear to be present at relatively constant background levels, while large phytoplankton (diatoms and dinoflagellates) are bloom organisms, fluctuating markedly in response to environmental conditions.

The problem with splitting phytoplankton and zooplankton into classes is that interaction of the size classes becomes extremely complex and not necessarily realistic. This is particularly the case if the small phytoplankton are grazed on by small zooplankton which are in turn grazed by the larger zooplankton. Coexistence of different functional components in a model is not guaranteed: models with competing functional groups may predict competitive exclusion of one group. The model of Moloney *et al*. (1991), for example, tends to show exclusion of large phytoplankton in undisturbed waters. In general, diverse phytoplankton assemblages in the real world tend to be "better behaved" than most model assemblages. The persistence of diverse phytoplankton communities all apparently competing for the same limiting nutrients and light has been referred to as the "paradox of the plankton" (Hutchinson 1961).

In the Port Phillip Bay model, we have separated phytoplankton into large and small size classes, with the large class potentially divided into diatoms (Si-requiring) and dinoflagellates. We have separated zooplankton into large and small size classes. We regard this level of resolution as being justified by the data, and as appropriate for the Study objectives.

2.2.2 Nutrient Recycling

In most models, the available nutrient (generally dissolved inorganic nutrient) is supplied through external loads and replenished through recycling in the sediment or water-column or both. (The model of Yangi *et al*. (1995) is forced with observed nutrient concentrations, but this approach is not applicable to any model that seeks to predict nutrient concentrations as a state variable). In some models, a proportion of organic matter involved in grazing or zooplankton mortality is assumed to be instantly remineralized to produce dissolved inorganic nutrient (eg. Tett *et al*. 1986, Frost 1987, Steele and Henderson 1992). These models are all open ocean euphotic zone or mixed layer models and do not explicitly represent organic detritus or dissolved organic matter. They represent the loss of detritus through sinking implicitly, by assuming a fixed fraction is exported from the euphotic zone. Regeneration of nutrients in deep water and vertical mixing or transport are assumed to maintain nutrient levels at the bottom of the euphotic zone. This approach is generally inappropriate for shallow waters, particularly where benthic and water-column processes are strongly coupled. However the model of Kremer and Nixon (1978) uses nutrient fluxes from the sediments which are independent of inputs.

Many models represent detritus explicitly. The detrital pool acts as a store of fixed nutrient, which introduces a delay into nutrient recycling. Particulate detritus sinks and thereby transports nutrients out of the surface layer into deep water or to the sediment. Dissolved organic matter (DOM) does not sink, and very large pools of refractory DOM are found in the open ocean and in coastal waters. Horizontal transport of particulate detritus and DOM from regions of high production to more oligotrophic areas can also be important. The model of Stigebrandt and Wulf (1987) does not have an explicit detritus pool but rather a general organic matter pool representing both living plankton and detritus, which can sediment out and decays on the bottom. Andersen and Nival (1988) investigate the effects of copepod vs salp grazing on phytoplankton. They explicitly modelled the production of different categories of detritus with differing settling velocities and hence retention efficiencies in the surface layer. Fennel (1995) has developed a two layer model with detritus in the lower layer and DIN in the upper layer. All living matter transported into the deep layer becomes detritus. This two layer approach is not really applicable to Port Phillip Bay, which is generally well-mixed. In their model of a French coastal Bay Chapelle *et al*. (1994) include a detrital pool which falls out and/or breaks down to DIN.

More complex remineralisation models use explicit models of detritivores. Fasham *et al*. (1990) explicitly model bacteria in the remineralisation of DOM in a pelagic model. The model of Pace *et al*. (1984) uses benthic detritus and water-column DOM with bacterial remineralisation and higher organisms grazing on the bacteria. The same is true of the ERSEM model of the North Sea (Radford 1993). There is still debate about the need to explicitly represent bacteria in models of nutrient recycling. Bacteria tend to represent a relatively small biomass that turns over rapidly. The question is whether modelling bacterial biomass explicitly improves predictions of detrital breakdown rates. Bacteria may also mediate grazer interactions by acting as a secondary food source for microzooplankton. We have chosen to explicitly represent particulate detritus and DOM, but not bacteria, in the Port Phillip Bay model. The role of bacteria is considered further in Chapter 3.

In systems where nitrogen is the key limiting nutrient, there are potentially sources and sinks associated with fixation of nitrogen gas and denitrification of nitrate to nitrogen gas. Atmospheric nitrogen gas represents an inexhaustible but biologically unavailable reservoir. These sources and sinks are important on long time scales in the global nitrogen cycle, and can play an important role in shallow basins that are poorly flushed. Denitrification has been modelled in the semi-enclosed North Sea (Radford 1993), and the Baltic Sea (Stigebrandt and Wulf 1987). These models use a simplified approach to the complex set of biogeochemical transformations and processes involved in denitrification. Sediment biogeochemical processes have been modelled in detail by Omori *et al*. (1994) and Blackburn and Blackburn (1993). In Port Phillip Bay, denitrification plays a critical role in maintaining water quality. Denitrification has been represented in the model using an empirical approximation analogous to that used for the North and Baltic Seas.

2.2.3 Multiple currencies.

Nitrogen and phosphorus are the two macronutrients most commonly regarded as limiting to algae and represented in models of eutrophication. Nitrogen is generally

thought of as limiting in marine systems, and phosphorus in freshwater systems, but exceptions to both rules occur. In systems where either may potentially be limiting, it is necessary to model both. Silicate can be limiting to diatoms (eg. Aksnes *et al*. 1995) and in systems where diatoms are important, it may be desirable to carry silicate as well. Phosphorus is present in great excess in Port Phillip Bay, and it is not necessary to include it, except as a diagnostic variable. On the other hand, diatoms play a dominant role in phytoplankton blooms in the Bay, and silicate depletion occurs seasonally. It has proved necessary to include silicate explicitly in order to predict bloom dynamics.

Under eutrophic conditions, the oxygen fluxes associated with photosynthesis and respiration can be large enough to significantly affect dissolved oxygen levels. In some systems, high external loads of organic matter impose a large direct oxygen demand. Oxygen depletion is a critical water quality indicator: anoxia leads quickly to catastrophic loss of benthic communities (Radford 1993). Oxygen levels also influence the process of denitrification (Blackburn and Blackburn 1993, Radford 1993). Oxygen can be modelled along with nutrients by explicitly including organic carbon or its oxygen equivalent. This has been done for a number of coastal basins subject to oxygen depletion, including Chesapeake Bay (Officer *et al*. 1984, Park *et al*. 1996), the Baltic (Stigebrandt and Wulf 1987), and the North Sea (Radford 1993). The estuarine model of Chapelle *et al*. (1994) also includes oxygen.

Wherever multiple currencies are involved, the model must specify the ratios in which these elements are taken up or released. The simplest approach is to assume that these ratios are constant, and the Redfield ratios for C:O:N:P:Si are frequently used for this purpose (Redfield 1934). More complex approaches draw on physiological theory to predict changes in composition with changes in relative nutrient availability (see Droop 1983).

2.2.4 Benthic communities

In shallow coastal waters, we must consider not only the role of sedimentation and nutrient cycling within the sediments, but also the contribution of flora and fauna at the sediment water interface. We distinguish three broad classes of epibenthic primary producers: microphytobenthos, macroalgae, and seagrass. We must also consider the role of filter-feeding animals. (Deposit feeders are treated implicitly through their contribution to organic matter remineralization within the sediment.)

Microphytobenthos (MPB) have been neglected in all ecosystem models known to the authors, although process models have been developed to address specific aspects of MPB ecology. For example, Montagna *et al*. (1995) has fitted different grazing functions to relate predation on MPB to production, and models have been used to estimate primary production (Pickney and Zingmark 1993). Larger benthic algae have been modelled by Solidaro *et al*. (1995). Seagrasses have been modelled by Bach (1993) and by Fong and Harwell (1994) who also modelled macroalgae. The paper of Bach (1993) referred to temperate species of eelgrass, that of Fong and Harwell (1994) to subtropical species. Since the principle seagrass in Port Phillip Bay is *Heterozostera tasmanica* and the Bay is temperate, the former is probably more relevant. The Fong and Harwell (1994) model uses only one currency (dry weight) while the Bach (1993) model, and the Solidaro *et al*. (1995) model, use Droop style kinetics (see Droop 1983)

with a varying C:N ratio. Norro and Frankignoulle (1995) include *Posidonia* in their model, but only as a constant nutrient sink at the time scales they are interested in. A generalised benthic vegetation component is included in the MIKE 21 EU eutrophication module (Ecological Modelling Centre 1993). Madden and Kemp (1996) have used a model specifically to investigate the response of benthic vegetation to the eutrophication of Chesapeake Bay.

The Kremer and Nixon (1978) model included filter-feeder grazing, but filter-feeder biomass was fixed and grazing was just a function of temperature and phytoplankton biomass. The ERSEM model contains a filter-feeder component (Radford 1993), and (unusually) an explicit model of deposit feeders. Raillard and Menesguen (1994) included oysters in a model similar to that of Chapelle *et al*. (1994). Their aim was to evaluate oyster production. Using estimates of filter-feeder abundance, Gerritsen *et al*. (1994) estimated the time taken for the waters of Chesapeake Bay to be filtered, taking account of the mixing regime induced by seasonal stratification. There are many models of the process of filtration (Riisgard and Larsen 1995), but few models of the dynamical response of mixed assemblages of filter feeders.

The Port Phillip Bay model explicitly represents microphytobenthos, seagrass, macroalgae and benthic filter feeders. In the PPBES, MPB were well studied and their estimated production is highly significant. Macroalgae were studied less and are thought to be less significant, although they may be locally important. The extent of seagrass distribution in the Bay is relatively limited: they have been included primarily as ecological indicators.

2.3 Spatial structure of the model

A defining characteristic of aquatic models is that the biogeochemical and ecological processes take place within a fluid medium in which the horizontal and vertical transport of constituents must be considered. At least in shallow coastal systems, these water column constituents and processes interact with the underlying sediment, which is fixed in place, although resuspension and transport of sediment can also be important. Pelagic ocean models (eg. Fasham *et al*. 1990, Tett *et al*. 1986) ignore the sediment, as do some models dealing with theoretical issues of plankton dynamics (eg. Steele and Henderson 1992). Models focused on the sediment in isolation are few in number and Blackburn and Blackburn (1993) is of most interest. Models which attempt to develop a consistent explanation of nutrient cycling in shallow coastal systems must address both water column and sediment: examples include Chapelle *et al*. (1994), the ERSEM model (Radford 1993), Stigebrandt and Wulf (1987) and the Port Phillip Bay model described here.

Models of water column constituents and processes are generally written in terms of constituent concentrations (ie. per volume), and describe the "local" rate of change of these constituents. These biogeochemical models are then nested within physical models, which describe the horizontal and vertical transport or exchanges of dissolved or suspended matter.

The level of horizontal and vertical resolution depends on the system under study and the model objectives. In systems with strong vertical mixing and weak vertical

gradients, the water column may be modelled as one well-mixed layer. Port Phillip Bay generally falls into this category. Many simple models of pelagic ocean systems have modelled only one vertical layer (the mixed layer) and imposed boundary conditions at the base of the mixed layer (eg. Evans and Parslow 1985, Fasham *et al*. 1990, Tett *et al*. 1986).

Coastal and estuarine systems can be subject to strong vertical stratification, while pelagic ocean systems often see seasonal stratification within the euphotic zone. Models may then incorporate multiple vertical layers. The simplest or computationally cheapest approach is to use two layers under stratified conditions. Some models use two layers at times or places where stratification is important, and revert to one layer when mixing dominates. The model of Chapelle *et al*. (1994), Stigebrandt and Wulf (1987) and the ERSEM model (Radford 1993) use two layers in deeper waters and one layer in coastal waters. Fennel (1987) uses two layers in summer and one in winter.

In principle, once one has developed a sound physical model of vertical transport, a model can be implemented with vertical resolution limited only by computational constraints. Increasingly sophisticated physical models of vertical mixing and turbulent closure have been developed in recent years (eg. Doney *et al*. 1995) and there is a rapidly developing move to vertically resolved pelagic biogeochemical models (Evans and Garcon 1997). Yangi *et al*. (1995) used a three layer model (10 m, 30 m and bottom) and Aksnes *et al*. (1995) used 11 layers in their model of a major North Sea bloom.

An alternative approach used by Woods and Onken (1982) modelled individual phytoplankton and their motion within the water column. This model was also a two layer model, the phytoplankton moving within the mixed layer and becoming trapped by the diurnal thermocline.

The level of horizontal resolution also depends on the physical context and the model objectives. Many pelagic models are developed as 1-D models of an idealised water column. However, it is recognised that there are important processes in basin and global biogeochemical cycles which 1-D models cannot address, and sophisticated and computationally expensive biogeochemical models based on ocean general circulation models are being developed by a number of research groups.

Increased horizontal resolution may be included either because the spatial distribution of properties is of interest as an output, or because spatial variation within a region is thought to be important for the behaviour of the region as a whole (ie. errors involved in averaging over these variations are too large). In small enclosed well-mixed basins, it may be a reasonable approximation to treat the entire system as a single compartment (eg. Kimmerer *et al*. 1993). Once one has developed a highly resolved physical model, there is in principle no obstacle other than computational constraints to prevent development of a highly resolved biogeochemical model. Highly resolved models are not only computationally expensive (this limits the number of numerical experiments which is possible), but also difficult to analyse and understand. Simple one-box models can provide useful insights into overall system behaviour.

In coastal regions, factors such as varying depth, nearness to coasts and to point input sources, and spatial variation in bottom type and benthic communities, may all

encourage the specification of greater spatial resolution. Models such as ERSEM (Radford 1993), and those developed by Kremer and Nixon (1978), Chapelle *et al*.'s (1994) and Tamsalu and Ennet (1995), all provide some level of horizontal resolution.

The full Port Phillip Bay model is based on a 3-D circulation and transport model package which allows considerable flexibility in the level of spatial resolution. The model has been run primarily at an intermediate level of resolution (60 boxes) which resolves the principal regions within the Bay, and the gradients within those regions. This level provides an appropriate resolution for the water column at time scales of a day or longer, and resolves broad gradients in sediment type, but not fine patchiness in benthic communities. It was chosen taking into account the computational costs and need for extensive numerical experimentation. Versions of the model with coarser spatial resolution, including a single cell model, have also been developed as an aid to model analysis.

2.4 Conclusions

This review has introduced briefly a range of conceptual approaches and structural choices developed for modelling nutrient cycles in coastal marine ecosystems. It has allowed us to introduce the scope and broad structure of the Port Phillip Bay model, and place it in the context of previous international modelling studies. The structure and process formulation is specified in detail in the next chapter.

An important lesson is that models of this kind are not developed *de novo*, but build on an established paradigm and extensive experience in modelling coastal systems. Within this broad paradigm, a choice is made in each new study of the level of complexity, in terms of modelled constituents, processes and spatial resolution. With regard to these choices, the Port Phillip Bay model stands at the moderately complex end of the model spectrum, in terms of trophic complexity, sediment-water coupling, use of multiple currencies, incorporation of benthic communities, and spatial structure. We feel that these choices are justified in terms of both the model objectives, and the scope of the field study and resulting data.

Within the general area of nutrient cycling and impacts in coastal systems, it is probably fair to say that models of planktonic ecosystems and biogeochemistry have received the most attention, and are most advanced in terms of both formulation and analysis. Sediment modelling (including denitrification) is less well covered by existing models as the processes are not so well understood. Models of macrophytobenthos and filter-feeders are even more poorly defined, but these are not so critical to nutrient cycling in Port Phillip Bay.

The Port Phillip Bay model does contain some innovative features, including the treatment of microphytobenthos, which is important in the Bay, and has been largely ignored by previous models and field studies. The separation of phytoplankton and zooplankton size classes is less common in older models, although separation of phytoplankton either by size or nutrient requirement has become increasingly common in recent models.

3 MODEL DESCRIPTION

This Chapter describes the state variables, equations and processes that together define the biogeochemical model used to simulate nutrient cycling, fate and impact in Port Phillip Bay. The Chapter starts by explaining the currencies and units used in the model, then introduces the state variables, and proceeds to a description of the model equations and processes.

3.1 Currencies and units

The model state variables represent the concentrations or biomass of the key components that interact to control the fate and impacts of nutrients. Components such as inorganic nutrients are defined as mass concentrations eg. as mg N m^{-3}, or mg P m^{-3}. For organic components such as phytoplankton or detritus, there is a choice of units or currencies to measure biomass. We have followed the common practice of using the limiting nutrient as a core currency to measure concentrations of these components.

Nitrogen is the principal limiting nutrient in Port Phillip Bay and its cycling, and in particular its removal, is critical to the functioning of the Bay. The model presented here is essentially a model of nitrogen cycling. Except where otherwise specified, concentrations of organic components are defined in terms of their nitrogen mass content ie. mg N m^{-3}. Epibenthic variables such as seagrass and benthic filter feeders are defined in terms of mass per unit area ie. mg N m^{-2}.

Although nitrogen is the focus of the model, we have included a capability to treat other currencies in the model for a variety of reasons. Organic carbon is not treated explicitly, but is treated implicitly to allow us to model oxygen production and consumption. Phosphate is abundant in Port Phillip Bay, at concentrations that are unlikely to limit or affect phytoplankton uptake and growth. However, because phosphate loads and concentrations have been well studied, and phosphate represents a useful diagnostic variable, we have included a capability to model P cycling. Silicate is included in the model because of evidence that silicate depletion and limitation of diatom growth may play an important role in phytoplankton and nitrogen dynamics (Harris *et al*. 1996).

The model deals with multiple currencies in a simple manner by assuming that the composition of organic matter (living and non-living) is fixed. This is a common assumption, at least for marine ecosystems, and we make the usual assumption that the composition follows the empirical (C:N:P:O) ratios defined by Redfield *et al*. (1963).

We have developed versions of the Port Phillip Bay model incorporating variable C:N and N:P ratios, but have not included these in the standard model. Including another currency explicitly effectively doubles the number of state variables in the model. We judged that the additional computational load was not justified, because carbon and phosphorus are not limiting and do not affect the core predictions of nitrogen fate and cycling. Errors in the Redfield approximation may affect the accuracy of predictions of phosphate or dissolved oxygen concentrations, and the use of the former as a diagnostic variable. While phosphate cell quotas can vary widely under phosphate limitation, this is unlikely to occur in the presence of excess phosphate. The assumption of fixed C:N

ratios is likely to involve substantial error in the case of benthic macroalgae (cf. Chidgey and Edmunds 1997), but we do not expect this to have a major effect on nitrogen cycling.

Variation in the N:Si ratio in diatoms probably does occur, and could affect the predicted phytoplankton dynamics, but associated errors are unlikely to outweigh other uncertainties in silica dynamics, and uncertainties concerning non-diatom bloom species.

Other nutrients have been implicated in phytoplankton dynamics. It has been suggested that iron limits oceanic production (Martin *et al*. 1990), but iron concentrations in coastal waters are likely to be much greater than the sub-nanomolar levels found in oceanic waters. Other trace metals including selenium, and also dissolved organic compounds in runoff, have been implicated in dinoflagellate blooms. Given the direct evidence for nitrogen limitation, any micronutrient limitation is more likely to affect phytoplankton composition than overall biomass.

Photosynthesis in the model is potentially light-limited and the available photosynthetically active radiation (PAR) in the water column and at the sediment surface is modelled explicitly. PAR is represented as W m^{-2}, but the units are not critical, except of course that they must be consistent with the units of the parameters defining light saturation intensities for photosynthesis.

3.2 Model State Variables

The biogeochemical model describes the flow of nitrogen through primary producers, consumers, detritus and inorganic nutrient pools. Each of these has been subdivided further into functional components. These are described in more detail below. A listing of the state variables, with symbols and units, is given in Table 3.1.

3.2.1 Primary Producers

Primary producers take up nutrients and incorporate them into organic matter. The standard model divides primary producers into five functional components: small and large phytoplankton, microphytobenthos, macroalgae and seagrasses. In the model equations, these are represented by the symbols PS, PL, MB, MA and SG respectively.

Phytoplankton play a key role in nutrient uptake, ecosystem production and water quality. We have chosen to divide phytoplankton into two size classes, which appear to play different functional roles and display different dynamics. Small phytoplankton generally have a fairly constant biomass, while large phytoplankton bloom in response to inputs and seasonal changes. In Port Phillip Bay, data on phytoplankton biomass and production has been collected for three size categories: picophytoplankton (<2 um), nanophytoplankton (2 to 20 um) and microphytoplankton (>20 um). These are standard operational definitions, but unfortunately they do not correspond well to functional groups, as the nanophytoplankton include both small flagellates which are not generally bloom organisms, and small diatoms which are. We chose to use only two size categories in the model, as we do not have good grounds to define and parameterise a third functional component based on size.

Given the silicate limitation observed in Port Phillip Bay, there is an argument for separating the large phytoplankton class into diatoms (Si dependent) and dinoflagellates. We have developed an experimental version of the model including diatoms and dinoflagellates.

Microphytobenthos are benthic diatoms which photosynthesise and grow in the top 1 to 2 cm of sediment. They are widespread in Port Phillip Bay, and have been shown to have a larger biomass than phytoplankton and to account for production equal to about half of that of the phytoplankton. They are therefore a major contributor to nutrient cycling in Port Phillip Bay, and have been represented explicitly, as volume concentration (mg N m^{-3}) in the upper layers of sediment.

The transport model allows for exchange of phytoplankton and microphytobenthos between the water column and the top layer of sediment, through sinking and resuspension. Microphytobenthos are assigned high sinking rates and settle out quickly. Phytoplankton which settle to the sediment are assigned an elevated loss rate, but remain viable if resuspended before dying.

Benthic macroalgae are abundant in northern Port Phillip Bay. Their estimated biomass varies seasonally from 200 to 1000 tonnes N Bay-wide, although these figures are quite uncertain (Chidgey and Edmunds 1997). This represents about 0.5-2.5 times the estimated biomass of phytoplankton. Given the much slower turnover of macroalgae, their production is likely to be an order of magnitude lower than that of phytoplankton. Only one functional class of macroalgae is represented in the model, although there is clearly a wide taxonomic, morphological and ecological diversity. The dominant group in terms of biomass appear to be filamentous algae, which may be largely drift algae.

The seagrass distribution in Port Phillip Bay is restricted to the shallow (< 5 m) areas mostly in the southwest. Their biomass and contribution to N cycling are thought to be relatively small. Seagrass have been included in the model because of their importance as an ecological indicator. Seagrasses may play a disproportionate role in the formation of very refractory detritus, which is lost to burial (Duarte and Cebrián 1996). However the very low nutrient content of this refractory detritus means that this flux is unimportant for nutrients.

3.2.2 Consumers

The model includes two size classes of herbivorous zooplankton, large and small, represented by the symbols ZL and ZS. The large zooplankton represent mesozooplankton, and consist primarily of crustaceans such as copepods. They are assumed in the model to feed only on large phytoplankton, and have relatively slow specific growth rates and loss rates. The small zooplankton represent microzooplankton, including zooflagellates, ciliates, etc, and are assumed to feed only on small phytoplankton. Small zooplankton are assumed to have high specific growth rates and loss rates, matching those of the small phytoplankton. The food sources of different zooplankton will be considered in more detail when the process of grazing is examined.

The feeding relationships among zooplankton and phytoplankton are simplified in the model. There is undoubtedly some feeding across size classes. Moreover, some protozoa

are facultative autotrophs and heterotrophs, a phenomenon referred to as mixotrophy. Under some conditions, mixotrophy may account for a significant proportion of grazing on phytoplankton (Jones 1994). The role of mixotrophs in Port Phillip Bay is unknown and we have not included this option in the model.

The sediments of Port Phillip Bay contain a diverse assemblage of suspension feeders, including molluscs, crustacea and polychaetes. These benthic filter feeders have been estimated to clear the entire water column of Port Phillip Bay once every 16 days (Wilson *et al*. 1993). This is much lower than the estimated zooplankton clearance rate, but the benthic filter-feeders may have important local effects in coastal areas, where the water column is shallow and their biomass may be larger. They can act to maintain ecosystem stability (Ott and Fedra 1977) and water clarity (Geritsen *et al*. 1994). Benthic filter feeders in the model are assumed to be relatively undiscriminating, removing small and large phytoplankton, small zooplankton and labile detritus from the water column. We have represented the diverse assemblage of suspension feeders by one functional component, given the symbol BF. This is a crude approximation (perhaps more obvious because these are macrofauna whose diversity is readily apparent). However, given their role in the nutrient cycle, the information available on distribution, abundance and autecology do not warrant subdivision of this group. Benthic filter feeders are assumed to have relatively low specific growth rates and loss rates compared with zooplankton.

3.2.3 Detrital Matter

Three forms of non-living organic matter are included in the model: labile particulate detritus, refractory particulate detritus and dissolved organic matter. These are represented by the symbols DL, DR and DON respectively. The particulate detrital pool contains a wide variety of particles, with diverse sources, ages, sizes and chemical composition. The model includes two functional components: fresh labile detritus breaking down on time scales of a few days, and semi-refractory detritus turning over on time scales of a year. This allows the model to treat perturbations to the nutrient cycle on time scales of days to years. There is a very large pool of particulate organic nitrogen in the sediments of Port Phillip Bay, which appears to have accumulated over periods of hundreds to thousands of years. This highly refractory component is not represented in the model. This is a minimal representation of detritus, but including more functional components is difficult to justify, given the lack of field procedures for distinguishing components according to turnover time or age. There could be an argument for subdividing particulate detritus on the basis of particle size or sinking rate, given the importance of sinking rate in sediment-water exchange and transport.

The pool of dissolved organic matter also contains a variety of compounds with diverse turnover rates. In oceanic waters there is a large pool of highly refractory DOM, whose average age has been estimated to be as much as 3400 years (Williams 1975). The bulk of this material is essentially irrelevant for the cycling of nutrients on the time scales of interest here. However the DOM pool also includes much more labile components. Highly labile sugars and amino acids released through cell lysis or messy feeding may be consumed by bacteria or break down on time scales of hours (Fuhrman 1987) to days (Holibaugh and Azam 1983). This material is not modelled explicitly, but is treated as though it was remineralised immediately to form dissolved inorganic nutrient. The

model includes a single DOM pool with an assumed turnover time of the order of a hundred days. This intermediate or semi-labile material accounts for the excess of DOM in Port Phillip Bay relative to oceanic water, and under present conditions constitutes the only significant form of nitrogen export to Bass Strait. Because it turns over on time scales, which are long compared with both phytoplankton uptake of inorganic N, and transport within the Bay, it plays a role in reducing N sequestration in coastal waters.

Each of these non-living organic pools is assumed to carry phosphorus and carbon along with nitrogen at Redfield ratios. However, detrital silica is produced only by diatoms, and has its own dissolution kinetics, so it is represented by a separate pool, with the symbol DSi.

3.2.4 Inorganic Nutrients

The model contains four inorganic nutrient pools: nitrate, ammonium, phosphate and silica (NO, NH, PO and Si).

As discussed in the preceding section, nitrogen is the key limiting nutrient. It would be possible to develop a model that represented dissolved inorganic nitrogen as a single pool. We decided to split this pool into nitrate and ammonia for several reasons. Nitrate and ammonia sources are to some extent spatially separated in Port Phillip Bay: WTP is the dominant ammonia source, while the Yarra and Patterson-Mordialloc systems are relatively more important as nitrate sources. The conversion of ammonia to nitrate (nitrification) is a critical part of the sediment biogeochemistry that leads to loss of nitrogen through denitrification. As the field program measured both nitrate and ammonia, we felt that modelling these pools separately could have important diagnostic value.

As discussed in the previous section, phosphate is generally not limiting, and was modelled as a diagnostic tracer. Silicate was measured in the field program, and silicate depletion was observed, apparently due to diatom uptake. Preliminary model results suggested that silicate depletion may limit phytoplankton blooms, and so it was included explicitly.

3.2.5 Dissolved Oxygen

In the water column, dissolved oxygen (DO) is affected by consumption and production of organic matter, and by exchange across the air-sea interface. Dissolved oxygen is an important water quality indicator, as oxygen stress can have major rapid ecosystem impacts. However, stratification is generally weak in Port Phillip Bay, and very low levels of dissolved oxygen were not observed in the water column during the study period.

Dissolved oxygen in pore water is depleted in sediments, and concentrations there play a critical role in mediating the key biogeochemical reactions, including nitrification and denitrification. Process models of sediment biogeochemistry must treat oxygen as an explicit variable, which can turn over on time scales of seconds to minutes. In the empirical models of sediment biogeochemistry used here, oxygen in the sediment is not

modelled explicitly, but the oxygen consumption in the sediment is calculated as an oxygen debt, and acts as a sink at the sediment-water interface.

3.2.6 Light

Light (ie. photosynthetically active radiation or PAR, symbol I) is a critical factor controlling primary production of both phytoplankton and especially phytobenthos. The surface irradiance is attenuated by suspended and dissolved material in the water column. The attenuation coefficient is calculated as a function of constituents in each layer, and the light intensities corresponding to both the bottom of the layer, and the layer mean, are calculated.

3.2.7 The Omission of Bacteria and Carnivores.

There are of course many potential variables, which are not represented in the model, and many potential levels of subdivision of those variables, which are included. This is inevitable, and the choice of model variables is a matter of judgement, based on the study objectives and the information available. There are two functional groups in particular whose omission deserves further discussion.

Heterotrophic bacteria have been included explicitly in a number of previous models, most notable Fasham *et al*. (1990). Bacteria in aquatic ecosystems play a number of important roles. The most important role is to attack, ingest and remineralize both particulate and dissolved organic matter, releasing dissolved inorganic nutrients. This role is represented implicitly in the model by assigning a breakdown rate to the detrital pools. Given the other uncertainties associated with the nature of detritus, and the lack of information on bacterial biomass, growth rates and loss rates in Port Phillip Bay, there is little reason to believe that an explicit model of bacterial dynamics would increase the accuracy of predicted detrital breakdown rates.

Bacteria can also serve as a food source for microzooplankton, and thereby divert organic matter which would otherwise be "lost" back to higher trophic levels. This alternative food source may have some impact on microzooplankton dynamics, and their interaction with small phytoplankton. The small phytoplankton - microzooplankton interaction is important under oligotrophic conditions, but much less important under the higher nutrient loadings of concern in Port Phillip Bay. Moreover, owing to the inefficiency of the microbial loop, relatively little bacterial production finds it way to higher trophic levels (Ducklow 1991). Recent studies have suggested that a large fraction of water-column bacterial production is not grazed but is killed by viruses instead (Weinbauer and Peduzzi 1995) leading to a further reduction in utilisation of bacterial production by higher trophic levels (Murray and Eldridge 1994).

Trophic levels higher than herbivores have not been treated explicitly in the model. A relatively small proportion of the total N flux flows through higher trophic levels, although these may of course be important for activities such as recreational and commercial fishing. Their principle effect in relation to water quality is to determine a loss rate for herbivores. Most biogeochemical models stop at the level of herbivores, or occasionally the next trophic level, and all face the problem of prescribing mortality

rates at one trophic level when the next level is not represented explicitly. This is known as the problem of trophic closure, and is discussed further in the next section.

Table 3.1: Model State Variables

Variable	Description	Units
PL	Large Phytoplankton	mg N m^{-3}
PS	Small Phytoplankton	mg N m^{-3}
DF	Dinoflagellates	mg N m^{-3}
MB	Microphytobenthos	mg N m^{-3}
MA	Macroalgae	mg N m^{-2}
SG	Seagrass	mg N m^{-2}
ZL	Large Zooplankton	mg N m^{-3}
ZS	Small Zooplankton	mg N m^{-3}
BF	Benthic Filter-Feeders	mg N m^{-2}
DL	Labile Detritus	mg N m^{-3}
DR	Refractory Detritus	mg N m^{-3}
DON	Dissolved Organic Nitrogen	mg N m^{-3}
DSi	Biogenic Silica	mg Si m^{-3}
NO	Nitrate + Nitrite	mg N m^{-3}
NH	Ammonia	mg N m^{-3}
PO	Phosphate	mg P m^{-3}
Si	Dissolved Silica	mg Si m^{-3}
O2	Dissolved Oxygen	mg O m^{-3}
I	Light (PAR)	W m^{-2}

3.3 Model Structure

This section presents the equations for the local rate of change of model state variables due to biogeochemical processes. The principal pathways of nitrogen represented by the equations are shown schematically in Figs. 3.1-3. The equations are listed here in abbreviated form using a simple convention to name individual source and sink terms, which represent the exchanges of nitrogen among state variables. The detailed formulation of the process submodels is given in the next section.

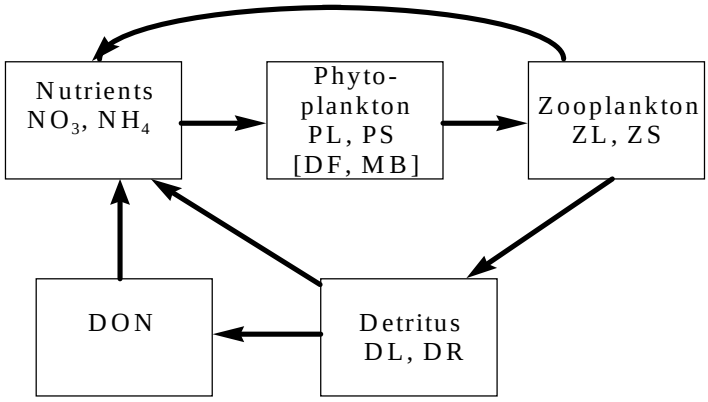

Figure 3.1 Principal state variables, nitrogen pools and pathways within the water-column in the Port Phillip Bay model. DIN is taken up by large and small phytoplankton, and potentially by dinoflagellates and suspended microphytobenthos. Phytoplankton are grazed by zooplankton, resulting in release of nutrients or the production of detritus. Detritus is remineralised to form inorganic nutrients, either directly or via DON.

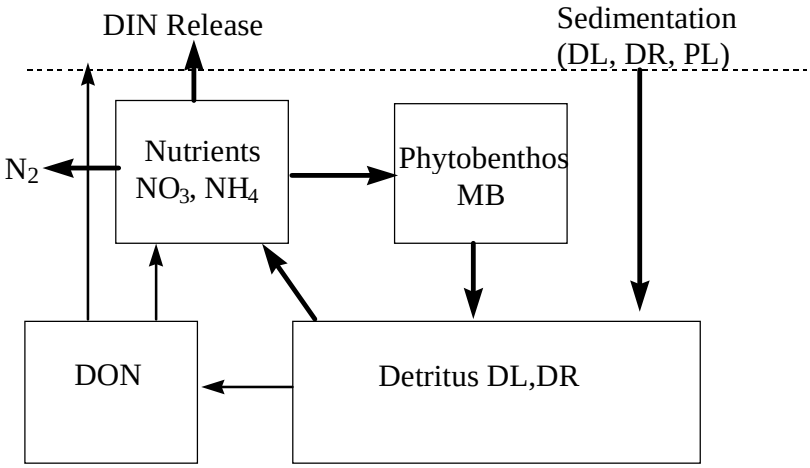

Figure 3.2. Principal state variables, nitrogen pools and pathways within the sediment of the Port Phillip Bay model. Nutrients are taken up by microphytobenthos which in turn die, producing detritus. Phytoplankton (which are not locally produced) also die to produce detritus, this mostly applies to PL, which sink out from the water-column. Detritus is then remineralised, either directly or via DON. However some nitrogen is lost as N_2 gas rather than being recycled.

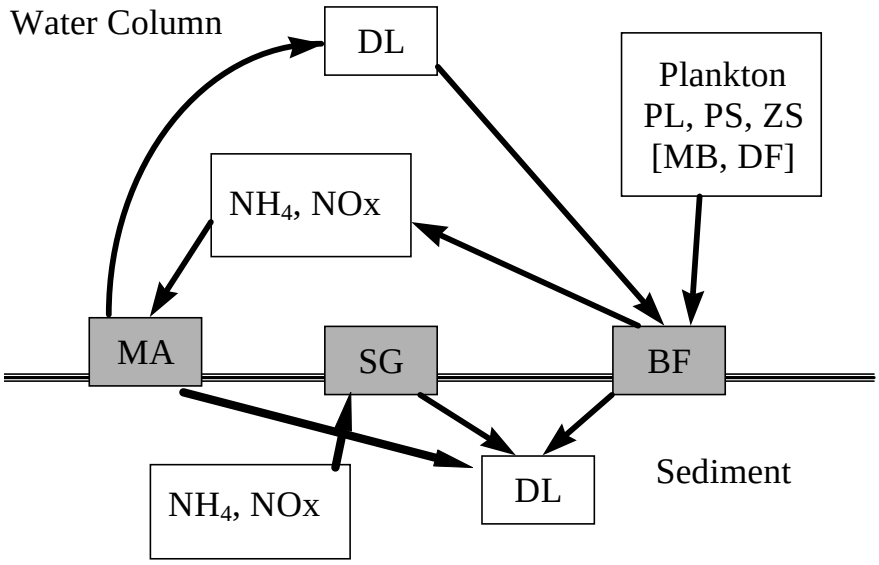

Figure 3.3. Nitrogen pathways involving epibenthic variables (grey boxes) in the Port Phillip Bay model.

Table 3.2 Model Equations

Large phytoplankton (diatoms) in the water-column dPL/dt = PLgrowth - ZLgrazePL - BFgrazePL	(E1)
Large phytoplankton in the sediment dPL/dt = - PLmortality	(E2)
Small phytoplankton in the water-column dPS/dt = PSgrowth - ZLgrazePS - BFgrazePS	(E3)
Small phytoplankton in the sediment dPS/dt = - PSmortality	(E4)
Dinoflagellates in the water-column dDF/dt = DFgrowth - ZLgrazeDF - BFgrazeDF	(E5)
Dinoflagellates in the sediment dDF/dt = - DFmortality	(E6)
Microphytobenthos in the water-column dMB/dt = MBgrowth - ZLgrazeMB - BFgrazeMB	(E7)
Microphytobenthos in the sediment dMB/dt = MBgrowth - MBmortality	(E8)
Macroalgae dMA/dt = MAgrowth - MAmortality	(E9)
Seagrass dSG/dt = SGgrowth - SGmortality	(E10)
Large zooplankton in the water-column dZL/dt = ZLgrowth - ZLmortality	(E11)
Small zooplankton in the water-column dZS/dt = ZSgrowth - ZSmortality - BFgrazeZS	(E12)
Benthic filter-feeders dBF/dt = BFgrowth - BFmortality	(E13)
Ammonia in water-column dNH/dt = - PLuptakeNH - PSuptakeNH - DFuptakeNH – MbuptakeNH - MAuptakeNH + ZLreleaseNH + ZSreleaseNH + BfreleaseNH + DONremin + DLremin +DRremin	(E14)
Ammonium in sediment dNH/dt = DLremin +DRremin + DONremin - nitrification – MbuptakeNH - SGuptakeNH	(E15)
Nitrate in water-column dNO/dt = - PLuptakeNO - PSuptakeNO - DFuptakeNO – MbuptakeNO - MAuptakeNO	(E16)
Nitrate in sediment dNO/dt = nitrification - denitrification - MBuptakeNO - SGuptakeNO	(E17)
Labile detritus in the water-column dDL/dt = ZLprodnDL + ZSprodnDL + MAmortality + Sgmortality - DLremin - DLsolDON - DLprodnDR - BFgrazeDL	(E18)

Table 3.2 Model Equations (cont.)

Labile detritus in sediment dDL/dt = PLmortality + PSmortality + DFmortality +BFprodnDL - DLremin - DLsolDON - DLprodnDR	(E19)
Refractory detritus in the water-column dDR/dt = DLprodnDR - DRremin -DRsolDON -BFtransDR	(E20)
Refractory detritus in sediment dDR/dt = DLprodnDR - DRremin -DRsolDON + BFtransDR	(E21)
DON in water or sediment dDON/dt = DLsolDON + DRsolDON - DONremin	(E22)
Oxygen in water-column dO2/dt = X_ON [PLgrowth + PSgrowth + DFgrowth + MBgrowth + MAgrowth + SGgrowth - ZLreleaseNH - ZSreleaseNH - BFreleaseNH - DLremin - DRremin -DONremin]	(E23)
Oxygen in sediment dO2/dt = X_ON [MBgrowth - DLremin -DRremin -DONremin]	(E24)
Phosphate in water-column dPO/dt = - PLuptakePO - PSuptakePO - DFuptakePO – MbuptakePO - MAuptakePO + ZLreleasePO + ZSreleasePO + BfreleasePO + X_PON[DONremin + DLremin +DRremin]	(E25)
Phosphate in sediment dPO/dt = X_PON[DLremin +DRremin + DONremin] – MbuptakePO - SGuptakePO	(E26)
Dissolved silica in water-column dSi/dt = DSisol - PLuptakeSi - MBuptakeSi	(E27)
Dissolved silica in sediment dSi/dt = DSisol - MBuptakeSi	(E28)
Particulate silica in water-column dDSi/dt = X_SiN[ZLgrazePL + ZLgrazeMB] - DSisol	(E29)
Particulate silica in sediment dDSi/dt = X_SiN[BFgrazePL + BFgrazeMB + PLmortality + MBmortality] - DSisol	(E30)

3.4 Processes

There are 30 equations defined in Table 3.2. (For many state variables, separate equations are prescribed for the water column and sediment.) The large number of individual source and sink terms fall into a relatively small number of categories. Growth of primary producers represents both an increase in biomass and a corresponding uptake of inorganic nutrient. Grazing by secondary producers represents both a loss term for primary producers and a growth term for the consumers. For both primary producers and grazers, a specific mortality term is prescribed. (Settling is also an effective removal term for several water-column components, but it is handled by the physical transport model.) Labile detritus is produced as a result of messy feeding, faecal pellet production and/or mortality, and is subsequently remineralised, or

transformed to refractory detritus or DON. Inorganic nutrients are produced either through remineralization of detritus or direct excretion by grazers. In the sediment, ammonia can be nitrified to produce nitrate, which can then be lost to nitrogen gas through denitrification.

The formulae or process submodels defining the source and sink terms are given below under these general categories. A discussion of the values to be assigned to the parameters involved in these process submodels is postponed to Chapter 4.

3.4.1 Primary Production

Model terms:

PLgrowth, PSgrowth, DFgrowth, MAgrowth, SGgrowth

Growth by primary producers is determined by multiplying a maximum specific growth rate by three factors: a nutrient limitation factor (hN), a light limitation factor (hI) and for benthic macrophytes a space limitation factor hS. So, for MA for example, we have:

MAgrowth = mum_MA . hN . hI . hS . MA (P 1)

Multiplicative models for nutrient and light co-limitation have been widely used (Fasham *et al*. 1990). A potential problem with multiplicative interactions involving several factors is that predictive growth rates become very low when each factor is moderately limiting. An alternative, Liebig's law of the minimum (ie. multiply mumax by the smallest factor) is more often applied to interactions among multiple nutrients (see below). More complex light-nutrient interaction models, involving changes in cell C:N and C:Chla in response to light and nutrient availability, could be implemented (eg. Tett *et al*. 1986, Radford 1993). However, we have chosen to use a simple model consistent with our decision to fix cell composition.

In the case of macroalgae and seagrasses, the model imposes a maximum biomass per unit area, and the growth rate is reduced as the biomass approaches the prescribed limit, reflecting competition for space or light.

Nutrient limitation of primary production

The model uses a Michalis-Menten (Monod) relationship between nutrient concentration and plant uptake (growth) rate. This approach is used widely for nutrient limited growth by phytoplankton in models (eg. Fasham *et al*. 1990, Radford 1993, Chapelle *et al*. 1994, Aksnes *et al*. 1995). More complex physiological models allow for variation in cell quota, and the decoupling of nutrient uptake and cell growth on short time scales (Droop 1968, Tett 1987). At the time scales resolved by the model (1 day and longer), the simpler Monod relationship is appropriate.

In the model, phytoplankton (PL, PS, and DF), suspended microphytobenthos and macroalgae are assumed to take up nutrients from the water column. Microphytobenthos and seagrass take up nutrients from the sediment pore water.

All plants take up ammonium, nitrate and phosphate. Diatoms and microphytobenthos take up silicate. Phosphate is assumed not to be limiting, and is not included as a potentially limiting nutrient in calculating plant growth rates. Ammonia and nitrate are potentially competing sources for inorganic nitrogen. The model does allow for ammonia inhibition of nitrate uptake, which can have important implications for ambient nitrate levels. There are a number of possible formulations of the ammonia - nitrate interaction (eg. Fasham *et al*. 1990, Radach and Lenhart 1995), some of which produce artifacts eg. higher growth at intermediate concentrations of both forms. The formulation used here is taken from Parker (1993) and avoids these problems. In this formulation, the total uptake depends only on the total concentration of dissolved inorganic nitrogen, DIN = NH + NO:

$$hN = DIN / (KN\_XX + DIN) \qquad (P2)$$

where KN_XX is the half-saturation constant for nitrogen-limited growth, and XX represents one of PL, PS, DF, MA, SG, MB. In the case of diatoms and microphytobenthos, we do need to consider the possible interaction of nitrogen and Si limitation. In this case, we do use Liebig's law of the minimum, so:

$$hN = \min[DIN/(KN\_XX+DIN), Si/(KS\_XX+Si)] \qquad (P 3)$$

where KS_XX is the half-saturation constant for Si-limited growth, and XX refers to one of PL and MB.

Photosynthesis

There are many different mathematical formulations of the relationship between plant growth and light intensity (see Platt *et al*. 1977). All agree that growth increases almost linearly with light level at low light intensities and saturates at higher light levels. Exposure to very high light levels can produce photoinhibition. Formulations ranging from a rectangular hyperbola to the hyperbolic tangent have been used to describe the relationship without photoinhibition. The data indicate that the transition from the linear to saturating parts of the curve occurs more abruptly than a rectangular hyperbola would predict, particularly when one is modelling growth rather than short-term photosynthesis. In practice, a simple bilinear model, first proposed by Blackman in 1905, is arguably as good as any, given the uncertainties and variabilities of parameters and environment (Lederman and Tett 1981). This formulation is not convenient for some purposes, but is useful for applied simulation models (eg. the MIKE 21 EU eutrophication model, Ecological modelling centre 1993). Given that hI is a relative growth factor scaled between 0 and 1, the bilinear model becomes

$$hI = \min[I/KI\_XX, 1] \qquad (P 4)$$

where KI_XX is the light saturation intensity for growth of primary producer XX.

In the model, we assume that phytoplankton are mixed rapidly throughout each layer, and respond to the mean daily light intensity in the layer. Benthic plants are assumed to respond to the mean daily light intensity at the sediment surface. There are a number of potentially complex issues relating to the interaction of time scales of light exposure and

the non-linear relationship between light and photosynthesis (eg. Prézelin and Matlick 1980), but these can be effectively subsumed into changes in KI.

Space Limitation

Available space for colonisation by macroalgae and seagrasses also limits growth, and this is represented as:

$$hS = (1-MA/MAmax) \quad \text{(P 5a)}$$

or $$hS = (1-SG/SGmax) \quad \text{(P 5b).}$$

Parameters MAmax and SGmax fix the maximum possible biomass per unit area, in the absence of any losses. For all other primary producers, space is not limiting and hS = 1.

3.4.2 Secondary Production

Model terms

ZLgrowth, ZSgrowth, BFgrowth

This section is concerned with grazing and its consequences: increase in grazer biomass, production of detritus and release of inorganic nutrients. There are three classes of grazers represented explicitly: small zooplankton, large zooplankton and benthic filter feeders. The generic processes involved are food capture and ingestion, assimilation and respiration.

Specific ingestion rates are prescribed as a function of food density (the functional response). Ingestion and growth are connected through growth efficiencies, which are usually prescribed as constants (Wilson *et al*. 1993). The losses occurring between ingestion and growth must then be partitioned between particulate detritus (ie. material not assimilated) and excretion of inorganic nutrients following respiration.

Food selection.

The model carries several potential food classes for grazers: small and large phytoplankton, small zooplankton, and detrital particles.

As discussed earlier, the small zooplankton class represents protozoans such as zooflagellates and ciliates. These are thought to ingest primarily small phytoplankton and bacteria (Lucas *et al*. 1987, Sherr and Sherr 1987). In the model, small zooplankton feed only on small phytoplankton.

The large zooplankton class represents primarily crustaceans such as copepods. In Port Phillip Bay about half the zooplankton are copepods (mostly *Paracalanus indicus*) and another 23% are Cladocera (Kimmerer and McKinnon 1985). At the micron scale of zooplankton feeding apparatus, Reynolds numbers are very low, and viscous effects dominate. Sieving of fine particles is only possible if water is trapped and sieved under pressure. Most copepods use feeding appendages to direct currents past the mouthparts and seize particles from the flow (Rubenstein and Koehl 1977). Some oceanic

euphausids and copepods (such as *Neocalanus*) living in regions dominated by small phytoplankton have an ability to capture prey down to a few microns diameter, but most species found in coastal waters (eg. *Calanus*) feed on larger phytoplankton (Fortier *et al*. 1994). Large copepods may feed as omnivores on small zooflagellates, but we have not included this effect in the model. The large zooplankton in the model feed only on large phytoplankton (PL, DF and suspended MB).

Gelatinous zooplankton such as salps pass water through fine filters under pressure (Morris and Diebel 1993), and can capture a large range of particle sizes. Indeed salps are capable of filtering particulate melanin particles of 200 nm diameter (Flood *et al*. 1992). Although larvacea are found widely through Port Phillip Bay, they are less abundant than are crustacean zooplankton (Kimmerer and McKinnon 1985). Since the role of gelatinous zooplankton in Port Phillip Bay is secondary, we have not included them as a separate functional component.

The benthic filter feeders in the model are assumed to be indiscriminate, taking small phytoplankton, large phytoplankton, small zooplankton and detritus particles according to their relative concentrations.

Functional response.

In a classical paper, Holling (1966) discussed the theoretical and empirical basis of the functional response relating ingestion per consumer (G) to food density (P). He identified three functional forms:

I) $G = \min (C.P, Gmax)$ (bilinear),

II) $G = C.P / (1 + C.P/Gmax)$ (rectangular hyperbola),

III) $G = C.P^2 / (1 + C.P^2/Gmax)$ (sigmoid or switching).

The parameter Gmax represents a maximum (food saturated) ingestion rate at high food densities, while C is a measure of grazing efficiency at low food densities. In Type I and II, the parameter C has units of volume cleared per grazer per unit time, and represents a maximum clearance rate.

A variant of Type III is the threshold functional response (Frost 1975):

IIIa) $G = C.(P-P_t)^+ / (1 + C.(P-P_t)^+/Gmax)$

In the case of zooplankton, there is empirical support for all of these functional forms. Although the differences among them may seem relatively subtle, they can have important effects on the stability and dynamical behaviour of phytoplankton - zooplankton interactions. These are discussed later.

In this model, we have used the rectangular hyperbola without thresholds, Type II, as the standard formulation. However, rather than specify the maximum ingestion rate Gmax, we have specified the maximum growth rate, "mum". This is related to Gmax through the growth efficiency E, so that mum = Gmax . E, or Gmax = mum / E.

The formulation for small zooplankton is simplest, as these feed on only one food type:

$$ZSgrazePS = ZS.PS.C\_ZS/(1 + PS.C\_ZS.E\_ZS/mum\_ZS) \quad (P\ 6)$$

Large zooplankton feed potentially on three food types, and these are assumed to be equally available and taken in proportion to their relative concentration:

$$ZLgrazePL = ZL.PL.C\_ZL/(1 + (PL + DF + MB).C\_ZL.E\_ZL/mum\_ZL) \quad (P\ 7)$$

$$ZLgrazeMB = ZL.MB.C\_ZL/(1 + (PL + DF + MB).C\_ZL.E\_ZL/mum\_ZL) \quad (P\ 8)$$

$$ZLgrazeDF = ZL.DF.C\_ZL/(1 + (PL + DF + MB).C\_ZL.E\_ZL/mum\_ZL) \quad (P\ 9)$$

Benthic filter feeders also feed on multiple food types, but are assigned different (lower) growth efficiencies on detritus (E_BFDL) than on living particles (E_BF):

$$BFgrazePS = BF.PS.C\_BF/(1 + C\_BF.(E\_BF.(PS+PL+DF+MB+ZS) + E\_BFDL.DL)/mum\_BF) \quad (P\ 10)$$

$$BFgrazePL = BF.PL.C\_BF/(1 + C\_BF.(E\_BF.(PS+PL+DF+MB+ZS) + E\_BFDL.DL)/mum\_BF) \quad (P\ 11)$$

$$BFgrazeMB = BF.MB.C\_BF/(1 + C\_BF.(E\_BF.(PS+PL+DF+MB+ZS) + E\_BFDL.DL)/mum\_BF) \quad (P\ 12)$$

$$BFgrazeDF = BF.DF.C\_BF/(1 + C\_BF.(E\_BF.(PS+PL+DF+MB+ZS) + E\_BFDL.DL)/mum\_BF) \quad (P\ 13)$$

$$BFgrazeZS = BF.ZS.C\_BF/(1 + C\_BF.(E\_BF.(PS+PL+DF+MB+ZS) + E\_BFDL.DL)/mum\_BF) \quad (P\ 14)$$

$$BFgrazeDL = BF.DL.C\_BF/(1 + C\_BF.(E\_BF.(PS+PL+DF+MB+ZS) + E\_BFDL.DL)/mum\_BF) \quad (P\ 15)$$

Increases in grazer biomass are obtained by multiplying ingestion by the relevant growth efficiencies:

$$ZSgrowth = E\_ZS.ZSgrazePS \quad (P16)$$

$$ZLgrowth = E\_ZL.(ZLgrazePL + ZLgrazeMB + ZLgrazeDF) \quad (P17)$$

$$BFgrowth = E\_BF.(BFgrazePS + BFgrazePL + BFgrazeMB + BFgrazeDF+BFgrazeSZ) + E\_BFDL.BFgrazeDL \quad (P18)$$

3.4.3 Mortality

Losses due to grazing are defined explicitly for small and large phytoplankton and suspended microphytobenthos. For zooplankton and the epibenthic animals and plants, losses due to predation and/or grazing are represented implicitly as part of "natural mortality". The simplest and most common formulation of mortality is to assume a constant specific mortality rate, so that the biomass removed per unit time increases linearly with biomass ("linear mortality"). One can interpret this as the effect of a constant density of predators with a linear functional response. An alternative formulation allows the specific mortality rate to increase linearly with biomass, so that the biomass loss per unit time is proportional to biomass squared ("quadratic mortality"). This formulation has been strongly advocated by Steele and Hendersen (1981). One can interpret this as the effect of a population of predators, which increases with prey density (ie. linear numerical response), combined with a linear functional response.

Other more complex formulations can be derived by combining the various functional responses discussed earlier with various assumptions about the numerical response of predators. Because the predators are not represented explicitly as a dynamical state variable, the lags or delays in the numerical response are not represented, and so any of these formulations must be treated as an empirical approximation. One would generally expect the numerical response of predators to be slower than that of prey, and in fact the quadratic mortality formulation has often been justified in terms of aggregation or switching behaviour by predators rather than an instantaneous numerical response; that is, as part of a sigmoid functional response.

Note that the zooplankton loss term in P-Z models is often assumed to include basal metabolic losses as well as losses due to mortality. However, metabolic rates often co-vary strongly with ingestion, and here we have assumed that losses due to metabolism are a fixed proportion of ingestion, and are accounted for in the assumed growth efficiencies.

These different formulations of mortality are important because they have different implications for the behaviour and stability of ecosystem interactions. In particular, a quadratic mortality rate, combined with a saturating functional response, automatically imposes an upper limit on grazer biomass. These implications are discussed in more detail in later chapters. Given that all formulations represent fairly crude approximations, the choice among them needs to be justified empirically (in terms of overall model performance). In this model, we have used a mixture of linear and quadratic mortality formulations. These selections are justified briefly below, and in more detail in later Chapters. We use "mL" to denote linear mortality coefficients, and "mQ" to denote quadratic mortality coefficients.

Phytoplankton which have sedimented out are subject to elevated mortality due either to an unfavourable environment or to removal by deposit feeders. This loss is modelled as linear mortality:

PLmortality = mL_PL.PL (P 19)

PSmortality = mL_PS.PS (P 20)

DFmortality = mL_DF.DF (P 21)

We assume that there is tight coupling between microphytobenthos and a community of grazers in the sediment. Some of these, such as the meiofauna, may have quite rapid numerical responses. We have therefore used a quadratic mortality formulation for microphytobenthos:

$$MBmortality = mQ\_MB.MB^2 \quad \text{(P 22)}$$

We have also imposed a quadratic mortality loss term on small and large zooplankton and benthic filter feeders. Given that predators on these components are likely to have slow numerical responses, these should arguably be interpreted as reflecting sigmoid functional responses on the part of predators.

$$ZLmortality = mL\_ZL.ZL + mQ\_ZL.ZL^2 \quad \text{(P 23)}$$

$$ZSmortality = mL\_ZS.ZS + mQ\_ZS.ZS^2 \quad \text{(P 24)}$$

$$BFmortality = mQ\_BF.BF^2 \quad \text{(P 25)}$$

For both macroalgae and seagrass, we have used a linear mortality term. Recall that a maximum biomass has already been set for these benthic macrophytes through the growth term. However, we have added additional loss terms for these components. Very high bottom stresses or sediment erosion rates lead to physical loss of macroalgae, and this is represented as an additional specific loss rate that increases with macroalgal biomass:

$$MAmortality = mL\_MA.MA + erosion\_rate.mS\_MA.MA \quad \text{(P 26)}$$

Seagrass take up nutrient from the sediment rather than the water column. However, when water column nutrient concentrations are high, they are susceptible to overgrowth by epiphytes (Madden and Kemp 1996). To account for this, we have added an additional specific loss rate for seagrass that is proportional to the concentration of dissolved inorganic nitrogen:

$$SGmortality = mL\_SG.SG + DIN.mS\_SG.SG \quad \text{(P 27)}$$

3.4.4 Detritus production and remineralization.

The fraction of food captured, which is not converted to new grazer biomass (ie. 1 - E), is either released as detritus (through messy feeding or as fecal pellets), or metabolised and the inorganic nitrogen excreted. The model assigns a fixed proportion (FDG_XX) of the total waste to detritus. It also assigns a fixed proportion (FDM_XX) of mortality losses to detritus production. It follows that:

$$ZSprodnDL = (1 - E\_ZS).FDG\_ZS.ZSgrazePS + FDM\_ZS.ZSmortality \quad \text{(P 28)}$$

$$ZLprodnDL = (1 - E\_ZL).FDG\_ZL.(ZLgrazePL + ZLgrazeMB + ZLgrazeDF) + FDM\_ZL .ZLmortality \quad \text{(P 29)}$$

$$BFprodnDL = (1 - E\_BF).FDG\_BF.(BFgrazePS + BFgrazePL + BfgrazeMB + BFgrazeDF) + (1 - E\_BFDL).FDL\_BF.BFgrazeDL$$

+ FDM_BF . BFmortality (P 30)

All of the direct mortality losses by primary producers are converted to labile detritus.

Labile organic detritus breaks down rapidly at a fixed rate r_DL. Most is assumed to be metabolised by bacteria and converted to ammonia. Of the remaining more refractory material, part (FDR_DL) is converted to refractory particulate detritus, and part (FDON_D) is released as refractory DON. The refractory detritus in turn is attacked by bacteria and breaks down at a slower rate r_DON. Most is converted to ammonium, with a small fraction (FDON_D) released as DON. DON breaks down at a fixed rate r_DON (Fig. 3.4). Thus:

DLremin = DL . r_DL (P 31)

DRremin = DR . r_DR (P 32)

DONremin = DON . r_DON (P 33)

DLprodnDR = DL . r_DL . FDR_DL (P 34)

DLsolDON = DL . r_DL . (1 - FDR_DL) . FDON_D (P 35)

DRsolDON = DR . r_DR . FDON_D (P 36)

The model maintains a separate pool of particulate biogenic silica DSi, as this is produced only by diatoms and microphytobenthos. All of the PL and MB mortality and grazing losses produce particulate biogenic silica according to the Si:N ratio, X_SiN. Biogenic silica dissolves with a fixed turnover time so that the rate of production of dissolved silicate is given by:

DSisol = RSi . DSi (P 37)

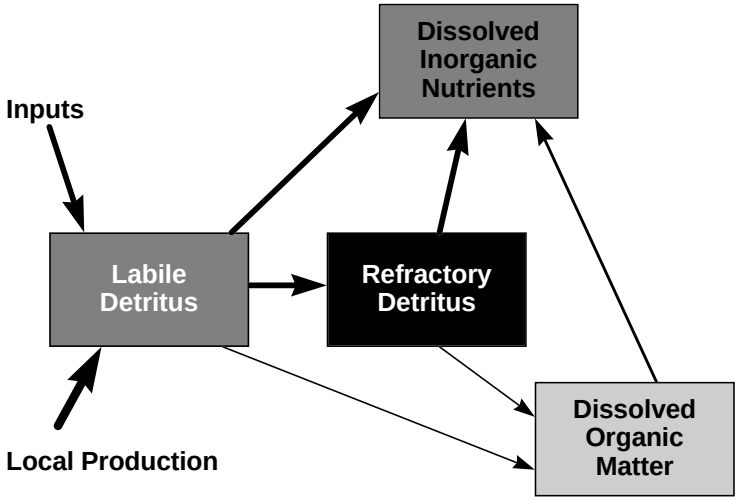

Figure 3.4 Model pathways for the decay of detrital matter

3.4.5 Inorganic Nutrient Uptake and Release.

Dissolved inorganic nutrients are taken up as a result of primary production, and released through remineralization of detritus and grazer excretion. Most of these terms have already been defined above.

Nutrient uptake by primary producers.

Increases in biomass through primary production are assumed to correspond to uptake of inorganic nutrients (nitrogen, phosphorus and, for diatoms, silica) at constant (Redfield) ratios. Given that nitrogen is the core currency, changes in biomass are measured in nitrogen units, and the model specifies the ratio of P to N, and Si to N, as X_PN and X_SiN respectively. Thus, for primary producer PL:

$$PLuptakePO = X\_PN.PLgrowth \quad (P\ 38)$$

$$PLuptakeSi = X\_SiN.PLgrowth \quad (P\ 39)$$

The uptake of DIN is partitioned between ammonia NH and nitrate NO according to Parker's (1993) model of ammonia inhibition of nitrate uptake. According to this model, total uptake is proportional to DIN/(KN + DIN), and ammonia uptake is proportional to NH/(KN + NH) (ie. ammonia is taken up in absolute preference). It follows that nitrate uptake is proportional to NO . KN / ((KN + DIN) . (KN + NH)). When these rates are expressed as fractions of total uptake, one obtains:

$$XXuptakeNH = XXgrowth.(NH/(KN\_XX+NH)).(KN\_XX+DIN)/DIN \quad (P\ 40)$$

$$XXuptakeNO = XXgrowth.(NO/DIN) \,.\, KN\_XX/(KN\_XX+NH) \quad (P\ 41)$$

where XX refers to one of PL, PS, DF, MB, MA, SG.

Nutrient Release from Grazers

Grazer losses through growth inefficiency and mortality which are not assigned to labile detritus are assigned to ammonia:

$$ZSreleaseNH = (1 - E\_ZS).(1 - FD\_ZS).ZSgrazePS + (1 - FDM\_ZS).ZSmortality \quad (P\ 42)$$

$$ZLreleaseNH = (1 - E\_ZL). (1 - FD\_ZL).(ZLgrazePL + ZLgrazeMB + ZLgrazeDF) + (1 - FDM\_ZL) .ZLmortality \quad (P\ 43)$$

$$BFreleaseNH = (1 - E\_BF).(1 - FDG\_BF).(BFgrazePS + BFgrazePL + BFgrazeMB + BFgrazeDF + BFgrazeZS) + (1 - E\_BFDL).(1- FDL\_BF).BfgrazeDL + (1 - FDM\_BF) \,.\, BFmortality \quad (P\ 44)$$

The remineralization of detritus (DLRemin and DRRemin) defined above produces ammonia and phosphate at Redfield ratios. In the sediment, ammonia in the pore water can be nitrified, producing nitrate, which in turn can be denitrified to produce nitrogen gas, which is biologically unavailable and lost to the system.

Process models of nitrification and denitrification are necessarily complicated. These models must resolve very sharp spatial gradients in dissolved oxygen, not only in the shallow oxic layer at the sediment surface, but also potentially around burrows. The time scales involved range from seconds for oxidation of sulphide to years for accumulation of refractory detritus. Process models have been proposed in the literature, and a version has been implemented for Port Phillip Bay (see Chapter 6), but these models are not appropriate for incorporation into an integrated system model. Instead, we have used a simple empirical model based both on qualitative results from process models, and on observations from the Port Phillip Bay field program.

The empirical model partitions ammonia released through remineralization among ammonia, nitrate and N_2 gas according to the sediment respiration rate or equivalently the remineralization (ammonia production) rate, which is a measure of oxygen stress in the sediment. The fraction of the ammonia produced, which is nitrified, decreases linearly from a maximum value (Dmax) at zero remineralization rate to zero at or above a remineralization rate R_0. Of the nitrate produced, the fraction denitrified increases from zero at zero sediment respiration to 100% at or above a remineralization rate R_D. Thus, as sediment remineralization rate increases from zero, denitrification efficiency (ie. the fraction of ammonia which is denitrified) increases to a maximum at R_D, and declines to zero at R_0.

$$\text{Remin} = \text{DLremin} + \text{DRremin} + \text{DONremin} \qquad \text{(P 45)}$$

$$\text{ReminNet} = (\text{Remin} - \text{MBgrowth})^{+} \qquad \text{(P 46)}$$

$$\text{Nitrific\_eff} = \text{Dmax} \,.\, (1 - \text{ReminNet} \,.\, \text{SLT} / \text{R\_0})^{+} \qquad \text{(P 47)}$$

$$\text{Denitrific\_eff} = \min (\text{ReminNet} \,.\, \text{SLT} / \text{R\_0}, 1) \qquad \text{(P 48)}$$

$$\text{Nitrification} = \text{ReminNet} \,.\, \text{Nitrific\_eff} \qquad \text{(P 49)}$$

$$\text{Denitrification} = \text{Nitrification} \,.\, \text{Denitrific\_eff} \qquad \text{(P 50)}$$

Note that R_0 and R_D have units of mg N m^{-2} d^{-1}, while remineralization rates are calculated as rates per m^3 of sediment, so ReminNet must be multiplied by the sediment layer thickness SLT in P46 and P47.

3.4.6 Light and Temperature.

Light attenuation is calculated in the biogeochemical module, as it depends on the concentrations of water column constituents. This module also allows for the effect of temperature on biogeochemical rate constants.

Light

Surface light (total daily average solar irradiance) is prescribed as part of the external forcing of the model. This surface irradiance is converted to subsurface PAR. Attenuation with depth within a layer between depths z1 and z2 is calculated as:

$$I(z) = I(z1).\exp(-k.(z-z1)) \qquad \text{(P 51)}$$

and the mean light intensity over the layer as:

$$\langle I \rangle = (I(z1) - I(z2)) / (k.(z2-z1)). \qquad \text{(P 52)}$$

The attenuation coefficient k is calculated as a sum of terms representing contributions from different constituents:

$$k = k_W + kDON \,.\, DON + kDL.(DL + DR) + kPN.(PL + PS + DF) \qquad \text{(P 53)}$$

Here, kw represents the background attenuation due to seawater and background DON, kDON the specific attenuation coefficient for modelled DON, kDL the specific attenuation coefficient for modelled detritus, and kPN the specific attenuation coefficient for phytoplankton (with biomass measured in nitrogen units).

Many models use only chlorophyll to modify attenuation (eg. Fasham *et al*. 1990). Kremer and Nixon (1978) use a non-linear function of chlorophyll, Chl,

$$k = k_w + k_{Chl1} \,.\, Chl + k_{Chl2} \,.\, Chl^{2/3} \qquad \text{(P 54)}$$

based on formulae derived for ocean waters. The non-linear dependence allows implicitly for co-variation of other constituents with chlorophyll, and possibly effects of cell size and packaging in bloom species. This formula is also used by Chapelle et al. (1994) with the modification that k_w depends on sea state. Raillard and Ménesguen (1994) represent the effects of inorganic seston on attenuation. We have not allowed for these effects explicitly, because the transport model is not yet calibrated for suspended inorganic particulates.

3.4.7 Temperature

Water temperature is either provided by the hydrodynamic model, or approximated by an empirical seasonal cycle, which is probably adequate for most purposes:

$$T = 15 + 5.\cos(2.\pi.[day-31]/365) \qquad \text{(P 55)}$$

Kremer and Nixon (1978) used a similar seasonal formulation for Narragansett Bay.

The rate parameters in the model are all specified for a temperature of 15 °C. A temperature correction is then applied at each time step by multiplying the base rate by

$$Tcorr = Q_{10}^{\,(T-15)/10} \qquad \text{(P 56)}$$

All rate parameters (those with units involving t^{-1}) are corrected in this way, using a fixed value of Q_{10}, except R_0 and R_D, the parameters controlling the shape of the denitrification curve. These last two parameters are really proxies for oxygen depletion. Among non-rate parameters, only light saturation intensities (KI_XX) are affected by temperature. This is consistent with the assumption that the maximum growth rate is temperature sensitive, but the initial slope, α, of the PvsI curve is not.

3.5 Physical Structure and the Transport Model

The underlying hydrodynamic and transport models are described in detail by Walker (1997a, b). The transport model divides the Bay into horizontal boxes, and each box can then be divided vertically into a number of water column and sediment layers or cells. In the standard version of the model, there is only one water column layer and one sediment layer in each box. There are 59 horizontal boxes in the standard version of the transport model, plus a boundary Bass Strait box (Fig 3.5). For purposes of analysis, we have grouped these boxes into 8 regions (see also Chapter 7). A version of the transport model using these 8 regions as coarse boxes has also been implemented (Walker 1997b).

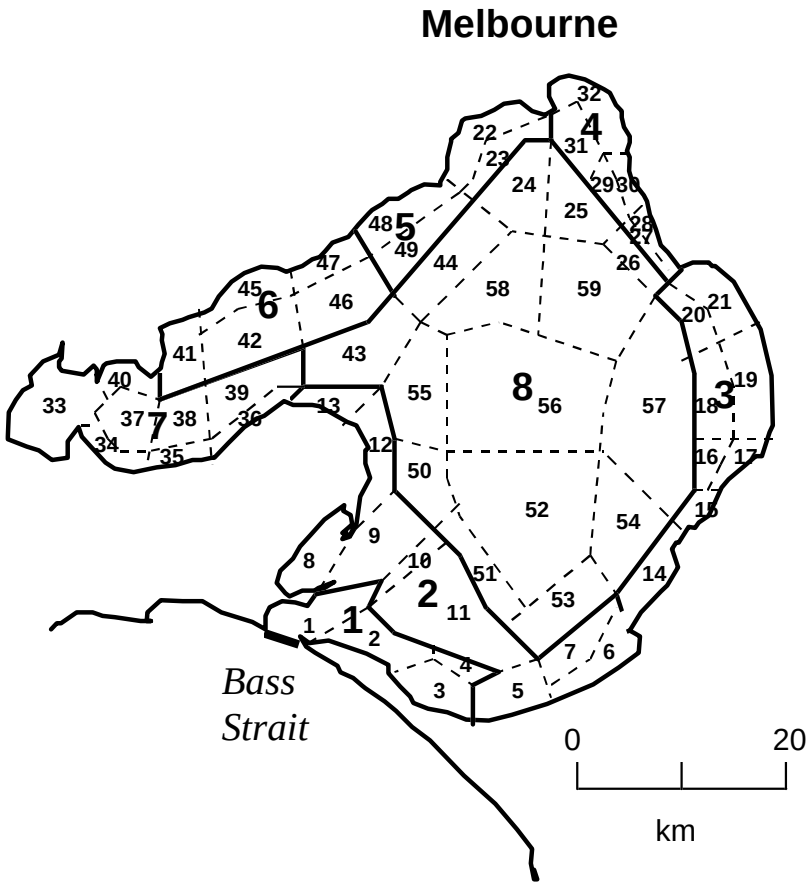

Figure 3.5 The horizontal spatial structure of the Port Phillip Bay model. The thin lines and small numbers define standard transport model boxes. The thick lines and large numbers represent the 8 regions or coarse boxes.

The concentrations of each state variable are defined in each water column or sediment cell, as appropriate, except for epibenthic variables which are specified as mass per square metre at the sediment-water interface in each box. At the beginning of each transport model time step, the concentration fields are passed to the biogeochemical model. Changes due to biogeochemical processes are integrated over the transport model time step, using a simple forward difference method. However, because the biogeochemical equations can become stiff, an adaptive time step is used. The relative change in any variable over a biogeochemical time step is not allowed to exceed a specified tolerance. Thus there may be many biogeochemical time steps for each physical time step.

After the local biogeochemical changes have been computed for each cell, the new tracer fields are returned to the transport model, and subjected to horizontal and vertical exchanges. The physical exchanges between water column cells due to advection and mixing are derived from the hydrodynamic model using a particle tracking technique described by Walker (1997a). The effects of bioirrigation and bioturbation in the sediment, and sinking and resuspension of particulate material, are also implemented in the transport model.

The particle-tracking technique allows the transport model to apply realistic exchanges among boxes over long time steps. (The standard physical time step used in the model is 1 day.) However, the long time step can cause problems in the treatment of sinking, resuspension and vertical mixing of particulates. This is less important in the standard model version, which has only one water column layer, but has created problems in trial implementations of models with multiple layers.

The separate integration of biogeochemistry and transport can also cause problems in treating interactions between "fast" biogeochemical reactions and large physical fluxes due to vertical mixing, sinking, and sediment-water column exchanges.

The physical transport model has the capability in principle to simulate concentrations of suspended inorganic sediment, taking into account external inputs, resuspension and sinking. However, this has not yet been calibrated (Walker 1997b). This has implications for the treatment of light attenuation in the biogeochemical model (see later), but these are not considered to be overly serious. Sinking rates of organic particles (detritus and phytoplankton) are specified in the transport model. These are dealt with in detail in this report, as they critically affect the nutrient cycle in the Bay.

There are some subtle bookkeeping issues involved in the sediment and epibenthic models. The dissolved constituents in pore water are expressed per unit volume of pore water, but concentrations of particulate fractions in the sediment are expressed as mass per unit volume. These measures are related by the sediment porosity ie. proportion of sediment volume occupied by pore water. Corrections for porosity must be made in calculating exchanges between dissolved and particulate constituents.

4 MODEL PARAMETER VALUES

In this chapter we discuss the values to be assigned to the integrated model parameters. We include settling velocities used by the P8B transport model because they are important controls on the behaviour of the integrated model. Comparison of model results and observations, and tuning of the model parameters, are dealt with in later chapters. The *a priori* information includes parameter values used by other models introduced in Chapter 2.

The PPBES included a number of experimental process studies which provide direct estimates of or constraints on parameters, which can be used to refine the literature values discussed in the first half of this chapter. These studies include the grazing experiments (Beattie *et al*. 1996), primary production study (Beardall *et al*. 1996), microphytobenthos study (Beardall and Light 1997), macroalgal study (Chidgey and Edmunds 1997), sediment study (Nicholson *et al*. 1996) and water-column data (Longmore *et al*. 1996). The last two reveal interesting information on the denitrification parameters and light attenuation respectively.

We note again that all model rate parameters are standardised to a temperature of 15 °C.

4.1 Primary Production

The parameters involved in primary production include maximum growth rates, light saturation intensities, nutrient half-saturation constants and maximum biomasses (of benthic macrophytes). Since phytoplankton are subdivided in different ways by different authors, the parameter values for the large and small phytoplankton classes defined in our model are discussed together.

4.1.1 Maximum growth rates

mum_PL; mum_PS; mum_DF

Maximum growth rates of phytoplankton depend on the type of phytoplankton, diatoms generally having larger growth rates than dinoflagellates (Aksnes *et al*. 1995) or flagellates (Radford 1993). Size of phytoplankton is not a reliable guide to maximum growth rates. Maximum growth rate can correlate inversely with cell size (Banse 1976, Langdon 1988), correlate weakly inversely (Banse 1982, Sommer 1989) or correlate directly (Prezelin *et al*. 1986). In systems such as Port Phillip Bay, where the large size fraction is dominated by diatoms, it may be reasonable to assign a higher growth rate to larger cells. Within diatoms or within flagellates, it is arguably reasonable to assign similar growth rates to small and large cells.

Taylor and Joint (1990) use 0.7 d^{-1} in a model of the Celtic Sea for large phytoplankton and 1.74 d^{-1} for small phytoplankton. In ERSEM (Radford 1993) the values are 2.5 and 2 d^{-1} for North Sea diatoms and flagellates respectively. Chapelle *et al*. (1994) use 0.45 d^{-1}, corresponding to 1.27 d^{-1} at 15 °C. Tett *et al*. (1986) reviewed growth rates from 5 studies to obtain maximum growth rates of nutrient saturated algae. They found a mean of 1.95 d^{-1} at 21.4 ^{o}C, a Q10 of 2 gives 1.25 d^{-1} at 15 ^{o}C, the mean temperature in Port

Phillip Bay. Aksnes *et al*. (1995) used maximum growth rates of 0.86 d^{-1} for flagellates and 1.3 d^{-1} for diatoms at 0 °C. Using their Q10 of 1.88, these correspond to 2.2 and 3.3 d^{-1} at 15 °C. These values are rather higher than those from other sources, but do refer to a diatom adapted to bloom in early spring in the northern North Sea and hence scaling growth up for the milder temperatures in Port Phillip Bay may not be appropriate. Fasham *et al*. (1990) use a value of 2.9 d^{-1} off Bermuda: at temperatures of 20-27 °C this corresponds to reasonable values (1.26-2.05 d^{-1}) at 15 ^{o}C. In a major review of phytoplankton growth rates, Eppley (1972) derived a formula $\log_{10} \mu = 0.0275T - 0.07$, as the upper envelope of observed growth rates μ. This gives a growth rate of 2.2 d^{-1} at 15 °C, and a Q10 of 1.88. A summary range of about 1-2.5 d^{-1} includes most maximum growth rate values presented here, when corrected to 15 °C. The higher values in this range apply to diatoms, the lower ones to flagellates.

In the PPBES, phytoplankton growth rates were estimated from nutrient enriched grazing dilution experiments conducted under ambient temperature and light intensities of 100 µE m^{-2} s^{-1} (about 20 W m^{-2}) on a 12 h light: 12 h dark cycle. This light intensity should be close to saturating.

Estimates of mum_PL from the nutrient saturated grazing-dilution experiments are about 2.5 d^{-1} in summer (Beattie *et. al*. 1996). Allowing for summer temperatures of 20 °C, and a Q10 of 2, this converts to about 1.77 at 15 °C. Similar estimates can be made for mum_PS, where the growth rate from grazing experiments is closer to 1.75 and so converts to 1.24 d^{-1} at 15 °C.

Short-term photosynthesis (^{14}C) experiments measured light saturated productivity (P^B_M: mg C (mg Chla)$^{-1}$ h^{-1}) (Beardall *et al*. 1996). These can be converted to an estimated daily growth rate if the L:D cycle and the C:Chla ratio are specified. Measurements for microphytoplankton yielded a Bay-wide mean value for P^B_M of 3.7 mg C (mg Chla)$^{-1}$ h^{-1}. If C:Chla = 50:1, then for a 12:12 L:D cycle this translates into 0.89 d^{-1}. Nanophytoplankton have a somewhat higher mean value for P^B_M of 4.9 mg C (mg Chla)$^{-1}$ h^{-1}, corresponding to 1.17 d^{-1}. Observed P^B_M values for picoplankton give a mean value of 5 mg C (mg Chla)$^{-1}$ h^{-1} or 1.2 d^{-1}. There is a clear seasonal signal in P^B_M with highest values in February. However these growth rates are nutrient limited. The largest phytoplankton have a much smaller growth by this estimate than was the case from the enriched grazing experiment, while the values for the picophytoplankton are quite similar. This is consistent with the respective half saturation values derived from the grazing dilution experiments (see below).

mum_MB

Typical maximum microphytobenthos productivity under light saturation was estimated from the literature at 1.5 mgC (mg Chla)$^{-1}$ h^{-1} (Beardall and Light 1994). For a C:Chla ratio of 50, and allowing for a 12:12 L:D cycle, this gives a maximum specific growth rate of 0.35 d^{-1}.

MPB photosynthetic rates in Port Phillip Bay were measured by Beardall and Light (1997). Observations of oxygen evolution in sediment chambers in the deepest parts of the Bay suggest MPB can adapt to very low light levels (Nicholson *et al*. 1996). Unfortunately, MPB photosynthesis experiments were only conducted to 10 m depth. Measurements of MPB productivity under light saturation yielded values of P^B_M of 7 mg

O_2 (mg Chla)$^{-1}$ h^{-1} at 1 m and 5 mg O_2 (mg Chla)$^{-1}$ h^{-1} at 10 m. For a C:Chla ratio of 50 and a 12:12 L:D cycle, this is equivalent to growth rates of 0.6 and 0.45 d^{-1}, somewhat higher than the literature estimate of about 0.35 d^{-1} discussed earlier. The standard deviation of field observations in Port Phillip Bay was about 0.37 d^{-1}. This gives a range of maximum growth rates of 0.1-0.75 d^{-1}, lower values being associated with lower saturation light intensities.

mum_MA

Growth rates for macroalgae are in the range 0.019 - 0.3 d^{-1} according to Nielsen and Sand-Jensen (1990). A maximum value of 0.2-0.3 d^{-1} is typical for *Ulva*, or for *Enteromorpha* (common off Werribee). Solidaro *et al*. (1995) used a value of 0.45 d^{-1} for the maximum growth rate of *Ulva* in the Lagoon of Venice. Productivity of *Caulerpa*, which is common in Port Phillip Bay, is about 5 mg C (g dry wt)$^{-1}$ h^{-1} and, given a C content for macroalgae of about 20-50% of dry weight (Campbell 1995), its growth rate is about 0.12-0.3 d^{-1}. Because macroalgae include a wide range of species from different habitats, this parameter is inherently uncertain. However the bulk of biomass in Port Phillip Bay occurs in the form of drift algae, not slow growing kelps or very rapidly growing eutrophic species such as *Ulva* and *Enteromorpha*. The middle part of the growth range 0.05-0.2 d^{-1} is likely to be appropriate, although this may underestimate productivity by *Ulva* and *Enteromorpha* close to nutrient inputs.

Unfortunately, macroalgal growth rates in Port Phillip Bay were not directly measured in PPBES. The observed seasonal changes in biomass (Chidgey and Edmunds 1997) suggest high growth rates may occur. For example, between December 94/January 95 and March 95, macroalgal biomass increased by an order of magnitude off Wedge Point and 2 orders of magnitude at 8 m. This would suggest as much as 5% growth per day, but as the biomass is predominantly drift algae, part of the increase may be due to advection and physical accumulation.

mum_SG

A review of specific growth rates of seagrass found these to mostly range from about 0.01 to 0.05 d^{-1}, but reported values as high as 0.11 d^{-1} (Hillman *et al*. 1989). According to Zimmerman *et al*. (1994), *Zostera* productivity at light saturation ranged from 0.41to1.22 μmol C (g fresh wt.)$^{-1}$ min^{-1}. Assuming 10% of fresh wet is C and a 12 h day, this gives a specific growth rate range of 0.035 to 0.1 d^{-1}. Short *et al*. (1995), investigating the effect of eutrophication on *Zostera marina*, found growth rates of 0.04-0.05 d^{-1} under optimal conditions. These values are in the upper part of the range of Hillman *et al*. (1989) and, since Port Phillip Bay seagrass is dominated by *Heterozostera tasmanica*, values from the range 0.035-0.1 d^{-1} may be appropriate.

4.1.2 Light saturation intensity

KI_PL; KI_PS; KI_DF

Light saturation intensity varies widely with phytoplankton type and size and with season and depth. Generally phytoplankton adapt to the light regime so that this parameter has a value related to the ambient light intensity (Talling 1955). The process of light adaptation has been modelled by Geider *et al*. (1996). Typical literature values are given in Table 4.1.

Table 4.1. Literature values of KI (PAR, W m^{-2})

Source and location	Phytoplankton category or season		
Prezelin *et al.* 1986	0.6-1 μm	1-5 μm	>5 μm
warm core 2m	26	26	95
coastal 2m	8	25	40
warm core chl max	5	25	40
front chl max	2		10
Furnas & Mitchel 1988	<2 μm	>2 μm	
Coral Sea 10 m	80	100	
Coral Sea 100 m	25	20	
Platt *et al.* 1983	<1 μm	>1 μm	
Atlantic 36 N 65-89 m	20	20	
Kirk 1983	February	July	October
Danish coastal	85	233	160
Rhyther 1956	Diatoms	Dinoflagellates	Chlorophytes
	43	99	17

Light saturation intensities for phytoplankton photosynthesis in Port Phillip Bay can be directly estimated from the results of Beardall *et al*. (1996). These studies do not indicate much difference among size fractions. The mean microphytoplankton saturation irradiance (PAR), calculated from alpha and P^B_M, is 96.7 μmole m^{-2} s^{-1} (sd 45). For nanophytoplankton and picophytoplankton, the observed values are 109.2 (sd 42) and 98.9 μmole m^{-2} s^{-1} respectively. These correspond approximately to 20 W m^{-2}, with a range of 10-30 W m^{-2}. There is little seasonal variation for microplankton and although there does appear to be a maximum for nanoplankton in summer 94-95 there is little evidence of a maximum in the summer of 93-94. Picophytoplankton do show consistent seasonal patterns in light saturation intensity with a seasonal range of about 80-120 μmole m^{-2} s^{-1}(maximum in January and minimum in June). Beattie *et al*. (1997) used 100 μmole m^{-2} s^{-1} for their incubation experiments.

KI_MB

An initial literature review of saturation levels produced an average value of about 250 μmoles m^{-2} s^{-1} (Beardall and Light 1994) or about 50 W m^{-2}, and a critical or compensation light intensity of about 38.9 μmole m^{-2} s^{-1} or 8 W m^{-2}. The latter value is inconsistent with sediment chamber observations of MPB photosynthesis in central Port Phillip Bay at about the 1% light level. Saturation intensity for a sediment algae community in Nivå Bay was 3.4 W m^{-2} (Round 1981) which indicates values could be substantially lower than the average. The minimum saturation level reported in the review of Beardall and Light (1994) was 48 μmole m^{-2} s^{-1} (9.6 W m^{-2}).

While MPB can grow in the Bay centre, they are absent or inactive there at times, and also have low biomass in deep water off Werribee. This suggests that light limitation plays a significant role. In Port Phillip Bay, measured saturation intensities were 12-400 μmole m^{-2} s^{-1} or 2.5-80 W m^{-2} (Beardall and Light 1997). Analysis of the observations from Port Phillip Bay shows a mean light saturation irradiance of 23 and 12 W m^{-2} at 1 m and 10 m respectively, with a standard deviation of 12 and 7.7 W m^{-2}. Unfortunately, the photosynthesis-irradiance experiments were conducted only with samples from depths of 10 m and shallower. It seems likely that the lowest values are applicable in the deeper parts of the Bay.

KI_MA

Growth of macroalgae is saturated at 20 - 40 W m^{-2} according to Mann (1982). Lüning (1981) separated macroalgae into eulittoral, sublittoral and deep forms with saturation intensities of 80-120, 30-44 and 12-14 W m^{-2} respectively. Given that a single variable represents all macroalgae in our model, the saturation intensity must be low to enable growth of low light adapted algae. Like microphytobenthos, macroalgae are found at considerable depth in Port Phillip Bay and biomass peaks at 8 m (Chidgey and Edmunds 1997). They must be able to adapt to low light. A range of about 5-20 W m^{-2} is appropriate for these deep growing algae.

KI_SG

Hillman *et al*. (1989) reviewed a range of values for light saturation of seagrass growth of 20-40 W m^{-2}. Zimmerman *et al*. (1994) fitted a range of light saturation values for Californian *Zostera*. Depending on which of two models was used this ranged from 77-317 or 58-238 μmol m^2 s^{-1} (15-65 or 12-50 W m^{-2}) PAR. Since most seagrass growth is restricted to coastal regions less than 5 m deep in Port Phillip Bay, a high value is appropriate and so the range 30-60 W m^{-2} is used.

4.1.3 Nutrient half-saturation constant for growth.

KN_PL; KN_PS; KN_DF

In some models phytoplankton growth and nutrient uptake may be decoupled (Droop 1983), in which case the uptake half-saturation constant can far exceed the growth limited half-saturation constant (with a corresponding maximum uptake rate far higher than the maximum growth rate). However in our model, uptake and growth are not decoupled and so we use the much lower nutrient half-saturation constant for growth. Observed values of this parameter range from 0.01-4.21 μg at L^{-1} (0.14-50 mg N m^{-3}: Goldman and Glibert 1983). Values vary with the type and size of plankton cells and the environment they come from. Most coastal phytoplankton are in the range 0.84-8.8 mg N m^{-3} (same reference). A review by Hein *et al*. (1995) derived a similar interquartile range, approximately 2-10 mg N m^{-3} for ammonia, and 2-6 mg N m^{-3} for nitrate. Even such factors as cell motion through the water increase uptake since they increase diffusion to the cell surface (Munk and Riley 1952). Fasham *et al*. (1990) use 0.5 μg at L^{-1} (7 mg N m^{-3}) for oceanic species. Tett *et al*. (1986) used 0.3 μg at L^{-1} (4.2 mg N m^{-3}).

Large phytoplankton tend to have higher half saturation values than do small ones (Eppley *et al*. 1969). In the Celtic Sea ecosystem model of Taylor and Joint (1990), two model options are investigated. In the first, KN for small phytoplankton is equal to that for large cells, while in the second, the ratio is 0.3. The standard value for large phytoplankton in that model is 0.1 μg at L^{-1} or 1.4 mg N m^{-3}. In the North Sea model (Radford 1993) the values are 1.4 mg N m^{-3} for diatoms and 0.7 mg N m^{-3} for flagellates. These very low values are more appropriate for ocean systems. Kremer and Nixon (1978) used 21 and 14 mg N m^{-3} for a coastal system. Aksnes *et al*. (1995) use a formula for KN which varies with temperature, but their values of KN for diatoms and flagellates are always in the ratio 4:3.

Other values from a review by Raymont (1980) are listed in Table 4.2. The literature generally supports values for KN in the range 1-20 mg N m^{-3}, with higher values in coastal waters. Observation and theory generally supports larger half-saturation constants for larger cells.

Table 4.2 Half saturation constants for DIN based growth (from Raymont 1980)

	Nitrate		Ammonium	
Location	**µg at L^{-1}**	**mg N m^{-3}**	**µg at L^{-1}**	**mg N m^{-3}**
Oligotrophic				
Tropic Pacific	.07	0.98	.42	5.88
N Pacific Gyre			.15	2.1
Mediterranean	0.1-0.3	1.4-4.2	<0.1	<1.4
Eutrophic				
Tropic Pacific	0.98	13.72	1.3	18.2
SubArctic Pacific	4.2	58.8	1.3	18.2
Peru Coast			1.1	15.4
Culture				
Oceanic Sp.	0.1-0.7	1.4-9.8	0.1-0.5	1.4-7
Diatoms	.4-5.1	5.6-71.4	.5-9.3	7-130
Flagellates	0.1-10	1.4-140	0.2-2.4	2.8-33.6

We are able to refine estimates of half-saturation concentrations using data obtained directly from Port Phillip Bay. In the grazing dilution experiments (Beattie et al. 1996), enrichment of samples by 1.5-2 µmoles DIN caused substantial increases in growth rates. For picophytoplankton, unenriched growth rates in spring and summer were typically 0.5 d^{-1} except at Wooleys Reef where they were closer to 1. Enriched growth rates were about 1.5 d^{-1} at all locations. Given an initial concentration of about 0.3-0.5 µmoles DIN, these figures imply half saturation constants of about 0.2-0.75 µmoles DIN (4-9 mg N m^{-3}). The lowest figures apply at Wooleys Reef. There is no significant difference between N concentrations at Sandringham and Wooleys Reef (averaging 0.4 µmoles DIN), in spite of the difference in response.

Patterns for the effect of enrichment on larger phytoplankton are more difficult to determine. Again populations at Wooleys Reef are less affected by enrichment, growth rates doubling in autumn and winter, but hardly changing at other times. Interpretation of results at other sites is complicated by some apparent negative growth rates, which imply growth is underestimated. However when growth is positive, the effect of enrichment is to greatly increase growth rates, except off Werribee in August when there is no effect. This absence of effect off Werribee also applied to picoplankton in August, and so probably reflects the high ambient ammonia concentrations there. As a general statement it seems safe to say saturation of growth for large phytoplankton requires higher DIN concentrations than for small phytoplankton. Therefore half saturation constants are well above the background 0.3-0.5 µmoles N L^{-1} but below the enriched 1.8-3 µmoles N L^{-1}. A range of 0.5-1.8 µmoles L^{-1} or 6-20 mg N m^{-3} DIN seems appropriate.

Given the constraints available it seems that half saturation constants should be contained within a range of 4-9 and 6-20 mg N m^{-3} for PS and PL respectively.

KN_MB

We do not have independently determined values for microphytobenthos half-saturation values. However, these are probably from the upper range of diatom values that are of order 20 to 100 mg N m^{-3} (Table 4.2). Because a one-layer sediment model is used, MPB experience artificially high DIN pore water concentrations, and KN_MB is scaled accordingly. Throughout most of Port Phillip Bay, MPB are not generally nutrient limited and thus they are not sensitive to the value of this parameter.

KN_MA

In a review of nutrient uptake by both micro- and macro- algae, Hein *et al*. (1995) found interquartile ranges for the uptake half-saturation constant for macroalgae of about 50-200 mg N m^{-3} for ammonia and 50-100 mg N m^{-3} for nitrate. Maximum uptake rates are mostly in the range 0.1-1 d^{-1}, based on values per g dry weight and an N content of 0.4-4% dry weight from Hein *et al*. (1995). This is roughly three times the maximum growth rate, and it follows that half-saturation constants for growth should be about three times lower than half-saturation constants for uptake, or about 15 to 30 mg N m^{-3}. This is still significantly larger than KN for phytoplankton growth. The ability of macroalgae to store nutrients allows them to take advantage of episodic nutrient supply. Their effective half-saturation constant may appear to be lower if the model does not resolve nutrient patchiness.

KN_SG

Like microphytobenthos, seagrasses take up nutrients from the sediment pore water. It is difficult to relate uptake to pore water concentrations, which are, in any case, artificially high in the model (see above). Seagrasses are nutrient limited in much of southern Port Phillip Bay where most beds are located (Bulthuis *et al*. 1992). This parameter was fitted to match observed seagrass distributions.

KS_PL

Half saturation constants for silicate from a variety of studies are listed by Raymont (1980) at 0.2-3.4 mmole m^{-3} or about 8-80 mg Si m^{-3}. The model of Aksnes *et al*. (1995) includes N, P and Si limitation. It uses a slightly modified Michalis-Menten formulation. The equivalent ratios of the half saturation constants by weight are 0.144 for KP:KN (ie. Redfield ratio) and 1.36 for KSi:KN. Kremer and Nixon (1978) use 14 and 1.4 mg Si m^{-3} for winter and summer populations. The ERSEM model uses 8.4 mg Si m^{-3} for diatoms. Excluding the very lowest and highest values we would expect KS_PL to be in the range 8-40 mg Si m^{-3}.

KS_MB

Microphytobenthos experience high pore water concentrations of silicate which are unlikely to limit growth. Since MPB are not Si limited, we use a low value equal to that for planktonic diatoms. This should not affect model predictions.

4.1.4 Maximum macrophyte biomass

Limited area and availability of suitable habitat impose an upper limit on macrophytobenthos biomass.

MAmax

The maximum biomass of kelps on reefs can be several kg wet wt m^{-2}. However relatively little of Port Phillip Bay's bed consists of rocky substrate, so the overall biomass of rocky reef macrophytes is very limited. Biomasses of *Caulerpa* off Werribee rose to 399 g dry wt m^{-2} and very large blooms of drifting *Cladophora* also occur (Brown 1980). Based on data obtained during PPBES by Chidgey and Edmunds (1997), the *Caulerpa* biomass is equivalent to ca 10000 mg N m^{-2}. Light and Woelkerling (1992) observed wet weight biomasses of up to 3 kg m^{-2} at Wedge Point, near the WTP outfalls. Chidgey and Edmunds (1997) observed biomasses of up to 4.6 kg m^{-2}. They estimated the maximum N biomass to be nearly 20000 mg N m^{-2}, although the next highest was only 11000 mg N m^{-2} at Altona Bay.

SGmax

Maximum standing crop in seagrass beds, worldwide, averaged 315 and ranged from 50-854 g dry wt m^{-2} (Duarte 1989), but in Port Phillip Bay the maximum reported biomass is about 220±58 g dry wt m^{-2} (Bulthuis *et al*. 1992). Of this 1.5-2.5% is N (Klumpp *et al*. 1989). This gives a range of 2000-5000 mg N m^{-2} for the densest seagrass beds in Port Phillip Bay.

4.2 Secondary Production

In this subsection we are concerned with the parameters that control production of grazers, both zooplankton (ZL and ZS) and benthic filter-feeders (BF). The relevant parameters are maximum clearance rates, maximum growth rates and ingestion efficiencies.

4.2.1 Maximum clearance rates

C_ZL

Given the explicit assumption in our model that the large zooplankton fraction feeds exclusively on larger phytoplankton, we have used data from crustacean grazing studies. Average copepod filtration rates reported by Marshall (1973) were 1500 ml $(mg\ dry\ wt)^{-1}\ d^{-1}$. At typical N:dry wt ratios of 7 to 12% (Ikeda 1974), this corresponds to 0.015 $m^3\ (mg\ N)^{-1}\ d^{-1}$. However the range is 2 orders of magnitude: 0.0002-0.050 $m^3\ (mg\ N)^{-1}\ d^{-1}$. The geometric mean is 0.005 $m^3\ (mg\ N)^{-1}\ d^{-1}$. In a review prepared for PPBES, Holloway & Jenkins (1993) list 29 values from the literature. Excluding the smallest and largest two values, these range from 0.00198-0.23 $m^3\ mgN^{-1}\ d^{-1}$. The interquartile range is 0.0033-0.06. Given the wide range of values, the arithmetic mean is not very useful, since it is dominated by a few large values. The geometric mean is 0.0229 $m^3\ mgN^{-1}\ d^{-1}$. In ERSEM the value used is 0.006 $m^3\ (mg\ N)^{-1}\ d^{-1}$ (Radford 1993).

For copepods the actual filtration rate varies with food availability (Frost 1975). We are interested in maximum filtration rates. The geometric mean of maximum filtration rates quoted in Holloway and Jenkins (1993) is 0.05 m^3 $(mg\ N)^{-1}$ d^{-1}. The comparable figure for Marshall (1973) is 0.02 m^3 $(mg\ N)^{-1}$ d^{-1}. From Marshall (1973), we can obtain a relationship between maximum filtration rate and copepod length (Fig. 4.1):

$$ml\ copepod^{-1}\ d^{-1} = 24L^{1.8}$$

Filtration rate per unit mass should then fall by the 1.2 power of length. As copepods in Port Phillip Bay tend to be dominated by smaller species, filtration rates are likely to be higher than mean literature values.

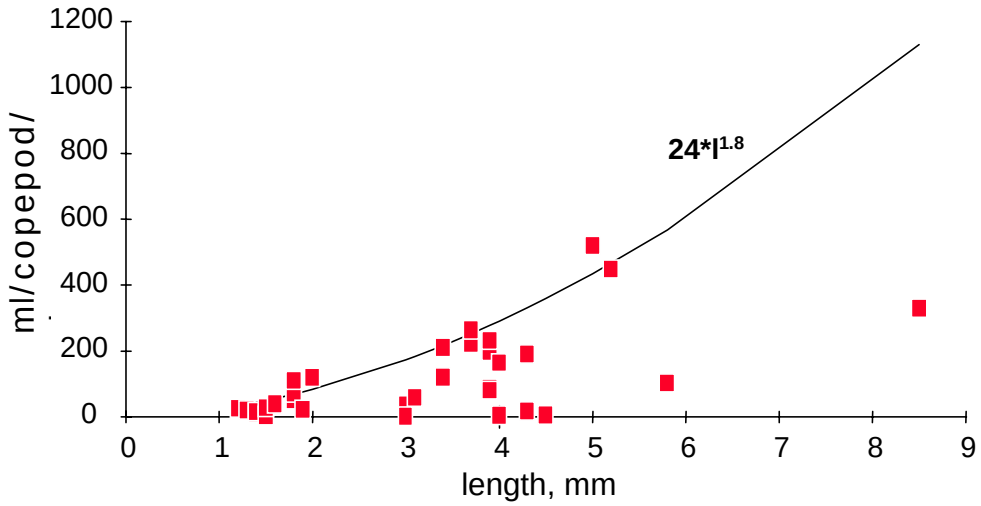

Figure 4.1 Dependence of copepod filtration rates on body size (data from Marshall 1973).

Filtration rate also depends on food particle size. Frost (1972) derived a relationship:

$$\text{Filtration rate} = 2.61 \log(V) - 4.84\ \mu l\ copepod^{-1}\ h^{-1}$$

for *Calanus pacificus*, where V is prey volume in μm^3. Filtration rate on 20 µm cells would be 30% less than on 100 µm cells. Thus filtration may vary significantly depending on the size of prey, even within coarse phytoplankton size fractions.

Due to the dominance of small crustacea in Port Phillip Bay (Kimmerer and McKinnon 1985), we have chosen a range of 0.02-0.08 m^3 $(mg\ N)^{-1}$ d^{-1} for the maximum clearance rate of large zooplankton.

C_ZS

The filtration rates of microzooplankton were surveyed by Sherr and Sherr (1987). Filtration rates ranged from 2000-500,000 body volumes per hour. However, they contended that the lower part of the range consisted of old measurements and that more recent measurments ranged from 30,000-500,000. Given 7% of wet wt as body carbon (Moloney and Field 1989) and Redfield C:N, these translate into 2 - 35 L $(mg\ N)^{-1}$ h^{-1},

or 0.05 - 0.8 m^3 (mg N)$^{-1}$ d^{-1}. Lucas *et al*. (1987) listed flagellate clearance rates of 7-2030 µL h^{-1} animal^{-1} which, if the grazers are assumed spherical and have the same C and N contents as previously assumed for ciliates, is equivalent to 0.004 - 4 m^3 (mg N)$^{-1}$ d^{-1}. Ciliates (Lucas *et al*. 1987) had grazing rates of 100-7000 µL h^{-1} animal^{-1} or 0.00168-0.13 m^3 (mg N)$^{-1}$ d^{-1} which is comparable to Sherr and Sherr's (1987) full range. Assuming ciliates are typical grazers on the PS fraction, a range of 0.05-0.6 m^3 (mg N)$^{-1}$ d^{-1} would appear appropriate but, if flagellates are very important, clearance rates could be higher.

C_BF

Typical filtration rates by benthic filter feeders are about 50-100 L (g dry wt.)$^{-1}$ d^{-1} (Wilson *et al* .1993) or 0.0005-0.001 m^3 (mg N)$^{-1}$ d^{-1}. The mean of the filtration rates listed in Wilson *et al*. (1993) is 0.00063 m^3 (mg N)$^{-1}$ d^{-1} with a SD of 0.00078; if one large value is removed these become 0.00055 and 0.00053 m^3 (mg N)$^{-1}$ d^{-1}. According to Wilson *et al*. (1993), the mean filtration rate for molluscs is 0.00047 m^3 (mg N)$^{-1}$ d^{-1} with SD of 0.000345, and the geometric mean is 0.00030 m^3 (mg N)$^{-1}$ d^{-1}. They calculated that molluscs account for 47% of filtration in Port Phillip Bay. They did not give specific filtration rates for benthic crustaceans, although these were estimated to account for 25% of total filtration in Port Phillip Bay. The only one of the top ten benthic species by biomass in Port Phillip Bay that has a listed filtration rate in Wilson *et al*. (1993) is *Mytilus edulis,* whose filtration rate is 0.001-0.00185 m^3 mgN^{-1} d^{-1}. Filtration by oysters has a maximum value of 48 L g^{-1} dry wt. d^{-1} (Raillard and Ménesguen 1994); this is roughly 0.0005 m^3 (mg N)$^{-1}$$d^{-1}$. Oysters' filtration rates decrease if seston levels exceed 200 mg L^{-1}. Such high levels are not common in Port Phillip Bay but may occur in Hobsons Bay. Gerritsen *et al*. (1994) calculated the total clearance rate by benthic filter feeders for Cheasapeake Bay using the formula:

$$C = 0.120\ W0.75$$

where C is m^3 ind^{-1} d^{-1} and W is the individual dry weight (g). For a 1 g animal this gives 0.0012 m^3 (mg N)$^{-1}$ d^{-1}, a 100 g animal would give 0.0004 m^3 (mg N)$^{-1}$ d^{-1}.

Clapham (1996) has measured filtration rates of the fan-worm *Sabella spallenzanii* at 1.4 L (g dry wt)$^{-1}$ h^{-1} at 13 °C and 4 L g dry wt^{-1} h^{-1} at 20 °C, or 0.00034 and 0.00096 m^3 (mg N)$^{-1}$ d^{-1} respectively. These rates are consistent with data for other species cited above.

4.2.2 Maximum growth rates

mum_ZL

The maximum specific ingestion rate for copepods varies from 4-60% d^{-1} according to Raymont (1983). However some zooplankton grow faster than this, and Raymont (1983) lists growth rates of 15-60% d^{-1}, depending on development stage and food type, for a second set of copepods. Holloway & Jenkins (1993) provided ranges of specific ingestion rates for eight Port Phillip Bay zooplankters and maximum values of these ranges varied from 0.04-3.6 d^{-1} with a mean of 1.4 and a geometric mean of 0.95 d^{-1}. For a gross growth efficiency of 0.5, this means that maximum growth rate should range from 0.02-1.8 d^{-1}. Removal of one particularly high set of estimates leave a range of 0.2-

1 d^{-1} with mean 0.6 d^{-1} and geometric mean 0.4 d^{-1}. Observed production/biomass ratios provide a lower bound for maximum growth rates. Conover (1979) reviewed P/B ratios from a variety of species in different environments; the range is about 1-78% d^{-1}. We can ignore the lower part of this range as food limited, and the higher ratios are summer-time values from either a subtropical Bay or shallow rivers, which are about 10 ^oC warmer than Port Phillip Bay. Conversion with our Q10 of 2 gives a maximum growth rate of up to 0.38 d^{-1}.

Kiørboe and Sabatini (1995) reviewed metabolic processes in copepods and found an average growth rate of 0.289 d^{-1}, which was independent of body size but varied with development state and the species' reproductive method. Fasham *et al*. (1990) use a maximum specific ingestion rate of 1 d^{-1} with an assimilation efficiency of 75%, which gives (after deduction of mortality (0.05) and excretion (0.1)) a maximum growth rate of 0.6 d^{-1}. Chapelle *et al*. (1994) use 0.3 d^{-1} for maximum specific ingestion rate at 0 °C or, given a Q10 of 2, 0.84 at 15 °C. However only 60% of this is assimilated and there is basal metabolism of 0.06 d^{-1} (at 15 ^oC), so the maximum growth is 0.44 d^{-1}.

The dominant copepod species in Port Phillip Bay is *Paracalanus indicus*. Specific ingestion rates for *Paracalanus* of 0.2-2 d-1, averaging 1.5 d^{-1}, were derived from the review of Holloway and Jenkins (1993). This would indicate that maximum growth rates could be as high as 0.75, or even 1 d^{-1}. However in nearby Western Port the dominant *Acartia tranteri* had a maximum growth rate of 0.2 d^{-1} (Kimmerer and McKinnon 1987). We have a range of maximum growth rates of 0.1-1 d^{-1}. Excluding data from Holloway and Jenkins (1993), and the lower values from Conover (1979), most estimates are in the range 0.2-0.4 d^{-1}.

mum_ZS

Zooflagellates have a minimum doubling time of 2.5-3 hours, at 20 ^oC (Fenchel 1987), which corresponds to a specific growth rate of around 5.5 d^{-1}, or 4 d^{-1} at 15 ^oC. Ciliates have minimum doubling times of about 10 h (ie. maximum specific growth rates of 1.7 d^{-1}) (Fenchel 1987). Verity (1985) reports maximum growth rates for tintinnids of about 2 d^{-1}. The formula $\ln \mu = 0.1438\ T - 0.3285 \ln (V \times 10^{-3}) - 1.3815$ was developed for ciliate maximum growth rates by Montagnes *et al*. (1988), where μ is growth rate, T is temperature, and V is volume in μm^3. In Southampton water, ciliates range in volume from 10^3 - 10^6 μm^3 (Leakey *et al*. 1992), but dominant forms were always less than 10^5 μm^3. According to the formula of Montagnes *et al*. (1988), at 15 ^oC, μ for the dominant small forms ranges from 0.5 - 2.17 d^{-1}. A range of 0.5-4 d^{-1} covers all likely maximum growth rate estimates.

mum_BF

Wilson *et al*. (1993) estimate an annual Production:Biomass (P:B) ratio of 2.8 y^{-1} for benthic fauna in Port Phillip Bay. This implies a minimum value for mum_BF of 0.0077 d^{-1}, even if no food limitation occurs. The P:B for Port Phillip Bay is high compared with other coastal areas listed by Wilson *et al*. (1993) (0.52-2.76 y^{-1}), so this may be close to a food-saturated value. However, other data indicates benthic filter-feeders may require very high food concentrations to saturate growth (Sprung 1993). The filter-feeding polychaete *Nereis diversicolor* can grow at 0.03-0.04 d^{-1} under eutrophic conditions (Vedel and Riisgård (1993). A range of 0.005 to 0.04 d^{-1} appears appropriate.

4.2.3 Growth efficiency

This parameter turns captured prey into biomass production. It allows for messy feeding, losses in assimilation (faecal pellet production), and metabolic losses (respiration). Separation of these components is described later by the appropriate FDG parameters. Note that all Si ingested is turned into detrital silica, so there is effectively a version of these growth efficiency parameters for Si which equals zero.

E_ZL

There is considerable data on the gross growth efficiency of crustacean zooplankton. Four major studies are listed by Raymont (1983): Conover (1968); Marshall (1973); Harris and Paffenhöfer (1976); and Paffenhöfer (1976). Conover (1968) lists gross growth efficiencies ranging from 0.4-60%, the interquartile range is 7-25%. Marshall (1973) looked at the growth efficiencies of different growth stages of *Calanus*, *Rhincalanus* and *Acartia* feeding on different prey types: this varied from 5-72%, but in most cases lay between 20 and 40%. Harris and Paffenhöfer (1976) examined growth efficiencies of two types of copepods by growth stage and food concentration and found a range of 8-45%, with most observations within15-25%. Paffenhofer (1976) found growth efficiencies of 13-45% (mean 28.5%). Zooplankton tend to have lower C:N ratios than Redfield (Ikeda 1974) and therefore their gross growth efficiency must be higher for nitrogen than carbon. Nitrogen gross growth efficiencies for zooplankton typical of Port Phillip Bay were reviewed by Holloway and Jenkins (1993): for *Paracalanus parvus* this was 0.37; *Acartia tonsa* 0.5-0.6 and 0.4 in two studies; and for *Penilia avirostrus* 0.4-0.58. We therefore consider the range 25-50% to be appropriate for N gross growth efficiency in Port Phillip Bay.

E_ZS

Lucas *et al*. (1987) showed growth efficiencies of 40% for flagellates and 34% for ciliates. Verity (1985) found gross growth efficiencies for two species of ciliate of 35-57%, values declined with temperature. Leakey *et al*.'s (1992) calculations of budgets for Southampton Water use a 40% ciliate gross growth efficiency. Taylor and Joint (1990) use a 30% conversion of picophytoplankton C to microzooplankton C value in their model. Moloney *et al*. (1986) transfer 65% of protozoan production to faeces + urine, this leaves 35% for modelled gross production. Frost's (1987) model uses a 50% growth efficiency for tintinnids. We therefore have a range of 0.3-0.6 for E_ZS, but, for similar reasons to E_ZL, we expect slightly higher values to apply for N than for C.

E_BF

The review by Wilson *et al*. (1993) estimates Bay-wide filter-feeder organic matter ingestion at 305 10^3 tonnes y^{-1}, with 44% assimilated, and 39% of that excreted, implying a gross growth efficiency of 17%. Unfortunately, the ingestion rates appear to be incompatible with calculated clearance rates and observed POC concentrations. Assimilation efficiencies from the literature ranged from 11-93% (Wilson *et al*. 1993). Exclusion of filter-feeders fed on bacteria or seston reduces the range to 30-93%. In the model, E_BF refers to growth efficiency on phytoplankton and protozoan food and we expect this upper range to apply. In the absence of clearer evidence, we have adopted the 0.25-0.5 range derived for zooplankton.

E_DLBF

Filter-feeders assimilate detritus much less efficiently than they do phytoplankton. Wilson *et al*. (1993) list assimilation efficiencies from three pairs of experiments in which animals graze on phytoplankton or seston: *Pyura praeputialis* 75±10% and 34±13%; *Plaecopecten magellanicus* 72-88 and 29-50%; and clams 82% and 21-22%. It is clear detritus is a much less suitable food, but the exact assimilation efficiency will depend on the type of detritus. If the percentage losses to respiration are similar to those for filter-feeders growing on phytoplankton, we would expect E_DLBF to be about 0.25-0.5 times E_BF. Since, in the model, we exclude refractory detritus from this ingested material, a value in the upper part of this range is most appropriate.

4.3 Mortality

The significance of the effects on ecosystem models of quadratic versus linear mortality was discussed in chapters 2 and 3. Here we discuss *a priori* limits to parameter values, which are scarcely applicable to quadratic parameters since they are empirical and must be tuned to local system behaviour and observed biomasses.

ml_PL

Mortality of large phytoplankton only applies in-sediment to cells that have fallen out of the water column. The value of 0.14 d^{-1} (decay time of 1 week) has been used as a default.

ml_PS

This parameter also only applies in the sediment and is unimportant as PS do not sink. The same value as for PL is used.

ml_DF

This parameter is unimportant since DF do not sink. The same value as for PL is used.

ml_MA

The underlying macroalgal loss rate, excluding stress due to storm events, is considered to be slow, but faster than for seagrasses. Macroalgae tend to live for several weeks to months. Round (1981) shows *in situ* growth rates for Nova Scotian macroalgae of 10-50% per month. Since growth must equal mortality on average, this argues for a mortality range of 0.003-0.016 d^{-1}. However, these species were large brown algae, which have relatively low growth rates (Nielsen and Sand-Jensen 1990) and so in Port Phillip Bay higher values might be expected. We assume a range of 0.01 to 0.03 d^{-1}.

ml_SG

Mediterranean seagrasses turn over in the course of about 50-100 days (Kraemer and Mazzella 1996) so mortality is about 1-2% d^{-1}. However, in the model, total loss rates are made up of basal mortality (ml_SG) plus additional losses due to nutrient stress (mS_SG), so that ml_SG should be less than observed mortality rates in eutrophic conditions. Conversely *Heterozostera tasmanica*, the commonest seagrass in Port

Phillip Bay, is comparable to the relatively rapidly growing *Zostera* forms (up to 2.5% d^{-1}, Kraemer and Mazzella 1996) for which mortality must be higher. Duarte (1989) found most P:B measurements for seagrasses to lie from 1-5% d^{-1}.

ml_ZL

Large zooplankton have generation times of weeks to years. Development time for a range of small copepods is 2.5-4.5 weeks (Kiørboe and Sabatini 1995). Given fecundity and generation time, we could calculate typical loss rates, but these are likely to be concentrated at early life history stages. Fasham *et al*. (1990) use a zooplankton mortality rate of 0.05 d^{-1}. Chapelle *et al*. (1994) use 0.025 d^{-1} at 0 °C or 0.07 d^{-1} at 15 °C and Raillard and Ménesguen (1994) use 0.035 d^{-1} (0.1 d^{-1} at 15 °C). This parameter is not actually used in model runs presented here so we will not explore it further. However, the quadratic mortality coefficient mQ_ZL should be chosen to produce similar loss rates at typical biomass levels.

ml_ZS

Microzooplankton in situ growth rates are often close to maximum growth rates (Leakey *et al*. 1992), implying that mortality rates may approach the 0.5-4 d^{-1} earlier derived for maximum growth. Taylor and Joint (1990) used linear mortality rates of 0.15 d^{-1} or 0.3 d^{-1}, but their model also includes a quadratic mortality term. A value of around 1 d^{-1}, depending on growth and ingestion, is appropriate for our model. Use of a large constant specific mortality rate, combined with a very high maximum growth rate, tends to make microzooplankton populations very unstable if subject to fluctuations in food supply. We use quadratic mortality for almost all the model runs (see Harris *et al*. 1996).

mQ_MB, mQ_ZL, mQ_ZS, mQ_BF

These parameters describe quadratic mortality rates on microphytobenthos, large and small zooplankton and benthic filter-feeders. Since they vary with biomass they must be tuned to local conditions in Port Phillip Bay and hence must be fitted during model calibration (Chapter 7). We have little data on the biomass of grazers, which is a limitation in estimating these parameters. Microphytobenthos biomass is better known and so mQ_MB is better constrained in model calibration.

mS_MA

This is the coefficient multiplied by bottom stress to calculate mortality due to physical stress in shallow waters. It has been fitted to reproduce the observed biomass distribution (see Chapter 7).

mS_SG

This parameter multiplies DIN concentrations to determine additional seagrass mortality due to growth of epiphytes. Given typical values of DIN of order 10 mg N m^{-3} and mum_SG of 0.05-0.1 d^{-1}, this must be less than 0.01 to allow seagrass growth, and greater than 0.0001 d^{-1} $(mg\ N)^{-1}$ m^3 to have any effect. Short *et al*. (1995) found concentrations of 150 mg N m^{-3} severely reduced growth rates of eelgrass in 30 cm deep mesocosms. This concentration is higher than is found in most of the Bay. Assuming that, at 30 cm, seagrass is growing at the maximum rates described earlier, this suggests a minimum value for mS_SG_T15 of about 0.0003-0.0006 d^{-1} $(mg\ N\ m^{-3})^{-1}$.

4.4 Detrital Production and Breakdown

4.4.1 Detrital production

There are four sources of detritus in the model: inputs from external sources, direct mortality of primary producers, waste products of grazing, and grazer mortality. The first two sources are assumed to produce only labile detritus, but the last two sources can also release ammonia. Waste products of grazing include messy feeding, faecal pellets, and excreted ammonia as a result of grazer metabolism. Mortality of grazers includes predation by carnivores that will also release ammonia directly. The gross growth efficiencies E determine the proportion of grazed material that is converted to zooplankton growth. Of the remainder, a proportion FDG is released directly as labile detritus, while 1-FDG is released as labile ammonia. Similarly, a proportion FDM of grazer mortality is converted immediately to detritus, and a proportion 1-FDM is release as labile ammonia. Note that some other models include respiration with the loss (mortality) term, so that these parameters are not directly comparable with parameters used in those models. In practice the FDG and FDM parameters are usually all given the same value (either 0.5 or 0.25). The exception is for benthic filter feeders feeding on labile detritus (FDG_BFDL), where we assume that a much higher proportion is not assimilated and is released as labile detritus.

FDG_ZL

Some 10-30% of ingested material is released by grazing crustacean zooplankton due to messy feeding (Jumars *et al*. 1990). Faecal production can also be significant, Anderson and Nival (1988) used 30% for copepods and 45% for salps as the percentages of ingested material lost as faeces. As mentioned above, it is difficult to compare model parameters directly, but most models (eg. Tett *et al*. 1986; Fasham *et al*. 1990; Taylor and Joint 1990) are consistent with values for FDG_ZL of 0.25 to 0.5.

FDG_ZS

Since the waste products of grazing on large and small zooplankton both join a single detritus pool, but in reality those produced by ZS settle more slowly and thus have more chance of breaking down before they hit the bottom, there is an argument for decreasing the proportion of detritus so produced to compensate. However Taylor and Joint (1990) in similar circumstances, use the same value for proportions of detritus and ammonia produced by ZL and ZS; this is about 0.5, depending on how their DON production is treated in our model. We would expect the range to be similar to the 0.25-0.5 appropriate for FDG_ZL, with slightly more emphasis towards lower values.

FDG_BF

In the model of Raillard and Ménesguen (1994) all oyster waste products are solid. Wilson *et al*. (1993) review ingestion rates and DIN production by filter-feeders, but the figures given are not sufficient to usefully constrain the proportions of waste released as detritus. In the absence of other information, we have used values comparable to those for zooplankton ie. 0.25 - 0.5.

FDGDL_BF

When detritus is consumed by filter-feeders much of it is rejected as pseudofaeces, so the proportion not respired should be greater than is the case for live plankton. If we assume respiration is equivalent regardless of food source, as discussed under E_BFDL, we would expect the difference between E_BF and E_BFDL to be due to solid waste. This would mean a range of about 0.6-0.9 for FDGDL_BF.

FDM_ZL

Predation on zooplankton results in waste product formation. If higher trophic levels have similar assimilation efficiencies and gross growth efficiencies to herbivorous zooplankton, then FDM should be similar to FDG. We therefore use a range of 0.25-0.5.

FDM_ZS

This is a result of grazing on ZS, probably by predators of comparable size and metabolic rate to large herbivorous zooplankton. We assume the same range as for FDG_ZL: 0.25-0.5.

FDM_BF

The nature of predation on benthic filter-feeders is poorly understood. We assume FDM_BF is similar to other FDM parameters (0.25-0.5).

4.4.2 Detrital breakdown

r_DL, r_DR

The model includes two detrital pools, referred to as labile and semi-labile. These are defined by their specific breakdown rates, which are assigned values of 0.1 d^{-1}, and 1 y^{-1} respectively. Changing these rates would correspond to a different operational definition of detrital fractions.

r_DON

DON turnover rates in seawater vary from hours (Fuhrman 1987) to thousands of years (Williams 1975). Some 20-40% of primary production is directly released as labile DOM, but most of this is recycled very rapidly, on time scales of hours (Hedges 1992), and is not considered in the model. The very refractory components (tens to thousands of years) account for a very small flux (Hedges 1992), and are treated in the model as a constant background. A large fraction (ca 50%) of the DON (and even more DOC) in marine systems varies on seasonal time scales (Williams 1995). It is essentially this component that we aim to model, and we assign the DON pool a turnover time somewhat less than 1 year.

There is some remaining ambiguity about the processes underlying DON in Port Phillip Bay. Measurements in the inflows to the Bay do not distinguish DON from PON. We have assumed that most of the organic N input to the Bay is in the form of PON, and that the DON export from the Bay is supported primarily by production of DON within the Bay, which is certainly important in other marine waters (Williams 1995; Druffel *et*

al. 1992). However, we cannot rule out the possibility that most of the organic N load to the Bay is in the form of refractory DON, and that this accounts for DON export, as observed in the Severn Estuary (Mantoura and Woodward 1982).

There were no experimental studies in PPBES focused on DON dynamics. The mean pool of DON is reasonably well-known, but this does not constrain turnover rates. Estimates of the Bay-wide DON pool changed by 15% between months, and on one occasion (June-July 1993) dropped nearly 30% in one month. However, these estimates are based on a relatively small number of fixed stations. Given the problems of sampling bias indicated even for tracers sampled underway (see Chapter 7), we do not believe it is appropriate to use the month to month changes to estimate DON breakdown rates.

r_DSi

The ERSEM model uses a value of 0.007 d^{-1} (Radford 1993). In an updated version of the same model, Ruardij and Van Raaphorst (1995) use a value of 0.17 d^{-1}, although dissolution is actually slower than this because it is inhibited by dissolved Si in the interstitial water (which is not the case in our model). Observations of Si fluctuations in the Bay provide reasonable constraints on this parameter during model calibration.

FDR_DL

This is the proportion of detritus breakdown resulting in refractory detritus. Breakdown of the phyoplankter *Skeletonema costatum*, common in Port Phillip Bay, was followed by Pett (1989). 67% broke down over time scales of hours to weeks. Then 29% broke down over months and 4% with a time scale of years, thus refractory material, by our definition, is 4-33% of detritus produced. Duarte and Cebrián (1996) in a review of the global fate of primary production estimated that, globally, coastal phytoplankton detrital production recycled within a year was 1.8 Pg C, while that still unrecycled after a year was 0.18 Pg C. This means about 9% of detritus is left after a year so, for our pool that breaks down on a one year time-scale, 18% must be converted to refractory forms. A similar proportion was estimated by Duarte and Cebrián (1996) for microphytobenthos production, but of macroalgal production only 1% was refractory, and for seagrasses about 50% of detritus is refractory (24% left after 1 year). For the bulk of detrital production a figure of order 0.2 seems appropriate for FDR_DL.

FDON_D

This parameter is the proportion of detrital breakdown producing DON. In Taylor and Joint's (1990) model of the Celtic Sea, DOM forms in the ratio 1:2.5 with detritus, making DOM formation 28% of total non-living organic matter formation. However this DOM is rapidly taken up by bacteria (depending on respective concentrations), whereas our DOM turns over very slowly. This figure therefore represents an overestimate. Similarly Fasham *et al*. (1990) channel 100% of detrital nitrogen, that is not grazed and does not fall out, through a labile DON pool. In practice, FDON_D and r_DON are adjusted to obtain the observed DON pool and export flux for the Bay.

4.4.3 Denitrification

R_0

Increased sediment respiration is known to suppress denitrification by preventing nitrification. In Chesapeake Bay denitrification ceased in summer when sediment N flux (100% ammonia by this stage) reached 300-400 µmoles N m^{-2} h^{-1}, or 100-130 mg N m^{-2} d^{-1} (Kemp *et al*. 1990). Sloth *et al*. (1995) enriched sediment with organic matter and found that denitrification ceased at 70 mg N m^{-2} d^{-1}. Regression of denitrification against total N flux for the data reviewed by Seitzinger (1988) gives a value for R_0 of 400 mg N m^{-2} d^{-1} or (if values where total N flux is less than 35 mg N m^{-2} d^{-1} are removed) 300 mg N m^{-2} d^{-1} (Fig. 4.2). The reason for removing these low N flux values is that, in our model, denitrification efficiencies are also suppressed at low sediment respiration rates, below R_D. Seitzinger's data support this; the correlation coefficient increased from 0.3 to 0.55 when low N fluxes were removed.

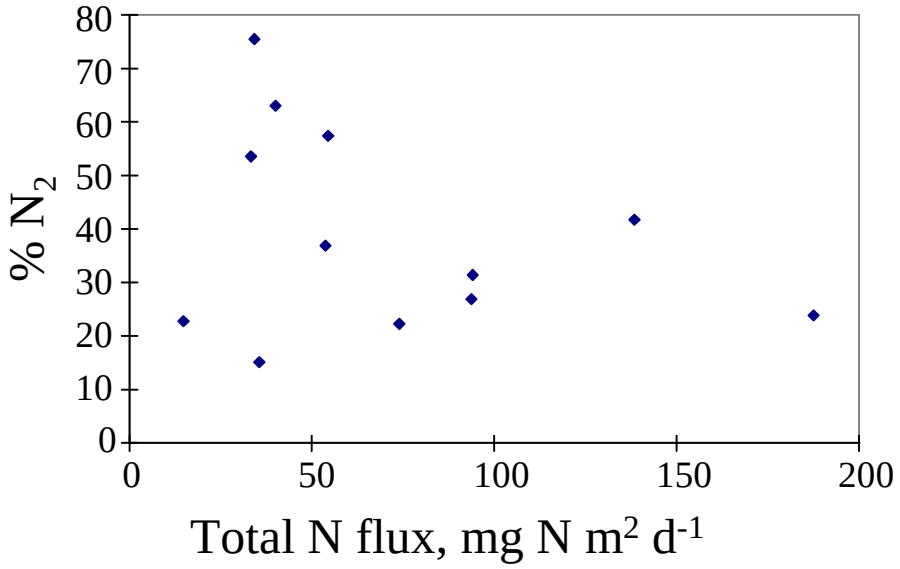

Figure 4.2 N_2 evolution as a percentage of total N flux from Seitzinger et al. (1988).

The sediment chambers deployed in Port Phillip Bay measured carbon and oxygen flux and DIN release. These were used to estimate denitrification losses, assuming Redfield ratios for organic matter. This assumption was supported by direct measurements of N_2 release (Fig. 4.3).

Regressions of denitrification efficiency on respiration rate provided direct estimates of Dmax and R_0. This regression is very dependent on a few observations at high respiration rates, located in one region (Hobsons Bay). The early sediment chamber results yielded a value of R_0 of about 250 mg N m^{-2} d^{-1}. However, with the inclusion of more data, a value of 384 mg N m^{-2} with 95% confidence limits of 240-970 mg N m^{-2} d^{-1} was obtained. However two new data points with high respiration rates and high apparent denitrification efficiencies also showed much lower than expected P and Si release, suggesting that the N imbalance in those experiments was not denitrification.

Exclusion of these points gives an intercept of 267 mg N m^{-2} d^{-1} and range of 183 to 501 mg N m^{-2} d^{-1}. In calculating R_0 and Dmax by regression, one should exclude data points with respiration rates less than R_D. For the PPBES data set, removal of those points for which respiration was less than 12 mg N m^{-2} d^{-1} has little effect on the slope or intercept. The upper 95% confidence limit for R_0 was reduced to 480 mg N m^{-2} d^{-1}. Given both the statistical uncertainty and the unusual nature of the environments which currently receive high loadings (shallow, near freshwater inputs) the use of a fixed value for this parameter throughout the Bay is questionable.

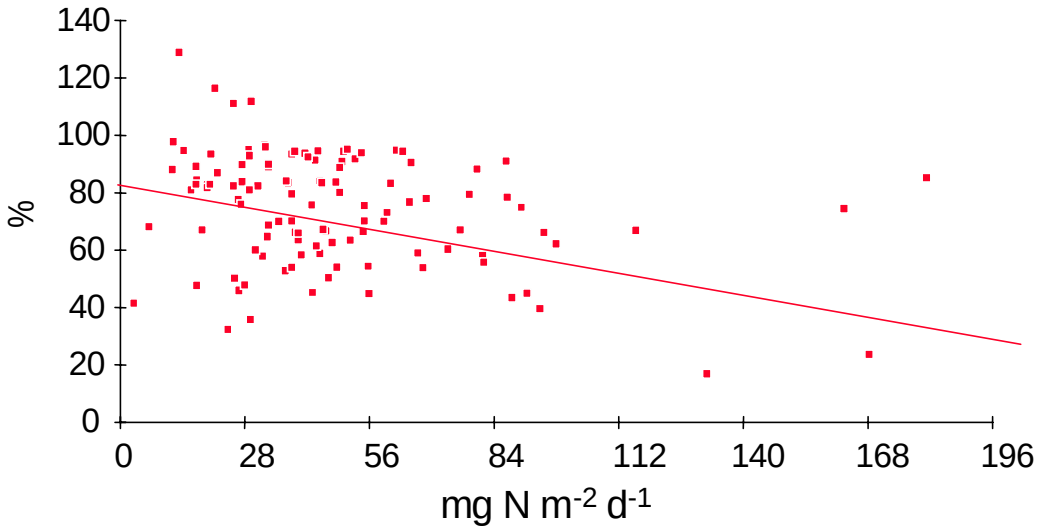

Figure 4.3 Denitrification versus respiration rate from PPBES sediment chamber deployments.

R_D

In data from several locations plotted by van Raaphorst *et al*. (1990), denitrification efficiency peaked at respiration rates equivalent to 3.5-14 mg N m^{-2} d^{-1}. Seitzinger (1988) reviewed denitrification as a percent of total N release for a variety of coastal temperate and warm temperate systems. Highest denitrification efficiencies occurred at respiration rates between 35 and 50 mg N m^{-2} d^{-1}. In Fig. 4.3 there are some low denitrification efficiencies at respiration rates below 30 mg N m^{-2} d^{-1}, but some high values also occur at 10 mg N m^{-2} d^{-1} or less. A range of 4 to 20 mg N m^{-2} d^{-1} appears appropriate for R_D.

Dmax

Simple diffusion models would seem to indicate this should be no larger than 0.5 if the DIN is produced within the sediment. However much higher values are sometimes observed (Seitzinger 1988). These can exceed 100% if nitrate is imported from the water-column (Seitzinger 1987).

According to the sediment chamber observations and regression (Fig. 4.3), the 95% confidence range for Dmax is approximately 0.7-0.9. However, the denitrification efficiencies in Fig. 4.3 are calculated based on dark respiration (ie. gross sediment respiration). These should be corrected for microphytobenthic photosynthesis, which

would reduce the net sediment respiration rate, and the apparent denitrification efficiency. Unfortunately, MPB studies were not co-located with sediment chamber studies, and it has not proved easy to make this correction rigorously. The regression estimate of Dmax is therefore likely to be an overestimate, but it is not clear by how much. The correction may be small, as maximum denitrification efficiencies were observed in the Bay centre, where MPB production is generally low. There are other issues associated with the interaction between MPB and denitrification, which are addressed in Chapter 6.

4.5 Composition

X_ON

This is the oxygen:nitrogen ratio involved in formation and remineralization of organic matter. For each mg of N this is about 16 mg O_2 (Chapelle *et al*. 1994).

X_PN

This is assigned a Redfield (1934) ratio of 0.143 (by weight), which has been used in other models eg. Aksnes *et al*. (1995), Radford (1993).

X_CN

This is the Redfield (1934) ratio of 5.6 (by weight) as used by, for example Taylor and Joint (1990). Although all organic matter in the model is treated as having Redfield composition, which is a convenient and powerful assumption, this may not apply to all organisms or all classes of detritus. Macrophytobenthos and seagrass can have much higher C:N ratios.

X_CHLN

Most literature sources refer to C:Chla ratios, which depend on the physiological status of phytoplankton. Parsons *et al*. (1984) review phytoplankton composition and propose a range of 25-60 mg C mg $Chla^{-1}$. Other model C:Chla ratios are 15-45 (Frost 1987), 50 (Tett 1987; Tett *et al*. 1986; Fasham *et al*. 1990), 45 (Fasham *et al*. 1983), 35 (Harris 1986) and 25 (Parsons and Kesseler 1983). Most values lie between 35 and 50, corresponding to 6 to 9 mg N mg $Chla^{-1}$ at Redfield C:N ratio. We have compromised between Harris and Fasham to use a default value of 40 mg C mg $Chla^{-1}$, or 7 mg N mg $Chla^{-1}$.

X_SiN

The silica:nitrogen ratio applies only to diatoms, both phytoplankton PL and benthic diatoms MB. Si:N ratios can vary because diatoms respond to Si limitation by decreasing the cell quota (thickness of Si frustules). Aksnes *et al*. (1995) used a molar ratio of 0.875, or 1.75 by weight. In the ERSEM model, diatoms have a maximum Si quota of 0.01785 mmoles $(mg\ C)^{-1}$ (Radford 1993), or 3.5 mg Si $mg\ N^{-1}$. According to Raymont (1980), in the oceans silica is used at a ratio of 15:1 with respect to P (by atoms) and so the Redfield ratio is approximately 1:1 with respect to N by atoms, or 2:1 by weight. However, this ratio applies to all organic matter production and consumption, of which diatoms form only a part. As the other references indicate, the Si:N ratio in diatoms can exceed the Redfield ratio.

4.6 Light attenuation, temperature dependence and sinking rates.

4.6.1 Light attenuation

Surface solar irradiance values are read into the model from an external forcing file (see previous Chapter) and converted to PAR. They are then attenuated over the water column. The bulk attenuation coefficient for total irradiance, k, depends on levels of chlorophyll, detritus, and DON in the water column.

The data collected at vertical stations in PPBES included both in-situ light attenuation and concentrations of the key optical constituents (Longmore *et al*. 1996). These are chlorophyll a, particulate N, and DON, and suspended particulate matter, NFR. We have estimated specific attenuation coefficients for these constituents in Port Phillip Bay by multiple regression of the measured attenuation coefficients on the observed constituent concentrations. Because the transport model representation of suspended inorganic matter model is not yet calibrated, we carried out the regrssion with and without NFR. The chlorophyll contribution was masked in this analysis, because it forms a relatively minor component of attenuation. For some analyses we therefore removed an attenuation due to chlorophyll of 0.025 m^2 $(mg\ Chl)^{-1}$, based on literature values.

k_w

Attenuation by pure seawater is low, less than 0.03 m^{-1}. However, in the model this parameter includes attenuation due to background DON (ie. DON at oceanic concentrations). Most other models incorporate attenuation by all constituents except chlorophyll in k_w. A value of 0.15 m^{-1} is used by Taylor and Joint (1990) for Celtic Sea background attenuation. Frost (1987) use 0.1 m^{-1}, but this is for the much clearer North Pacific.

Regression of k on DON, particulate N, chlorophyll and non-filterable residual gives an intercept of 0.016 m^{-1}, which is lower than the value of about 0.025 m^{-1} expected for pure seawater, but within 1 standard error of it (s.e. = 0.026). If we deduct the background (Bass Strait) DON concentration (70 mg N m^{-3}), before carrying out the regression, we get an intercept value for k_w of 0.084 m^{-1} with s.e. of 0.016. Omission of NFR (and background DON) from the regression leaves k_w = 0.093 m^{-1} with s.e. = .016. If we fix chlorophyll specific attenuation to literature values (0.025 $m^2(mg\ Chl)^{-1}$) the intercept is 0.03 m^{-1} if NFR is included, and 0.057 m^{-1} if it is excluded.

k_PN

This parameter can vary depending on N:Chl a ratios, accessory pigments, and cell packaging effects. Attenuation due to chlorophyll itself is usually around 0.025 m^2 $(mg\ chla)^{-1}$ (Tett 1990), or for a N:Chla ratio of 7:1, 0.0035 m^2 $(mg\ N)^{-1}$. Frost (1987) uses a slightly lower value of ca 0.0029 m^2 $(mg\ N)^{-1}$. Fasham *et al*. (1990) use a value of ca 0.002 m^2 $(mg\ N)^{-1}$.

Multiple regression of attenuation on DON, NFR, particulate N and chlorophyll gives an estimate of 0.008 m^2 mg Chl^{-1}, s.e. = 0.0057, with marginal significance (P=0.16). This regression translates into 0.00114 m^2 $(mg\ N)^{-1}$ with s.e. 0.0008, about a third of the literature value. This low value may be an artifact, due to covariation of Chl a with the other constituents. Omission of NFR gives an even lower value of 0.0012, s.e. 0.0055;

this is not significantly different from zero (P=0.83). While the regression suggests a marginal effect of chlorophyll on light in the Bay under current conditions, we have retained the literature values for k_PN because of its potential importance under conditions of increased eutrophication.

k_DON

Certain organic compounds, such as humics, absorb light more strongly so there need not be a direct relationship between concentration of DON, and light absorption by DOM. Furthermore, in order to simplify the modelling of exchange with Bass Strait, the value of DON in Bass Strait has been set to zero and thus the value in Port Phillip Bay represents the excess over Bass Strait DON, which is assumed to be refractory.

The multiple regression of Port Phillip Bay attenuation against water column constituents yields values for k_DON of 0.00092 m^2 mg N^{-1} (s.e. 0.0002) with NFR included, and 0.00085 m^2 mg N^{-1} (s.e. 0.0002) without NFR. These values are slightly reduced to 0.00085 and 0.0007 m^2 $(mg\ N)^{-1}$, if chlorophyll attenuation is set to literature values.

k_DL

Despite its name this specific attenuation coefficient applies to both refractory and labile detritus. Prieur and Sathyendranath (1981) estimate a specific attenuation coefficient for seston of 0.03 m^2 g^{-1} dry weight, giving about 0.3 m^2 $(g\ N)^{-1}$ or 0.0003 m^2 $(mgN)^{-1}$.

Regression of Port Phillip Bay observations gives a very strong relationship between attenuation and total particulate N. Estimates of k_DL are 0.0033 and 0.0046 m^2 $(mg\ N)^{-1}$, with se 0.0006. Removal of literature based chlorophyll attenuation gives similar values for k_DL of 0.0031 and 0.04 m^2 $(mg\ N)^{-1}$. These are much higher than literature estimates and are close to literature values for phytoplankton. This may indicate a high proportion of relatively fresh detritus with high pigment content, or a strong correlation of organic detritus and pigment.

k_IS

Currently the sediment resuspension model is not fully calibrated and so we assume a fixed contribution to attenuation from suspended inorganic sediment. The regression of Port Phillip Bay observations gives 0.011 m^2 $(g\ dry\ wt)^{-1}$ (s.d. 0.002), or 0.012 m^2 $(g\ dry\ wt)^{-1}$ if chlorophyll attenuation is fixed at literature values. However, since the sediment resuspension model is not yet fully calibrated, we have used a constant value for attenuation due to inorganic suspended sediment. The mean suspended sediment concentration (2.5 to 3.3 g dry wt m^{-3}) corresponds to an average attenuation due to suspended inorganic sediment of 0.025-0.04 m^{-1}.

The estimated attenuation values give

$$k = 0.082 + 0.0035.PN + 0.0008.DON + 0.0044.(DL+DR)$$

For mean values of PN = 10, DON = 87 (+70), and DL+DR = 28 mg N m^{-3}, these constituents contribute, respectively, 0.035, 0.07 and 0.16 m^{-1}. NFR's contribution to attenuation (part of the first, constant, term) is comparable to chlorophyll. The observed mean attenuation is 0.337 m^{-1}, and the calculated mean attenuation is 0.346 m^{-1} with

our approximations. Note that the biased (coastal) nature of site locations means that the role of particulate N is likely to be exaggerated. However it clearly does play a key role in attenuation.

4.6.2 Temperature dependence

Q10

Aksnes *et al*. (1995), after Eppley (1972), use 1.88 as a Q10 for phytoplankton. Chapelle *et al*. (1994), citing the same source (Eppley 1972), use a Q10 of 2. Eppley (1972) cites values of Q10 of 2.1-2.3 from other studies, but derives a value of 1.88 from a review of observed growth rates. Kremer and Nixon (1978) also used Q10=2. Radford (1993), on the other hand, used 4. Huntley and Lopez (1992) used a formula equivalent to Q10=2.7 for copepod grazing rates. Kiørbe and Sabatini (1995), using data from Huntley and Lopez (1992) and others, derived a Q10 of 3 for zooplankton growth related processes. Moloney and Field (1989), when reviewing production and respiration of marine organisms, use a Q10 of 2 to correct zooplankton respiration and 3 for ingestion. They also use Q10 of 2.45 for bacterial maximum nutrient uptake, and 2 for diatom photosynthetic rates. Norwiki (1994) looking at denitrification rates obtained denitrification Q10s of 1.8-4.5. The filtration rate of *S. spallenzanii* has a Q10 close to 2.7 (Clapin 1996). Tumbio and Downing (1994) found a Q10 of 2-2.5 was required to fit benthic secondary production. It is difficult to find compelling arguments against using a single Q10 of about 2 to cover all rate processes. The model retains the option to modify Q10 values for individual parameters.

Experimental data on picophytoplankton photosynthesis parameters P^B_M and KI demonstrate Q10s closer to 1.5 in Port Phillip Bay, and larger phytoplankton show no seasonal signal for these parameters (Q10=1). In the case of microphytobenthos, P^B_M shows a Q10 of slightly more than 2 and KI a Q10 of 2-3 depending on site. KI_MB averaged over all sites and depths in summer is approximately twice the winter value.

A similar seasonal change is apparent in sediment respiration, being approximately double in summer at all sites where seasonal data are available (6, 16 and 37), although the magnitude of fluxes differs among sites. However this signal could be the product of either increased detritus flux to the sediment (sediment respiration rates were also correlated with primary production in the overlying water column) rather than temperature-driven variation in the detritus breakdown rate r_DL.

4.6.3 Sinking rates

Because of the implementation of sinking and vertical mixing in the transport model, once sinking rates per day exceed the water column depth, all material is lost to the water column. This is potentially a problem in shallow waters.

w_DL

The exact sinking rate depends on the nature of the detritus. It can vary from negligible (or even negative) to over 1 km d^{-1} in the case of salp faeces (Silver and Bruland 1981). Certainly much phytoplankton detrital material reaches the floor of even the deepest

oceans shortly after blooms (Theil *et al*. 1988). However much material does recycle in the upper water-column and little copepod faecal pellet material may leave the euphotic zone (Bathman *et al*. 1987, Martens and Krause 1990). Taylor and Joint (1990) used 1 m d^{-1}.

Sediment deposition rates were measured as part of the PPBES by You *et al*. (1996). Deposition rates were recorded at three sites in the Bay centre, Hobsons Bay and Corio Bay. Settling velocities were recorded for sediment + organic matter and for sediment alone. From these we can calculate an average organic matter deposition of approximately 0.2, 0.3 and 0.4 g h^{-1} m^{-2}. Sediment concentration, with and without organic matter were also recorded at about 10 cm from the bed for the three sites. The residual organic matter averages about 3, 10 and 2 g m^{-3}. From these figures we can calculate settling velocities of 1.6, 0.5 and 3.6 m d^{-1}. These data indicate detrital settling velocities lie in the range 0.5-5 m d^{-1}. We cannot separate this organic matter into labile and refractory components.

w_DR

Since this includes more degraded material, and to the extent that it contains large flocs or marine snow, settling velocity is likely to be less than that of labile detritus. After refractory material is resuspended from the bed during storms, the coarse fraction will sediment out very quickly. We are interested in the fine fraction that remains suspended for extended periods, and use a relatively slow sinking rate. The data of You *et al*. (1996) described under w_DL also applies to w_DR.

w_DSi

This material consists of the tests of diatoms and so is likely to be found in relatively large fast sinking particles such as nearly whole cells or faecal pellets.

w_PL

Settling by live diatoms was determined by Smayda (1970) at 0.74 m d^{-1} and for mixed communities at 1 m d^{-1}. Flocculation can increase settling, particularly at high densities (Jackson 1990) and decreased nutrients may also enhance sinking (Logan and Aldredge 1989). Aksnes *et al*. (1995) used a range of 0.3-3 m d^{-1} sinking for diatom, depending on Si levels. In the ERSEM model (Radford 1993), sinking rates vary from 0-45 m d^{-1}, and exceed zero once nutrient-limitation reduces growth by more than 25%.

4.7 Summary of Parameter Ranges

The parameter ranges we have chosen based on the literature and on results of the PPBES process experiments discussed in this chapter are listed below (Table 4.3). Also shown are the parameters which were used in the standard model run si142, which represents the end result of model calibration against observations (see Chapter 7). This run uses the quadratic version of zooplankton mortality and therefore ml_ZL and ml_ZS are zero. This run also does not include dinoflagellate dynamics and so the growth rate of this component is set to zero.

Table 4.3 Parameter ranges, standard values used in run si142, and units.

Parameter	Range	Standard value	Units.
mum_PL	1-2.5	1.7	d^{-1}
mum_PS	1-1.75	1.24	d^{-1}
mum_DF	1-1.75	0	d^{-1}
mum_MB	0.1-0.75	0.35	d^{-1}
mum_MA	0.05-0.2	0.1	d^{-1}
mum_SG	0.035-0.1	0.05	d^{-1}
KI_PL	10-30	10	W m^{-2}
KI_PS	10-30	10	W m^{-2}
KI_DF	10-30	10	W m^{-2}
KI_MB	2.5-12	3	W m^{-2}
KI_MA	5-20	5	W m^{-2}
KI_SG	30-60	60	W m^{-2}
KN_PL	6-20	15	mg N m^{-3}
KN_PS	4-9	7	mg N m^{-3}
KN_DF	5-15	30	mg N m^{-3}
KN_MB	fitted	200	mg N m^{-3}
KN_MA	5-50	20	mg N m^{-3}
KN_SG	fitted	5	mg N m^{-3}
KS_PL	8-40	20	mg Si m^{-3}
KS_MB	fitted	20	mg Si m^{-3}
MAmax	5000-20000	10000	mg N m^{-2}
SGmax	1000-5000	2000	mg N m^{-2}
C_ZL	0.02-0.08	0.08	m^3 $(mg\ N)^{-1}$ d^{-1}
C_ZS	0.005-1	0.4	m^3 $(mg\ N)^{-1}$ d^{-1}
C_BF	0.0005-0.001	0.0005	m^3 $(mg\ N)^{-1}$ d^{-1}
mum_ZL	0.2-0.4	0.375	d^{-1}
mum_ZS	0.5-4	2.5	d^{-1}
mum_BF	0.005-0.04	0.01	d^{-1}
E_ZL	0.25-0.5	0.5	
E_ZS	0.25-0.5	0.5	
E_BF	0.25-0.5	0.5	
E_DLBF	0.1-0.25	0.2	
ml_PL	0.03-1	0.14	d^{-1}
ml_PS	0.03-1	0.14	d^{-1}
ml_DF	0.03-1	0.14	d^{-1}
ml_MA	0.01-0.03	0.02	d^{-1}
ml_SG	0.01-0.02	0.01	d^{-1}
ml_ZL	0.025-0.06	0	d^{-1}
ml_ZS	0.5-4.0	0	d^{-1}
mQ_MB	fitted	0.000035	d^{-1} $(mg\ N)^{-1}$ m^3
mQ_ZL	fitted	0.02	d^{-1} $(mg\ N)^{-1}$ m^3
mQ_ZS	fitted	0.15	d^{-1} $(mg\ N)^{-1}$ m^3
mQ_BF	fitted	0.000001	d^{-1} $(mg\ N)^{-1}$ m^3
mS_MA	fitted	80000	d^{-1} $(unit\ erosion)^{-1}$
mS_SG	fitted	0.015	d^{-1} $(mg\ N)^{-1}$ m^3

Table 4.3 Parameter ranges, standard values used in run si142, and units. (cont.)

Parameter	Range	Standard value	Units.
FDG_ZL	0.25-0.75	0.25	
FDM_ZL	0.25-0.75	0.25	
FDG_ZS	0.25-0.75	0.25	
FDM_ZS	0.25-0.75	0.25	
FDG_BF	0.25-0.75	0.25	
FDGDL_BF	0.6-0.9	0.75	
FDM_BF	0.25-0.75	0.25	
r_DL	0.1	0.1	d^{-1}
r_DR	0.0036	0.0036	d^{-1}
r_DON	fitted	0.0176	d^{-1}
r_DSi	0.02-0.2	0.05	d^{-1}
FDR_DL	0-0.5	0.2	
FDON_D	<0.28	0.05	
R_0	183-480	200	mg N m^{-2}
R_D	3.5-20	10	mg N m^{-2}
Dmax	0.7-0.9	0.7	
X_ON	16	16	mg/mg
X_PN	0.143	0.143	mg/mg
X_CN	5.7	5.7	mg/mg
X_CHLN	4.4-10	7	mg/mg
X_SiN	2-4	3	mg/mg
k_w	0.05-0.1	0.1	m^{-1}
k_PN	0.0035-0.005	0.0035	m^2 (mg N)$^{-1}$
k_DON	0.0007-0.0011	0.0009	m^2 (mg N)$^{-1}$
k_DL	0.036-0.055	0.0038	m^2 (mg N)$^{-1}$
k_IS	0.009 - 0.013	0.0	m^2 (g dry wt)$^{-1}$
Q10	1-4	2	
w_DL	0.5-5	3	m d^{-1}
w_DR	0.5-5	2	m d^{-1}
w_DSi	0.1-10	2.5	m d^{-1}
w_PL	0.3-3	2.5	m d^{-1}

5 FORCING DATA

This Chapter reviews briefly the data that are used to force the integrated model. Physical forcing data such as freshwater runoff, winds and tides are dealt with separately in the physical transport model (Walker 1997a,b). Here, we discuss the major point source and diffuse nutrient loads to the Bay, and surface irradiance that drives photosynthesis.

The integrated model uses a nominal 1-day time step, and nutrient loads are specified at daily intervals. However, none of the nutrient sources are monitored with this frequency, and the time series of loads must be generated from the observations by interpolating or modelling. The interpolation methods and models are explained below.

The principal nutrient sources for the Bay are the Western Treatment Plant (WTP), the Yarra River and the Patterson River and Mordialloc Creek complex (Fig. 5.1). Inputs from the minor creeks of Werribee River and Kororoit River are included in the model, but these are based on very limited data. Atmospheric inputs and the boundary conditions at Bass Strait are also treated explicitly.

We have attempted to prescribe nutrient loads as well as physical forcing for the period 1990 to 1995. The specific nutrients treated are ammonium, nitrate, organic N, dissolved inorganic phosphate (DIP), organic P, and Si. In the model, we have assumed that organic N and organic P are involved in biological processes at Redfield ratios, and therefore it is not necessary to specify the organic P load separately.

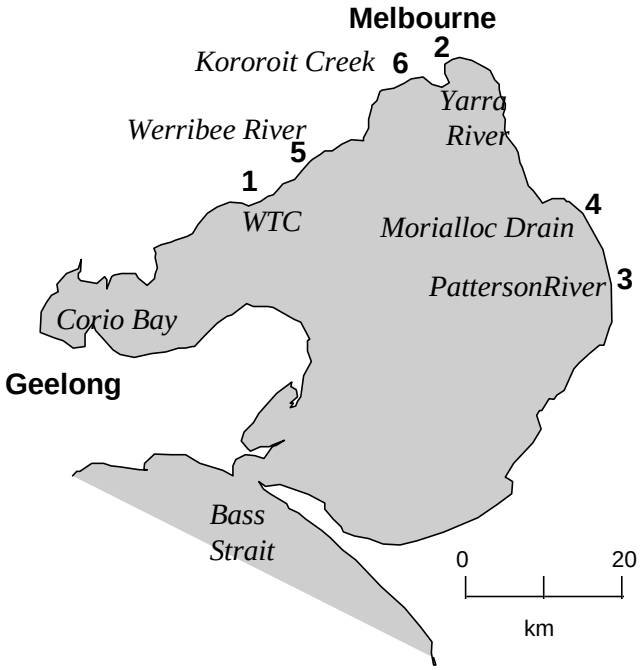

Figure 5.1 Principle Nutrient Input Sources for Port Phillip Bay (Ranked in Order of Total N Input)

Annual average nutrient inputs from the principal sources for the period 1991 to 1994 are shown in Table 5.1. These demonstrate the dominance of WTP as a source of NH_4, total N and phosphate. The Yarra and the Patterson - Mordialloc system are important sources of nitrate. The Yarra and WTP are major sources of detrital N. (One might expect the nature of the detrital N from these two sources to differ, but there is no data on the composition of the organic N. In fact, we do not have data for the principal sources distinguishing dissolved and particulate organic N. In the model, we assume that the TKN is all labile detrital N.)

Table 5.1 shows significant interannual variation, with N and Si inputs being significantly lower in 1994, which was a dry year. The effect is somewhat dampened by WTP whose inputs remain relatively constant year to year, although even WTP shows lower N inputs and a switch from ammonium to nitrate in 1994, indicating that nitrification and denitrification at WTP was more effective in the dry year. The annual phosphate load to the Bay is relatively constant. The large drop in output from the Patterson in 1994 merely reflects effects of diversion of flows and is matched by increased phosphate discharge from Mordialloc Creek.

Table 5.1 Water borne nutrient inputs to Port Phillip Bay (Murray 1994; Sokolov 1996)

Yarra, West Gate Bridge	**NH_4 t y^{-1}**	**NOx t y^{-1}**	**Lab_Det_N t y^{-1}**	**SiO_4 t y^{-1}**	**DIP t y^{-1}**
1991	132	507	966	1678	81
1992	182	615	1439	2154	99
1993	173	499	1259	1805	92
1994	104	276	437	824	77
mean	148	474	1025	1615	87
WTP					
1991	2969	172	959	1188	895
1992	2971	208	831	1313	957
1993	2341	437	887	1315	1036
1994	1964	456	882	1136	1047
mean	2561	318	890	1238	984
Mordialloc					
1991	203	142	188	519	103
1992	182	186	281	722	118
1993	95	122	230	538	81
1994	100	145	345	571	148
mean	145	149	261	587	113
Patterson					
1991	84	233	338	1371	57
1992	76	257	430	1788	64
1993	50	208	380	1651	51
1994	13	82	108	562	16
mean	56	195	314	1343	47
Total					
1991	3390	1055	2452	4756	1137
1992	3412	1267	2982	5977	1239
1993	2662	1268	2757	5309	1261
1994	2182	960	1773	3093	1289

The development of time series of loads for individual sources is discussed in more detail below.

5.1 Western Treatment Plant

WTP is the major source of phosphate and ammonium inputs to Port Phillip Bay, but not nitrate or TKN. However ammonium is the major N form, so that WTP dominates inputs of total N to the Bay as well. Nutrient and metal concentrations are monitored weekly, together with flow, at the four drains exiting WTP (Murray 1994). This allows the calculation of total instantaneous loads once per week. Since these loads show relatively small short term variation, this weekly interval is regarded as sufficient to give an accurate estimate of seasonal fluxes into the Bay. We have generated daily time series by linearly interpolating the weekly observed values.

Silicate data is not currently collected at WTP. An estimate of Si input was obtained by multiplying water discharges by a constant concentration of 8 mg L^{-1} based on estimates of WTP Si loads and discharges in the Phase One Study (MMBW/FWD 1973). Freshwater discharge from WTP has since increased, and use of this Si concentration leads to an estimated current annual discharge of about 1000 tonnes Si (see table 4.1)

The time series of calculated daily loads from WTP are plotted in Fig. 5.2 Loads of organic nitrogen show little seasonal or interannual variation. The load is somewhat reduced early in the year (ie. in late summer), but this is not the case in 1994. The nitrate load is low and fairly constant, but increases in 1993 and 1994 with summer peaks at the beginning and end of 1993, and in the winter of 1994. The phosphate load has a pronounced seasonal variation in 1991 and 1992, with a 5-fold variation between winter maxima and summer minima, but this reduces to a factor of less than 2 in 1993 and 1994. The ammonia load is of particular interest, as this is the dominant source of the limiting nutrient. It is highly seasonal in 1991-92, changing from about 18 tonnes per day in winter to less than 1 tonne per day in summer. In 1993 the peak is slightly lower, at about 15 tonnes per day, and in 1994 less than 10 tonnes per day. However, the duration of the winter peak increases in these years, so that there is less interannual variation in the annual load than in the peak load.

The autocorrelation of ammonium discharge is very high (Fig. 5.3) This is because the seasonal cycle is much more important than fluctuations with period of less than a week, and indicates that measurement intervals of one week are adequate to resolve most of the variation in ammonium inputs. Phosphate shows a very similar pattern. Nitrate inputs are also moderately highly correlated over a period of a week or more. After this they seem to show a nine month maximum correlation. This is a coincidence caused by a relatively small number of large discharges of nitrate. Organic N shows low autocorrelation at lags beyond one week, but evidence of a weak seasonal cycle. Runoff (and therefore Si) has similar autocorrelation to nitrate for lags less than three months, but at longer lags shows evidence of a regular seasonal cycle.

Although the short-term autocorrelation for ammonia is high, there is significant week to week variation in ammonia fluxes at times of moderate loading. We illustrate this in Fig. 5.4 where the discharge in week x+1 is plotted against discharge in week x. The summer minima and the two levels of winter maxima are visible as clusters of points.

Week to week variation can be as much as a factor of 2 at medium loads. Some of the week to week changes (up to ±12 %) can be accounted for by the underlying seasonal cycle.

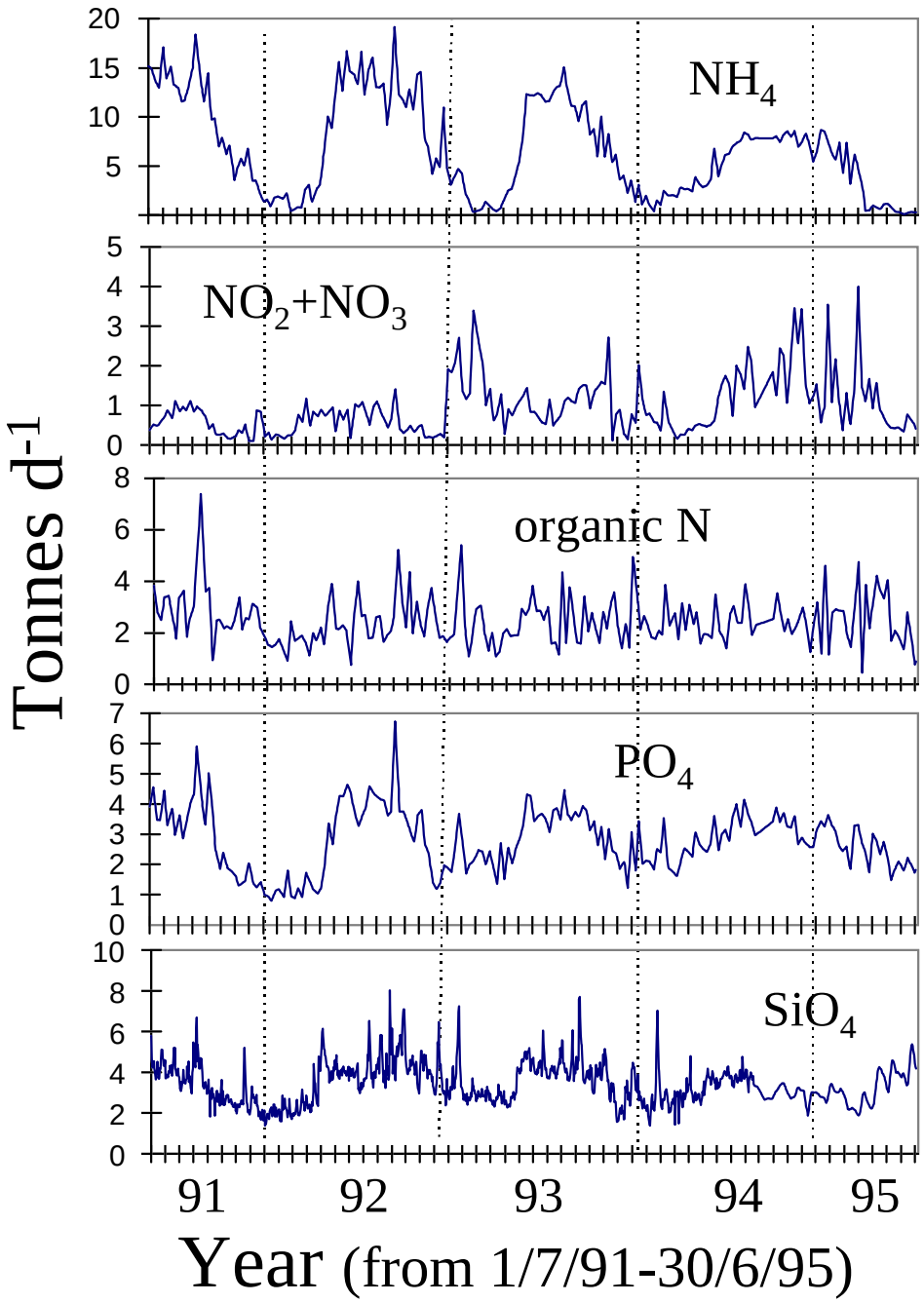

Figure 5.2 Inputs to Port Phillip Bay of ammonia, nitrate + nitrite, organic nitrogen, phosphate and silica from the Western Treatment Plant 1/7/91-31/6/95. Inputs from concentrations and flows measured by Melbourne Water except Si which is estimated.

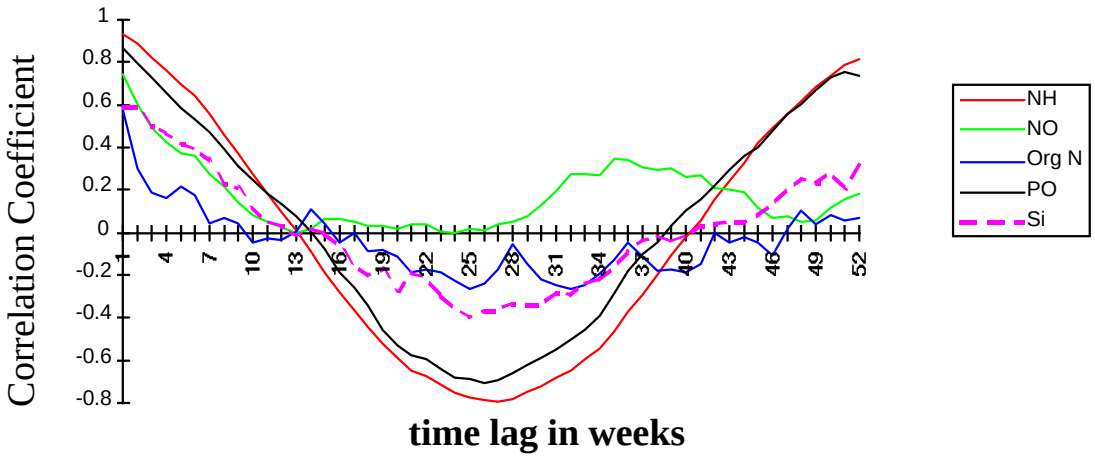

Figure 5.3 Autocorrelation of WTP inputs for 1991-3.

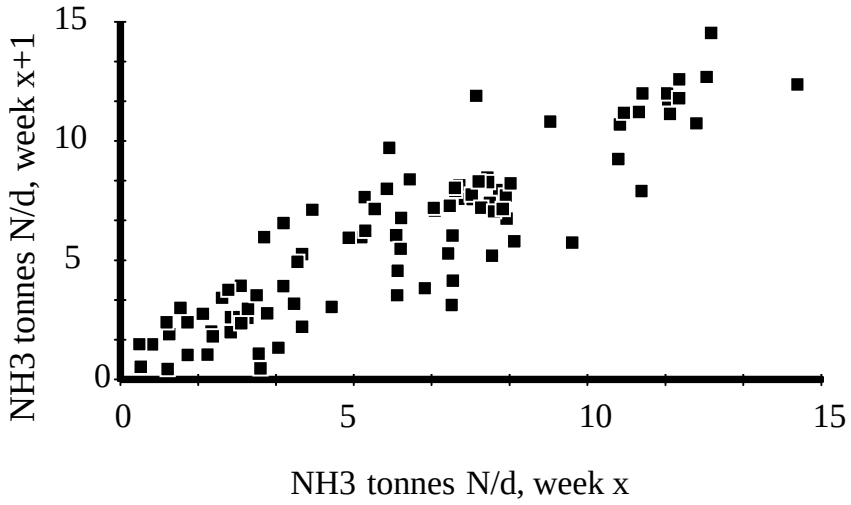

Figure 5.4 Week to week variation in inputs of ammonia 93-94.

5.2 Major riverine inputs

Annual average inputs from creeks and drains (other than the Yarra River) were investigated by NSR consultants (1993). Annual average loads are useful for identifying and ranking significant nutrient sources. However, as noted earlier, the model requires time series of daily loads.

Direct observations of loads (ie. concentrations and discharge) have generally been made intermittently and often infrequently. Even for the three major rivers, the data are not sufficient to directly interpolate to get daily loads. However, for these rivers, automatic flow gauges provided good time series of daily freshwater discharge.

In order to estimate daily loads, simple catchment models were developed by Sokolov (1996), who formulated models linking nutrient loads to runoff, and estimated the parameters in these models by fitting them to the observed loads. The models allow for

a dynamic reservoir of nutrients in catchments. Nutrients accumulate in the catchment at a fixed rate, and are washed out at a rate that depends on the catchment reservoir and the runoff. Thus the load depends not only on the current runoff, but also on the recent history of runoff.

The formulae as derived by Sokolov (1996) are:

$$dM/dt + \beta M = Aw$$

where M is the catchment reservoir, A is the area of the catchment, w is the input rate to the catchment, βM is the load, and:

$$\beta = \min \{\alpha[(F_t - F*)/(F_{max} - F*)]^{\gamma}, 0\}$$

There is also a constant direct input to the system that defines the load when runoff is less than the transitional flow $F*$.

The parameters in these models were estimated for the Yarra and Patterson-Mordialloc system by fitting predicted loads to observed loads. Runoff and loads in the Patterson-Mordialloc system are complicated because flood waters are diverted from the Mordialloc drain into the Patterson River. This has been incorporated into Sokolov's models.

In the case of the Yarra, loads associated with freshwater inputs to the Yarra estuary have been monitored, but the integrated model requires loads into the Bay at the mouth of the estuary to be specified. The PPBES commissioned an intensive six month program monitoring concentrations and flows near the mouth of the Yarra (at Westgate Bridge). Sokolov (1996) then fitted an empirical model that extrapolates freshwater loads to the mouth of the Yarra (Fig. 5.5).

Inputs from the rivers are extremely variable because flow is highly variable. Discharges at intervals of a week or more are very weakly correlated (Fig. 5.6). This means that weekly measurements, or modelled inputs, could not be expected to describe inputs, as they do in the case of WTP. This illustrates the importance of good catchment models. This applies particularly to organic N and nitrate, which are the most important of the riverine inputs. Even in the case of ammonia and phosphate, the seasonal cycle accounts for about half the total variance, and the remaining signal shows almost no autocorrelation at one week.

The combined discharges of inorganic N and P from the Patterson River and Mordialloc Creek are comparable to those of the Yarra River, although organic N discharges are rather lower. Mordialloc Drain discharges are relatively constant with weak seasonal signals. Patterson River discharges are extremely variable with transient peaks, some seasonality, and very low loads throughout 1994.

The Yarra and Patterson-Mordialloc models have been fitted to data for the period 1988-94 and daily estimates of freshwater discharges. Predicted loads are available for the period 1988-1995 at Westgate Bridge and 1988-mid-1995 for the Patterson-Mordialloc. The mid 1991- mid 1995 period was selected for model forcing (Fig 5.5, 5.7

and 5.8). As well as nutrients, the catchment models have also been calibrated to predict a range of toxicant loads.

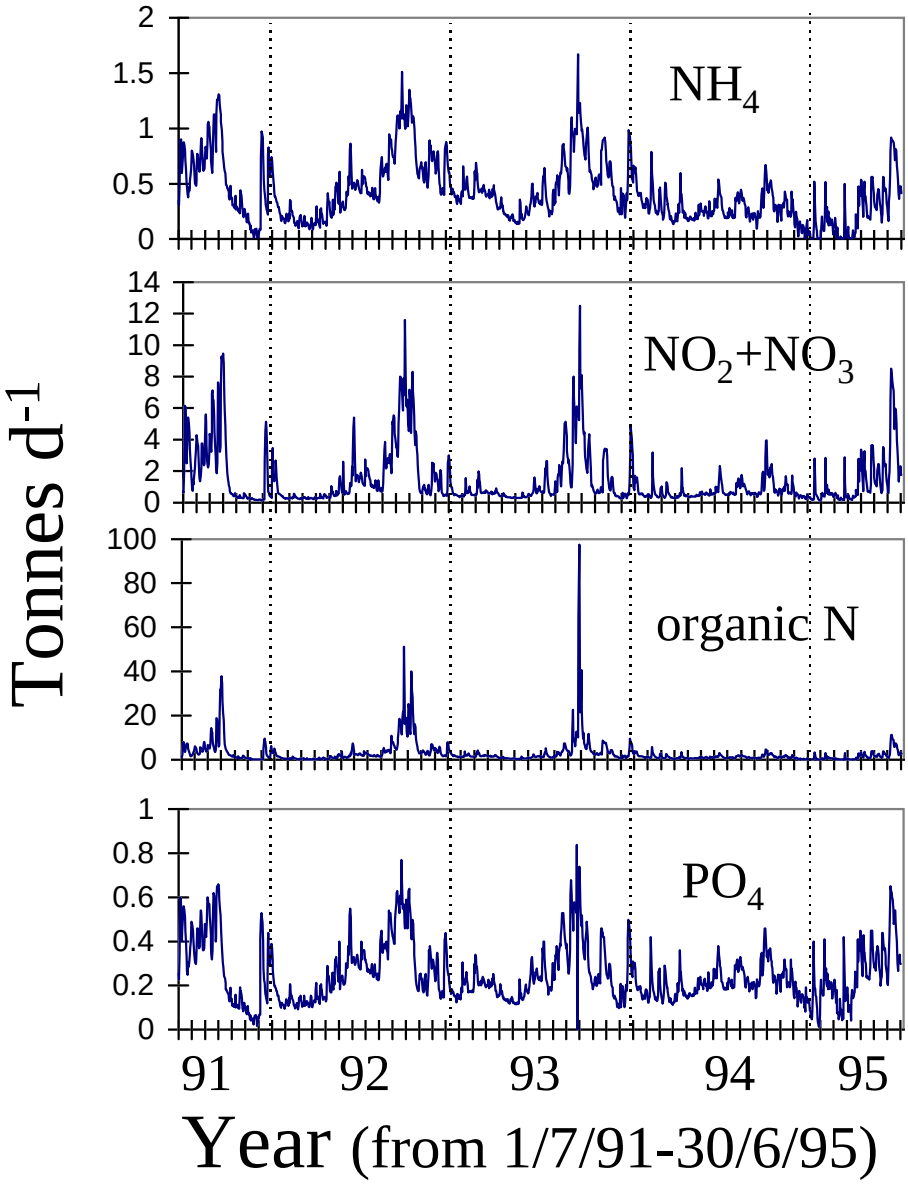

Figure 5.5 Inputs to Port Philip Bay of ammonia, nitrate + nitrite, organic nitrogen and phosphate 1/7/91-31/6/95 from the Yarra River, as predicted by the model of Sokolov (1996).

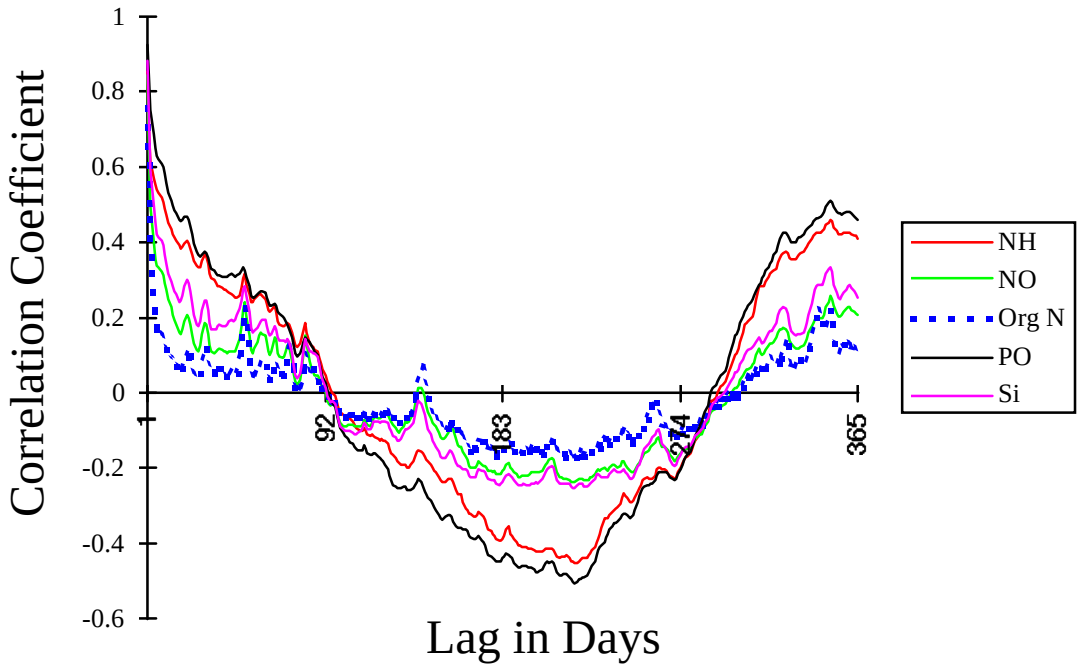

Figure 5.6. Autocorrelation of Yarra discharges.

Silicate was not included in the historical catchment monitoring program, but was measured in the PPBES Westgate monitoring program. From this last data set, Sokolov (1996) derived a relationship between NFR and Si loads:

$$\text{LoadSi} = -3808 + 365.\text{L\_NFR}^{0.3270}$$

which has been used to estimate Si loads from the Yarra. However this formula does not work in the Patterson-Mordialloc systems. For this system, a constant concentration of 8 mg Si L^{-1} was assumed, based on the analysis of catchments and loads in Phase One (MMBW/FWD 1973), and multiplied by runoff to obtain Si loads. By this calculation, discharge from the Patterson River is a very significant source of Si, and one that exhibits very large interannual variation. Estimated silicate loads from each source are shown in Fig. 5.9.

To the extent that Si inputs into Port Phillip Bay are important (see Chapter 7), the lack of recent monitoring of Si loads is a problem. Assuming that Si is not buried in the Bay, the total annual load must match the annual export. The mean Si pool in the PPB water column is estimated at ca 3300 tonnes. For a flushing time of 1 year, and allowing for a correction for the Bass Strait concentration amounting to 10 to 20%, this implies a mean annual load of about 2700 to 3000 tonnes Si y^{-1}. This is certainly comparable with our estimates of the catchment load. The estimated water column Si pool varies over months from 1025-6658 tonnes, reflecting variation in inputs and storage in sediments.

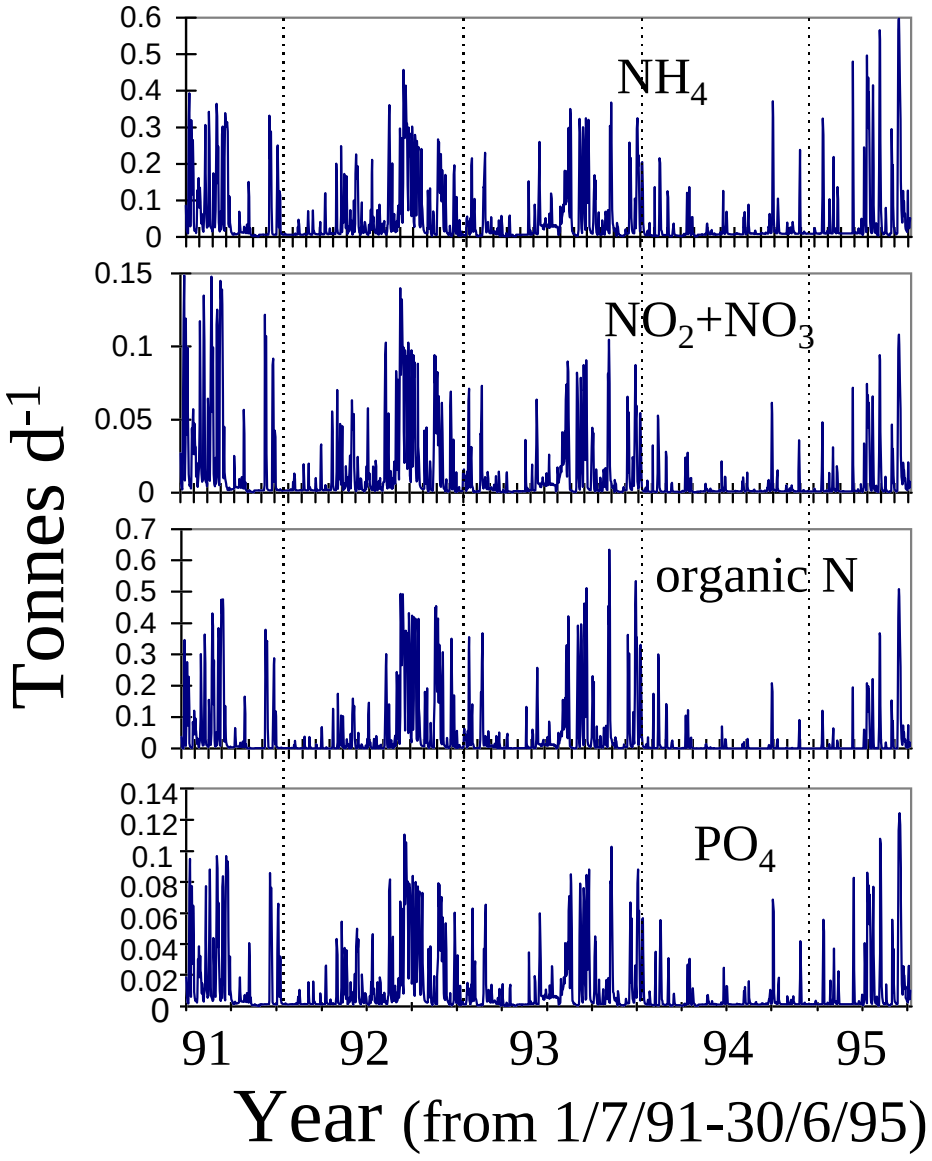

Figure 5. 7 Inputs to Port Phillip Bay of ammonia, nitrate + nitrite, organic N and phosphate from the Patterson River 1/7/91-31/6/95, as predicted by the model of Sokolov (1996).

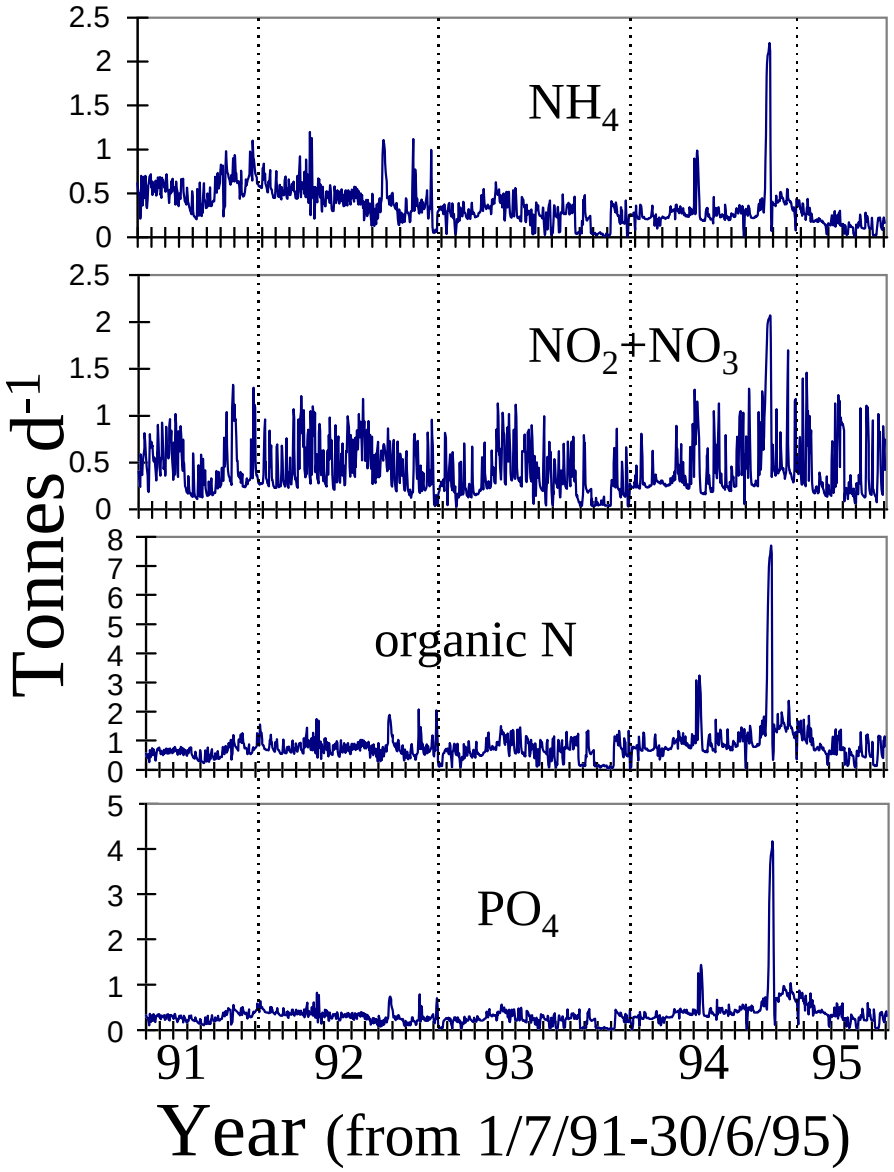

Figure 5.8 Inputs to Port Phillip Bay of ammonia, nitrate + nitrite, organic N and phosphate 1/7/91-31/6/95 from the Mordialloc River, as predicted by the model of Sokolov (1996).

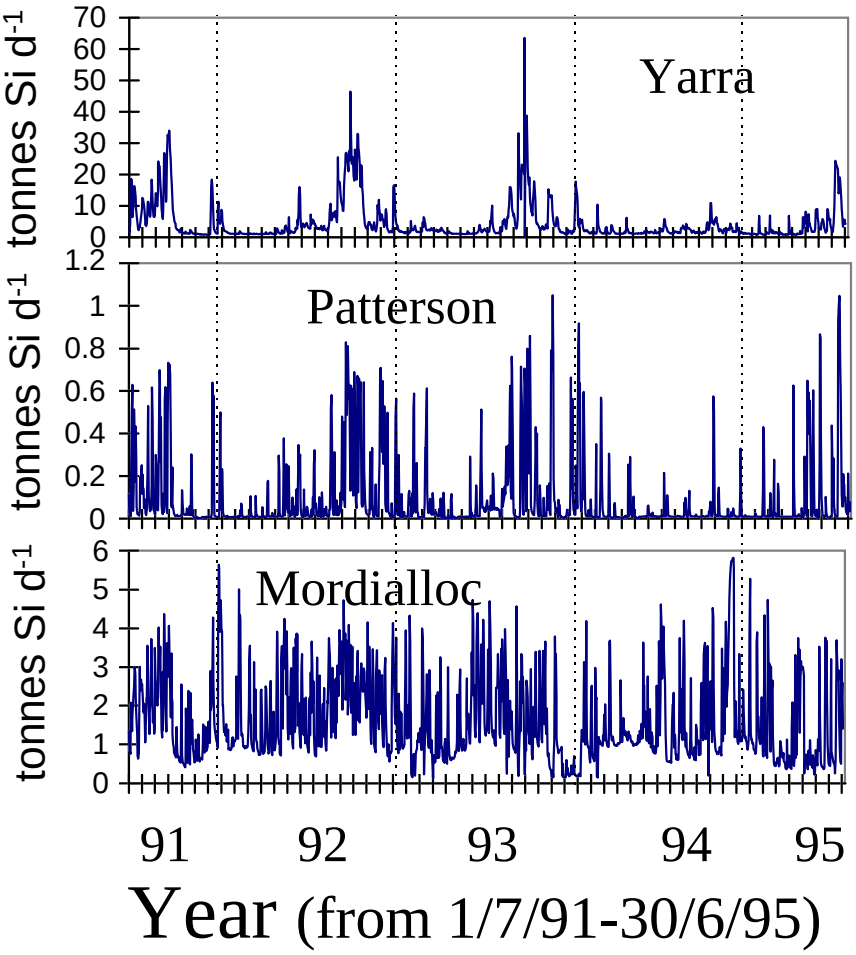

Figure 5.9 Silicate discharges from Yarra, Patterson and Mordialloc Rivers 1/7/91-31/6/95. The data is estimated by methods explained in the text.

5.3 Inputs from minor creeks

The estimates of annual loads prepared by NSR (1993) indicate that average nutrient inputs from other creeks and drains are generally negligible compared with the WTP, Yarra and Patterson-Mordialloc contributions. (This is not necessarily the case for toxicants.) However, there is subsequent evidence that inputs of nutrients from the Werribee River and Kororoit Creek in a single runoff event lasting a few days in 1993 exceeded by a considerable margin the NSR estimates of annual load from these catchments. There are no direct data on nutrient concentrations in runoff during this event, but if one uses the measured runoff volume, and the typical concentrations under normal flow conditions (NSR Consultants 1993), the event N load for the Werribee River was about 300 tonnes N. An indirect estimate of 75 to 125 tonnes N was obtained based on nitrogen-salinity relationships measured near the mouth of the Werribee River (Harris *et al*. 1996). We have used both of these estimates in model experiments to

examine the local impact of intense runoff events of this kind. As Fig. 5.10 shows, runoff from the Werribee River was insignificant at other times.

Time series of loads from Werribee River and Kororoit Creek were estimated by multiplying runoff by mean concentrations (mg L^{-1} of N, P or Si) from Kororoit Creek and Werribee River, based on NSR (1993) and Phase One data (MMBW/FWD 1973) (Table 5.2).

Table 5.2. Mean concentrations (mg L^{-1}) in runoff from Kororoit Creek and Werribee River (NSR 1993; MMBW/FWD 1973).

	NOx	NH4	OrgN	PO4	Si
Kororoit	1.7	0.5	3.1	1.05	10
Werribee	2.3	0.08	0.52	0.75	10

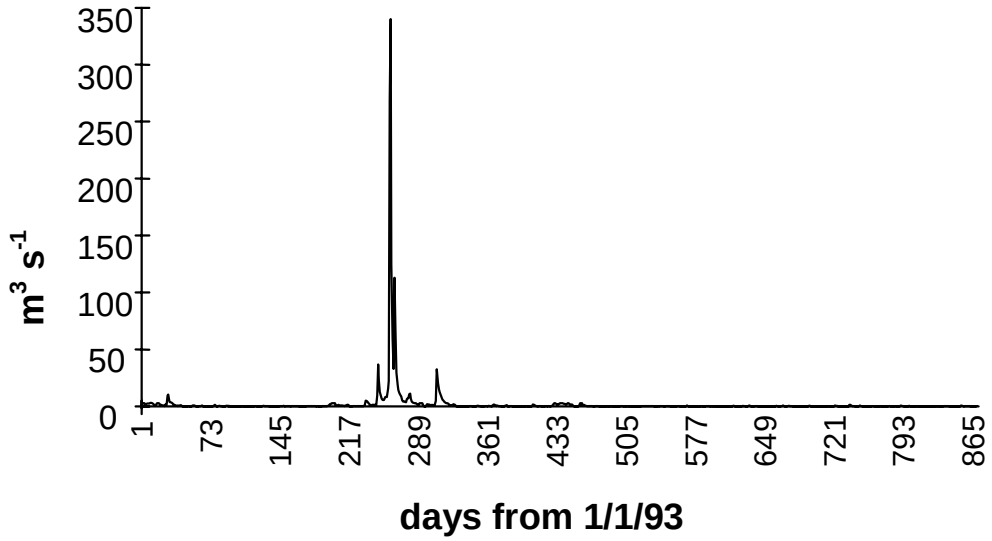

Figure 5.10 Flows in the Werribee River 1993-5

5.4 Bass Strait boundary conditions

The fixed monitoring sites in Port Phillip Bay were extended during the study to include a station N1 located at the Heads, to provide data on the nutrient and chlorophyll concentrations involved in exchange with Bass Strait. This area is subject to strong tidal currents, and potential aliasing from the tides. In 1993, the station was sampled only once on each monthly survey without regard to tide. In 1994, the station was sampled twice at midtide inflow and midtide outflow (Figs. 5.11-5.15).

Analysis of nutrient profiles from station N1 indicates that there may be significant differences in depth averaged concentration in inflowing and outflowing water. However the difference between the values at midtide inflow and outflow in 1994 is less than the range of concentrations recorded in 1993 when measurements were taken without respect to tide. (One would expect the extreme concentrations to be recorded at the end of the ebb and flood.) This suggests the extreme values were missed in 1994

and thus Bass Strait concentrations may be overestimated. In general, one would expect Bass Strait concentrations to correspond to the lower envelope of observed concentrations, except in the case of nitrate, where Bass Strait may act as a source.

Analysis of data from station N1 shows no significant seasonal pattern in observed concentrations. Given the uncertainties due to sampling and tidal aliasing, and the lack of any apparent seasonal pattern, we have adopted constant boundary conditions at Bass Strait. Fortunately the slow exchange with Bass Strait makes the model insensitive to this boundary condition (except of course for local predictions over the outer Sands). This would not be the case in other estuarine systems with high flushing rates.

Chlorophyll varies from 0.5 to 1.5 mg m^{-3} (Fig. 5.11), and we have used 1 mg m^{-3}. Ammonia concentration is somewhat less than 0.5 μM (Fig. 5.12), and we have used a concentration of 5 mg m^{-3} as our boundary condition. There is no clear seasonal signal, but some suggestion of a decline through the period of observation.

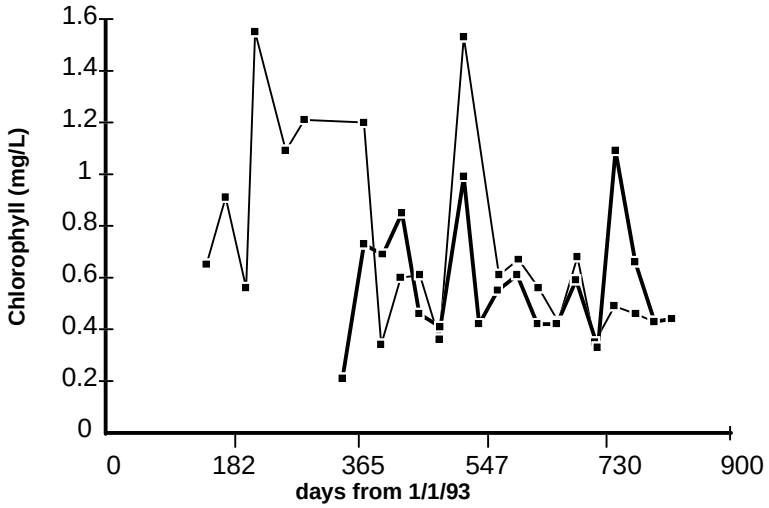

Figure 5.11 Chlorophyll on ebb (thick line) and flood (thin line) tides at Port Phillip Bay Heads (N1E and N1F).

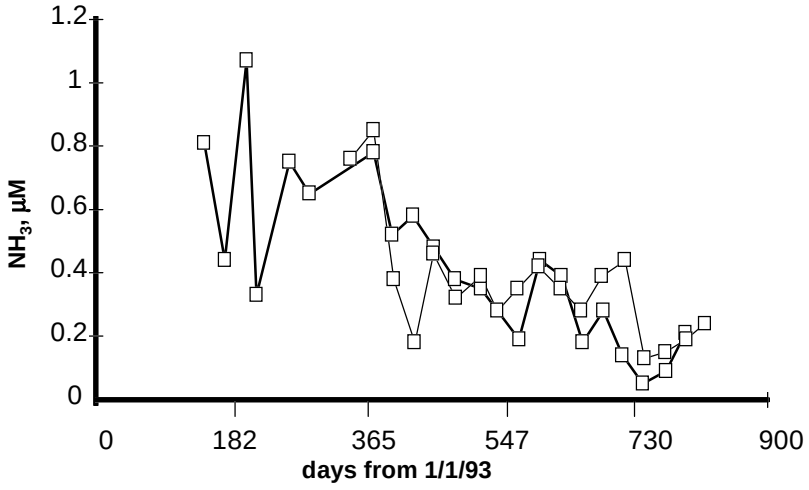

Figure 5.12 Ammonia on ebb (thick line) and flood (thin line) tides at Port Phillip Bay heads (N1E and N1F).

Nitrate/nitrite and phosphate are both about 0.5 μM (Fig. 5.13, 5.14) and this value has been used as the boundary condition. It could be argued that 0.25 μM might be more consistent with the phosphate flood observations and other Bass Strait observations (Gibbs *et al*.1986). NOx does appear to show a marked seasonal cycle in 1994, with a maximum in winter, although this is obscured by the large variation recorded in 1993.

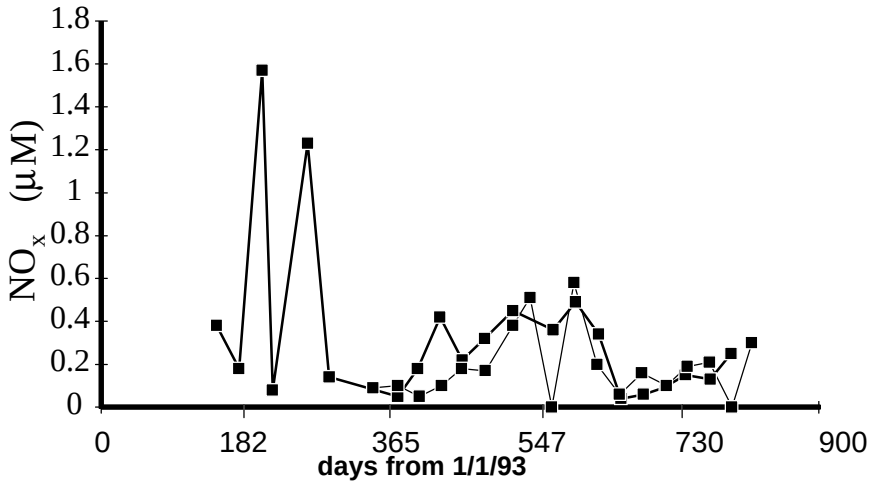

Figure 5.13 Nitrate + nitrite on ebb (thick line) and flood (thin line) tides at Port Phillip Bay heads (N1E and N1F)

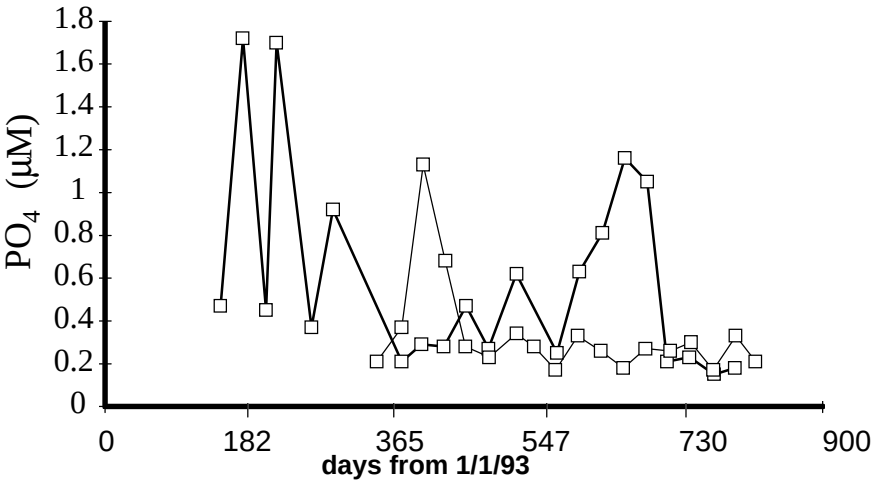

Figure 5.14 Phosphate on ebb (double line) and flood (single line) tides at Port Phillip Bay heads (N1E and N1F)

Dissolved organic nitrogen (DON) in Port Phillip Bay is in excess of Bass Strait concentrations. We expect oceanic and Bass Strait waters to contain a background level of very refractory DON, which would not participate significantly in biogeochemical cycles in the Bay. We have made the simplifying assumption that the DON in Bass Strait is refractory, and that it is only that portion of DON in Port Phillip Bay in excess of the Bass Strait concentration that is represented by the model DON (ie. produced and remineralized according to the model dynamics described in earlier chapters). Accordingly, the Bass Strait concentration for the model DON is set to zero.

The observed Bass Strait concentration must be subtracted from observations in order to compare them with model predictions. Based on the observations, we have used a constant Bass Strait background of 6 μg at N L^{-1} or 80 mg N m^{-3}. There is some evidence of seasonal variation in DON at station N1, with higher values in summer (Fig. 5.15). If we assume that the winter minimum in Bass Strait does represent truly refractory DON, then strictly speaking, we should impose a seasonal cycle in DON at the boundary between zero and about 2 μg at N L^{-1}.

Silicate concentrations in Bass Strait are of order 0.5 μM, or 14 mg m^{-3} (Gibbs *et al*. 1986). Observed silicate concentrations at site N1 (Fig. 5.16) are also generally less than 1 μM. The silicate concentrations show occasional much larger peak values, but there is no obvious pattern at seasonal or other time scales.

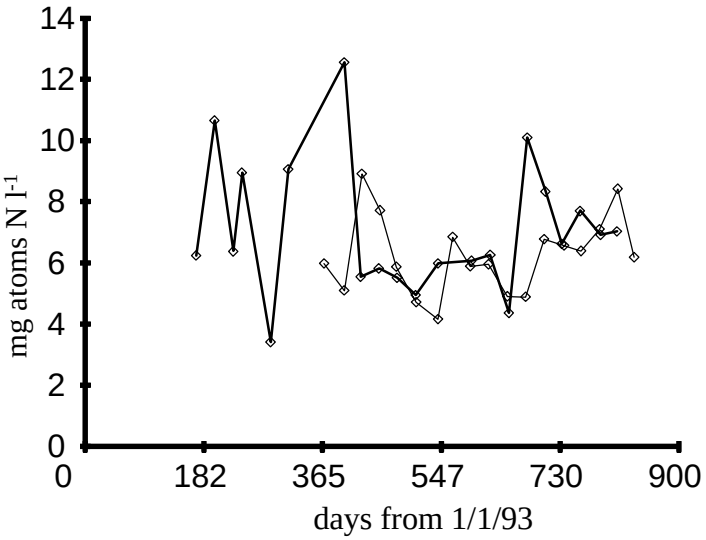

Figure 5.15 DON concentration on ebb (thick line) and flood (thin line) tides at Port Phillip Bay heads (N1E and N1F)

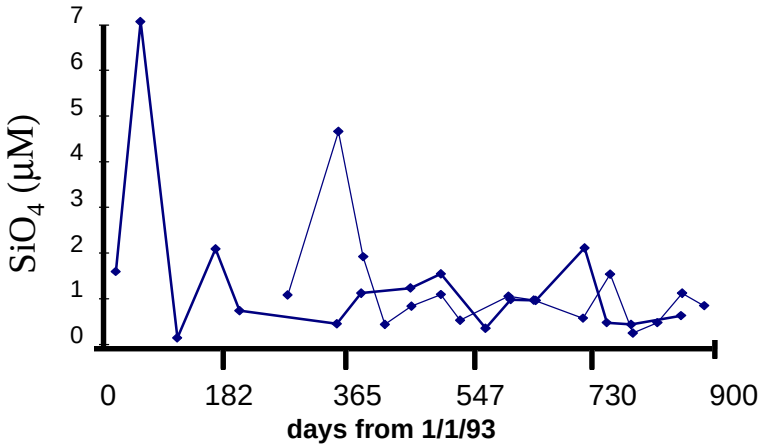

Figure 5.16 Silicate concentration on ebb (thick line) and flood (thin line) tides at Port Phillip Bay heads (N1E and N1F)

We have no independent data on zooplankton concentrations in Bass Strait. Zooplankton concentrations at the boundary were based on typical modelled Bay-centre values in order to minimise exchange across the boundary and thereby minimise boundary effects in the Sands.

The Bass Strait boundary concentrations used in the model are listed in Table 5.3.

Table 5.3. Bass Strait boundary conditions for biogeochemical model variables.

PL	3 mg N m^{-3}
PS	3 mg N m^{-3}
DF	2 mg N m^{-3}
Chl	1.14 mg N m^{-3} (0.86 for model versions without dinoflagellates)
ZL	7 mg N m^{-3}
ZS	2 mg N m^{-3}
NH_3	5 mg N m^{-3}
NOx	5 mg N m^{-3}
PO_4	15 mg P m^{-3}
DON	0 mg N m^{-3}
SiO_4	14 mg Si m^{-3}

5.5 Atmospheric and groundwater inputs

We currently have only crude estimates of annual atmospheric nitrogen loads, and no estimates of annual P or Si loads (Beer *et al*. 1992). We have specified nitrate and ammonium loads of 500 tonnes N y^{-1} each, distributed uniformly over the entire Bay and throughout the year. We have not included estimates of N_2O loads, which are assumed to be biologically unavailable. An atmospheric load of 1000 tonnes N y^{-1} is a significant contribution to the N budget, and, given the uncertainties surrounding this estimate, atmospheric inputs deserve more attention in future studies.

A review of groundwater inputs suggested that these are small compared with surface inputs, and unlikely to contribute significantly to the Bay's nutrient budget (Hydrotechnology 1993). Because groundwater integrates surface inputs over a long period, there are unlikely to be groundwater input events comparable to those observed for surface streams such as Werribee River. Groundwater inputs could be significant in terms of benthic fluxes in particular locations of limited spatial extent.

5.6 Irradiance, temperature and other physical forcing

Observed total irradiance inputs are used in the model. The data were also used to drive heating in the physical model. The total short-wave irradiance is converted to PAR by multiplying by 0.5. PAR data was available from June 1994 to the end of October 1995 (You *et al*. 1996) but not for the entire period of the model. Fortnightly PAR data is available from the fixed sites, but this temporal resolution is too coarse to be useful.

Temperature was calculated using the sinusoidal seasonal curve derived in Chapter 3. This simple model provides a good fit to observations (Fig. 5.17). Throughout the Study period, thermal stratification is weak, and the effect of any vertical gradient in temperature on biological rate processes is negligible.

Forcing for the physical hydrodynamic and transport models is discussed by Walker (1997a,b). Forcing data sets for these models have been obtained for the period 1990 to 1995, and the models have been run and calibrated over that period.

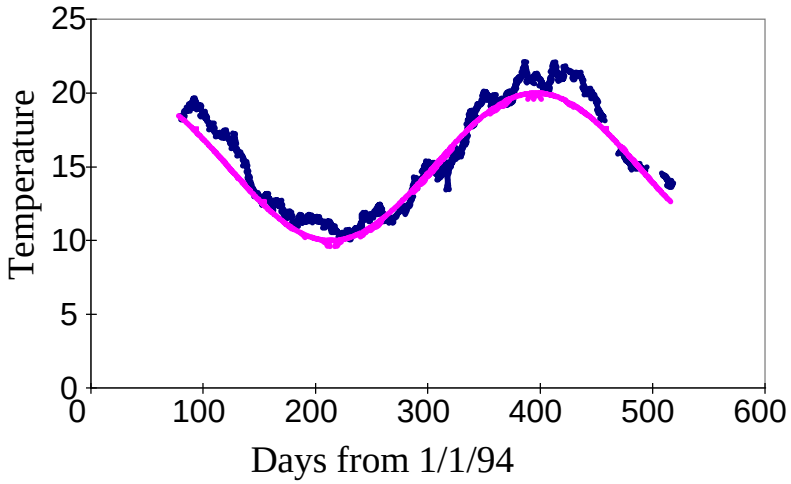

Figure 5.17 Midday water temperatures at Hovel Pile as recorded in 1994 and 95, and sinusoidal fit to daily average temperature.

5.7 Discussion

Specifying the time-dependent nutrient loads into a system as large as Port Phillip Bay is not a straightforward task. The PPBES was not designed to include catchment studies: it was originally envisaged that catchment studies would proceed in parallel with the PPBES. Apart from WTP itself, monitoring of nutrient loads to Port Phillip Bay has not been carried out on a consistent basis. The Study has been forced to rely heavily on historical data, and on the catchment models developed by Sokolov. While these appear to perform well, there are uncertainties related to event resolution, and to the siting of monitoring stations upstream from discharges to the Bay. The latter is a particular problem for the Yarra estuary, and it would be desirable to have a longer time series of data to calibrate Westgate load models.

It is highly desirable that monitoring programs be implemented in the catchment to allow improvement and updating of estimates of loads to the Bay. Monitoring design should take the needs of catchment models into account, specifically with regard to sites and sampling frequency and timing with respect to runoff events. Given the role of silicate identified by the PPBES, this nutrient should be added to catchment monitoring programs. It is also desirable that estimates of atmospheric loads (both annual averages and temporal and spatial variation) be improved.

6 MODEL ANALYSIS

In Chapter 2 we described ecosystem modelling approaches ranging from very simple budgets to dynamic spatially resolved models. This technical report is intended primarily to describe the development and calibration of the dynamic spatially resolved simulation model presented in Chapter 3. However, results derived from simpler models and analyses, presented in this chapter, provide valuable insight into the Port Phillip Bay ecosystem, and the behaviour of the full model. The Chapter begins with simple mass balances of Bay-wide inputs and outputs, and then introduces the concepts of recycling and export efficiencies which link external loads to primary production. We then introduce and analyse simple one-box models of nutrient recycling in planktonic systems, and consider the factors that control water column recycling efficiencies. We briefly describe the key results from process-based models of sediment biogeochemistry, and then discuss simpler empirical denitrification submodels and their implications for the Bay-wide response to increasing nutrient loads. Finally, we extend the discussion to include local and transient responses of the full model.

6.1 Baywide mass balance

The simplest analysis of Port Phillip Bay's nutrient dynamics is a comparison of inputs and outputs of nutrients for the Bay as a whole. The difference must represent a net sink or source of nutrients within the Bay itself. We have a reasonably good knowledge of inputs (Chapter 5) and, for reasons that will be explained here, we are also able to constrain exports quite tightly. This means in particular that we are able to demonstrate convincingly, and quantitatively, the importance of interior sinks of nitrogen in Port Phillip Bay.

We are concerned here with inputs and exports of total N, total P and total Si, including dissolved and particulate, inorganic and organic forms. Estimates of inputs were obtained as described in Chapter 5. If we approximate Port Phillip Bay as a single well-mixed box, the export to Bass Strait can be estimated as:

$$\text{Export} = (\text{average concentration in PPB} - \text{concentration in Bass Strait}) \cdot \frac{\text{Bay volume}}{\text{flushing time}}$$

It is important to remember that this equation is approximate, and the approximations can involve substantial errors. In Port Phillip Bay, exchange through the constricted entrance and across the Sands is limited, and estimated flushing times (based on salinity budgets) are long, of order one year, compared with mixing times for the Bay interior. This means that the one-box approximation is likely to be good, especially for conservative tracers. For non-conservative tracers with dynamics that are fast compared with interior mixing times, especially DIN and phytoplankton N, there may still be substantial errors in using average Bay-wide concentrations to estimate export.

According to the one-box approximation, for a flushing time of one year, the annual export is equal to the mass of excess tracer (ie. excess over Bass Strait concentrations) in the Bay water column. Estimates of Bay-wide pools are subject to statistical problems

of interpolation and extrapolation (Longmore *et al*. 1996). In an effort to address spatial heterogeneity and biased sampling (coastal regions were more likely to be visited than the central Bay), a variety of statistical approaches were used to calculate mean concentrations from the data collected by the PPBES field program. The detailed monthly surveys provided an adequate basis for estimates of Bay-wide pools. In the case of Si, which is extremely variable in time, but fortunately less variable in space, the Bay-wide pool varied strongly from month to month. It is only because we have a large number of estimates of the Bay-wide pool in all seasons that we can compute annual average pools and exports.

The pool of total P is dominated by inorganic phosphate, and phosphate concentrations are high and relatively uniform throughout the Bay, except for elevated concentrations near inputs, and the mixing gradient across the Sands. As noted previously, this distribution is consistent with the behaviour of a conservative tracer. Although P participates in biogeochemical cycles in the Bay, it is present in such excess that it behaves approximately conservatively. The estimate of annual P export (1200 tonnes P y^{-1}) from the equation above is close to the estimated annual load of 1500 tonnes P y^{-1}, indicating that net burial rates of P within the Bay are low compared with annual loads.

Si is more difficult to deal with than P because the Si concentration varies widely on seasonal and shorter time scales, driven by variation in loads, phytoplankton uptake and release from sediments. Temporal and spatial averaging errors increase uncertainty about the mean pool size, and the applicability of a one-box flushing model is less clear. As noted in Chapter 5, the annual load of Si is also not well known. However, the mean estimated Bay-wide Si pool of 3300 tonnes (May 93 - March 95, Longmore *et al*. 1996) is certainly within error bounds about the (uncertain) estimate of the annual load of about 4200 tonnes Si y^{-1} presented in Chapter 5. We conclude, as for P, that there is no firm evidence for high rates of Si burial in the Bay.

The total N pool in Port Phillip Bay is about 3600 tonnes, and consists primarily of DON, which like phosphate has a spatial distribution consistent with that of a conservative tracer. (Some of this DON may be of terrestrial origin, highly refractory and practically conservative.) However, there is a large pool of refractory DON in the oceans, and the concentration in Bass Strait is approximately 2/3 that of the Bay, so that the estimate of net export is less than 1600 tonnes N y^{-1}. Since annual loads are of the order of 7000 tonnes N y^{-1}, it is apparent that most of the N input is not exported from the Bay, and is either buried in sediments or lost to denitrification.

6.2 Internal nutrient turnover

Continuing the theme of Bay-wide mass balance, we now consider the relationship among primary production, recycling and export fluxes in both the water-column and in the sediment.

DIN concentrations in the water-column are low and relatively constant, except in the close vicinity of sources, and the Bay-wide DIN pool is small, of order 300 tonnes N. On the other hand, estimates of annual primary production are large, of order 30000

tonnes N y^{-1}. It follows that the DIN pool turns over quickly, about 100 times per year, and that, at least throughout much of the Bay most of the time, phytoplankton N uptake and DIN supply are in close balance. The particulate organic matter produced by phytoplankton has one of two fates: it is either remineralised in the water column, releasing DIN, or falls to the sediment. The organic matter reaching the sediment is either buried or remineralised, and the DIN released is either returned to the water column through diffusion and bioirrigation, or lost to denitrification. These cycles are shown schematically in Fig. 6.1.

We thus have two steady-state mass balance equations, one for supply of DIN to the water column:

Primary Production = External Load + Water Column Recycling + Sediment Release

and one for the fate of organic matter:

Primary Production = Water Column Recycling + Denitrification / Burial + Sediment Release

We define an export efficiency for the water column f_w as the fraction of primary production exported to the sediment. (This is analogous to the export efficiency or "f-number" defined for pelagic systems.) We also define f_d as the proportion of organic matter reaching the sediment which is either buried or lost to denitrification. As we discuss later, there is evidence that denitrification is the dominant loss term, and at times we refer to f_d as the denitrification efficiency. It follows from these definitions that:

$$\text{Water Column Recycling} = (1-f_w) \,.\, \text{Primary Production}$$

and

$$\text{Sediment Release} = f_w \,.\, (1-f_d) \,.\, \text{Primary Production.}$$

Substituting in the above equations, and reaaranging, we obtain the result:

$$\text{Primary Production} = \text{External Load of DIN} / (f_w \,.\, f_d)$$

This equation is important because it relates the external load to primary production, which is in turn closely related to phytoplankton biomass, water quality and the degree of eutrophication. It says that primary production is amplified over the external load by an amount which increases as water column export efficiency and denitrification efficiency decrease. For Port Phillip Bay currently, this amounts to an amplification of about four to five times.

In these equations, we have ignored the external export of N to Bass Strait, which is small compared with external loads and internal fluxes (see previous section). Under this approximation, the external load must equal the loss to denitrification and/or burial. It is possible to modify the equations to include the effect of export to Bass Strait. This becomes important at higher loads (see Section 6.7).

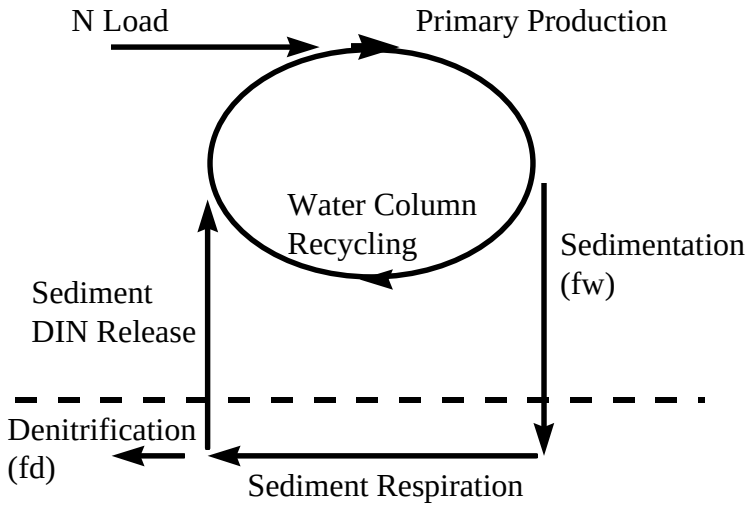

Figure 6.1 Cycling of nitrogen through the water column and sediment.

Input to the Bay is around 7000 tonnes N y^{-1} and estimates of phytoplankton production range from 25,000 to 35,000 tonnes N y^{-1} (see Chapter 7) implying a range for f_w . f_d of 0.2 to 0.28. Total primary production that results in consumption of water-column N should also include macroalgal primary production. The value of this is unknown, but given an estimated mean biomass of order 500 tonnes N (Chidgey and Edmunds 1997), additional annual production of a few thousand tonnes N is expected (for more discussion, see Chapter 7).

The export efficiency from the water-column to the sediment (f_w) depends on the nature of the water-column community and the local environment. Communities dominated by small, heavily grazed phytoplankton are likely to have lower export efficiencies than communities where large phytoplankton dominate production. Macroalgal production is less likely to be grazed and most of its production may be exported as detritus to the sediment. The details of the interactions of these communities are complex and are discussed in more detail in section 6.4.

Port Phillip Bay differs from some other emBayments in that the flushing time is long, and denitrification rather than export to Bass Strait is currently the principal process for removing N. However, if conditions in the Bay changed so that the denitrification efficiency f_d approached zero, the above analysis predicts a rapid increase in primary production. As discussed in section 6.4, a more complete analysis shows that, as f_d approaches zero, levels of DIN or chlorophyll will increase to the point where flushing replaces denitrification as the principle N loss, and the Bay becomes severely eutrophied.

According to the simple analysis presented above, DIN release from the sediments equals the external N load times ($1/f_d$ -1). Nicholson *et al*. (1996) have made two estimates of DIN release from sediment for Port Phillip Bay of 8100 and 3600 tonnes N y^{-1}. Since input to the Bay is approximately 7000 tonnes N per year, these estimates of sediment release imply mean values of f_d of 46 or 66%. We have simplified by

neglecting the export of DON from Port Phillip Bay, which represents another loss term. When this is accounted for, estimates of f_d are slightly lower.

6.3 Steady-state pool sizes

In this section we continue to use one-box models and focus on the nitrogen cycle in the water column. We consider steady-state solutions for simplified dynamical models of interactions among nutrients, phytoplankton and zooplankton (so-called NPZ models). These solutions can be obtained as explicit or implicit mathematical expressions relating nutrient loads and biological parameters to the steady-state pool sizes. The solutions provide considerable insight into the response of marine ecosystems to changes in nutrient loads, and the dependence of model predictions on process formulation and parameter values.

Naturally, steady-state solutions do not tell us about the transient response of the system to perturbations and cannot be used in situations where perturbations and transients are major features of system behaviour. At high loadings, some formulations of the model may exhibit internally generated instabilities even under constant loadings (Rosenzweig 1971). A steady state analysis cannot describe such behaviour, but it can indicate the conditions under which steady-state solutions disappear or become unstable.

The simplest practical models of nitrogen cycling in planktonic systems are N-P or N-P-Z models which represent the interactions of a simple nutrient-phytoplankton-(zooplankton) system. We present some of the key results for N-P-Z models here; more details will be presented elsewhere (Murray and Parslow, in preparation). A simple version of the N-P-Z model has the form:

$$dP/dt = \mu_I\, P\, N/(K_N+N) - gZP - m_p P$$

$$dZ/dt = egZP - m_Z Z$$

$$dN/dt = I_X + f_M m_Z Z + f_G(1-e)gZP - \mu_I\, PN/(K_N+N)$$

Many of the parameters in this simple model are identical to ones used in the final model; however others differ because of the simplifications involved. For this reason a modified nomenclature is adopted in this section. (We have used the N-P-Z notation here because it is widely used in the literature. We note the potential for confusion between the use of "P" for phytoplankton in this section, and its use to denote phosphorous elsewhere in the report, and hope the reader will bear with us.) Here I_X is the input of N to the water column, including input recycled by breakdown of detritus, but not that recycled directly from grazing. The parameters are μ_I, the light-limited nutrient-saturated growth rate; K_N, the half saturation constant for growth on DIN; g, the clearance rate; e, the zooplankton growth efficiency; and f_G and f_M, the proportions of zooplankton waste and mortality respectively which are released as DIN. The parameter m_p is the specific mortality rate of phytoplankton and m_Z is the specific loss rate of zooplankton.

Steady-state solutions are obtained by setting the time derivatives to zero.

Setting dZ/dt = 0, we obtain:

$$egZP = m_Z Z$$

so $P = m_Z/eg.$

Setting dP/dt = 0 and dN/dt = 0, and summing, we obtain:

$$gZP + m_p P = I_X + f_M m_Z Z + f_G(1-e)gZP$$

and, after rearranging:

$$Z = (I_X - m_p P)/(gP - f_M m_Z - f_G(1-e)gP).$$

Back substituting gives:

$$N = K_N(gZ + m_p) /(\mu_I - m_p - gZ)$$

The solution for Z breaks down if loading is too low ($I_X < m_p P$). There is another solution with Z = 0:

$$P = I_X/m_p$$

$$N = K_N m_p(\mu_I - m_p)$$

The key features of these results are maintained for more complex formulations of zooplankton grazing. If the grazing functional response is given by the function *G*(P), then the steady state solution for P is given implicitly by $G(P) = m_Z/e$, and P is still a constant, independent of nutrient load. For example, if $G(P) = gP/(1 + egP/g_{max})$ (Type II functional response, g_{max} is the maximum growth rate) then:

$$P = m_Z/(eg. - m_Z g/g_{max}).$$

The steady-state equations for Z and N in terms of P are still valid.

These steady state solutions of the simple model show the following characteristic response of N, P and Z to changing loads: at low loads, Z = 0, N is a constant independent of load and P increases linearly with load; at higher loads, P is a constant independent of load, Z increases linearly with load and N increases at an accelerating rate (Fig. 6.2). If the nutrient load is increased further, it eventually reaches a level where it exceeds phytoplankton uptake capacity, even at maximum growth rate, and N begins to accumulate. At this point, the steady-state solution breaks down, and is replaced by limit cycle solutions involving large amplitude blooms. (In fact, the steady-state solution becomes unstable at somewhat lower loads.) Once N concentrations start to accumulate to significant levels, N export through flushing, which is ignored in this simple model, becomes important. If flushing is included, it has the effect of restoring a

steady-state solution at very high loads, with Z reaching an asymptotic level, and N increasing linearly with load. However, for most realistic grazing responses, this solution is still unstable, and large amplitude blooms occur.

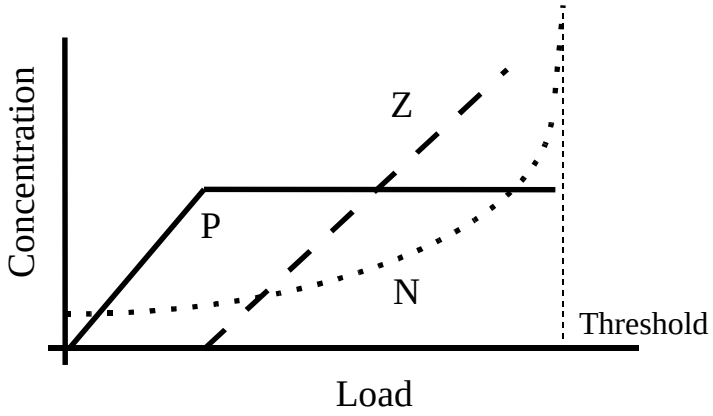

Figure 6.2 Variation in concentrations of N, P and Z with load under linear zooplankton mortality.

The most striking aspect of this analysis is the prediction that phytoplankton biomass can remain constant while loads increase, until suddenly a threshold load is exceeded, and large blooms occur. Behaviour of this type would have serious management implications. However, this prediction depends on the formulation of the interaction between phytoplankton and zooplankton. The steady-state phytoplankton concentration in this model is determined entirely by zooplankton parameters, and in particular by the balance between the zooplankton specific growth rate, and the (constant) zooplankton specific mortality rate.

Other formulations of zooplankton mortality have been suggested. Steele and Henderson (1992) have argued that the zooplankton specific mortality rate should increase with zooplankton biomass, reflecting switching or aggregation by zooplankton predators. Under this assumption, zooplankton losses are proportional to Z^2. We refer to this as quadratic zooplankton mortality, and the first version as linear zooplankton mortality. If one substitutes the quadratic mortality term in the above model, one can obtain a steady-state solution as before. Now, setting $dZ/dt = 0$ yields $P = m_{QZ}Z/eg$; ie. P and Z increase in proportion as load increases. NPZ models incorporating quadratic zooplankton mortality no longer predict steady-state solutions with constant phytoplankton biomass independent of load. After some algebra, one can obtain the relationship:

$$Z = \{ -m_p/g + [(m_p/g)^2 + 4\gamma e I_X/m_{QZ}]^{1/2} \} / 2\gamma,$$

where $\gamma = (1 - e.f_M - f_G(1-e))$.

According to this result, at very low loads, when phytoplankton losses are dominated by natural phytoplankton mortality, Z and P increase linearly with load. However, as loads increase further, and grazing losses dominate over natural phytoplankton mortality, Z and P increase in proportion to the square root of load (Fig. 6.3). The steady-state relationship between N and Z derived for the linear mortality model still holds for the

quadratic mortality model. It follows that the steady-state value of N increases in an accelerating way. Eventually, this steady-state also breaks down. The reason is that P increases only like the square root of the load, so that eventually the N load must exceed the maximum phytoplankton uptake capacity and nitrogen starts to accumulate. As before, the model then needs to be extended to allow for export of N through flushing. This restores a steady-state solution in which N is large, phytoplankton growth is nutrient saturated, and P and Z approach asymptotic maximum values. This steady-state solution at high loads is now stable.

However, if we replace the simple and unrealistic grazing formulation by a Type 2 functional response, the model behaviour at high loads becomes potentially more complicated. There is now a maximum possible zooplankton biomass, given by $Z = g_{max}/m_{QZ}$, and consequently a maximum clearance rate. If the nutrient saturated phytoplankton growth rate exceeds this maximum clearance rate, then phytoplankton biomass can escape zooplankton control. In this case, once Z approaches its maximum level, P increases linearly with further increases in loading. Although steady-state solutions of the quadratic mortality model always exist at high loads, their stability is not assured. For some parameter combinations, these steady-state solutions are unstable, and stable limit cycle solutions exist.

The dependence of steady-state solutions of the quadratic mortality model on loads can be summarised as follows. P and Z increase linearly at very low loads, and as the square root of loads as these increase further. N increases at a rate which is faster than P or Z. Then either zooplankton reach their maximum net growth rate and phytoplankton escape grazing control, or phytoplankton reach their maximum growth rate, and grazing controls phytoplankton biomass. In the latter case N increases linearly with further increases in loads, which are balanced primarily by export of DIN through flushing. In the former case, P increases linearly with load, N declines, and loads are balanced primarily by export of P. In more realistic models, factors such as self shading also limit growth rates of phytoplankton, arresting and then reversing the fall in N.

The implications of the two zooplankton mortality formulations for management are very different. Under linear zooplankton mortality, the models predict a sudden breakdown in the water-quality of the Bay as loads cross a threshold level. Under quadratic mortality, a more gradual decline in water quality is predicted, and monitoring chlorophyll will give a good indication of the state of the Bay. If the linear mortality model applies, then chlorophyll will not increase significantly until the ecosystem has already crossed a load stability threshold. As argued in the Port Phillip Bay final report, if we look widely across all water bodies, chlorophyll concentrations do show increases of perhaps an order of magnitude between oligotrophic clear oceanic waters and mesotrophic coastal waters (such as Port Phillip Bay) without exhibiting gross instability. Indeed in Port Phillip Bay, the Bay centre chlorophyll levels declined substantially between the high nutrient input in 1993 and the much lower input in 1994. This tends to suggest that the quadratic mortality formulation is more realistic.

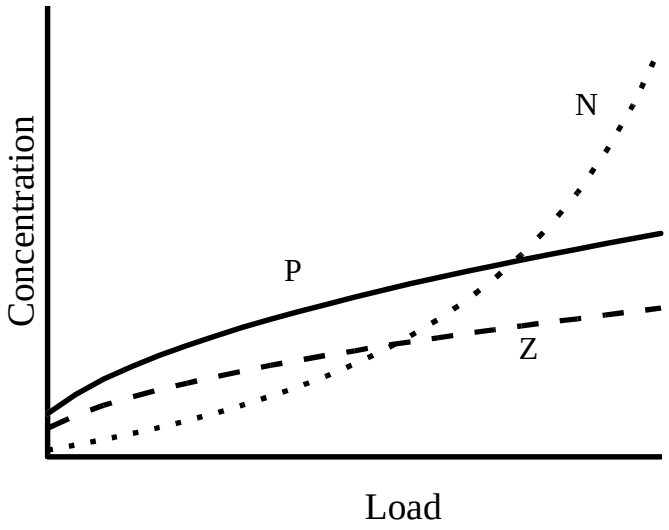

Figure 6.3 Variation in concentrations of N, P and Z with load under quadratic zooplankton mortality.

The one-box steady-state analysis presented in this section offers some useful insights into the behaviour of more complex models, and of real systems close to steady-state. However, the results should be interpreted and applied with caution. Real systems are subject to spatially and temporally variable loads, and will produce blooms and transients even if the underlying dynamical model is stable. These effects are examined in detail using the numerical model in Chapter 7, and a qualitative analysis of some of these effects is presented in Section 6.8.

6.4 Factors controlling water-column recycling efficiencies.

In this section we consider the factors which control the fate of organic matter produced in the water column: ie. the relative magnitude of water-column recycling and export to the sediment. This principally depends on the nature of the plankton community and the outcome of competition among different primary producers. Even simple models of competition are complicated and highly non-linear. We have not obtained exact analytical solutions, but are able to present qualitative guidelines that we use in the investigation of the full dynamical model in Chapter 7.

In the models used in this study, inorganic nutrients are produced in the water-column through zooplankton excretion, or through remineralisation of suspended detritus. Because Port Phillip Bay is shallow, and detritus is assumed to sink quickly, most detritus reaches the sediment, and remineralisation of suspended detritus is a relatively small term. Zooplankton excretion of DIN is assumed to be a fixed proportion of zooplankton ingestion. Thus, the water column recycling efficiency depends on the fraction of production, which is grazed, as opposed to the fraction, which dies and/or sinks out of the water column.

Because large diatoms sink rapidly and small phytoplankton and motile dinoflagellates do not, it follows that, in diatom-dominated communities, a smaller proportion of production is grazed, and a larger fraction is exported to the sediments. Grazing on small phytoplankton may also result in more DIN release in the water column than grazing on large phytoplankton. Large zooplankton produce large rapidly sinking faecal pellets, while microzooplankton produce small slow sinking pellets which are more likely to break down in the water-column. Grazing is thought to make a minor contribution to macroalgal losses, and most macroalgal production is thought to be converted to detritus, and transported to the sediment.

We now consider the interaction of different phytoplankton groups. Phytoplankton groups can only co-exist if they are exploiting different niches. They compete for light and nutrients, and are subject to different grazers. In a spatially and temporally varying environment, coexistence may occur because different groups do better in different places or at different times.

The models used here allow coexistence of small and large phytoplankton classes even at steady state. One reason for this is zooplankton grazing, which tends to limit phytoplankton populations and maintain high phytoplankton growth rates, and hence high nutrient concentrations. This means that as populations of one class rise, so do the corresponding zooplankton populations and hence the grazing losses. This feedback can break down if phytoplankton populations approach levels which saturate zooplankton grazing. Due to their very high growth rates, microzooplankton can generally keep populations of small phytoplankton relatively low, even in the face of transient perturbations.

For the simplest model formulation, with linear zooplankton mortality m_Z and constant clearance rate g, the steady state solution for P is:

$$P = m_Z/eg.$$

More complex versions of the grazing functional response yield similar solutions. Microzooplankton have high clearance rates g (per unit biomass) but also high mortality rates, compared with mesozooplankton. The relative dominance of small and large phytoplankton in the model at steady-state can be tuned by adjusting clearance rates and mortality rates.

The models used here assume small and large zooplankton feed exclusively on small and large phytoplankton respectively. This kind of simplified trophic structure cannot be extended easily to larger numbers of size classes. For models with linear zooplankton mortality, each time an additional phytoplankton-zooplankton class is added, the steady-state phytoplankton biomass for the new class is added to the total biomass. For models with quadratic zooplankton mortality, the total phytoplankton biomass increases like the square root of the number of classes. In both cases, there is an upper limit to the number of classes that can coexist. It is clearly unrealistic for total phytoplankton biomass to depend on the arbitrary resolution of size structure, and models, which incorporate large numbers of size or functional classes need to allow more complex trophic interactions.

As noted in Section 6.2, levels of primary production are determined by external loads and internal recycling efficiencies. One might expect increases in nutrient supply and

primary production to favour large phytoplankton, which are intended to represent bloom organisms (diatoms) with higher maximum growth rates but lower affinity for nutrients. Under a linear zooplankton mortality formulation, the steady-state balance between small and large phytoplankton does not vary smoothly with nutrient supply. Over some intermediate range of nutrient loads, the steady-state biomasses of both classes are independent of load. As loads decrease, large phytoplankton and large zooplankton will disappear at the point where nutrient concentrations become too low to support large phytoplankton loss rates due to sinking. As loads increase, eventually the steady-state solution will become unstable, and both classes will fluctuate, with large phytoplankton becoming increasingly dominant on average.

Under a quadratic mortality formulation, the ratio of small to large phytoplankton varies more smoothly with nutrient load. Small phytoplankton are favoured at low loads and low nutrient concentrations, while large phytoplankton are favoured at higher loads. However, depending on the parameter values, it is possible for the model to have a steady-state solution at very high loads in which small phytoplankton escaping grazing control and reach very high biomass, in the process driving nutrient concentrations too low to support the sinking losses of large phytoplankton.

If phytoplankton biomass is high enough, there will be a reduction in light levels through increased attenuation (self-shading), and light rather than nutrients may limit growth. This will tend to favour large phytoplankton, which are assumed to have higher light-limited growth rates. However the competitive outcome under light limitation is not clear-cut, as the loss term for large phytoplankton is higher due to sinking. Si limitation may also prevent domination by large phytoplankton (diatoms) at high nitrogen loads. (Because denitrification efficiency decreases with loading, Si limitation may result even if Si loads increase along with nitrogen.) If a non-diatom bloom functional group (eg. dinoflagellates) is included in the model, it is possible for this class to dominate at high loads under Si limitation, which may be a more realistic outcome.

As different factors affect the outcome of competition between phytoplankton classes at different loadings, it follows that different parameters play important roles at different times and in different parts of the Bay. For example P vs I parameters and light attenuation have little impact at current loadings, but at high loadings their role is important in determining composition and total maximum biomass of phytoplankton. It is likely that large phytoplankton, which are most severely nutrient limited, will be more sensitive to changes in relative nutrient half-saturation constants. Large phytoplankton are also sensitive to changes in their settling velocity in relation to water depth, as sinking losses represent a major competitive disadvantage at low loads. Small phytoplankton, which are less nutrient limited, are more sensitive to grazing parameters at low to moderate loadings.

Observations suggest that eutrophic systems are generally dominated by bloom algae rather than by picophytoplankton. It appears that the latter are suppressed by grazing even at nutrient levels sufficient to saturate growth. (It is possible of course that in nature this is partly due to mixotrophy by some bloom microphytoplankton.) In the case of the quadratic zooplankton mortality formulation, it is possible through a steady-state analysis to derive conditions on small phytoplankton and zooplankton parameters which

ensure grazing control of small phytoplankton is maintained even at high nutrient loads and concentrations.

Macroalgae compete with phytoplankton for nutrients and therefore reduce water-column production. It is possible to carry out an analysis of macroalgae similar to that undertaken in section 3 for N-P-Z models. The details of this analysis will be presented elsewhere (Murray and Parslow, in preparation). We present the key conclusions below.

At high phytoplankton densities, macroalgae are deprived of light and cease to grow, so it is at low to medium phytoplankton levels that macroalgae play a significant role. Under the assumption of linear zooplankton mortality, phytoplankton biomass is constant, and their effect on macroalgae, at least through light attenuation, is small and independent of primary production. Phytoplankton biomass is not constant for the quadratic zooplankton mortality model, but at low to moderate biomasses, phytoplankton still make only a minor contribution to light attenuation in the Bay.

Macroalgae and phytoplankton are assumed to compete for dissolved inorganic nutrients in the water column. At low loadings, at steady state, low DIN will favour the component with best ability to compete at low nutrient levels. This is a function of the nutrient half-saturation constant and the relative values of maximum growth rate and intrinsic mortality rates. In fact, small phytoplankton, which have zero intrinsic mortality at very low biomass (they do not sink and, at very low biomass, support few grazers), will always be present regardless of loads, and are likely to drive nutrients to levels which will not support significant macroalgal biomass. In low nutrient conditions in the real world, macroalgae rely on variability in nutrient concentrations, as they can persist for longer periods between loading events and may have the capacity for rapid luxury uptake of nutrients.

As steady-state loadings and nutrient concentrations increase, macroalgae become more effective competitors, and remove N that would have supported phytoplankton growth. This may delay the onset of algal blooms. Further increases in nutrient loads will result in high persistent phytoplankton biomass or, at least, large blooms (depending on the model formulation). As this occurs, macroalgae may decline due to light limitation, leaving more nutrient to support phytoplankton production. Thus, in water bodies of the right depth, one might predict a rapid switch between macroalgal dominated and phytoplankton dominated states. Most of Port Phillip Bay is too deep for macroalgae to dominate, at least at current levels of light attenuation. However, in water bodies with extensive shallow areas, including many coastal lagoons in Australia, very large macroalgal blooms occur under eutrophic conditions.

Only a small proportion of the nitrogen taken up by macroalgae is released in the water column, and they are very efficient at exporting detritus to the Bay floor. This makes their impact on primary production disproportionate to their productivity. Consider a case in which 50% of phytoplankton production and zero macroalgal production are recycled in the water-column. For each tonne of N released from the sediment, 2 tonnes of phytoplankton production is possible. Each tonne of DIN used in macroalgal production results in the loss of not one but two tonnes of potential phytoplankton production. Although macroalgal production is apparently much smaller than phytoplankton production in Port Phillip Bay, it can have a significant impact on local nutrient cycling (see Chapter 7).

6.5 A dynamic process model of sediment-nutrient dynamics

In this section we describe briefly a process model of sediment biogeochemistry which we developed to investigate controls on denitrification. This model was not incorporated directly in the full Port Phillip Bay integrated model since it is too computationally expensive. The process model results were used in formulating the simple empirical submodel used in the integrated model.

The key transformations of nitrogen in the sediment, and their relationship to other biogenic elements, are shown schematically in Fig. 6.4. Breakdown of organic matter in the sediment produces ammonia which, depending on the availability of oxygen, may be oxidised to nitrate through nitrification. Under anoxic conditions, nitrate may itself become an oxygen donor, and is converted to N_2 gas, a process known as denitrification. Both nitrification and denitrification are carried out by specialised bacteria. Ammonia, nitrate and N_2 gas are all potentially exchanged between pore water and the overlying water column through diffusion and bioirrigation. Process models of the sediment nitrogen cycle need to prescribe the local rates of these transformations and their effects on concentrations of the key variables (especially oxygen), as well as the transport processes within the sediment and across the water-column - sediment interface. There are serious difficulties associated with the spatial and temporal structure and resolution of these models that we discuss later.

Examples of the underlying equations prescribing the local rates of change are given by Blackburn and Blackburn (1993) or by Omori *et al*. (1994). We used a modified version of the model of Omori *et al*. (1994):

$$dDet/dt = -breakdownO - breakdownA$$

$$dO/dt = -breakdownO - S_{ox}.S(i).O(i) + R2.denitrification - nitrification$$

$$dNH/dt = N:C\ .\ (breakdownO + breakdownA) - nitrification$$

$$dNO/dt = nitrification - denitrification - deitrificationS$$

$$dS/dt = breakdownA - S_{ox}S(i).O(i) - R.deitrificationS$$

Here, Det represents particulate organic carbon, O represents oxygen, NH ammonia, NO nitrate and S sulphide. Breakdown of organic matter occurs through aerobic breakdown above a threshold oxygen concentration:

$$breakdownO = B.(O\text{-}T_{ox})^{+}.Det$$

and anaerobic breakdown which is inhibited by oxygen:

$$breakdownA = E.Det/(L.(O\text{-}Tox)^{+} + F)$$

Note that we use $(O\text{-}T_{ox})^{+}$ as a shorthand for $\max\{ (O\text{-}T_{ox}), 0\}$.

Nitrogen dynamics consist of ammonia production, nitrification and nitrate reduction. Ammonia production is just a result of organic matter breakdown. Nitrification occurs above a specific oxygen threshold

$$nitrification = NH.Q.(O\text{-}T_{nit})^{+}$$

and denitrification occurs below another threshold or in the presence of sulphide.

$$\text{denitrification} = NO.Q2.(T_{den} - O)^{+}.Det$$

$$\text{denitrificationS} = S.Q3.NO$$

There are three oxidation agents in the model, oxygen, nitrate and sulphate, which interact in association with the reduced forms of ammonia and sulphide. In practice, sulphide is so rapidly oxidised in the presence of oxygen that sulphide can be represented as negative oxygen. This simplifies the model, and eliminates an extremely fast reaction, which would otherwise require a very short time step.

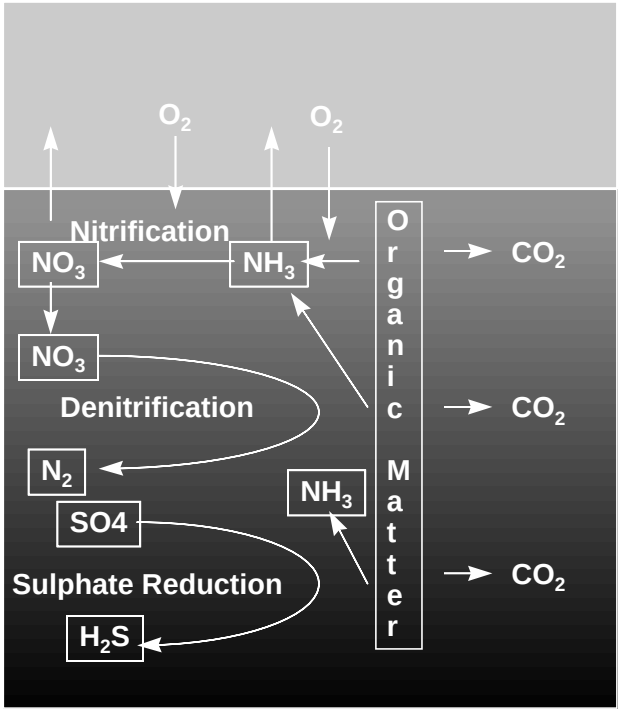

Figure 6.4 Nitrogen transformations involved in sediment biogeochemistry. Organic matter breaks down releasing ammonia and consuming oxygen, nitrate or sulphate. Ammonia is oxidised in the presence of oxygen to form nitrate. In the absence of oxygen, nitrate may be reduced either to support respiration or the oxidation of sulphide.

Transport terms in the model are fundamentally different for particulate detritus and for the other pools that exist in dissolved form. The external input to the sediment system is, at least in this simplified form, fallout of organic matter from the water-column and vertical transport of oxygen from bottom water.

Detrital fallout ends up on the sediment surface where it is mixed down by biological activity (bioturbation) or simply buried by subsequent fallout of organic and inorganic sediments. If the supply of organic or inorganic sediment is rapid relative to breakdown, then burial can act as a sink term and organic material accumulates in the sediment interior. Sediment profiles suggest this is not important in Port Phillip Bay, except possibly in Hobsons Bay. Bioturbation can result in random local mixing, modelled as enhanced diffusion, or it may have a more directed nature, with surface material being

carried to depths by surface foraging animals, or subsurface sediment being expelled on the surface by burrowers (which effectively increases the burial rate).

Transport of dissolved material occurs partly as a result of molecular diffusion but also as a result of animals pumping water into their burrows (bioirrigation). Again, bioirrigation can cause enhanced diffusion or it can result in direct exchange of pore water between deep sediments and the surface. Alternatively, oxygenated surface water can be injected into the sediment interior and can then find its own way to the surface, resulting in broad upward advection of pore water. These processes can have marked biogeochemical effects. In oxygenated burrows, for example, breakdown of detritus can result in ammonia formation and its oxidation to nitrate. If the burrow water is expelled rapidly, the nitrate or ammonia may be released to the overlying water column. If the burrow water diffuses or is pumped into the sediment, then it becomes anoxic and the nitrate is reduced to N_2.

This sediment biogeochemistry process model proved very computationally expensive. This is because it involves processes occurring on timescales ranging from seconds (oxidation of sulphide) to years (burial of detritus). It is possible to remove the sulphide reaction by the device of using negative oxygen described above, but this still leaves processes such as oxidation of ammonia or consumption of oxygen on time scales of minutes. The establishment of near-equilibrium profiles of particulate matter takes years, while the establishment of porewater profiles occurs on time scales of days. It makes sense to separate these time scales, and model pore water processes using pre-specified particulate profiles. However, this is not entirely satisfactory since these profiles change in response to biogeochemical parameters and loads.

There are other difficulties with these models associated with the representation of physical structure within the sediment. The model developed here, like many others, is a 1-D vertical model. Concentrations within each depth layer are assumed to represent mean concentrations of particulates or of dissolved constituents in pore water, averaged over the layer. However, these properties almost certainly vary three-dimensionally, at both micro-scales, associated with sediment grains, organic particles and micro and meiofauna, and at larger scales associated with macrofauna and burrows. Because the reaction equations are highly non-linear, use of average concentrations can involve serious errors, and parameters such as threshold concentrations need to be adjusted to compensate. This is not necessarily adequate. There have been attempts to investigate the effects of 3-D structure. Modelling of the effect of burrows has been undertaken by Aller (1980, 1984) and bioturbation by Robbins (1986). However, more work is needed.

Despite these weaknesses, these sediment biogeochemistry models do produce results that are believed to be at least qualitatively robust (Fig. 6.5). At low organic matter loadings (sediment respiration rates), oxygen penetrates deep into the sediment so nitrate reduction is suppressed, leading to nitrate release and low denitrification efficiencies. At high loadings, the sediment becomes anoxic and so nitrification is suppressed leading to ammonia release, and low denitrification efficiencies. At intermediate loadings, both nitrification and nitrate reduction co-exist, leading to high denitrification efficiencies. Denitrification efficiencies approaching 100%, as observed in Port Phillip Bay, are difficult to replicate with simple diffusion models. They require a high degree of overlap between the oxygen ranges for nitrification and for nitrate

reduction. This could be explained as the effect of microscale variation in the sediment. However, an alternative interpretation is that burrowing organisms are responsible for this anomaly. Burrow walls are potentially highly favourable environments for nitrification and denitrification, particularly in the presence of directional flow (nitrification occurring at one end of the burrow and denitrification at the other), or episodic irrigation, or injection of water into the sediment.

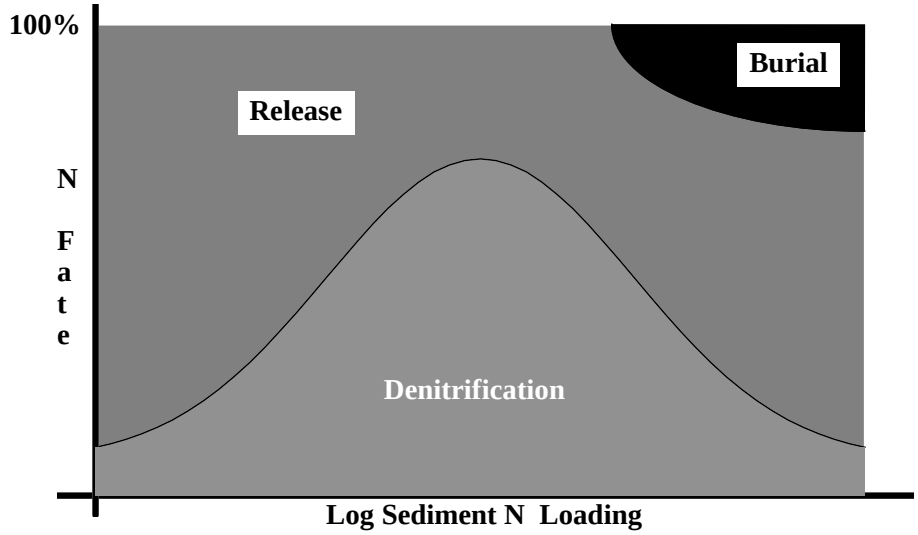

Figure 6.5 Conceptual diagram of the fate of nitrogen under different sediment respiration regimes. At low loadings nitrification is favoured but not nitrate reduction and so there is little denitrification. At high loadings ammonia is not oxidised and so denitrification cannot occur. Some loss may occur due to burial of detritus. At intermediate loadings nitrification can occur and so can nitrate reduction. It is here that denitrification is most efficient.

6.6 Sediment response to loading and microphytobenthos production

As we have just discussed, there are problems associated with sediment process models including computational requirements, parameterisation, and unresolved processes. We therefore decided to produce a simpler model based on the sediment process model results, and empirically fit this model to the observations of sediment-water column fluxes from chamber experiments. This empirical model is shown schematically in Fig. 6.6, and formulated as follows.

The fraction of ammonia production which is nitrified (f_n) is assumed to decrease slowly with increasing net sediment respiration rate R, and reach zero at R = R_0:

$$f_n = f_n^{max} . (1 - R/R\_0)^+$$

where $(1-R/R\_0)^+$ is shorthand for max {(1-R/R_0), 0}. The fraction of nitrate production, which is denitrified (f_{nd}) is assumed to increase rapidly with increasing R, and reach a maximum value of 1 at R = R_D:

$$f_{nd} = f_{nd}^{max} \cdot \min \{ R/R\_D, 1.\},$$

where R_D << R_0. Provided the respiration rate R exceeds R_D, the fraction of ammonia production which is lost to denitrification (f_d) is given by:

$$f_d = Dmax \cdot (1 - R/R\_0)^{+},$$

where Dmax is the maximum denitrification efficiency.

When coupled to the overlying water column, this effect of sediment respiration on denitrification efficiency results in a positive feedback: elevated DIN ⇒ increased water column production ⇒ increased sediment respiration ⇒ lower denitrication efficiency ⇒ greater nutrient release from sediments ⇒ elevated DIN.

Note that, in the range R_D < R < R_0, the total denitrification loss rate is given by:

$$fd.R = Dmax \cdot R \cdot (1 - R / R\_0).$$

That is, the denitrification flux fd.R depends quadratically on R, and reaches a maximum value at R = R_0/2, given by 0.25 . Dmax . R_0. This maximum value constitutes a theoretical upper limit to the denitrification loss rate per unit area.

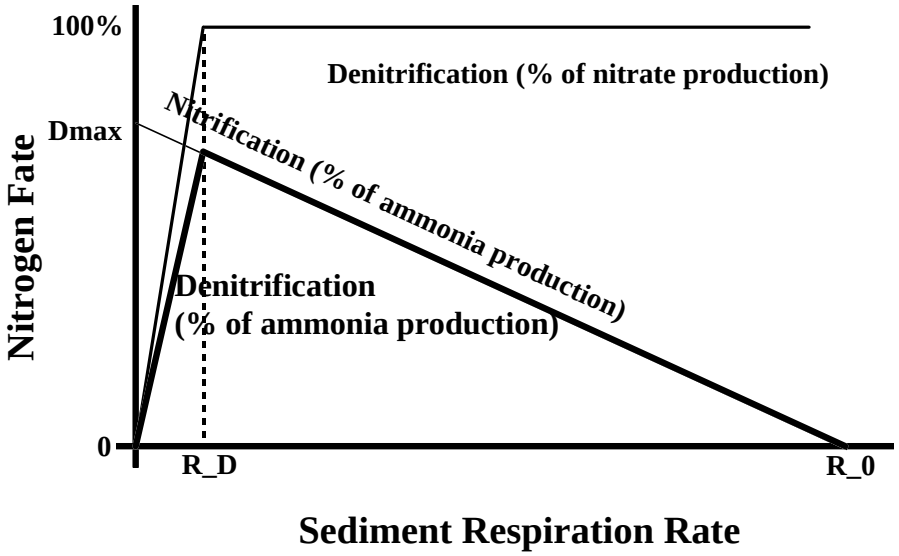

Figure 6.6 A schematic representation of the simple empirical denitrification model.

As discussed in earlier sections, under current conditions of low DIN and biomass, the export of nitrogen from Port Phillip Bay to Bass Strait via flushing is low. The observations suggest that almost all of the nitrogen load to the Bay is accounted for by denitrification. This means that we can roughly equate the sediment denitrification loss rate to the external load of nitrogen to the Bay, I_t. If the external load was increased, we would expect water column production and export, and net sediment respiration rate, to increase in such a way that the loss to denitrification continued to balance the external

load. However, once the net sediment respiration rate reaches R_0/2, the system reaches its maximum denitrification capacity. Further increases in sediment respiration rate result in lower denitrification fluxes and therefore further increases in load cannot be balanced by denitrification. One would then expect an accumulation of inorganic N or organic N in the water column until export from the Bay through flushing matched the difference between external load and denitrification loss. Because of the low flushing rates in Port Phillip Bay, this would require a large increase in water column concentrations over current values. Thus, the denitrification capacity corresponds essentially to an assimilative capacity for the system.

The magnitude of the theoretical denitrification capacity is obviously of considerable interest. The sediment chamber data (see Chapter 4) indicate that R_0 is approximately 250 mg N m^{-2} d^{-1}, equivalent on a Bay wide basis to a flux of 170,000 tonnes N y^{-1}. However, the appropriate value of Dmax depends on the interaction of MPB uptake with denitrification in the model.

MPB are bottom living single celled algae, usually diatoms. In Port Phillip Bay, their estimated production, at around 15000 tonnes N y^{-1}, is comparable to the net sediment respiration rate of around 12000-15000 tonnes N y^{-1}. They therefore have a major effect on nutrient fluxes within the sediment.

We have considered two submodels of the effect of MPB on denitrification: one in which MPB intercept DIN which would otherwise be released from the sediment (the "facilitative" model); and one in which MPB act as as competitors for nitrification and take up NH_4 before it enters the nitrification / denitrification pathway. Under the facilitative submodel, MPB enhance the effective denitrification efficiency by trapping DIN which would otherwise escape, and converting it back to organic matter, which is ultimately cycled back through the remineralization-nitrification-denitrification loop. Under the alternative "neutral" model, MPB take up DIN before denitrification occurs, and the cycling of N through MPB is irrelevant so far as the denitrification loop is concerned: it sees only the production of DIN corresponding to net sediment respiration. In both cases, MPB production supports dark respiration which is not matched by any N release from the sediment. This can make denitrification appear much more efficient than it really is, if care is not taken to accurately measure net sediment respiration over a day-night cycle.

The important difference between the two MPB interaction submodels is that under the facilitative submodel, denitrification efficiency falls as MPB production falls, whereas this does not occur under the neutral model. As nutrient loads increase and phytoplankton biomass rises, bottom light levels drop and so MPB production falls. Under the facilitative submodel, this leads to decreased denitrification efficiency, increased DIN release to the water column and hence more phytoplankton, creating a potentially important positive feedback in eutrophication.

The current version of the Port Phillip Bay model uses the neutral submodel of the MPB-denitrification interaction. In other words, MPB production does not enhance denitrification. Sediment chamber results show maximum denitrification efficiencies in central Port Phillip Bay where bottom light levels are low, and MPB production at times is negligible. These observations are incompatible with a uniformly applied facilitative submodel. It may be that MPB does enhance denitrification in shallow water but, in the

absence of direct evidence of this, we chose not to use different process submodels in coastal and offshore regions of the Bay.

Under the neutral submodel, the Port Phillip Bay observations are consistent with a value for Dmax of 0.7. Under the facilitative submodel, the total denitrification loss is given by R_G.Dmax.(1 - R / R_0), where R_G is the gross sediment respiration rate, equal to net respiration rate R plus MPB production. Given that on a Bay-wide basis, R/R_G is about 0.5, it follows that Dmax must be assigned a value of ca 0.3 in order for the Bay-wide loss to denitrification under the facilitative submodel to match the observed denitrification loss.

Estimating the maximum denitrification capacity of the Bay for the facilitative sub-model is not so straightforward. If MPB production increased in proportion to net sediment respiration, then the two sub-models would give identical results. However, MPB are exposed to elevated DIN concentrations in pore water, and their production is generally not N limited, except possibly in the Sands. Therefore, MPB production does not increase in proportion to nitrogen loads and thus the ratio R_G/R decreases. MPB production may in fact be suppressed by the declining bottom light levels that result from elevated phytoplankton production, further reducing R_G/R. In the worst case, MPB production ceases as R approaches R_0/2, and the maximum denitrification capacity is again given by 0.25.Dmax.R_0, but with Dmax = 0.3.

For the facilitative sub-model, the changes in phytoplankton biomass, light attenuation and MPB production with loading also depend on the zooplankton mortality formulation. For quadratic zooplankton mortality (see section 6.3) phytoplankton biomass rises with loading, MPB production is reduced by declining bottom light and so the maximum denitrification capacity is close to the lower estimate. Under linear zooplankton mortality, phytoplankton biomass, bottom light levels and MPB production are relatively independent of load, and hence the denitrification capacity is somewhat higher.

The two submodels of MPB imply significantly different denitrification capacities for Port Phillip Bay of around 30000 and 13000 tonnes N y^{-1} respectively. In the final report (Harris *et al*. 1996), using the MPB facilitative sub-model with a slightly lower estimate of Dmax (0.25), the maximum denitrification capacity was estimated to be about 10,000 and 15,000 tonnes N y^{-1} respectively under the quadratic and linear zooplankton mortality formulations.

Using the full numerical simulation model with Dmax = 0.7 and R_0 = 200 mg N m^{-2} d^{-1}, the predicted denitrification capacity is 15-20,000 tonnes N y^{-1} (see Chapter 8). For this value of Dmax, the simple one-box steady-state analysis predicts a denitrification capacity of 22000 tonnes N y^{-1}. The difference results from spatial and temporal variation in sediment respiration rate in the simulation model, and the non-linear (quadratic) local relationship between denitrification and respiration rate. Thus, when the mean Bay-wide respiration rate equals R_0/2, local rates may be substantially above or below R_0/2, and the average denitrification loss rate will be less than 0.25.Dmax.R_0.

6.7 The overall response of the Bay to changing loads

Two aspects of the model principally determine the broad response of Port Phillip Bay to changes in loading. The most important of these is the denitrification model that determines the assimilative capacity. The other important aspect is the zooplankton mortality formulation, which determines the response of the plankton to changes in loads. To a lesser extent, macroalgae influence the Bay at low to moderate loads by competing with phytoplankton for nutrients, and changing recycling efficiencies. Light attenuation influences this competition and, at very high loads, determines the maximum phytoplankton biomass. All these factors have been considered separately elsewhere in this chapter but this section addresses their joint effect. This matter is considered in more detail in the Port Phillip Bay final report (Harris *et al.* 1996).

Since, except at very low loadings, denitrification efficiency decreases with increased loading, there is a non-linear response of nutrient fluxes in the Bay to increased loadings. An increase in external load leads to a disproportionate increase in primary production and sediment respiration (Fig. 6.7). Once the external load exceeds the Bay-wide denitrification capacity, water column concentrations of DIN and organic N accumulate until export to Bass Strait again balances the external load. Because of the very long flushing time, this requires very high phytoplankton biomass and production, and the resulting sediment respiration increases to the point where denitrification ceases altogether and the only loss term in the model is export to Bass Strait. That is, production increases catastrophically as the denitrification capacity is exceeded.

According to the simple model, this failure of denitrification may not be easily reversed. A decrease in loading to a level below the denitrification capacity will not result in a restoration of water quality while the sediment respiration rate remains above the denitrification cut-off R_0. Instead, the external load must be cut to the point where phytoplankton production in the absence of denitrification is sufficiently low that sediment respiration falls below R_0. In other words, the combined water column and sediment system is likely to exhibit hysteresis (Fig. 6.7).

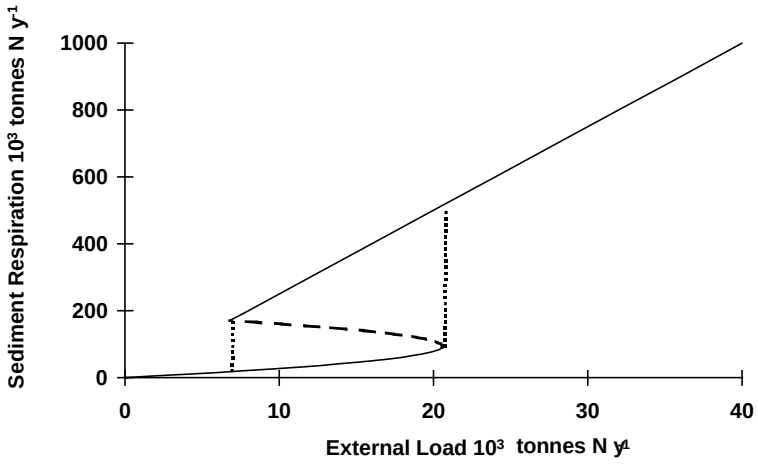

Figure 6.7 Schematic diagram of the effect of changes in load on sediment respiration rate predicted by simple one-box models. Once load to the Bay exceeds the denitrification capacity, the system switches to a new state with much higher production and sediment respiration, where loads are balanced by export to Bass Strait. In order to return to the low production state, loads must be cut significantly.

The implications for the pelagic and benthic ecosystems of the severe eutrophication expected following a failure in denitrification are of course severe, and the time scales for their recovery are unclear. If the high denitrification efficiencies currently observed are partly due to the presence of benthic macrofauna and their burrows, then ecological and water quality recovery may be linked dynamically.

The modelled response of the plankton to changes in the nutrient load to the water column depends on the zooplankton mortality formulation used. If linear zooplankton mortality is used then the phytoplankton biomass will remain constant as loading increases until a threshold is crossed and the steady-state solution breaks down, being replaced by cyclic blooms of phytoplankton. This second threshold, if real, would be of significant concern in itself for managers. There is also potential for such a switch in plankton behaviour to trigger the failure of denitrification, since declining blooms are likely to result in very high organic loads to the sediment.

The quadratic zooplankton mortality model predicts that phytoplankton biomass will increase smoothly in response to increased loads, eventually escaping effective grazer control. Thus the two models predict respectively either large episodic blooms or a large continuous bloom at very high loads. In either case these are highly undesirable outcomes. The magnitude of the blooms is eventually limited by the effects of self-shading on phytoplankton growth rates.

A third problem may be the collapse of macroalgal beds at high loadings. This occurs when shading by phytoplankton prevents growth. Since macroalgae compete with phytoplankton for nutrients, decreases in macroalgae will increase phytoplankton production and biomass, causing further loss of macroalgae. At current levels, phytoplankton make only a small contribution to light attenuation, and this feedback is weak. However, this feedback will become much more important at higher nutrient loads, when phytoplankton biomass starts to dominate light attenuation. Since phytoplankton production is much more likely to be recycled in the water-column than is macroalgal production, changes in macroalgal production have disproportionate effects on phytoplankton. While the balance between external loads and denitrification losses is maintained, the interaction between macroalgae and phytoplankton affects water column recycling efficiency and overall primary production, but not the net sediment respiration rate or denitrification efficiency.

Microphytobenthos are also affected by changes in light attenuation due to phytoplankton biomass. Under the facilitative submodel, decreases in MPB production do result in decreases in denitrification efficiency, leading to more release of nutrient from sediments, and increases in phytoplankton production and biomass. The effect of this positive feedback is to sharpen the transition from mesotrophic to eutrophic conditions.

This analysis is still based on a one-box horizontally-averaged treatment. As noted in the preceding section, the effect of spatial variation is to lower the theoretical denitrification capacity, but also to blur the catastrophic transition between a denitrification-dominated (mesotrophic) and an export-dominated (eutrophic) regime. When spatial effects are included, deterioration may start at lower loads, but the hysteresis effect may not be as marked as for a one-box model. As loads are decreased following eutrophication, a recovery in denitrification in part of the Bay may be

sufficient to trigger recovery over the whole Bay. The effects of transients and spatial variation may also blur the contrast between the steady-state behaviour of one-box models using different zooplankton mortality formulations.

6.8 Transient and spatial effects

The full simulation model developed for Port Phillip Bay includes the effects of physical transport, and is subject to spatial and temporal variation in forcing. The analyses described in previous sections are generally based on approximations of the system by a well-mixed one-box system subject to steady-state forcing. These approximations provide a useful basis for understanding the large-scale or average response of the Bay at longer time scales. However, there are transient and local properties of the Bay, such as blooms around major inputs or in response to major runoff events, which are of intrinsic interest to managers. Because many of the processes are non-linear, there is also potential for these local or transient effects to modify the Bay-wide behaviour. These transient and local effects are not as easily treated by qualitative analysis, and the full simulation model is designed to address these. Nonetheless, some useful insights can be obtained rather simply.

There are a number of scales of time and space over which variation can occur. Interannual or long-term changes in loads or parameters can reasonably be investigated using steady state analysis. Seasonal behaviour can also be treated by steady-state analysis, at least in the case of plankton and other ecosystem components with turnover times of days to a few weeks. Responses to changes in loads at these longer time scales can be analysed using the results already reported in this chapter. However short term phenomena such as the response to Yarra floods must be treated as transients. Spatial features, most notably blooms off Werribee, also reflect local instabilities and can be considered as transients from a Lagrangian perspective.

Yarra Floods

When the Yarra River floods, as in late 1993, the waters of Hobsons Bay and adjacent northern and eastern coastal waters show elevated nutrient levels followed by elevated chlorophyll. There is not much response in the Bay centre or south. The observed changes reflect an initial imbalance between nutrient inputs and the uptake capacity of the existing phytoplankton. The increase in nutrients results in increased growth of phytoplankton, which escape grazer control and bloom. Blooms tend to be dominated by large phytoplankton (diatoms), as they have higher maximum growth rates than small phytoplankton, and large zooplankton have a slower numerical response. The extent and duration of the bloom depends on the rate of input and local retention of nutrient, the maximal and background rates of phytoplankton growth, and the background concentrations of phytoplankton and zooplankton.

The effect of Yarra floods on Bay centre chlorophyll and nutrients is marginal; the Bay appears to be too large to show much in the way of direct effects of floods. In the 2 weeks of the September 1993 flood (the largest event in the 1993-94 period) the Yarra input amounts to 475 tonnes of N, about 6% of that year's total N input. Only 103 of those tonnes are in the form of DIN, which is about a third of the average DIN pool in

the Bay. It follows that local retention and thus build-up of nutrient is essential for a significant effect to occur.

Werribee Inputs

The response of plankton in Hobsons Bay to flood inputs from the Yarra River is explicable in terms of the lags involved in phytoplankton and zooplankton responses to a sudden nutrient increase. Blooms and high nutrient concentrations also occur off Werribee, but inputs from this source are reasonably constant, at least on time scales of weeks appropriate to phytoplankton responses. The local response appears to be driven by the mixing of low nutrient, low biomass offshore water with the high nutrient inputs from WTP.

One could model physical exchange between the water just off the WTP input and the rest of the Bay either in terms of a diffusive mixing process, or as an advective process such as long-shore transport. In a diffusive model, a phytoplankton bloom can be expected if the nutrient-saturated phytoplankton growth rate exceeds the local dilution rate due to mixing, while the maximum zooplankton growth rate is less than the local dilution rate. This is likely to be the case for large phytoplankton and zooplankton, but not small phytoplankton and zooplankton.

In an advective model, from a Lagrangian perspective, the source acts exactly like a transient nutrient spike, and the transient response described for the Yarra will apply.

The offshore water contains relatively low phytoplankton and zooplankton populations. As these mix with the high nutrient coastal waters the phytoplankton population begins to grow rapidly. As phytoplankton biomass increases, so does zooplankton growth rate. However, by the time zooplankton populations are beginning to catch up with the phytoplankton, the water is transported away from the nutrient source. As a result the process begins anew with more offshore water, and the zooplankton never catch up with the phytoplankton.

6.9 Conclusion

Simple approximate models are a very powerful tool for gaining insight into the underlying processes and feedbacks that control the Port Phillip Bay ecosystem. They also provide insight into the relationship between model structure and function, allowing unrealistic model behaviours to be identified and avoided. This insight into model behaviour is also a great advantage when it comes to selecting or tuning parameter values in the full simulation model. The real Bay is subject to spatial and temporal variation in forcing which can act synergistically through a variety of non-linear interactions. Prediction and analysis of the resulting spatial and temporal pattern of responses requires the full dynamic simulation model, discussed in the next Chapter.

7 SIMULATION MODEL CALIBRATION AND ANALYSIS.

In Chapter 3, we provided a detailed description of the full, process-based numerical model of the Port Phillip Bay nutrient cycle. In Chapter 4, we discussed in detail the "a priori" information available on the model parameters, both from the literature and from process experiments carried out as part of the Port Phillip Bay Study. It was clear there that, while some parameters were quite tightly constrained, a number of key parameters are subject to large a priori uncertainties, while some parameters, such as quadratic mortality coefficients, are essentially empirical, and can only be estimated within the model context. Calibration of the dynamical model output against the Study observations imposes a powerful but indirect set of additional constraints on the parameters. In this chapter, we describe the process and outcome of model calibration against the observations.

While the process of model calibration is primarily concerned with refining parameter estimates, one cannot completely separate parameter estimation from process formulation. One of the strengths of the PPBES has been the integration of the field program and the modelling. The model formulation was revised during the Study to take account of field results, and model formulation and parameter estimation have been closely coupled. The model formulation described in Chapter 3 represents the outcome of this process. While this chapter concentrates on parameter estimation within the context of that model version, we do point out interactions between model formulation and parameter values where these are significant.

The model formulation described in Chapter 3 is moderately complex, with 14 state variables and 80 parameters. The model complexity is increased further by the spatial resolution, with the Bay divided into 59 horizontal compartments (boxes). As we explained in Chapter 3, we have tried to keep the model as simple as possible: ie. to introduce additional state variables and processes only where these are important in controlling the nutrient cycle in the Bay and/or the impact of changes in that cycle on important ecosystem properties. Similarly, we have tried to choose a spatial resolution that is just sufficient, to resolve the variation in nutrient cycling within the Bay, and the effects of transport on the nutrient cycle.

The level of complexity in the model has important implications for the process of model calibration. The model run time on a fast workstation is short enough (ca 30 minutes) to allow extensive numerical experimentation. By comparison, the run-time of the hydrodynamic model is long enough that only a small number of runs (of order one or two) would have been possible if the ecological model had been directly coupled to the hydrodynamic model. On the other hand, there is increasing interest by ecological and biogeochemical modellers in the use of formal parameter estimation techniques, using either directed search or Monte Carlo methods, to maximise the goodness of fit or likelihood of model predictions given the observations. The Port Phillip Bay model run-time was too long, and the number of parameters too large, to allow the use of these formal methods.

The calibration process adopted has consisted instead of a directed but heuristic search through parameter space to identify parameter combinations providing better agreement

between model predictions and observations. We have used numerical experiments extensively to assess the effect on model predictions of changes in selected parameters. The qualitative understanding achieved through the analysis of simple or approximate models, described in Chapter 6, has been critical to the success of this process. This understanding has changed what could have been an undirected wander through a many-dimensional parameter space into a series of numerical experiments to either confirm hypotheses based on analysis of simple models, or to study particular "new" phenomena appearing in the full model.

We have chosen one particular parameter set as representing "best" agreement between model predictions and observations. For this "standard" run, we present the corresponding model predictions, and their comparison with observations, in some detail. We also present a local (linear) sensitivity analysis about this solution. However, we have ourselves been frustrated by modelling reports in which a "best" solution is presented as an outcome of an invisible calibration process. We try here to present sufficient information about the numerical experiments, and the hypotheses and understanding associated with them, to convey both a picture of the process itself, and perhaps more importantly, an understanding of the dependence of the full model on parameter values, and a feel for the key remaining uncertainties in the model parameters and predictions.

The spatial and process complexity of the model, and the variety and complexity of the available data sets, represent another kind of challenge. We have many kinds of data, on a variety of spatial and temporal scales, to compare with model predictions. We have also faced choices about the kinds of predictions and comparisons to present in this Report. It is not feasible to provide comprehensive information for all model state variables in all locations at all times for even one model run. We have adopted a hierarchical approach to both the calibration process itself, and the presentation of results in this chapter. We focus first on model predictions and model-data comparisons at the level of Bay-wide annual averages of key pools and fluxes. We then look at the major regional and seasonal patterns in the Bay. Finally, we focus on certain key events that are restricted in time and place.

The chapter is divided into seven sections. The first section describes briefly the data sets available for model calibration. The second section describes the preprocessing methods (eg. spatial and temporal averaging) needed to compare observations with model output, and their results. The third section describes the key numerical experiments involved in the calibration process, and the results, primarily in terms of Bay-wide pools and fluxes. The fourth section describes the standard "best" solution, and presents detailed comparisons of predictions and observations for this solution at a variety of spatial and temporal scales. It also discusses results of numerical experiments at these spatial and temporal scales. The fifth section compares model predictions and observations focusing on specific local or transient phenomena. The sixth section presents a local sensitivity analysis about the standard solution. The last section briefly summarises the key conclusions from the model-data comparison.

7.1 Data sets used in model calibration and testing

There are three sorts of data that play a role in the model's formulation, calibration and testing. The forcing data used to drive the model were discussed in Chapter 5 and will not be considered further here. The use of results from process experiments to directly constrain parameters was discussed in Chapter 4 under the corresponding parameter headings. The third type of data consists of field observations of variables (concentrations or fluxes) which can be compared with model predictions, and used for model calibration or testing. In this section, we summarise these data, and discuss the technical issues involved in comparing model predictions and observations.

The Port Phillip Bay study produced a very large and diverse data set, much of it useful in model calibration. While larger data bases exist for areas such as the North Sea (Radach and Moll 1993), the combination in the PPBES data set of water-column, sediment, and epibenthos pools and fluxes, together with input loads and physical transport, is arguably unprecedented. The size, diversity and comprehensive nature of this data set has made the modelling task particularly rewarding, and particularly challenging.

The major data sets, which are suitable for model validation, are briefly summarised below. Futher details of all of these data sets can be found in the Technical Reports cited.

7.1.1 Underway transect data

As part of the PPBES, 25 cruises were undertaken between March 93 and March 95. The cruises followed a path designed to sample the key horizontal gradients in the Bay, and measured surface water properties continuously from a shallow underway intake. These surveys measured surface values of NO_2, NO_3, NH_4, PO_4, SiO_4, chlorophyll a, and oxygen. NO_2 is of minor importance and is combined with NO_3 as NO_X for model purposes. The data have already been subjected to extensive analysis by Longmore *et al.* (1996). Results of short-term intensive underway surveys off Werribee and Hobsons Bay have been presented and analysed by Longmore *et al*. (1996).

7.1.2 Fixed site water-column measurements

A series of 11 sites were visited fortnightly, and vertical profiles obtained using pumps and discrete bottle samples. These sites provide more temporal resolution (fortnightly vs monthly), vertical structure and more variables (dissolved and particulate organic N, P and C, and light attenuation). For a subset of these sites, monthly data are available over a longer time period (1990 to 1995).

Vertical stratification in physical properties is generally weak in Port Phillip Bay, except at times of high runoff and/or locally near freshwater inputs. Vertical stratification in biogeochemical variables is most significant for chlorophyll and NO_X. Surface measurements alone could lead to underestimation of the depth-averaged chlorophyll by ca 20%, and overestimation of depth-averaged NO_X by 20%(Longmore *et al*. 1996). Stratification is more common in Hobsons Bay, and oxygen levels there decrease measurably in bottom waters. The lack of bottom water oxygen depletion over most of

the Bay implies vertical mixing on time scales of hours to a few days, given that sediment oxygen consumption rates are of order 50 mmol m^{-2} d^{-1}.

7.1.3 Phytoplankton database

A long-term data-base of phytoplankton abundance and species composition has been collected and analysed (Magro *et al.* 1996). The data include phytoplankton counts at monitoring sites that are different from the station sites included in Longmore *et al.* (1996). These data have not been used directly for model calibration, but the qualitative results (eg. diatom dominance of net phytoplankton) have guided model formulation. More use could potentially be made of these data in analysing and modelling factors controlling bloom composition, including silicate limitation.

7.1.4 Phytoplankton production measurements

The phytoplankton photosynthetic parameters and production estimates presented by Beardall *et al*. (1996) are extremely useful both as direct constraints on model parameters, and as calibration data for predicted fluxes. Their report describes seasonal variation in both light saturation intensity and light saturated productivity, the model parameters controlling photosynthesis. The estimated fluxes include both local column primary production at sampled sites, and estimates of Bay-wide primary production. Like other process studies, the phytoplankton productivity experiments could be carried out only at a limited number of sites, and this does present problems in scaling up to Bay-wide flux estimates.

7.1.5 Zooplankton grazing experiments

A very useful data set was obtained from experimental analysis of microzooplankton grazing in Port Phillip Bay. These experiments provided data on light-saturated growth rates of phytoplankton under both nutrient-limitation and nutrient-saturation, as well as microzooplankton clearance rates. The data consist of monthly estimates of growth rates and clearance rates over a single year at six sites (Beattie *et al*. 1996).

This data set confirms the high growth rates of phytoplankton indicated by production measurements. These constitute an important constraint on the model. The data are most useful in directly constraining the maximum growth rates of phytoplankton, and half-saturation constants for growth on ammonia (see Chapter 4). The observations can be compared with local or regional model predictions of growth rate and grazing rate, although again the spatial coverage is limited.

7.1.6 Benthic chambers

The results of the benthic chamber experiments, which directly measured oxygen, carbon and nutrient fluxes across the sediment-water interface, are presented by Nicholson *et al*. (1996). This data set is crucial to our understanding of Port Phillip Bay. Again, data are only available at a few locations and times. A monthly time series of measurements was made at only one location, off Werribee. The data have been most useful in the formulation and parameterisation of empirical submodels of sediment

biogeochemistry, particularly the dependence of denitrification efficiency on sediment respiration rates. The data have been used to directly estimate Bay-wide fluxes, although large uncertainties in these estimates due to the limited spatial and temporal coverage have been recognised. Both Bay-wide and regional fluxes are compared with model predictions.

7.1.7 Sediment cores

Extensive sets of sediment cores were collected on three occasions, providing quite good spatial coverage at regional scales, but limited seasonal coverage. Cores were sectioned and profiles obtained of both dissolved constituents (nitrate, ammonium, phosphate, silicate, DON, DOP) and particulate organic N, P and C. The data are reported by Nicholson *et al*. (1996). These data are potentially useful for calibrating vertically-resolved sediment biogeochemistry process models, of the kind outlined briefly in Chapter 6. They are not so useful for calibrating the integrated model. The gradients in pore water concentrations near the surface of the sediment can be used to estimate diffusive fluxes, but the sediment chamber results indicate that bioirrigation is important, and diffusive fluxes underestimate sediment-water exchanges.

Over most of the Bay, there are very weak vertical gradients in particulate organic N and C in the top 30 cm of sediment. This indicates that the large pool of organic matter in the sediments is quite refractory, turning over on time scales long compared with sediment bioturbation time scales estimated at tens of years. Because this organic matter is highly refractory, it cannot be compared with the labile and semi-labile detritus pools represented in the model.

A separate report (Burke 1995) presents measurements and interpretation of microprofiles of oxygen penetration of the sediments. The data are restricted to 9 sites over a two week period, and have been more useful in guiding model formulation than in quantitative calibration. The very short depth of direct penetration of oxygen (ca 1 mm) shows that benthic respiration rates near the sediment surface are very high. Estimates of diffusive oxygen flux based on near-surface oxygen gradients accounted for about half the oxygen consumption measured by sediment chambers, the rest (presumably) occurring through burrow walls. Again, these are potentially important constraints on sediment process models, but not on the integrated model with its simple empirical sediment submodel.

7.1.8 Microphytobenthos

Benthic microalgae have turned out to play a crucial role in Bay-wide primary productivity that was not expected when the Study began. Their estimated annual Bay-wide production is only slightly less than that of the phytoplankton, and they may play an important role in regulating sediment-water exchanges of DIN (see Chapter 6). Reports by Beardall and Light (1994, 1997) present and analyse data on the distribution, productivity and light-dependence of microphytobenthos. The underlying data set has limited spatial and temporal resolution, consisting of one intensive spatial survey of biomass, and monthly measurements of biomass and photosynthetic parameters at three depth ranges at each of three locations. These data have been interpolated and extrapolated to provide monthly estimates of Bay-wide biomass and production, but

better spatial and temporal coverage is desirable. Both Bay-wide and local flux estimates are compared with model predictions. Given its potential importance (discussed in Chapter 6), there are strong arguments for further process studies to better resolve the interaction between microphytobenthos production, sediment respiration and denitrification efficiency.

7.1.9 Macroalgae

The macroalgae of Port Phillip Bay have been surveyed by Chidgey and Edmunds (1997) as part of the PPBES. Macroalgal biomass, species composition and chemical composition were measured along 5 onshore-offshore transects, at 2m depth intervals from 4 m to 10 m, at 3 month intervals over one year. There was a clear pattern of highest biomass at 8 m and lower biomass at both 4 m (shallowest) and 10 m (deepest). This depth distribution imposes important constraints on model predictions and parameters, particularly the light saturation intensity that determines how deep macroalgae can grow. The model cannot reproduce the decrease in macroalgal biomass in shallow waters unless a loss term related to bottom stress is introduced. (Most of Port Phillip Bay has soft sediments, and the dominant macroalgal form in terms of biomass is loosely attached filamentous algae.) The observations have been used to provide direct constraints on the parameter that sets the upper limit to macroalgal biomass. There is considerable uncertainty involved in scaling up results from the 5 transects to estimates of Bay-wide biomass.

The Study did not include direct measurements of macroalgal production. The observed seasonal variation in biomass provides some lower bounds for growth rates and loss rates. The model represents all macroalgae by one state variable, so that the species composition data has not been used in model calibration. More detailed macroalgal models would be required to investigate impacts of changes in loads on macroalgal composition.

7.1.10 Seagrass

A map of seagrass in Port Phillip Bay based on historical data was presented by Bulthuis *et al*. (1992). Seasonal data for Swan Bay (Bulthuis and Woelkerling 1983) showed minima of about 2000 mg N m^{-2} in January and June and maxima of 3-4000 mgN m^{-2} in April and September. Their estimate of biomass assumes that 30% of biomass is present as rhizomes, but rhizomal biomass was not measured and this percentage may well vary seasonally. The results refer to only one location noted for its seagrasses, and so the maximum values have been used as an upper limit for seagrass biomass.

7.1.11 Benthic filter-feeders

The literature review of Wilson *et al*. (1993) is useful mostly in constraining parameters (discussed in Chapter 4). However it also contains estimates of Bay-wide fluxes of DIN release, and an estimate that benthic filter-feeders turn over Port Phillip Bay in about 16.5 days. Given the turnover time of phytoplankton biomass is approximately 2-3 days, this means benthic filter-feeding is a relatively minor loss term for phytoplankton. However, locally, in shallow waters, filter-feeders may play a more important role.

There were no comprehensive surveys of the distribution or physiology of benthic filter-feeders conducted as part of the Study. Studies of benthic fauna were designed to look at long-term changes in particular regions (Poore 1992). The model includes only a single state variable to represent the biomass of a complex community of benthic filter-feeders, each with their own dynamics and life history strategies. This is a crude representation: the best we might hope for is to get the regional and seasonal distribution of total clearance rates and nutrient release approximately correct. During the Study, data on the spatial distribution of the introduced sabellid worm were collected by MAFRI (Harris *et al*. 1996). These were concentrated along the west and north of the Bay, a distribution in agreement with model predictions based on food concentrations. However, other filter feeders (eg. scallops, Hall 1994) have different distribution patterns.

7.1.12 Other data

The CASI mapping exercise produced distributions of benthic communities based on optical classification with high spatial resolution to a depth of ca 7 m. Historical data, including the Status Review (Hall 1994), Mickelson's (1990) report on oxygen, the Phase One report (MMBW/FWD 1973) and Newell's (1990) report, contain useful data for qualitative comparison. Sediment biomarker analyses (O'Leary *et al*. 1994) pointed to the importance of phytoplankton, and diatoms in particular, as a source of organic matter in the sediments.

7.2 Spatial and temporal scales in observations

As we have just seen, the spatial and temporal coverage of the observations varies considerably, from the monthly underway transects and fortnightly site samples for water column nutrients and chlorophyll, to very limited combinations of sites and times for some process studies. As we discussed in the introduction to this chapter, we can expect model-data comparisons at different time and space scales to highlight different model processes and parameters. For both these reasons, we have found it very useful to carry out model-data comparisons at a hierarchy of scales.

The coarsest scale we have considered is that of Bay-wide annual averages. The PPBES main field program extended roughly over two years, from May 1993 to April 1995. This period includes both a high load year and a low load year. The observations allow us to estimate Bay-wide averages for most of the key pools and fluxes over each of these two years. Agreement with these annual Bay-wide averages represents a basic requirement of model performance.

7.2.1 Bay-wide pools

Bay-wide pools of nutrient in the water-column have been estimated by Longmore *et al*. (1996). In early surveys in particular, coastal waters were more intensively surveyed than were central waters, so simple averages of observations may well be biased. Three different methods were used by Longmore *et al*. (1996) to estimate Bay-wide pools from underway data: simple means, inverse distance weighting and double spline interpolation.

Table 7.1 Mean Bay-wide content of nutrients (tonnes of N, P or Si) and chlorophyll (tonnes Chl a) (from Longmore *et al*. 1996).

Year/Method	NH_4	NO_2	NO_3	PO_4	SiO_4	Chl	Phyto N
May 93-April 94							
Simple Mean	284	24.2	134	1612	4100	31.3	219
Inverse Distance	249	18.8		1651	4304	26.5	185
Double Spline	208	17.7	89	1500	4263	22.5	157
May 94 - March 95							
Simple Mean	151	14.0	74	1558	2478	22.2	155
Inverse-Distance	130	11.8		1549	2436	21.1	148
Double Spline	118	11.6	60	1420	2342	19.6	137
93-95 Double Spline	163	75	15	1460	3303	21.1	148

Overall means for these variables in the 1993-95 period based on the double spline interpolation are shown in the last row of Table 7.1. These estimates are considered most reliable, and have been used for model calibration. The variation among different interpolation methods provides a crude measure of the uncertainty due to sample coverage. According to the size-fractionated studies of Beardall *et al*. (1996), chlorophyll is divided roughly equally among the three phytoplankton size classes: micro (29%), nano (39%) and pico (32%).

The annual and Bay-wide average DON pool is also estimated by Longmore *et al*. (1996). However DON concentration was only measured at the fixed sites and therefore the spatial average involves more uncertainty than for variables measured underway. The model predicts the DON excess over background oceanic (Bass Strait) concentrations. Observations at site N1 suggest that this background DON concentration should be approximately 80 mg N m^{-3}, equivalent to a Bay-wide pool of about 2000 tonnes of N (see Chapter 5). The status review estimate of the total DON pool was 4000 tonnes N (Skyring *et al*. 1994) but the simple mean estimate for the study period was 3300 tonnes N (Longmore *et al*. 1996). This would be equivalent to a DON pool of about 1300 tonnes N in excess of Bass Strait levels. Given the spatial and temporal coverage of the data used to estimate DON, both in the Bay and at the Bass Strait boundary, there is probably an uncertainty of several hundred tonnes N in the excess DON pool size.

Estimates of nitrogen pool sizes are available for two other important model variables: macroalgae and microphytobenthos. Macroalgal biomass Bay-wide is estimated as varying seasonally between 200 and 1000 tonnes N (Chidgey and Edmunds 1997). The annual average pool size is ca 500 tonnes N. Microphytobenthos biomass is around 300-400 tonnes N, more than twice the phytoplankton N pool (Beardall and Light 1997). We have no estimates of Bay-wide seagrass biomass but beds extend over 100 km^2 or 5% of the Bay (Bulthuis et al. 1992). If we use the seagrass density measured in Swan Bay (2-4000 mg N m^{-2}: Bulthuis and Woelkerling 1983) this gives 200-400 tonnes N. However seagrass densities in Swan Bay are generally higher than in other areas. Of four local leaf densities surveyed by Bulthuis *et al*. (1992), the lowest was less than 20% of Swan Bay leaf density (Bulthuis and Woelkerling 1983) and the average was about 50% of Swan Bay levels. Even within these areas seagrass distribution is often patchy. This density and area gives a crude range of estimated values for seagrass biomass of 40-200 tonnes N.

The pools of detrital organic C and N in the sediment estimated by Nicholson *et al.* (1996) are very large, ca 147,000 tonnes N in the top 20 cm. However, the vast bulk of sediment organic N is clearly highly refractory, and the labile and moderately refractory detritus pools represented in the model cannot be distinguished from the background material. The estimated particulate N pool in the water-column of 696 tonnes N (Longmore *et al.* 1996) also presumably includes a mixture of labile, semi-labile and refractory material, as well as phytoplankton N. Interestingly, the measured C:N ratio of suspended detritus decreased throughout the period 1990 to 1995, and approached the Redfield ratio towards the end of this period. This suggests a change in composition from refractory to more labile material.

We have no direct data on the zooplankton biomass in Port Phillip Bay for the Study period. Mean densities of larger zooplankton in 1982-83, were 1480 m^{-3} (Kimmerer and McKinnon 1985), and about 80% of these were crustacea. *Paracalanus parvus* (which is very similar to Port Phillip Bay's dominant copepod *Paracalanus indicus*) and most *Acartia* sp. have weights in the region 1.5-5 μg C (0.3-0.9 μg N). However, about 10% of the crustaceans in Port Phillip Bay were an order of magnitude larger (40-50 μg C per individual). Including these larger zooplankton approximately doubles average weight, and gives a biomass of 1-3 mg N m^{-3}, equivalent to about 50 tonnes N Bay-wide. Theoretically, we might expect the biomass of crustacean zooplankton to be comparable to that of large phytoplankton (Sheldon *et al.* 1972), which would be about 3-5 mg N m^{-3}.

We do have an estimate of biomass for benthic filter feeders of 27100 tonnes (ash free dry wt) Bay-wide (Wilson *et al.* 1993). This corresponds to about 2500 tonnes N.

The pool sizes derived from this discussion are summarised in Table 7.2. The best estimates of Bay-wide water-column nutrient pools were found by Longmore *et al.* (1996) by double spline interpolation onto a 300 m grid. The estimates based on simple averages of observations are also shown, since these (biased) estimates were compared with similarly biased estimates based on model predictions, using a procedure described below.

Table 7.2. Bay-wide average pool sizes and concentrations from cruises.

Variable	Best Estimate		Cruise Average	
	tonnes	mg m^{-3}	tonnes	mg m^{-3}
Chl	21.1	0.84	26	1.04
PL+PS (Phyto N)	147	5.9	182	7.3
NH_4	163	6.5	224	9.0
$NO_2 + NO_3$	90	3.6	109	4.4
PO_4	1460	58.4	1589	64
DON (excess)	800	32	1300	52
		mg m^{-2}		
MA	500	250		
MB	350	175		
BF	2500	1250		

7.2.2 Bay-wide fluxes

It is arguably the extent and variety of flux data that make the PPBES data set exceptional. If any single summary flux describes the state of the Port Phillip Bay ecosystem, it is the level of phytoplankton primary production.

Estimates of phytoplankton primary production in Port Phillip Bay have fluctuated over the years as data has accumulated. Newell (1990) estimated 20000 tonnes N y^{-1}, which was revised to 10400 tonnes N y^{-1} by Skyring *et al*. (1994). The PPBES phytoplankton study (Beardall *et al*. 1996) found an average productivity of 364 mg C m^{-2} d^{-1} or ca 43000 tonnes N per year. However this is a simple average of observations, and does not necessarily allow adequately for horizontal variation in phytoplankton biomass, growth rates, or water column depth. If we convert back to production per unit volume we get productivities for offshore and coastal waters of 0.85 and 2.69 g N m^{-3} y^{-1} respectively. If we assume 80% of the Bay is offshore, we get a production of 30418 tonnes N y^{-1}. To allow for the fact that our definition of the offshore region may not correspond to the actual extent of low productivity water, we use a range of 70% to 90% of the Bay's volume, and this gives a range of productivity estimates of 25,800-35,000 tonnes N y^{-1}.

It is difficult to confirm this crude estimate of sampling bias, given the limited spatial coverage of the observation set. However, the primary production fields predicted by the model show a comparable bias. In the standard model run, the annual Bay-wide phytoplankton production is around 30000 tonnes N y^{-1}, while averaging the model production at the sampling sites yields a figure of about 40000 tonnes N y^{-1}, comparable to the average obtained by Beardall *et al*. (1996).

Although we have no direct estimates of macroalgal production, the estimated N biomass of 200-1000 tonnes will probably support production of a few thousands of tonnes N y^{-1}. The depth at which much of the macroalgal biomass is found would preclude high growth rates, while the seasonal variation in biomass indicates that annual production is at least of the same order as maximum biomass. A net growth rate of 1-5% d^{-1} (10-50% of our default maximum growth rate of 0.1 d^{-1}) would give a range of 2000-9000 tonnes N y^{-1} if we take 500 tonnes N as an annual average biomass. Given an annual macroalgal productivity of 1 mg C m^{-2} as a world-wide average (Duarte and Cebrián 1996) and a C:N ratio of 12 (DeBoer 1981) then, if 10% of the Bay-bed is suitable habitat, productivity of 6000 tonnes N y^{-1} would be expected. Macroalgal productivity in Port Phillip Bay is thus comparable with productivity in other areas.

We have estimated seagrass biomass at 40-200 tonnes N. The turnover time of this biomass is of the order of 50-100 days (Kraemer and Mazzella 1996), implying annual production is probably 120-1200 tonnes N y^{-1}, about an order of magnitude less than macroalgal production.

Nutrients to support phytoplankton and macroalgal production in the water column come from four sources. These are the external loads, recycling in the water column (including breakdown of input detritus), release from the sediments and release by benthic filter-feeders. These recycling terms are referred to as WRc, SRc and FRc. Since we are interested in water column primary production, we define these terms in the sense of supply of DIN to the water column. WRc is thus the net N released from all heterotrophic processes in the water column. For SRc, however, we are interested in the

net release from the sediments and thus SRc must equal net DIN production in the sediment (detrital remineralization minus denitrification losses minus MPB and seagrass production). In the model, filter-feeders excrete N directly into the water-column, and thus their respiration, plus release of DIN following mortality, is used for FRc. Thus external DIN load + WRc + SRc + FRc equals phytoplankton + macroalgal production.

The value of the load and recycling terms can be constrained by observations. The direct input (excluding detrital N) is about 6000 and 5000 tonnes in 1993 and 1994 respectively, including inputs from the atmosphere and 300 tonnes from minor creeks in 1993 (see Chapter 5).

For benthic filter feeders, the estimated clearance time of about 16.5 days (Wilson *et al.* 1993), multiplied by mean phytoplankton concentrations, gives an ingestion rate of about 3000 to 4000 tonnes N y^{-1}. However filter-feeders are concentrated in regions of higher than average phytoplankton biomass, and also ingest detritus and some zooplankton, so a somewhat higher estimate, of order 5000 tonnes N y^{-1}, is appropriate. If we assume 75% of the labile organic nitrogen ingested by benthic filter-feeders is released as DIN, FRc is about 3750 tonnes N y^{-1}.

The average Bay-wide annual flux of DIN from the sediment during the PPBES has been estimated from the sediment chamber measurements at 8100 ± 3200 and at 3600 ±1900 tonnes N y^{-1}, depending on the assumptions made in spatial extrapolation (Nicholson *et al.* 1996). This large uncertainty is due to the limited spatial and temporal coverage that was feasible for these complex experiments. The lower range, which assumes very low fluxes in the Sands, is thought to be more realistic.

There were no direct measurements made of water-column recycling of DIN in PPBES (this flux can be measured using ^{15}N as a tracer.) The estimate provided here is based on mass conservation. Given primary production of 30000 tonnes N y^{-1} by phytoplankton and (very roughly) around 6000 tonnes N y^{-1} by macroalgae, and inputs consisting of 6000 tonnes N y^{-1} from external loads, 8000 tonnes y^{-1} from sediment release, and 4000 tonnes N y^{-1} from filter-feeder release, it follows that water column recycling is around 18000 tonnes N y^{-1}. The measured microzooplankton grazing rates represented approximately 2/3 of nutrient-limited phytoplankton growth rates. However, these rates do not include grazing by mesozooplankton on larger phytoplankton. If zooplankton grazing accounted for all 30000 tonnes N y^{-1} phytoplankton production, then water column recycling of 18000 tonnes would imply a recycling efficiency of 60%. Given that some phytoplankton production must be consumed by benthic filter-feeders, or lost to direct sedimentation, the recycling efficiency associated with grazing must be even higher. We must of course keep in mind that we are calculating differences of terms each involving substantial estimation errors. Still, given the observed high levels of phytoplankton production and the high denitrification efficiencies in the sediment, it is impossible to avoid the conclusion that water column recycling efficiencies must be high.

At steady-state, the annual loss of N due to denitrification in the sediments must match the inputs to the Bay minus the losses to Bass Strait. This net load is about 7000 tonnes N y^{-1}. Sediment respiration based on measured oxygen fluxes was estimated at 30000 and 18600 tonnes N y^{-1} under the two spatial extrapolation methods used (Nicholson *et*

al. 1996). However this oxygen flux gives gross respiration. The net sediment respiration (in N terms) must equal the sum of measured DIN release (3600 to 8100 tonnes N y^{-1}) plus denitrification, ie. 10600 to 15100 tonnes N y^{-1}. This level of net sediment respiration is also consistent with the observation that sediment respiration correlates well ($r^2 = 0.655$) at regional and seasonal scales with primary production, with a slope of 0.45 (Nicholson *et al*. 1996).

The difference between net sediment respiration and gross sediment respiration (8000 to 15000 tonnes N y^{-1}) must be supported by carbon and nitrogen fixed in the surface sediment ie. by microphytobenthos production. Estimates of Bay-wide MPB production (10000 to 15000 tonnes N y^{-1}) are entirely consistent with this explanation. Because measurements of MPB production and sediment chamber fluxes were carried out at different times and places, it is not possible to confirm this consistency at the scale of local measurements. Nevertheless, estimates of all major fluxes appear to be consistent at a Baywide level. The ratio of denitrification to net sediment respiration gives a high denitrification efficiency of 46-66% and an even higher "apparent denitrification efficiency" of 70-85%, if the gross respiration rate is compared with DIN release.

Major fluxes of nitrogen used to constrain the model solutions are shown in table 7.3. The ranges given are based on our current state of knowledge, and may not reflect the variation in historical estimates.

As discussed below, these annual Baywide mean pools and fluxes are quite powerful constraints on model parameters. However, the model has been designed to explain and predict spatial and temporal variation in key variables and fluxes at a number of space and time scales. We consider next the spatial and temporal patterns revealed by the field data, and the issues involved in model-data comparison at these spatial and temporal scales.

Table 7.3. Estimates of major nitrogen fluxes (tonnes N Bay-wide per year) in Port Phillip Bay

Flux	Estimate	Min	Max
Phyto. Prim Prod.	30000	25000	38000
MA Prim. Prod.	5000	2000	9000
MB Prim. Prod	12,000	10,000	15,000
SRc	8000	3000	10,000
FRc	3750	?	?
WRc	18,000	15,000	25,000
Denitrification	7000	6500	7500
S. Resp.	14,000	10,000	15,000

7.2.3 Spatial and temporal variation.

Based on the field results, one can distinguish three major regions in Port Phillip Bay: the central basin, the north-western and north-eastern coastal areas, and the southern Sands. These correspond to the Bay centre, surround and exchange zones defined in the

Phase One Study (MMBW/FWD 1973).The central basin is low in nutrients, relatively deep and dominated by phytoplankton production. The north-western and north-eastern coasts are the regions of highest external nutrient loads, with relatively high phytoplankton biomass and substantial macroalgal beds. The Sands are also shallow, but they are strongly flushed by Bass Strait waters and have lowest nutrient concentrations (especially phosphate) and low phytoplankton biomass. Most seagrass beds are found in shallow parts of the south of the Bay, except in those areas where bottom stress prevents colonisation.

Fig. 7.1 presents a partitioning of the Bay into 8 regional compartments. These represent supersets of the 59 boxes used in the transport model, and have been chosen to reflect the observed regional variation in the Bay. (To avoid ambiguity, we refer in this chapter to the boxes used in the standard 59-box transport model as "fine" boxes, and the 8 regional boxes as "coarse" boxes.) We have at times implemented transport and nutrient models with this coarse regional resolution, and the coarse boxes were also partly chosen with this in mind. For example, the Sands region is subdivided into northern and southern parts (coarse boxes 1 and 2), mainly for reasons related to physical transport (to better represent exchange with Bass Strait). The coastal region is subdivided into 5 regional boxes. Three of these are centred on major inputs: Patterson-Mordialloc (coarse box 3), Yarra River (coarse box 4) and WTP (coarse box 6). Corio Bay (coarse box 7) has no major direct inputs. It is influenced by inputs from Werribee, but has limited physical exchange with the rest of the Bay. Coarse box 5 in the north-west lies between the Yarra and WTP inputs, and is influenced by both, depending on the circulation. The Bay centre is represented by a single region, coarse box 8, but is subdivided into northern and southern components for some analyses.

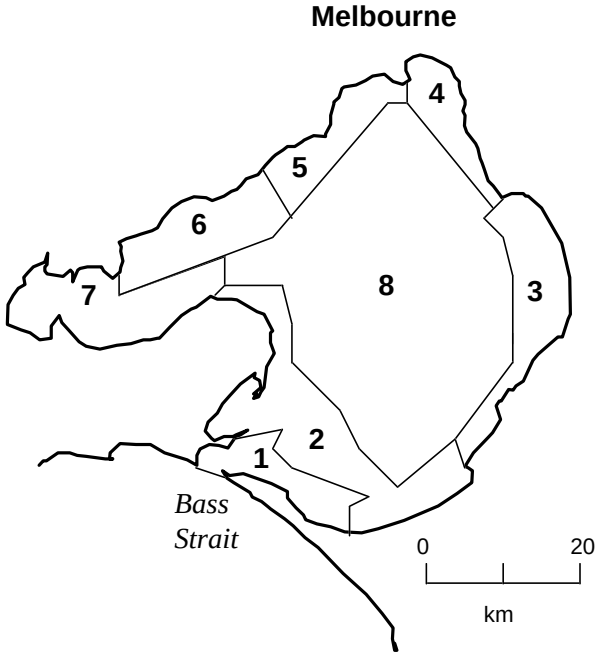

Figure 7.1 the 8 Box model regional structure of Port Phillip Bay. The regions are: 1 - the Heads; 2 - the Sands; 3 - East Coast; 4 - Yarra; 5 - North West; 6 - Werribee; 7 - Corio Bay; and 8 - the Bay Centre.

We consider that these regional boxes capture the key persistent spatial patterns within the Bay. Generally speaking, we would be satisfied if the simulation model reproduced the observed spatial and temporal patterns at this spatial scale. The transport and integrated model are run at a higher spatial resolution (the fine boxes, Chapter 3) partly because of concern about the interaction of horizontal transport and biogeochemical processes near inputs, and partly to address local phenomena, including effects of bottom depth on benthos.

Even at the regional box scale, the availability of data for model calibration is very uneven. In the case of the underway nutrient and chlorophyll data, there may be hundreds of observations in one box, but the cruise track may still be biased with respect to persistent spatial gradients within the box. In the case of variables such as DON, we have observations at only one or two fixed sites within a regional box, and the potential for bias is much greater. Even if a sampling point or cruise track is "unbiased" in some long-term statistical sense, there may still be considerable "noise" associated with any given observation. Many water column properties are known to be patchy at a range of length scales. Especially in areas of large mean gradients, near the major point source inputs and across the Sands, there is likely to be patchiness driven by turbulent stirring at scales which are not resolved by the transport model.

For variables with observations at fixed sites only, it arguably makes more sense to compare observations with model predictions at the finest model resolution (ie. fine box means rather than regional or coarse box means). Even for the underway data, we have the option of comparing transect means within fine boxes with the model predictions. Fine box concentrations predicted by the model must be regarded as (arithmetic) mean concentrations for the box volume, and should ideally be compared with comparable averages of the observations. Where we have only isolated observations at a site within a box, the question arises as to what level of agreement we should expect between a predicted average concentration and a single sample from a potentially patchy field.

We have investigated the relationship between spatial averages and point observations directly for those variables (nutrients and chlorophyll) where we can compare averages of underway concentrations along the cruise track with a fixed site measurement in the same fine box. Examples are shown for chlorophyll concentrations in Fig. 7.2. The correlation is quite high at site 6 (off Sandringham) and at site 1 (Blairgowrie). This reflects a relatively low spatial variance within the associated fine boxes, compared with the month-to-month variation in concentrations. The correlation is weaker at site m2 in the northern central Bay: the within-box spatial variance is in fact quite low near this site, but the mean concentrations are also low, and show relatively weak month-to-month variation. The worst agreement is obtained at site 11 off Werribee (and at site 9 in Hobsons Bay, not shown). The correlation at site 11 is still quite high, but the profile mean underestimates the cruise track mean by a factor of 2 or more when the latter exceeds 3 mg Chl m^{-3}. This bias reflects the particular location of the fixed site within strong local gradients near a major input.

We have also carried out an extensive analysis of the spatial and temporal patterns of variation in the underway data. This will be reported in detail elsewhere, but the key conclusions of relevance to model calibration can be summarised as follows. There are generally moderate levels of local spatial variation within fine boxes throughout the Bay

(coefficients of variation of about 0.3), with elevated levels in regions of large gradients (near the Yarra and WTP inputs and, in the case of phosphate and silicate, across the Sands). Elevated variance among fine boxes within regional boxes, and persistent mean gradients in fine box means, also characterise these high-gradient "mixing zones". The analysis confirms that the regional or coarse boxes capture most of the persistent spatial variation in the Bay, but that there are strong contributions from spatial-temporal interactions at fine box × monthly and region × monthly scales.

The intensive repeat surveys conducted off Werribee and Hobsons Bay, reported by Longmore *et al*. (1996), also show strong patchiness at scales of order 1 km, which are not resolved by the fine boxes. These patches change on time scales of hours to days, and will produce both high and variable spatial variances within fine boxes. The day-to-day variability in these patches is aliased by the monthly surveys, and appears as a contribution from monthly × fine box interaction terms. This kind of variation is not able to be predicted by the model.

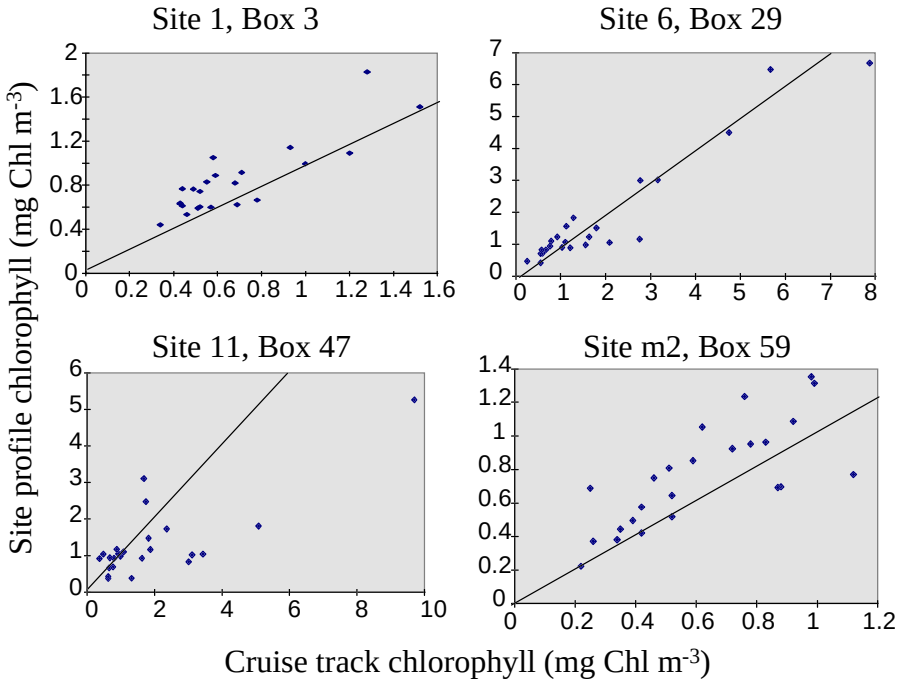

Figure 7.2 Chlorophyll concentrations (mg m^{-3}) obtained at fixed sites plotted against chlorophyll concentrations obtained from cruise tracks within the same fine box. The correlation coefficients are 0.85 for site 1, 0.95 for site 6, 0.78 for site 11 and 0.76 for site m2.

This fine scale spatial and temporal patchiness also shows up as relatively weak temporal autocorrelation at fixed sites, even at the two week sampling interval. At site 1, a strong long-term decline throughout the Study period results in a relatively high autocorrelation at a two week lag of 0.51. Off Werribee (site 11) there is no significant

fortnight-on-fortnight autocorrelation at all (-0.07). Other sites lie between these extremes.

The variance in most observed variables scales with the square of the mean, indicating that the data are generally log-normally distributed. A log-normal distribution is not unexpected, and is consistent either with turbulent stirring of gradients near sources, with exponential growth of biological populations, or with variation driven by a number of independent multiplicative factors. The exception is nitrate, which is present in such low mean concentrations, in some cases close to detection limits, that measurement errors result in inflated coefficients of variation.

Given a log-normal distribution, it is common practice to log-scale data before calculating statistics such as means and variances. This is equivalent to calculating geometric means and coefficients of variation of the unscaled data. However, the model prediction corresponds to the arithmetic mean of the corresponding fine box. In comparing model predictions and observations, one should either compute arithmetic means of the observations, or correct the geometric mean for bias.

For sites located in strong spatial gradients, especially site 9 in Hobsons Bay and site 11 off Werribee, the location of the site within the fine box may lead to bias, as we saw in Fig. 7.2. We have chosen fine box boundaries parallel to the shore to approximately follow depth contours at 5 m intervals. In some cases, this means that sampling sites fall close to fine box boundaries. In these cases, we have tried to use the underway data to choose the fine box which shows least bias between underway observations and site observations. However, it must be recognised that there are intrinsic limitations in the level of spatial resolution chosen for the model. If we want to model distributions at these fine scales near inputs, we will need to use finer spatial (and temporal) resolution in the model.

These analyses also have implications for model-data comparisons at different temporal scales. We expect the model to replicate reasonably well variation at seasonal and interannual time scales, and to respond correctly to major events, such as Yarra floods. However, it is unreasonable to expect the model to reproduce local, cruise-to-cruise fluctuations, especially given the observed small-scale patchiness and the likelihood of spatial and temporal aliasing in monthly observations at these scales. Even with perfect observations, it would be overly ambitious to expect to reproduce the exact time course of transient blooms off Werribee under high but slowly-varying loads. It is desirable that the model produce blooms of similar magnitude, duration and frequency, or more broadly, that the model should reproduce the observed statistical properties (mean and standard deviations) at regional scales.

Correlations of predicted and observed concentrations, or sums of squared residuals, are not necessarily appropriate measures of model performance under these conditions. The model could produce blooms of the appropriate magnitude and frequency without consistent phase relationships to observations. Phase lags are also potentially an issue for model-data comparisons in cases where we do expect some level of deterministic prediction, such as the response to high Yarra runoff events. The model may well produce responses of the correct magnitude, but either lagged or in advance of the observed response. Again, correlation or sum of squared errors may provide a

misleading measure of model performance, especially given that observations are made at monthly intervals.

In the case of the underway measurements of nutrients and chlorophyll, we have focused on comparing predicted and observed means and standard deviations at regional scales. However, the possibility of bias in cruise track locations within regional boxes is still a cause for concern, especially in those regional boxes with strong spatial gradients. Since it was not possible to correct for this bias using only the observations, we chose instead to compute a model regional mean which could be directly compared with the direct mean of the observations. This was done by computing a weighted mean of the model fine box values within the region, with the weights chosen according to the number of underway observations in each fine box. (Since this varied from one cruise to the next, the weights were recomputed for each cruise.) This weighted predicted mean should show the same bias as the observations. We can of course compute directly the model bias between a cruise-track weighted mean and a true (volume-weighted) mean.

There is still a potential problem in cases where spatial gradients are very steep, and the cruise track represents a biased sample within fine boxes. A good example occurs off Werribee (coarse box 6), where cruise tracks often run parallel to the coast near the boundary between coastal and offshore fine boxes. The difference between these fine boxes in the model is large, whereas the effect on observations of being on one side or the other of this imaginary line is small. These problems could only be addressed by increased spatial resolution in the model.

In calibrating the model, we have relied heavily on comparing cruise-track weighted regional means with observed regional means. We have also computed and compared cruise-track weighted Bay-wide means. This represents a small enough data volume that it is feasible to compare monthly observations and predictions of all underway variables graphically for each run. We have also computed and compared annual means and variances for these quantities.

We have computed means of the underway observations for each fine box, and graphically compared predictions and observations on a month by month basis at this level. However, the data volume involved is considerable, and we have used this approach primarily to assess and/or fine-tune the performance of the standard run, after calibration was largely complete. Because of the high levels of log-normal noise in fine-scale observations, it is appropriate to log-scale predictions and observations.

In the case of benthic variables such as macroalgae (Fig. 7.3), seagrass (Fig. 7.4: Bulthuis *et al*. 1992), microphytobenthos (Beardall and Light 1997), and sabellids (Harris *et al*. 1996) we have qualitatively compared observed and predicted spatial (and in some cases seasonal) distributions.

Because we have used a heuristic rather than formal minimum cost or maximum likelihood approach to model calibration, we have not been forced to specify quantitatively the weights attached to different observations, or to different spatial and temporal statistics. In the case of a consistent data set such as the underway data, it is possible to develop quantitative formal weights which reflect appropriately the spatial and temporal variation (patchiness) in the observations, and its effect on different spatial

and temporal statistics. However, *a priori* estimates of observation error in other data sets must be more subjective.

In practice, we have given most weight to observations which were assessed as having lower uncertainty, particularly the regional means derived from the underway data sets, and the annual and Bay-wide mean pools and fluxes. We have in some cases paid relatively little attention to date to variables where the model predictions were thought to be less critical, and the process errors involved were not thought to critically affect the key model outcomes. Examples include seagrass and nitrate, which are discussed further in the following sections.

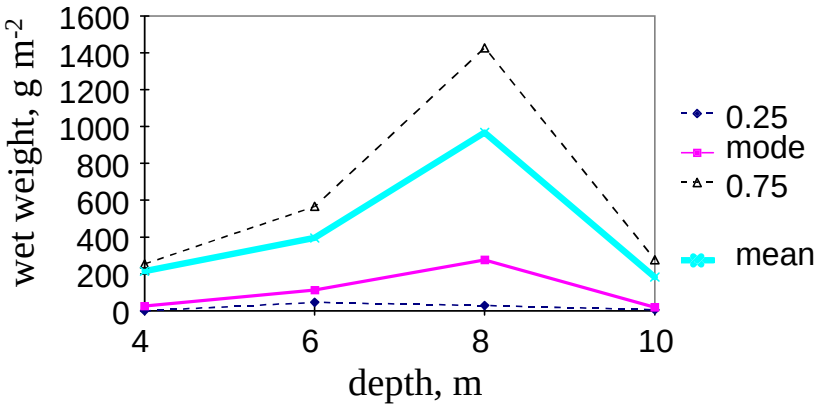

Figure 7.3 Mean, mode and interquartile range of macroalgal biomass, g wet weight m^{-2}, from all sites.

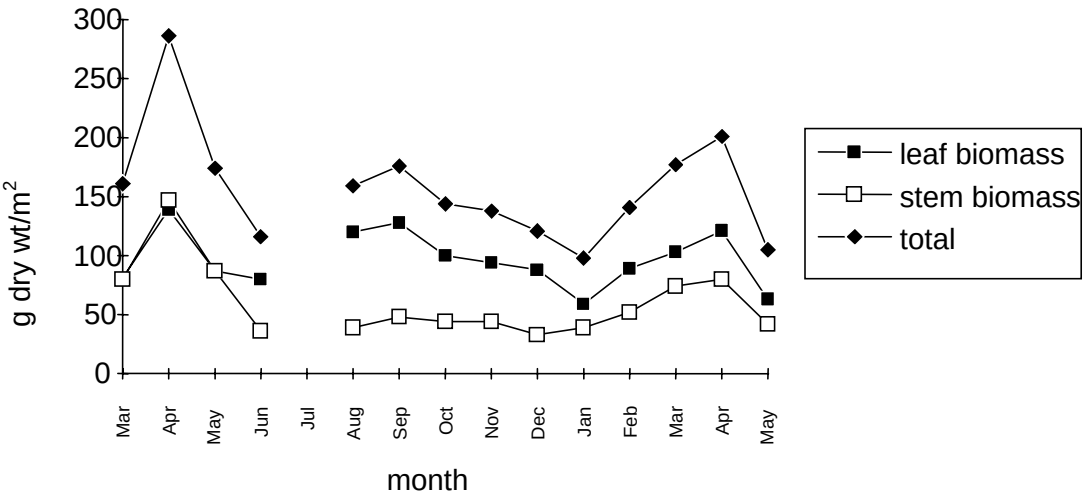

Figure 7.4 Seasonal Patterns in Seagrass above-ground Biomass in Swan Bay (1978-9)

7.3 Model Performance at Bay-wide, Annual Scales.

This section describes the results of numerical experiments undertaken as part of the model calibration procedure. We have not attempted to describe the historical sequence of experiments, but rather summarised the effects of changes in parameters on model predictions in relation to observations. This section focuses on the model performance at the level of Bay-wide annual means. Subsequent sections deal with model performance at other time and space scales.

Because of the number of parameters, and the nonlinear interactions among parameters, it is not feasible to systematically or comprehensively explore all parameter combinations. The numerical experiments described here involve changes in selected individual parameters or combinations of a small number of parameters. These selections were based on understanding derived from the qualitative analysis described in Chapter 6, and experience gained in running the full model. As noted earlier, the model structure and process formulation co-evolved with the calibration process. This is a potential complication, but in practice it has been fairly easy to distinguish effects of changes in model formulation, and these are noted where appropriate.

It is worth noting that the qualitative model analysis, and the use of Bay-wide annual averages for model calibration, are particularly useful in Port Phillip Bay because approximately 70% of the volume of the Bay falls within the central region, where the steady-state one-box approximation is arguably a good approximation at seasonal and interannual time scales. We can therefore proceed by determining parameter subsets, which produce approximately the right steady-state behaviour in the Bay centre, and then fine-tuning those subsets to obtain the correct behaviour at finer time and space scales in the coastal region.

Because of the potential for non-linear interactions among parameters, any approach that allows us to disaggregate or quarantine groups of parameters is particularly valuable for model calibration. A key separation of this kind can be made between water column and sediment parameters, at least at the level of Bay-wide annual fluxes. We noted in the discussion of annual budgets in Section 7.2 that, averaged over a year, the nitrogen loss to denitrification (plus the small loss to Bass Strait) must balance the external load, and that the net sediment respiration rate must balance the denitrification loss plus DIN release from the sediment. Thus, so long as the export to Bass Strait is small, the model must produce the correct net sediment respiration rate and DIN release if it produces the appropriate mean denitrification efficiency.

In the final version of the model, which uses the "neutral" formulation of the MPB-denitrification interaction, the local relationship between denitrification efficiency and net sediment respiration rate is determined entirely by the denitrification parameters Dmax, R_0 and R_D. It is quite straightforward to adjust these so as to produce the correct Baywide annual DIN release and consequently, the correct net sediment respiration. Because the local relationship between denitrification flux and net sediment respiration rate is non-linear, the mean Bay-wide denitrification efficiency in principle depends on the spatial and temporal pattern of sediment respiration rates, and consequently on a host of water column parameters. However, the effect of this non-linearity on Bay-wide fluxes is quite weak at current loadings. (It does become much more important as loadings approach or exceed the maximum denitrification capacity.)

Under the "facilitative" formulation of the interaction between microphytobenthos and denitrification, the effective denitrification efficiency also depends on levels of MPB production. The parameters controlling MPB production (growth rates, light saturation intensity, mortality rate) then interact strongly with the denitrification parameters in controlling Bay-wide denitrification efficiency. There is also a potential interaction via light attenuation between water column processes and microphytobenthos production. This latter interaction is generally weak at current loadings and chlorophyll levels, but would be important at higher loadings.

Using the standard "neutral" formulation of the MPB-denitrification interaction, the level of MPB production and biomass can be adjusted independently of both sediment DIN release and water column processes (subject to the comment concerning light attenuation) by manipulating MPB growth and mortality parameters. Note that at a given level of DIN release from the sediment, DIN concentrations in the sediment are determined by the physical parameters controlling exchange of pore water with the overlying water column. The MPB nutrient half-saturation parameter must be adjusted accordingly.

Many processes and parameters potentially interact to determine pools and fluxes in the water column, and it is more difficult to separate parameter effects. However, the qualitative analysis of Chapter 6 still suggests a useful line of approach. Given the external load and the DIN release from the sediment, the level of primary production is determined by the water-column recycling efficiency. Those parameters that prescribe the proportion of grazed material released as DIN, directly affect water column recycling efficiency, and can be adjusted to obtain the appropriate level of primary production. However, other parameters and processes (eg. sinking rates of diatoms and suspended detritus) indirectly affect water column recycling efficiency. Because different recycling efficiencies are associated with different primary producers and grazers, changes in parameters that affect the relative dominance of these groups also potentially change the overall primary production level. Thus, total primary production, and the relative production of different functional groups, must be adjusted together. This requires carefully planned sequences of numerical experiments.

We describe now the results of particular numerical experiments demonstrating the effects of changes in parameter values for both the sediment and the water column. In some cases, we refer to individual model runs by a run number. These numbers belong to two series of model runs. In the first series (numbers without a prefix), the model did not include Si limitation. In the second series (numbers with the prefix "si"), the model included Si cycling and Si limitation of diatoms.

7.3.1 Denitrification, sediment recycling and microphytobenthos.

The denitrification submodel has three parameters: Dmax, R_0 and R_D. The maximum denitrification efficiency Dmax directly controls Bay-wide denitrification efficiency and consequently overall primary production. As Dmax is varied between 0.5 and 0.9, phytoplankton primary production decreases from 39000 tonnes N y^{-1} at Dmax = 0.5 to 29000 tonnes N y^{-1} at Dmax = 0.7, and 22000 tonnes N y^{-1} at Dmax = 0.9. (An expanded version of this experiment is presented in Chapter 8 as a management scenario.)

The sediment respiration rate required to achieve maximum denitrification efficiency, R_D, is not well constrained by the sediment chamber observations, although it appears to be lower than 20 mg N m^{-2} d^{-1}. The exact value of this parameter is not particularly important at the current loads, because sediment respiration rates in most locations (with the possible exception of the Sands) are above 20 mg N m^{-2} d^{-1}. A decrease in R_D from 20 to 10 mg N m^{-2} d^{-1} caused only a 10% decrease in Bay-wide primary production. This decrease results from increased denitrification efficiency at locations with low sediment respiration rates: the DIN release dropped by 15% in the Sands. The associated reduction in pore water DIN does potentially have an impact on seagrass distribution, as seagrass occur in areas with low sediment respiration rates.

The sediment respiration rate at which denitrification efficiency drops to zero, R_0, is only weakly constrained by the observations to within a factor of ca 2 about 250 mg N m^{-2} d^{-1}. If R_0 is decreased to 125 mg N m^{-2} d^{-1}, DIN release from the sediment increases by about 60%. However, when R_0 is increased to 500 mg N m^{-2} d^{-1}, DIN release from the sediment decreases only marginally. This reflects the fact that, under current loads, predicted local sediment respiration rates are mostly well below 250 mg N m^{-2} d^{-1}. Of course, the response of the model to increased loads is particularly sensitive to R_0. If Dmax and R_D are fixed, the maximum denitrification capacity of the Bay varies like the square of R_0 (see Chapter 6). The uncertainty in R_0 discussed in Chapter 3, which cannot be resolved by calibration of the full model against observations, remains a major source of uncertainty in model predictions of responses to increases in load. This uncertainty is worth addressing through further process experiments.

As discussed in Chapter 6, we have developed two formulations of the interaction between microphytobenthos and denitrification, the so-called "facilitative" and "neutral" submodels. In the facilitative submodel, MPB intercept DIN which would otherwise be released to the water column, and convert it back into organic matter, which is recycled through the sediment remineralization-denitrification loop, increasing the effective denitrification efficiency. We noted in Chapter 6 that, in order to obtain the observed Bay-wide denitrification loss, one would need to use a much lower value of Dmax for the facilitative submodel (Dmax = 0.3) than for the neutral submodel. Not surprisingly, numerical experiments with the full model confirm this.

If one adopts the facilitative submodel, then changes in MPB production have a major effect on DIN release from the sediment, and therefore on water column production. When microphytobenthos were eliminated from a model version incorporating the facilitative submodel, phytoplankton primary production increased from 30000 tonnes N y^{-1} to 56000 tonnes N y^{-1}, while DIN release from the sediment increased from 6000 to 20000 tonnes N y^{-1}. (This change is approximately equivalent to decreasing Dmax from 0.7 to 0.3 in the neutral submodel.)

When Dmax values are adjusted correctly, the two submodels result in quite similar predictions of Bay-wide fluxes and pools at current loads. As discussed in Chapter 6, the facilitative submodel is more sensitive to increasing loads. However, the neutral submodel is more consistent with the sediment chamber observations: the facilitative submodel cannot reproduce observed high denitrification efficiencies in the Bay centre, where MPB production is often very low.

At current loads, the MPB biomass, production and spatial distribution are determined primarily by the MPB light-saturated growth rate, light saturation intensity, and the (quadratic) mortality rate parameter. The first and second are directly constrained by the results of the MPB photosynthesis-light experiments. The light saturation intensity strongly controls the predicted depth-distribution of MPB, and is best calibrated against the observed spatial distribution. The biomass and production levels overall are primarily determined by the choice of the mortality rate parameter, which is not constrained *a priori*, and is chosen to reproduce the observed Bay-wide biomass and production. Nutrient limitation is relatively unimportant for MPB production, except possibly in the Sands.

Because light-limitation is so important, MPB biomass and production are potentially strongly affected by changes in light attenuation resulting from increases in phytoplankton in the water column. However, the observed phytoplankton concentrations make only a small contribution to light attenuation, at least in the Bay centre. This interaction does become important at higher loads, when predicted chlorophyll values increase substantially. For example, the PPBES Final Report (Harris *et al*. 1996) describes a series of experiments (using the facilitative denitrification submodel and quadratic zooplankton mortality) in which total nutrient loads were increased by up to a factor of 5. At twice the current load, the predicted phytoplankton concentration increased ca 6 times, and MPB production was severely diminished. This effect of shading by phytoplankton on MPB production is an important positive feedback in eutrophication when the facilitative submodel is adopted, and the MPB light saturation intensity is an important parameter controlling the onset of this feedback. By comparison, using the neutral submodel, the predicted phytoplankton concentration increases only twice at doubled loads, and the decline in MPB production is quite small (see Chapter 8).

7.3.2 Phytoplankton growth and water-column recycling

The model has been implemented with multiple classes of phytoplankton. In the standard model version, there are two classes: small non-sinking phytoplankton and large phytoplankton that sink and require Si. There have been experimental runs in which the large phytoplankton are split into diatoms, which sink and need Si, and dinoflagellates, which do not sink or need Si for growth. These phytoplankton fractions (and their associated grazers) represent a considerable complication of the plankton model over a simple NPZ model. The justification for this complication is discussed in some detail in Chapter 3. It would be possible to calibrate a simpler plankton model to match the observed annual biomass and fluxes. The justification for the more complex model lies largely in its ability to reproduce spatial and temporal patterns within the Bay (and in the differences in the expected response to changes in loads).

During the PPBES, the biomass of small phytoplankton was relatively stable over much of the Bay, while large phytoplankton biomass was far more variable, both spatially and temporally (Beardall *et al*. 1996). These spatial and temporal patterns are discussed further in the next section. However, because large phytoplankton sink, the relative dominance of the two size fractions affects water-column recycling efficiency and hence total phytoplankton production in the model.

We consider first a set of experiments in which one fraction was removed from the model, keeping all other parameters fixed. Primary production rose from 30000 to 33000 tonnes N y^{-1} with the removal of PL, but fell to 20000 tonnes N y^{-1} when PS was removed. The water column recycling flux also changed, the corresponding values being 20000, 25000 and 13000 tonnes N y^{-1}. DIN release from the sediment hardly changed, as expected, being fixed by the external load and sediment denitrification efficiency. It was 5700, 5500 and 6000 tonnes N y^{-1} respectively in the three cases.

The mean Bay-wide biomass of each phytoplankton fraction increased in response to the removal of its competitor. Large phytoplankton alone increased from 1.6 to 3.7 mg N m^{-3}, and small phytoplankton alone from 3.2 to 4.1 mg N m^{-3}. However, in each case, the removal of one fraction led to a decrease in the total biomass (and total chlorophyll) compared with the biomass of 4.8 mg N m^{-3} with both fractions present. The concentration of ammonia increased in both cases, from about 8 to 12 mg N m^{-3}, but for rather different reasons. Ammonia concentrations are set primarily by the phytoplankton nutrient-limited growth rates. The small phytoplankton alone grow more rapidly, and hence require higher concentrations of the limiting nutrient. The large phytoplankton also have higher half-saturation constants for nutrient-limited growth.

Removal of an entire fraction of the phytoplankton is a rather drastic change. Many other parameters also affect the balance between the two size groups, sometimes in subtle and unexpected ways. We consider here the response of the size fractions to changes in nutrient loading and recycling, sinking rates (both the diatom sinking rate w_PL and detrital sinking rates), maximum growth rates, and nutrient half-saturation concentrations. Zooplankton parameters also strongly affect the phytoplankton biomass and production levels: these are dealt with in the next subsection.

The effective DIN loading to the water column is affected directly by changes in external loads (Harris *et al*. 1996) and indirectly by changes in denitrification efficiency and sediment release. Using the standard model version, when loads to the Bay were increased from 0.5 to 2 times current loads, the biomass of diatoms increased by a factor of 5, whereas small phytoplankton increased by only 50%. Similar changes in biomass and dominance were predicted using an earlier model version when Dmax was decreased from 0.9 to 0.3. However, when Dmax was cut from 0.3 to 0.1, causing very high DIN loads to the water column, both groups increased in biomass by about 50%. In general, one would expect large phytoplankton to respond most to increased nutrient loads, and the model behaviour is consistent with that expectation. However, diatoms can become silicate limited at very high nitrogen loads, resulting in an increase in small phytoplankton. These responses to changes in loads and Dmax are considered in more detail in Chapter 8.

The sinking rate of detritus determines the proportion of detritus which is suspended and remineralised in the water column, where it is not subject to high denitrification losses. Thus decreasing detritus sinking rates increases water column recycling efficiencies, and primary production. In one set of experiments, reducing the sinking rate of labile detritus from 5 to 1 m d^{-1} and of refractory detritus from 1 to 0.5 m d^{-1} caused primary production to rise from 27000 to 30000 tonnes y^{-1}. The mean biomass of large and small phytoplankton rose from 6.9 to 7.5 mg N m^{-3} and 2.2 to 2.4 mg N m^{-3} respectively. In a later set of experiments, decreasing sinking rates of labile detritus from 5 to 2 and then 1

m d^{-1} caused primary production to rise from 29000 to 34500 to 38500 tonnes y^{-1}, large phytoplankton biomass to rise from 2.26 to 2.6 to 2.79 mg N m^{-3} and small phytoplankton biomass to increase from 2.11 to 2.32 to 2.53 mg N m^{-3}. In these experiments, mean Bay-wide biomasses of large and small phytoplankton were almost equally affected.

There are interesting spatial effects of changes in detritus sinking rate. Because DIN is rapidly removed by phytoplankton blooms, advection of suspended detritus is an important mechanism for transporting nitrogen from coastal areas into the Bay centre. When sinking rates are high, detritus is rapidly transported to the sediment where it is locally recycled, and nitrogen tends to be trapped and recycled in coastal areas near inputs.

The sinking rates of detritus are not well-constrained *a priori* by independent measurements, and are only weakly constrained by their impact on recycling efficiency (many other parameters also affect recycling efficiency). The best indirect constraint on detritus sinking rates should be the observed concentrations of suspended detritus in the Bay, but these also include an unknown contribution from very refractory detritus, which is not represented in the model.

The sinking rate of large phytoplankton (diatoms) directly affects their loss rate, and consequently the balance between small and large phytoplankton, as well as the water column recycling efficiency. In one experiment, as diatom sinking rates were decreased from 2.5 to 1.75 to 1 m d^{-1}, primary production rose from 19500 to 23300 to 28200 tonnes N y^{-1}, large phytoplankton biomass increased from 2.5 to 3.5 to 4.9 mg N m^{-3}, while small phytoplankton biomass and mean ammonia concentrations remained unchanged. Results of an earlier series of experiments, in which the diatom sinking rate was changed from 5 to 1 m d^{-1}, are shown in Table 7.4. In all these cases, primary production increased about 20%, large phytoplankton biomass (PL) doubled, and small phytoplankton biomass (PS) decreased slightly. This is consistent with the more recent experiment, except that the relative effect on primary production is much larger in the more recent case. The explanation lies in changes to the macroalgal component between the two series. In the more recent series, macroalgal production was larger, and competition between macroalgae and diatoms more significant. As diatom sinking rates increased, total primary production shifted from phytoplankton to macroalgae, and the drop in phytoplankton primary production was magnified.

Table 7.4 The effect of PL sinking rate on primary production (tonnes N y^{-1}) and mean concentration (mg N m^{-3}) of large (PL) and small (PS) phytoplankton.

	5 m d^{-1}				1 m d^{-1}		
run	Prim. Pr.	PL	PS	run	Prim. Pr.	PL	PS
45	28357	1.42	3.14	45s	32922	3.22	2.83
58	28879	2.14	2.58	51	33877	4.34	2.26
65	32287	1.60	4.76	61	33191	4.37	3.28
66	28356	2.37	3.49	62	31974	5.21	2.58
50	28248	1.42	3.12	50s	32845	3.23	2.82

Phytoplankton growth rates are controlled by the maximum growth rates mum_PL and mum_PS, nutrient limitation, and light limitation. Under current conditions, nutrient limitation is much more important than light limitation. In coastal regions where nutrient levels are at times elevated and potentially saturating to growth, the water column is shallow and mean light levels are relatively high. In the Bay centre, mean water column light intensities are substantially reduced (by about a factor of 5) at current light attenuation levels, and light limitation does reduce phytoplankton growth rates at the observed values of the light saturation intensity KI. However, it would be difficult to distinguish effects of changes in KI from effects of changes in maximum growth rate.

Significantly, phytoplankton currently make a small contribution to light attenuation in the Bay centre (see Chapter 3). This means that the negative feedback of phytoplankton biomass on phytoplankton growth rates via self-shading is not important at current loads. Self-shading is likely to be important at high loads. Note that light attenuation at the bottom of the water column is quite severe: in the Bay centre, the bottom sees 1% or less of surface light. As noted earlier, the light saturation intensity is a critical parameter for all phytobenthos.

The data from the zooplankton grazing dilution experiments provided quite good *a priori* constraints on phytoplankton maximum growth rates. We have conducted a number of model experiments to investigate the effects of changes in these parameters, often in concert with changes in sinking rates or nutrient half-saturation constants. In one example (runs 45s and 51 in table 7.4), the maximum growth rate of large phytoplankton, mum_PL, was raised from 1.24 to 1.7 d^{-1}, while mum_PS remained at 1.24 d^{-1}. Increasing mum_PL led to an increase in PL biomass, a decrease in PS biomass and a slight increase in phytoplankton primary production. In another experiment, the maximum growth rate of both phytoplankton fractions was cut from 1.24 to 1 d^{-1}. The effect on phytoplankton biomass was quite small: PL fell from 2.9 to 2.6 and PS from 2.3 to 2.1 mg N m^{-3}. However, annual phytoplankton primary production fell substantially from 32000 to 26000 tonnes N y^{-1} and ammonia and nitrate concentrations doubled. This significant decrease in phytoplankton primary production resulted from a switch from phytoplankton to macroalgal production.

Phytoplankton maximum growth rates are important in controlling the outcome of competition between different phytoplankton fractions, and between phytoplankton and macroalgae. The standard version of the model sets mum_PL = 1.7 d^{-1}, and mum_PS = 1.24 d^{-1}, at 15°C. These values are consistent with the field results (grazing experiments) and, in combination with the nutrient half-saturation constants discussed below, yield an appropriate balance between large and small phytoplankton.

As discussed in Chapter 6, under simplifying steady-state assumptions, primary production is determined by external loads and recycling efficiencies, and phytoplankton biomass and growth rates given primary production are determined by zooplankton parameters. Given phytoplankton growth rates, nutrient concentrations are determined by the half-saturation constant KN. Thus we expect changes in KN to primarily affect ambient ammonia levels. However, because phytoplankton growth is nutrient-limited, changes in KN also strongly affect the outcome of competition between phytoplankton fractions, and hence indirectly recycling efficiencies and primary production.

Results of three numerical experiments involving KN, each consisting of a pair of runs, are shown in table 7.5. In the first two pairs, KN_PL was increased from 10 to 12 and KN_PS from 4 to 6 mg N m^{-3}. This increased the relative competitive ability of large phytoplankton, because the relative increase in KN_PS was larger. This led to an increase in diatom biomass, and a corresponding decrease in primary production, due to decreased recycling efficiency. (In these runs macroalgal production was negligible.) In the last pair, KN values for PL, PS and MA were all increased by 20%. This did not result in any competitive advantage to any primary producer, and so the only component changed was DIN (ie. ammonia plus nitrate), that increased by about 20%. Thus, the half-saturation constants can be easily adjusted to obtain the observed Bay-wide mean ammonia concentrations. However, predicting the correct spatial distribution of nutrient concentrations is more difficult. For example, the 20% increase in KN in run si328 led to an 8% increase in ammonia off Werribee, but an 18% increase in ammonia in the Bay centre (where ammonia concentrations are lower and more limiting to growth.).

Table 7.5 Phytoplankton primary production PP, phytoplankton biomass (PL and PS) and DIN (NO_x and NH_4) for selected runs with differing half-saturations (see text).

Run	KN_PL	KN_PS	PP	PL	PS	NO_X	NH_4
59	10	4	34211	1.16	6.49	0.38	3.16
60	12	6	31920	1.71	5.89	0.46	4.03
61	10	4	33191	4.37	3.28	0.38	3.34
62	12	6	31974	5.21	2.58	0.41	3.61
si142	10	4	29439	3.76	1.71	0.85	6.99
si328	12	4.8	29150	3.74	1.70	0.97	8.18

Changes to maximum growth rates and nutrient half saturation constants obviously have interactive effects on phytoplankton competition. In one experiment, mum_PL, mum_PS, KN_PL and KN_PS were all cut by about 40%. This had almost negligible effects on Bay-wide mean phytoplankton biomass, nutrient concentrations and total primary production, because the dependence of growth rate on ammonia at low ammonia concentrations was almost unchanged.

7.3.3 Grazing and zooplankton mortality

As mentioned in the previous chapter, zooplankton parameters play a strong role in determining steady state phytoplankton biomass. Not surprisingly they also play an important, and rather complicated, role in the dynamical model. There were no observations made of zooplankton biomass in the Study, and we must rely for calibration on the effects of zooplankton parameters on the observed pools and fluxes, particularly phytoplankton biomass. The role of zooplankton parameters is particularly important for small phytoplankton, which tend to be grazing limited. The zooplankton parameters most important in determining Bay-wide phytoplankton biomass are the maximum clearance rates C and the quadratic mortality coefficients mQ.

Table 7.6 shows results of a series of experiments in which the clearance rates of both large and small zooplankton were decreased together by either 25% or 50%. Overall, total phytoplankton biomass or chlorophyll increased as C decreased. We would expect the steady-state biomass of one phytoplankton group alone to scale like 1/C. In fact, small phytoplankton biomass increased by more than 1/C, while large phytoplankton biomass generally decreased. Because small phytoplankton are much more strongly grazing limited, a decrease in clearance rates of both grazers tilts the competitive advantage in favour of small phytoplankton. We see this reflected in the ambient nutrient concentration, which is largely controlled by small phytoplankton, which have lower half-saturation constants for growth. As PS biomass increases, their growth rate decreases, and so does the ambient nutrient concentration. Primary production increases, partly because of the increased water column recycling efficiency associated with a relative increase in PS. This version of the model used the facilitative MPB-denitrification interaction, so increases in overall phytoplankton biomass also decreased MPB production, and increased sediment recycling efficiency.

Table 7.6 Pairs of runs for which both C_ZL and C_ZS are altered. The % change in these parameters between pairs of runs is shown in the last column.

Run	PP	MPBP	PL	PS	PL+PS	NO_X	NH_4	ΔC
37	26985	17764	2.59	2.11	4.70	1.24	12.86	
39	31259	15376	2.53	5.40	7.93	0.50	4.38	-50%
51	33876	15705	4.33	2.26	6.59	0.45	4.41	
61	33191	15255	4.37	3.27	7.64	0.38	3.33	-25%
52	30954	16186	2.56	2.94	5.50	0.65	6.21	
64	31143	15683	1.97	4.39	6.36	0.49	4.24	-25%
58	28878	16465	2.14	2.58	4.72	0.62	5.61	
65	32287	15631	1.59	4.75	6.34	0.46	3.91	-25%

Table 7.7. Parameters corresponding to the runs shown in Table 7.6

Run	w_PL	mum_PL	mum_PS	mQ_BF	mQ_ZL	mQ_ZS	IK_PS	IK_PL	C_ZL	C_ZS
37	1	1	1	0.00001	0.015	0.15	10	10	0.1	0.4
39	1	1	1	0.00001	0.015	0.15	10	10	0.05	0.2
51	1	1.7	1.24	0.00001	0.02	0.2	20	20	0.1	0.4
61	1	1.7	1.24	0.00001	0.02	0.2	20	20	0.075	0.3
52	1	1.24	1.24	0.000005	0.015	0.15	10	10	0.1	0.4
64	1	1.24	1.24	0.000005	0.015	0.15	10	10	0.075	0.3
58	2.5	1.7	1.24	0.00001	0.02	0.2	20	20	0.1	0.4
65	2.5	1.7	1.24	0.00001	0.02	0.2	20	20	0.075	0.3

There are differences among these experiments in the response of the model to identical changes in grazing rates, and these can be related to differences in other parameters (Table 7.7). Among the three examples in which clearance rates were cut by 25%, the

magnitude of the shift from large to small phytoplankton increased from (51,61) to (52,64) to (58,65). In run 51, large phytoplankton have high maximum growth rates and low sinking rates, and are initially dominant. In run 52, they have low maximum growth rates and low sinking rates, while in run 58, they have high maximum growth rates but very high sinking rates. These results suggest that parameter sets which make diatoms stronger competitors for nutrient decrease the relative advantage accrued by small phytoplankton through general cuts to clearance rates.

In a more recent experiment, C_ZL and C_ZS were changed successively, with C_ZL reduced first by 50% and then C_ZS by 25%. The system started in a state dominated by small phytoplankton, changed to a state dominated by large phytoplankton, and then changed back to a state in which biomasses were approximately equal. The total chlorophyll concentration increased successively from 0.53 to 0.63 to 0.7 mg m^{-3}, while DIN dropped at each step.

We can summarize these results as follows. Zooplankton clearance rates fix the total phytoplankton biomass, and therefore the growth rate and ambient nutrient levels, for a given level of primary production. The balance between phytoplankton groups is particularly sensitive to clearance rates, which interact strongly with other parameters affecting the outcome of competition (phytoplankton maximum growth rates, nutrient half-saturation constants, and diatom sinking rates.) It is worth noting that clearance rates are only important provided phytoplankton densities are too low to saturate zooplankton ingestion. The sensitivity to clearance rates should be much lower in blooms, or under very high loads.

The analysis in Chapter 6 suggests that the zooplankton quadratic mortality coefficients mQ_ZL and mQ_ZS will co-determine the steady-state phytoplankton biomass, along with clearance rates. Results of a large number of experiments involving changes in these coefficients are shown in Table 7.8. In general, decreasing the zooplankton mortality coefficient for one size fraction leads to an almost proportional decrease in the biomass of the corresponding phytoplankton fraction, and a smaller compensatory increase in the biomass of the other phytoplankton fraction. When the mortality coefficient for either fraction is cut, the total phytoplankton biomass decreases, and the ambient nutrient concentration increases. Primary production is significantly affected in only one case (Runs 66 and 68). In these runs, diatoms have a very high sinking rate (2.5 m d^{-1}) so changes in the PL:PS ratio affect fluxes to the sediment strongly.

At low loads under steady-state conditions, we can trade off changes in clearance rates and mortality coefficients to obtain the same phytoplankton biomass levels, and neither is well constrained by model calibration. However, when phytoplankton biomass is high, clearance rates become unimportant, while the mortality coefficients (along with maximum zooplankton growth rates) determine the maximum zooplankton biomass, and the point at which phytoplankton production can overwhelm grazing. Maximum zooplankton growth rates are also potentially important in determining the evolution of transient phytoplankton blooms, in response to sudden nutrient additions.

Table 7.8. Effects of changes to zooplankton mortality parameters on primary production (PP), phytoplankton biomass (PL and PS) and DIN (NO_X and NH_4).

Run	PP	PL	PS	NO_X	NH_4	mQ_ZL	mQ_ZS
35	32922	3.22	2.83	0.59	5.82	0.02	0.2
36	32431	2.94	2.33	0.77	7.94	0.015	0.15
66	28356	2.37	3.49	0.53	4.49	0.01	0.2
68	25031	3.21	1.56	0.63	4.91	0.01	0.1
71	26100	1.64	4.29	0.88	8.27	0.01	0.1
74	25367	2.12	3.97	0.84	7.53	0.015	0.1
72	25396	1.49	4.37	0.96	8.79	0.01	0.1
75	24300	1.91	4.06	0.90	7.85	0.015	0.1
si8b	30188	2.68	2.34	1.55	6.87	0.015	0.15
si9	29849	3.42	2.16	1.24	6.00	0.02	0.15
si30	32241	2.43	2.27	1.31	6.53	0.015	0.15
si31	30890	2.80	1.57	1.44	7.12	0.015	0.1
si32	32041	2.40	2.28	1.39	6.59	0.015	0.1
si33	29988	3.30	1.46	1.25	6.14	0.02	0.1

7.3.4 Macroalgae and seagrasses

Macroalgae are a significant component of the total biomass in the Bay (Chidgey and Edmunds 1997). Although macroalgae were included in early versions of the model, data on the macroalgal biomass and distribution only became available late in the study. Calibration of macroalgal parameters consequently occurred late in the calibration process.

Table 7.9 compares Bay-wide fluxes and pools for two versions of the model, one (run si42) preceding calibration against macroalgal data, and the other (run si142) following calibration. Both runs have been calibrated against the water column and sediment pools and fluxes and they are essentially indistinguishable in terms of most of those pools and fluxes. The two runs differ substantially in that the later run produces much higher mean macroalgal biomass and annual production. (The macroalgal biomass is presented as mg N m^{-2}. The values given correspond to ca 500 and 120 tonnes N Bay-wide for runs si142 and si42 respectively). The higher values for macroalgal biomass and production in run si142 are more consistent with observations. One noticeable change in si142 is an increase in water column recycling efficiency. This is necessary in order to sustain the same level of phytoplankton production plus the increased macroalgal production. It was achieved by changing the parameters controlling the proportion of zooplankton ingestion and mortality released as DIN.

Macroalgal biomass and production are controlled by the parameters which determine macroalgal loss rates, and the growth rate parameters (maximum growth rate mum_MA, nutrient half-saturation constant KN_MA and light saturation intensity KI_MA). Macroalgae are generally weaker competitors for nutrients than phytoplankton and must make do with the light that reaches the bottom. Their principal advantages are lower natural loss rates, and of course the ability to remain in areas of the Bay with favourable conditions (high nutrients and high light). Because of this, Bay-wide macroalgal biomass and production is intrinsically related to their distribution within the Bay and

we cannot address macroalgal calibration without considering this spatial distribution. We noted earlier that the observed distribution of macroalgal biomass is rather surprising, with peak biomass at relatively large depths and low light intensities. We have attributed this to the inability of macroalgae to find secure attachment in soft substrate at shallow depths with high wave stress, and have represented this in the model by a loss term proportional to bottom stress. Run si42 included this bottom stress loss parameter mS_MA, but gave it a relatively low value compared with the stress-independent mortality parameter mL_MA. As a result, the predicted macroalgal biomass was concentrated in shallow depths near nutrient inputs (the inshore Werribee region), and was too low in Corio Bay and the north-east region. In order to avoid absurdly high values of macroalgal biomass in the inshore regions, it was necessary to assign low maximum growth rates, and a low Bay-wide biomass and production.

Table 7.9. Two runs of the model, with high and low macroalgal production. The mean Bay-wide fluxes are in tonnes N y^{-1} and the mean concentrations are in mg m^{-3}, except for macroalgae (mg N m^{-2}).

Run	phyto. pp	WRc	SRc	FRc	SResp	MPB Pr.	Den	MA Pr.
142	29439	19205	6232	4326	13171	12720	6939	5193
42	28416	15354	5889	3319	12975	10910	7086	2072
	DON	**PL**	**PS**	**Chl**	**NO_X**	**NH_4**	**PO_4**	**MA**
142	34.18	3.76	1.71	0.78	0.85	6.99	72.42	273
42	33.74	3.57	1.75	0.76	1.24	6.74	71.50	61

In run si142, the stress-related mortality was increased from a negligible level to one in which it became comparable to background mortality, and the maximum growth rate mum_MA was increased to compensate. This resulted in a much better fit to observations, with higher biomass in boxes of 5-10 m depth along the western and northern parts of the Bay, including Corio Bay and the entire north coast (Fig. 7.5). Very high biomass is still predicted off Werribee, reflecting the very high nutrient levels there. Biomass levels of this order have been observed, but are generally seasonally restricted, due to the unstable nature of the local bed (Light and Woelkerling 1992). Modelled inshore biomasses are maximal in spring or even late winter when nutrients are most abundant. (These boxes, being shallow, have reasonable light levels even in winter.) In the 5-10 m depth band away from Werribee, the maximum biomass occurs in summer, as light is critical at these depths.

While there is little difference between these two runs in terms of other Bay-wide pools and fluxes, the improved distribution of macroalgae in run si142 produces as a bonus improved spatial and temporal patterns of phytoplankton biomass. In the Werribee region, excessively prolonged phytoplankton blooms in run si42 terminate at the correct time in run si142. In the Bay centre, the interannual decrease through the 93-95 period in response to changes in loads is somewhat better replicated in run si142. These regional impacts on phytoplankton dynamics are dealt with in more detail in the next section.

Macroalgae are highly sensitive to changes in nutrient and light levels, and therefore respond strongly to changes in nutrient loads. Under increased nutrient loads, one might expect macroalgal biomass to increase in shallow waters near inputs, but to decline at depth as phytoplankton and light attenuation increase. These effects are addressed in the next Chapter.

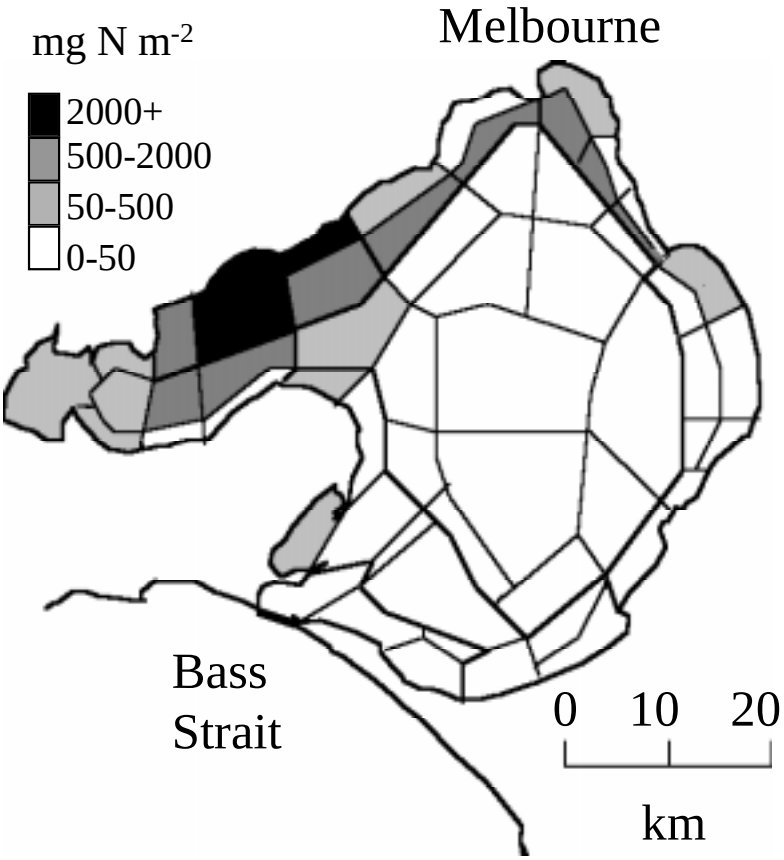

Figure 7.5 Map of predicted macroalgal distribution on 1/1/1995 (Run si142).

The differences between runs si42 and si142 do not accurately reflect the role of macroalgae in si142, since both runs have been independently tuned to produce appropriate phytoplankton productivity and biomass/nutrient distributions. If macroalgae are simply deleted from the model version used in run si142, the effects on plankton and sediment are considerable. Phytoplankton primary production, DIN, and large phytoplankton biomass all increase by about 30%. Release of DIN from the sediment declines, due to a decrease in the area of sediment subjected to high detritus inputs and suppressed denitrification. As one might expect, these effects are concentrated in areas supporting high macroalgal biomass. The biomass of large phytoplankton off Werribee and in Corio Bay doubles with removal of macroalgae, but changes relatively little elsewhere in the Bay (Fig. 7.6). Seagrass beds in the southern Bay are badly affected by removal of macroalgae, and those in Corio Bay disappear.

In summary, macroalgae in the model have a potentially significant, but mostly local, impact on the Bay ecosystem. Others have argued that macroalgae can compete effectively with phytoplankton for DIN in shallow, enriched waters (Fong *et al*. 1993). The observations collected as part of the study provide useful constraints on macroalgal biomass, but only weak constraints on macroalgal production. Additional information from process experiments on macroalgal growth rates, and their dependence on light and nutrient levels, of the kind collected for phytoplankton and microphytobenthos, would be very helpful.

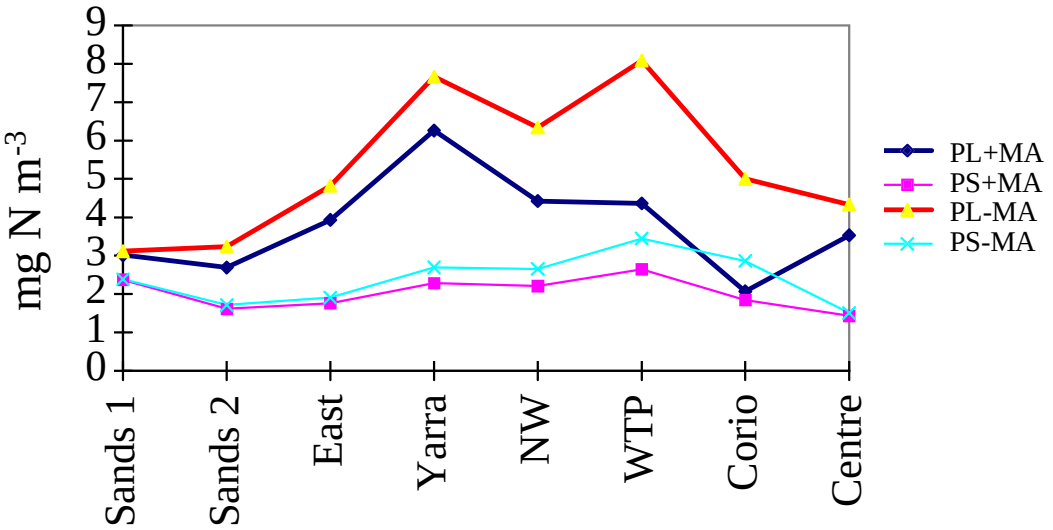

Figure 7.6 The biomass of large and small phytoplankton (PL and PS) in the presence (+MA) or absence (-MA) of macroalgae.

In the model, seagrasses draw their nutrients from sediment pore water, and are assumed to be adversely affected by high water column nutrient levels, which encourage the growth of epiphytic algae. The model currently overpredicts the extent of seagrass in the Sands (the model does not allow for the effect of sediment instability on seagrass colonisation), and underpredicts their extent along the southern shore of the Geelong arm (Fig. 7.7). The predicted seagrass biomass in Corio Bay is particularly sensitive to nutrient levels in the model. Versions of the model with low ambient nutrients produce high seagrass biomass there, while versions with high nutrient levels lose seagrass in Corio Bay. Modelled seagrasses in Corio Bay reach highest biomass generally by midsummer and maintain high biomass through to autumn. Biomass can fall quite quickly in winter and then rises slowly again through spring and early summer. This is similar to the observed pattern shown earlier. However, modelled seagrasses in Swan Bay, from which the observations came, do not behave like this. Here maximum model biomass is in winter. This timing appears to reflect the very shallow depth in Swan Bay, and its extreme nutrient limitation in the model. This is probably exaggerated because the model does not include local runoff and nutrient loads into Swan Bay.

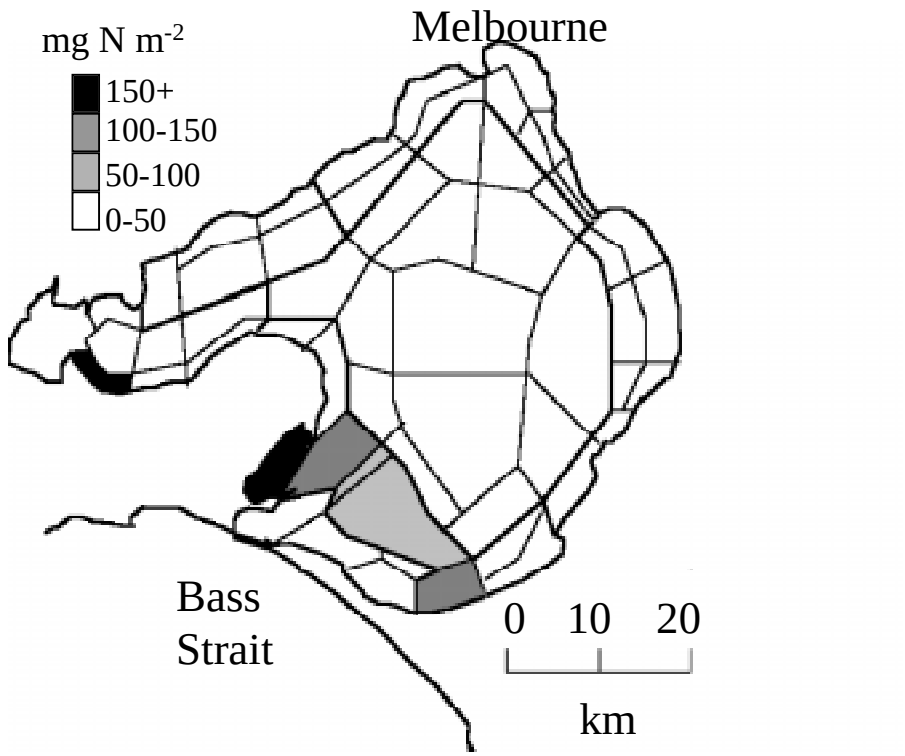

Figure 7.7 Map of predicted seagrass distribution on 1/1/1995 (Run si142).

7.3.5 Summary of the model performance at Bay-wide scales.

The model formulation and parameter set used in run si142 have been adopted as a standard, following model calibration. This version has also been used as the basis for a conventional parameter sensitivity analysis described in detail later. Table 7.10 compares predicted Bay-wide fluxes and pools with the "best" estimates based on observations. For the underway variables, cruise-track weighted annual means are presented for both observations and predictions.

The observed and predicted fluxes generally agree quite closely, certainly within the uncertainties in the observations. The predicted release of DIN from the sediment lies half-way between the low and high estimates from the observations. Model agreement with respect to pool sizes is also good, and well within observation errors, with two exceptions. The predicted nitrate pool is much too low, although the agreement for ammonia is very good. This suggests that either the model is underestimating the proportion of nitrate in the DIN released from the sediment, or overestimating the proportion of nitrate in phytoplankton uptake of DIN. Sediment chamber data do not suggest that the release of nitrate from the sediment is underestimated. The model currently uses the same KN values for nitrate and ammonia uptake, but allows for ammonia inhibition of nitrate uptake. Either the formulation of inhibition is inadequate, or a higher KN for nitrate uptake needs to be specified separately. The nitrate pool is relatively small, and to date we have not thought it worth while to improve the agreement at the expense of introducing a more complex nutrient-uptake model.

Table 7.10. Comparison of observed and predicted fluxes (tonnes N y^{-1}) and mean pool sizes (mg N m^{-3}, except for Chl in mg Chla m^{-3} and PO_4 in mg P m^{-3}). Predictions are based on the standard run si142. CW142 and Cruise refer to cruise-track weighted predictions and observations respectively.

	phyto. pp	WRc	SRc	FRc	SResp	MPB Pr.	Den	MA Pr.
si142	29439	19205	6232	4326	13171	12720	6939	5193
Observed	30000	18000	4-8000	3750	14000	12000	7000	5000
	DON	**PL**	**PS**	**Chl**	**NO_X**	**NH_4**	**PO_4**	**MA**
si142	34.18	3.76	1.71	0.78	0.85	6.99	72.42	273
Observed	32			0.86	3.5	6.5	58	250
CW 142				0.96	1.36	7.8	69.6	
Cruise	52			1.04	4.34	9	64	

If we compare the unweighted Bay-wide mean concentrations, phosphate concentration is significantly overpredicted by the model. This is surprising because phosphate is expected to act in the model almost as a passive tracer. There is no organic pool of P in the model large enough to account for the discrepancy in the Bay-wide average. However, the cruise-track weighted estimates of average pool size agree quite well. That is, the model predictions and observations agree (at least on average) in those areas which are sampled. This implies that most of the discrepancy in the unweighted means is due to bias in the cruise-track and errors in the spatial spline interpolation process used to estimate the Bay-wide pool from the under-way data. (Note that the cruise-track does not sample Corio Bay, where the model predicts high phosphate.) Any real discrepancy between the observed and predicted Bay-wide pool would have to be explained either by over-estimation of terrestrial loads, overestimation of the Bass Strait boundary concentration, overestimation of the flushing rate, or long-term burial of inorganic or refractory organic P in the sediment.

This good agreement of observations and predictions at Bay-wide, annual scales should be kept in perspective. It reflects the fact that, given the *a priori* constraints on model parameters, we have more than sufficient degrees of freedom to match predictions and observations for 16 key variables. Reproducing the spatial and temporal structure of the observations is potentially far more of a challenge, and we address this in the next section.

7.4 Spatial and temporal variation.

The model performance at Bay-wide, annual scales is, for the most part, relatively easy to understand and adjust on the basis of simple one-box steady-state models. We have used this process as an important first step in model calibration, and it has allowed us to constrain a number of model parameters, or combinations of parameters, quite tightly. Understanding and correcting the model performance at finer spatial and temporal scales is much more complicated. In presenting the results, we have continued the hierarchical approach, moving from persistent regional patterns to local events. In the following

sections, model predictions refer to predictions from the standard calibrated run (si142), unless otherwise indicated.

7.4.1 Regional variation.

The eight regional or coarse boxes presented earlier (Fig. 7.1) were chosen to resolve the major persistent spatial patterns in the observations of pools and fluxes. We present first a brief, largely qualitative, discussion of the modelled and observed behaviour by region. We then present a more quantitative comparison of model predictions and observations at regional scales for sediment fluxes, chlorophyll and ammonia.

Region 1 represents the entrance of the Bay. In all water-column variables, behaviour here is largely controlled by the Bass Strait boundary conditions. Aliasing of the tidal exchange across this region produces a regular cycle, with a period of a fortnight, in the model output. Mixing between Bay and ocean water across this region causes large gradients and large spatial standard deviations in variables that have elevated concentrations in the Bay centre (DON and PO_4). Gradients are weaker for phytoplankton and ammonia, but more variable in time.

Region 2 is similar to region 1. If anything, the regions are too similar in the model, which may reflect inadequate spatial resolution of the gradients across the sands. This region, which extends past Port Arlington and along the southern coast of the Geelong Arm, is the principle habitat of seagrass. The cycle due to tidal aliasing has much lower amplitude in this region (and disappears in the Bay interior). This region usually has the lowest predicted phytoplankton biomass and nitrate concentrations in the Bay (ie. lower than Bass Strait concentrations). For some parameter sets, the model (unrealistically) exports ammonium to Bass Strait, in which case ammonia levels are higher than in region 1. This region has a pronounced seasonal cycle with less observed (and predicted) interannual variation than more northerly boxes.

Region 3 is influenced by the inputs from the Patterson Mordialloc system. As a result it does exhibit strong interannual variation. This region is a long, narrow coastal strip, and water column properties are generally quite similar to those observed in the Bay centre, due to rapid mixing across the long boundary. Nitrate and phytoplankton levels may be higher than Bay centre values at times of high runoff. The model correctly predicts high ammonia concentrations associated with inputs in 1993, but tends for some parameter combinations to over predict ammonia levels in 1994.

Region 4 is the northeast coastal region, including Hobsons Bay, and is dominated by the Yarra. The decrease in Yarra runoff between 1993 and 1994 produces large interannual variation in this region. A large runoff event in 1993 produced a phytoplankton bloom with high chlorophyll concentrations, which some model runs capture well, and others fail to capture at all. The presence or absence of this bloom is therefore a critical test of the model's performance (although one which most runs do pass). This region is notable for high and variable nitrate and chlorophyll, dominated by large phytoplankton, and for high though less variable ammonia. In the sediments, observed denitrification efficiencies in upper Hobsons Bay sometimes approach zero in 1993. The model tends to overpredict microphytobenthos and macroalgae in this region. This is probably due to the fact that the current model version does not allow for

turbidity in the Yarra inflow. The Yarra flood response in this region is discussed in more detail later.

Region 5 is the north west coastal region, which is strongly influenced by inputs from both the Yarra River and WTP, depending on the direction of the circulation. Because inputs from these sources have different temporal patterns, and currents can change rapidly with winds, water column concentrations are highly variable, even in the case of more conservative tracers such as DON. Macroalgal growth in this box is sensitive to model parameters. The model predicts seagrass beds in this region if parameter sets are chosen which result in underestimation of DIN.

Region 6 (Werribee region) is in many ways the most interesting area in terms of the behaviour of the real Bay, and also in terms of model calibration. For many parameter combinations and formulations, the model predicts very large phytoplankton blooms off WTP which, in view of the large nutrient inputs and shallow water column with high light levels, seem quite reasonable at first sight. However only moderate blooms are observed. Understanding and removing this discrepancy has been one of the most challenging aspects of model calibration. This is discussed in detail later.

Region 7, Corio Bay, has the longest flushing time, and is the only interior region for which exchange with the rest of the Bay is limited. The predicted DON values in Corio Bay are high because of the slow flushing rate. Intermittent injections of water from the Werribee region produce transient blooms of large phytoplankton. The predicted seagrass biomass in this region is very sensitive to changes in model parameters that affect DIN concentrations. This sensitivity extends to MPB, which compete with seagrass for nutrients, and to macroalgae which are DIN-limited. Model predictions and observations agree that DIP is highest in this box in winter, while it is highest elsewhere in summer.

Region 8 is bounded approximately by the 10 and 15 m depth contour, and represents half the Bay by area and 70% by volume. It is an area of low nutrients and phytoplankton biomass. Variability is low, except for MPB which show strong spatial and seasonal variation due to light limitation in winter. The steady-state one-box simplification is potentially quite a good approximation for the water column in this region. The model tends to predict seasonal cycles in water column concentrations in this region, which are not apparent in the observations. Observations instead indicate a long term decline in chlorophyll and DIN through the Study period, apparently in response to decreases in loads. Reproducing this decline has been a significant challenge for model calibration, and this is also discussed in more detail below.

7.4.2 Spatial and temporal variation in sediment fluxes

One of the most important observations to emerge from the Port Phillip Bay study is the variation in denitrification efficiency in time and, most importantly, in space. It was observed that sediments near input sources showed lower denitrification efficiencies than Bay-centre sediments. The model explains this in terms of an empirical relationship between denitrification efficiency and sediment respiration rate, based on the sediment

chamber observations. The spatial pattern of denitrification efficiency predicted by the model should then match the observations provided the predicted pattern of sediment respiration rates also matches observations. For the standard run, denitrification efficiency is about 60% in regions such as the Bay centre or Corio Bay (approaching Dmax), but closer to 40% in Hobsons Bay and off Werribee. The apparent denitrification efficiency calculated using dark respiration rates (which include respiration of organic matter produced by MPB) is closer to 80-90% and 60% respectively. The model predicts complete suppression of denitrification at times in upper Hobsons Bay (fine box 32), in agreement with observation.

A seasonal change in sediment respiration rates by a factor of 2 occurs in both the observations and the model. In the Bay centre (fine box 52), model values are 10-20 mg N m^{-2} d^{-1} in winter and 30-40 mg N m^{-2} d^{-1} in summer, or approximately 0.7-1.5 and 2-3 mmoles N m^{-2} d^{-1} (Fig. 7.8). When this is multiplied by the Redfield C:N ratio, we get 5-10 and 12 to 20 mmoles CO_2 m^{-2} d^{-1}, which compare well with observed CO_2 fluxes at site 37 (8 to 23 mmoles CO_2 m^{-2} d^{-1}) in both magnitude and seasonal variation (Nicholson *et al.* 1996). DIN flux from the sediment also shows a maximum in summer, in line with observations.

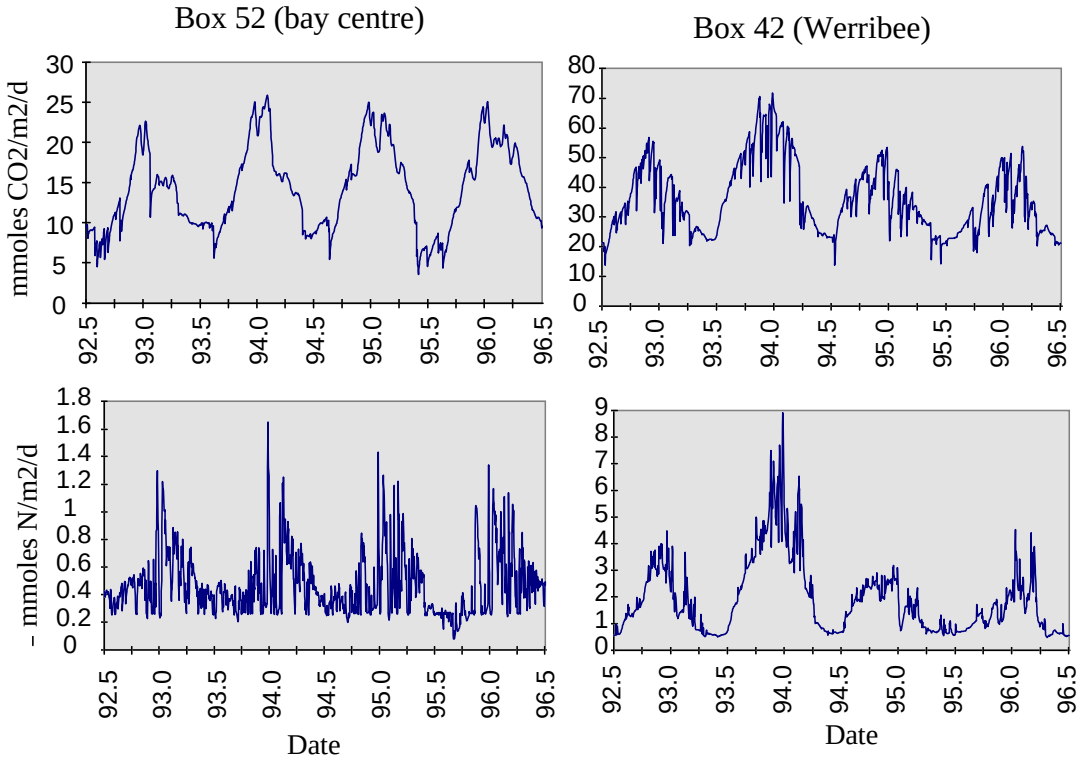

Figure 7.8 Standard model run: sediment respiration rate (mmoles CO_2 m^{-2} d^{-1}) and DIN N release (mmoles N m^{-2} d^{-1}) in fine boxes 52 (Bay centre) and 42 (Werribee region).

The winter variation in sediment fluxes in the Bay centre does help to constrain R_D. In model runs with R_D = 20 mg N m^{-2} d^{-1}, denitrification efficiencies decrease in winter as respiration rates fall below R_D, and DIN release from the sediment starts to increase. This is not consistent with observations. When R_D is reduced to 10 mg N m^{-2} d^{-1}, predicted denitrification efficiencies remain high in winter. The predicted DIN release in the Bay centre is then about 0.4 mmoles m^{-2} d^{-1} in winter and a highly variable 0.5-1 mmoles m^{-2} d^{-1} in summer. These results are generally comparable to observations, although the model has no mechanism to reproduce the DIN influx to the sediment observed in October 1994 (Nicholson *et al*. 1996).

Coastal seasonal patterns in DIN release are also reproduced reasonably well. Sediment fluxes were measured monthly from October 94 to June 95 at experimental site 6, which can be compared with model fine box 42. In the standard model run, the predicted DIN release in fine box 42 rises quite abruptly in January and February of 1994 to 2-3 (with peaks up to 4.5) mmoles N m^{-2} d^{-1} (Fig. 7.8) but declines in April to about 0.5 mmole N m^{-2} d^{1}. A very similar pattern is observed at site 6, except that high DIN release persists until June (when observation ceased).

The predicted pattern of DIN release is subject to strong interannual variation and there are strong gradients between boxes. Thus similar February peaks of DIN release occur in neighbouring boxes, but in fine box 45, off the WTP outfalls, they reach 15 mmoles m^{-2} d^{-1} (and denitrification is entirely suppressed), while further offshore in box 39, they only just exceed 1 mmole m^{-2} d^{-1}. Given these strong gradients, finer spatial resolution is probably required in order to compare model predictions with point observations in this region. In general, we regard the model's reproduction of sediment respiration rates and denitrification efficiencies as encouraging. This is important, given the critical role of denitrification in determining the trophic state of the Bay.

7.4.3 Chlorophyll spatial patterns

In this section we compare chlorophyll means and standard deviations predicted by the model with observations from the underway data. We have made the comparison at the fine box level to minimise problems of bias, but concentrate in the discussion of performance on the regional level. Underway data is available from all regions and about half of the fine boxes.

We first calculated the mean of underway chlorophyll concentrations within each fine box on each monthly cruise. These monthly means were treated as the basic observations. We then calculated the mean and standard deviations of monthly values over all 25 cruises, for each fine box. We dropped fine boxes which were missed on more than 3 cruises, except for fine box 45, which was used for the comparison in spite of being missed by four cruises, since it is the box into which WTP discharges. The mean and standard deviations of chlorophyll values predicted by the standard run were calculated over the 2 years from mid 93 to mid 95, this period being comparable to the observation period. The results are shown in Fig. 7.9 and Fig. 7.10.

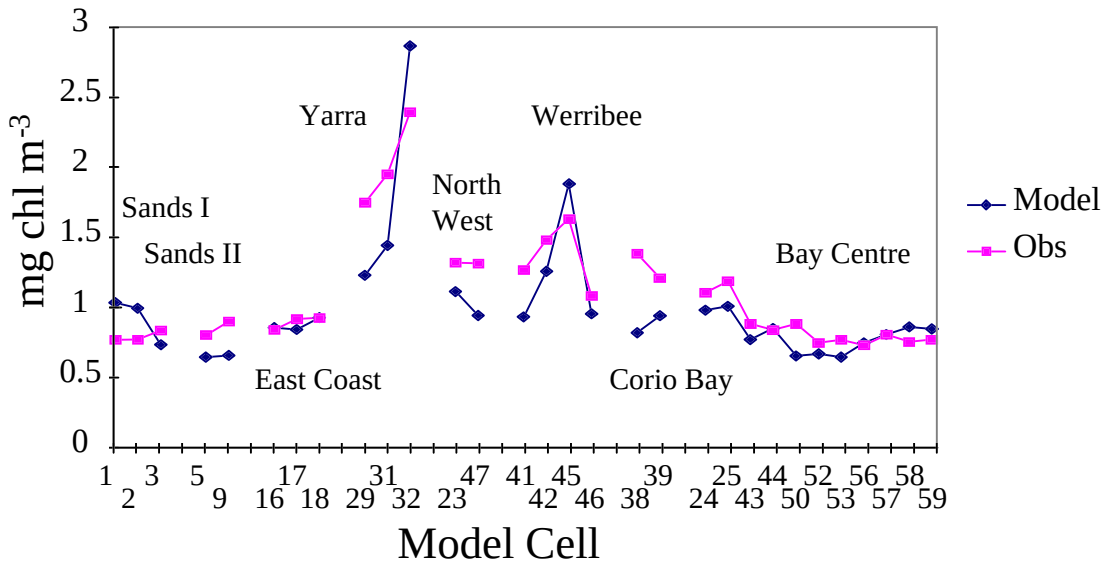

Figure 7.9 Annual mean values for chlorophyll: observations and model predictions by fine box.

The comparison between the model and observed mean chlorophyll concentrations is, in general, very good. The correlation is 0.846 and regression slope about 0.9.

In the Sands, the Bass Strait boundary condition is the dominant influence on chlorophyll levels. The slight discrepancy in the fine boxes closest to the Heads suggests that the boundary value for chlorophyll is slightly too high. In the northern Sands (region 2) the model underpredicts chlorophyll slightly. This could indicate that the Bass Strait value for zooplankton biomass is too high, or simply that the inputs to this region from the central Bay are slightly too low.

The regions most directly influenced by nutrient inputs are regions 3 to 7. Region 3 is very well simulated. The individual fine boxes covered by observations are all south of the inputs and dominated by exchange with the Bay centre, so the strongest effects of the Patterson-Mordialloc inputs are not included in this comparison.

In the Yarra region (box 4) the model predicts the correct average biomass, but the wrong distribution within the region. The model overpredicts chlorophyll in Hobsons Bay and underpredicts chlorophyll further from the Yarra mouth. The Hobsons Bay bloom is discussed in more detail later, but this error in distribution indicates that the modelled bloom develops too rapidly. This may be due to inadequate representation in the model of the effects of turbidity in the Yarra plume on phytoplankton growth in Hobsons Bay. Alternatively, it may be due to excessive smearing in the model at the scale of fine boxes. The fine scale measurements in Longmore *et al*. (1996) suggest that patches of high nutrient water may move downstream from Hobsons Bay without mixing strongly with Bay water containing phytoplankton "seed" populations. This could not be represented without greatly increasing the spatial resolution in the model. Predicted bloom development and mixing in Hobsons Bay may also be affected by vertical stratification, which is potentially important in the Yarra bloom, especially

during high runoff events. The model currently uses only one depth-averaged water column layer.

In the north-west region, the model significantly under-estimates chlorophyll. This error may be due to underestimation of local inputs. We discuss uncertainty in the loads from Kororoit Creek and the Werribee River, and the implications for local chlorophyll concentrations, in the next Chapter.

The model prediction of mean chlorophyll in the Werribee region (coarse box 6) is quite good, despite the strong gradients observed within and between fine boxes. There is again a tendency to overpredict close to the outfalls, and underpredict further away.

The model underpredicts chlorophyll in fine boxes 38 and 39, which lie on the outer margin of the Corio Bay region. It is possible that this is due to an overprediction of macroalgal production in this region; earlier runs with low macroalgal production yielded chlorophyll levels in this region more in accord with observations (but overpredicted levels off Werribee).

In the Bay centre there is a very good fit between model chlorophyll and observations. The model appears to capture the mean spatial gradient within this region, as well as the overall mean. Values in southern boxes (44, 50, and 52) are slightly underestimated, as in the northern Sands region.

The performance of the model in reproducing temporal variation as measured by the coefficient of variation across monthly cruises is more uneven (Fig. 7.9). Temporal variation in regions 3 and 6 (which receive inputs from Patterson-Mordialloc and WTP) is very well simulated. Variability in the northwest region is underpredicted, but, since the mean is also under-predicted, this may also reflect a problem with local inputs. The variability in Hobsons Bay is strongly overestimated. This is due to the excessive response of phytoplankton to inputs, the same problem that led to overprediction of mean chlorophyll there. In Corio Bay, and in northern fine boxes in the Bay centre, the observed temporal variability is well-reproduced.

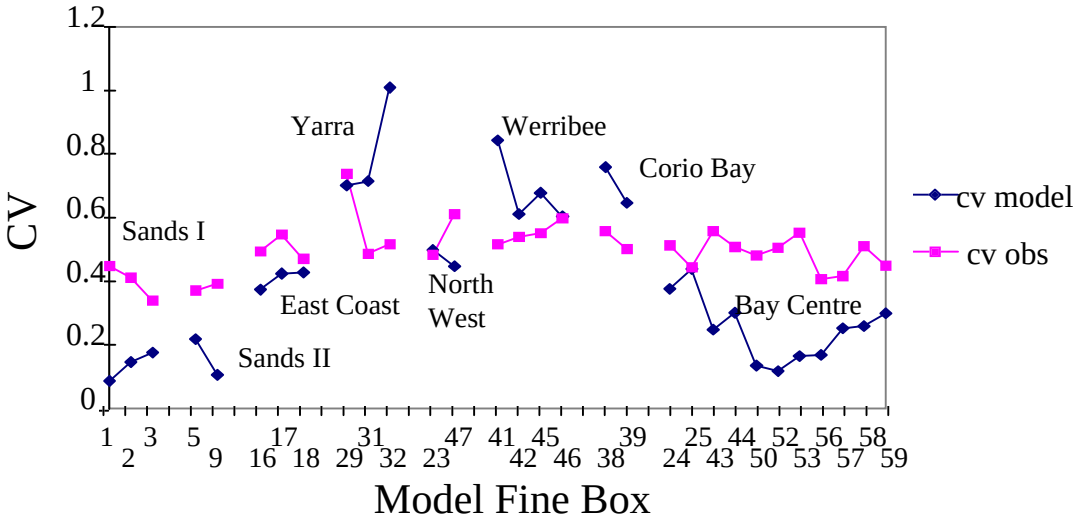

Figure 7.10 Coefficient of variation of chlorophyll over time: observation means and model predictions by fine box.

In the southern Bay centre, and regions 1 and 2 in the Sands, the model generates coefficients of variation, which are only a third to a quarter the observed values. The result is that there is a relatively poor correlation (ca 0.7) of predicted and observed fine box means across months. This underprediction is due to an inability of the model to represent the full extent of the interannual variation in chlorophyll in this region (see 7.5). The low model variability in the Sands may also reflect the fact that we impose a constant value as the Bass Strait boundary condition.

One would not expect the level of agreement between predictions and observations to be as high for variance as it is for means. The model captures well the high levels of variation in coastal regions near inputs, and predicts with appropriate attenuation the resulting variation in nearby waters in the northern Bay centre. It merely fails to propagate this low variation into the southern Bay.

A similar comparison of predicted and observed means and standard deviations has been carried out for ammonia. The performance is quite similar to that described for chlorophyll, and is briefly summarised here. Regional mean values are predicted well over most of the Bay, and are very good in regions 1, 2, 3 and 8. Underprediction in Corio Bay may reflect cruise track bias. Ammonia is overpredicted near the WTP outfalls. Analysis indicates that this is due to excessive trapping of ammonia through local consumption and remineralization. This is associated with the local overprediction of chlorophyll noted earlier, attributed to the model's spatial resolution. The model under predicts the coefficient of variation of ammonia. In the coastal regions, this is associated with underprediction of the mean. In the Bay centre, it is due to a failure to predict the full extent of interannual changes in ammonia concentration.

The excessive uptake of nutrients close to inputs is also reflected in underprediction of Si concentrations in Hobsons Bay.

Overall, we conclude that the model reproduces quite well the regional patterns in key water column variables. The comparison does not suggest any fundamental flaws in the model representation of nutrient cycling. The model performance could be expected to improve locally if spatial resolution was increased in regions of strong gradients. Some fine-tuning of boundary conditions may be indicated, and there may still be unresolved issues in the interaction between phytoplankton and macroalgae, and associated N trapping, in some coastal regions.

7.5 Transient Features

Calibration of a dynamical model against steady-state or annual average concentrations has the disadvantage that it generally provides very weak constraints on model rate parameters. In this Study, we have the considerable advantage of a diverse set of flux measurements, which provide much stronger constraints on rate parameters. We also have the advantage of descriptions of the spatial distribution for some key variables combined with a sound model of physical transport (Walker 1997a, b). As we have just seen, physical advection and mixing interact strongly with biological rate processes and parameters to determine local spatial distributions near inputs.

A third class of important constraints on rate parameters is provided by observations of transient responses to forcing at a range of time scales. We consider here the interannual change in Bay centre chlorophyll and nutrients in response to interannual changes in loading, the response to the elevated winter load of ammonia from WTP, and the bloom in the north-east of the Bay in response to Yarra flood events.

7.5.1 Interannual variation in Bay-centre chlorophyll.

Observed Bay-centre chlorophyll levels showed a very significant decline over the 93-94 period. This is assumed to be due to the decrease in nitrogen loading over the same period. Total nitrogen loads over the Study period are shown in Fig. 7.11.

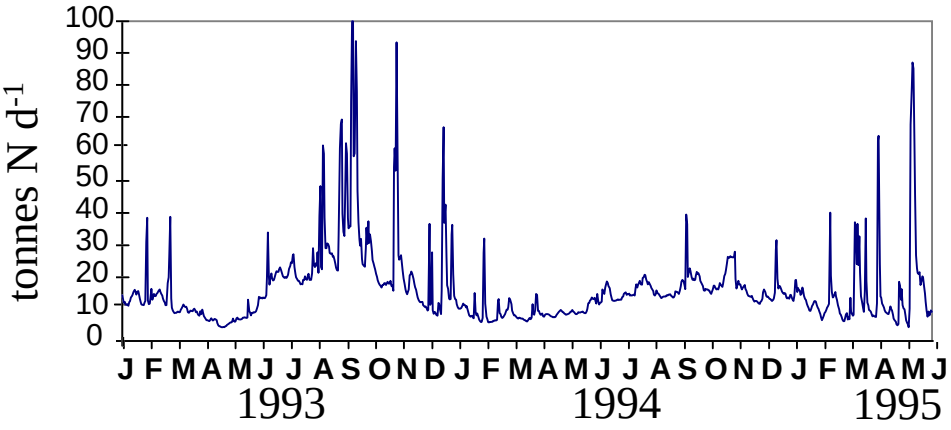

Figure 7.11 Total N inputs to Port Phillip Bay, 1/1/93 to 1/7/95 (a peak of 160 tonnes d^{-1} in September 1993 is truncated).

In Fig. 7.12, we compare predicted and observed chlorophyll concentrations in the Bay centre for three versions of the model. Run 45 used a sine curve approximation to the seasonal cycle in surface irradiance. The predicted seasonal change in chlorophyll is very smooth, and closely tracks the seasonal cycle in nitrogen loading. However, the predictions do not match the observations well: the amplitude of the seasonal cycle is too high, while the interannual variation is too low.

Most model runs predict a seasonal and interannual pattern of chlorophyll in the Bay centre similar to run 45. The amplitude of the predicted seasonal cycle in run si42 is lower than in run 45, but still larger than observed. Other runs in the Si series have a similar seasonal amplitude to run 45. At least one run in this series predicted a seasonal cycle with near-zero amplitude, but this run also showed near-zero interannual variation. The increase in short-term "noise" in run si42 is due to the use of observed daily surface irradiance.

The standard model run (si142) has much higher macroalgal biomass and production than other runs. This run does approximate better the observed long-term but noisy decline in Bay centre chlorophyll from October 1993 to August 1994. However, as in all other model runs, the model does not predict the high chlorophyll concentrations observed from May to September in 1993, and the very low chlorophyll concentrations

observed in October, 1994 to January 1995, and consequently fails to capture the full magnitude or duration of the interannual variation.

The problem in explaining the interannual variation in the Bay centre is that a 20% decline in annual nitrogen load appears to produce a 2-fold decline in phytoplankton biomass in the Bay centre. In a simple steady-state water column model, a 20% decline in load would be expected to produce a 10 to 20% decline in chlorophyll. Increasing the role of macroalgae in the model helps because macroalgae compete with phytoplankton for nutrient. If macroalgae are favoured under lower loads (due to lower light attenuation) and capture a larger share of the nutrient input, there is a disproportionate decrease in phytoplankton biomass of the kind observed. During July to September 1994, where the model does predict a major decline in chlorophyll and phytoplankton production relative to 1993, it also predicts a significant increase in the relative contribution of macroalgal production. However, we do not have observations to support this.

Of course, the interannual change in nutrient load is not evenly distributed in space and time. As one would expect, the seasonal DIN load from WTP differs little between the two years. The difference in load is accounted for almost entirely by the drop in inputs from streams and rivers, and in particular the lack of runoff from the Yarra in the spring and summer of 1994. The timing and magnitude of the nutrient load to the Bay centre depends on the efficiency with which nutrients from different sources are transferred from the coastal regions near inputs into the Bay centre. As discussed earlier, nutrients are intercepted in coastal regions by phytoplankton or macroalgal uptake, recycled locally through sediments, and partly lost to denitrification. Transport and remineralization of semi-labile detritus and DON provides a source of DIN to the Bay centre that varies on long time scales.

The weaknesses in the model's interannual Bay centre performance cannot be easily confined to a particular source or season. In 1993, the model underpredicts the Bay centre response to the winter WTP input, but predicts the response to the Yarra spring and summer inputs quite well. In 1994, the model predicts an appropriate response to the WTP winter input, but overpredicts chlorophyll during the spring and summer.

One could argue that we should not place too much weight on this particular issue in the overall model calibration. Changes in zooplankton parameters associated with shifts in zooplankton community composition could easily produce discrepancies of the kind observed. However, the interannual change in response to changes in loading is important because it may provide clues to the response of the Bay to long-term changes in loading. The results suggest that the Bay is somewhat more sensitive to changes in loading than the model predicts. This could mean, for example, that denitrification efficiencies in coastal sediments decline more steeply with increased loadings than our empirical submodel assumes. Alternatively, it could mean that the contribution of semi-labile organic matter is smaller than the model assumes. Finally, we note that Si limitation is particularly important in limiting phytoplankton blooms in coastal regions (see below). Silicate concentrations in the Bay centre are also observed at times to drop to levels that are potentially limiting to diatom growth. The model does not reproduce this behaviour, possibly because of problems in the simple model of recycling of

biogenic Si, or because of errors in the predicted inputs (we lacked data to directly calibrate Si load models).

Further numerical experimentation, longer time series of observations, and focused field experiments, are needed to address these hypotheses further.

Predicted Bay-wide phytoplankton production varies from about 27000 tonnes in 1993 to 31000 in 94, representing about 15% variation. By comparison, simulated North Sea gross production, over the entire period of 1962 to 1986, varied by 17% between the least and most productive years: 83.5 - 99.0 g C m^{-2} y^{-1} (Radach and Moll 1993). The mean Port Phillip Bay productivity (76 to 90 g C m^{-2} y^{-1}) is highly comparable in magnitude to the North Sea, although given that Port Phillip Bay is shallower, its productivity per cubic metre is higher.

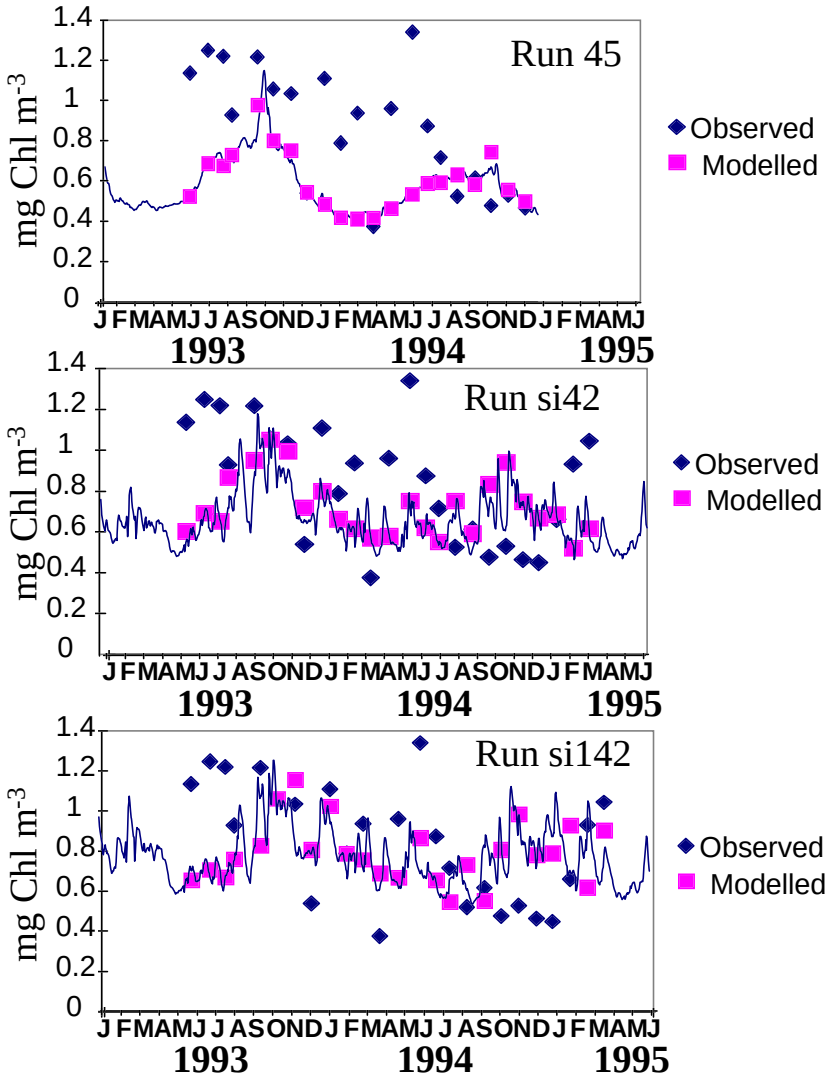

Figure 7.12 Box 8 chlorophyll, cruise track means (diamonds), cruise track-weighted model predictions (squares) and volume weighted model predictions (fine line) for model runs 45, si42, si142 Note that run 45 only covers 1993-94, whereas the other runs extend to mid 1995.

7.5.2 The Werribee region

Because 2/3 of the DIN inputs to Port Phillip Bay come from the WTP, it is unsurprising that blooms occur in this region. In calibrating the model, we initially found that the model over-predicted the magnitude of those blooms, and we encountered surprising difficulty in reducing the predicted phytoplankton concentrations. The key to solving this problem has been the inclusion of Si as a limiting nutrient.

We present results from the standard run si142 that includes Si-limitation (Fig. 7.13). The predicted chlorophyll concentrations in the Werribee region are restricted to 1-3 mg Chl m^{-3} for most of the time, in accord with observations. Inspection of the observed and predicted ammonia concentrations shows how surprising the absence of large blooms is. Very high ammonia levels are still present in spring and yet chlorophyll levels remain at quite low values by coastal water standards. The modelled ammonia concentrations exceed the observed summer minimum, possibly due to problems with offshore transport of detritus (a similar problem occurs in Hobsons Bay). An extremely high value of ammonia observed in June/July of both years is not predicted. Nitrate is persistently underestimated for several months in midwinter off WTP. The general problem with underprediction of nitrate was discussed earlier, but since DIN is not limiting in this period, the problem does not affect local chlorophyll dynamics.

In the model, phytoplankton biomass remains low as spring approaches, despite abundant DIN and light, because silicate is depleted to levels that limit phytoplankton growth. The agreement between predicted and observed silicate in the Werribee region is very good, considering the lack of data on silicate loads and cycling in the Bay.

In the absence of Si limitation, modelled bloom chlorophyll concentrations in the Werribee region were frequently 2 to 3 times those observed. Bloom concentrations in this region could be reduced, for example by increasing diatom sinking rates, but only at the cost of decreasing chlorophyll to unrealistic levels in the Bay centre or the Yarra region. Bloom concentrations off Werribee could also be reduced by allowing very high biomasses of benthic filter-feeders there. Because this region is comparatively shallow, changes in sinking rates, benthic filter-feeder biomass and macroalgal biomass have large impacts in this region compared with deeper parts of the Bay. While silicate limitation does appear to be the correct principal explanation for the observed patterns, the role of benthic filter feeders and macroalgae may still be significant. As we discussed earlier, the standard run si142 allows higher macroalgal biomass and production off Werribee. With lower macroalgal biomass, the spring phytoplankton blooms allowing for Si limitation are still somewhat prolonged in 1993, and too high in 1994.

Because only diatoms require silicate, the composition of the phytoplankton community is critical to the development and impact of Si limitation. In the standard version, the large phytoplankton class (PL) are assumed to be diatoms and require Si, while the small class (PS) do not. For parameter combinations where PS dominate in the model, Si limitation does not restrain phytoplankton biomass and large blooms can occur. The predicted accumulation of DIN occurs in the standard run because small phytoplankton are controlled by grazing.

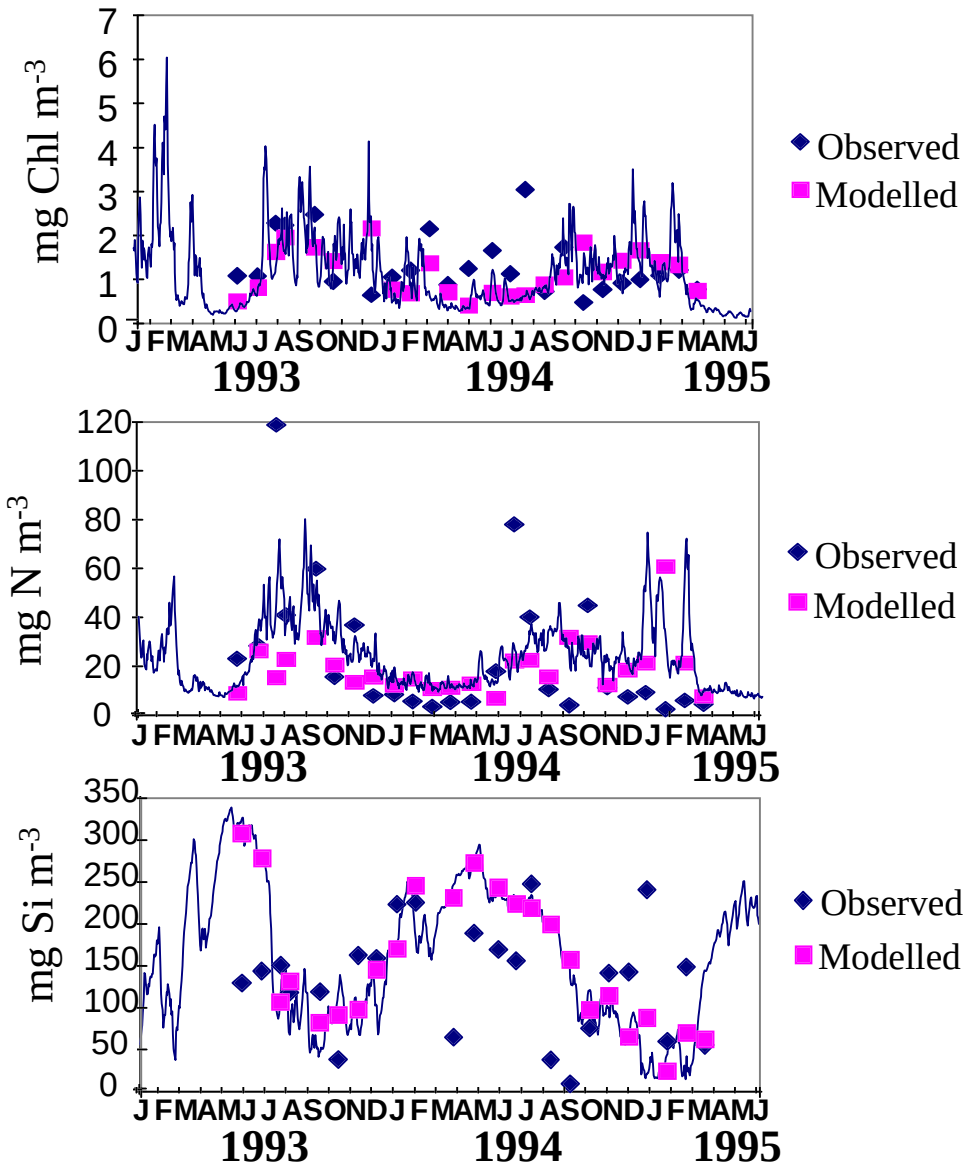

Figure 7.13 Box 6 chlorophyll, NH_4 and SiO_4 for run si142. Symbols as in Fig. 7.12.

One might expect that other phytoplankton bloom species, especially dinoflagellates, would become important under prolonged or widespread Si limitation. If Si-limitation and DIN accumulation occurred in the Bay centre, one would expect dinoflagellate biomass there to increase, and possibly act as a seed population for blooms off Werribee. Alternatively, dinoflagellate cysts in sediments could act as an alternative seed population. It appears to be the lack of Si limitation in the Bay centre (and hence the presence of a Si-dependent seed phytoplankton population), combined with Si limitation off Werribee, which explains the relatively low bloom concentrations there. If this explanation is correct, an increase in the Bay centre N:Si ratio could lead to increasing dominance by dinoflagellates (Doering *et al*. 1989). We have experimentally introduced dinoflagellates into the model as a slow-growing, non Si-limited phytoplankton class subject to weak grazing control. In the model, competition between diatoms and dinoflagellates tends to be unstable, producing occasional very large

dinoflagellate blooms. While large dinoflagellate blooms have been observed occasionally in the Bay, we are not confident that this model version captures the processes underlying their dynamics.

As we discussed earlier, observed chlorophyll concentrations off Werribee are very patchy, and show very low cruise-to-cruise autocorrelation at the level of individual fine boxes. Not surprisingly, the cruise by cruise correlation between the observed and modelled chlorophyll concentration in the Werribee region is equally low, about 0.05. The model is unable to predict individual patches and blooms, which are sub-gridscale and essentially random from the point of view of the model. As we discussed earlier, the model has been calibrated successfully against the seasonal and spatial pattern in bloom magnitude and frequency.

7.5.3 The Hobsons Bay bloom

A strong bloom event is observed in the Yarra region in 1993, and to a much lesser extent in late 1994, associated with high runoff from the Yarra River. The nature of the Yarra nutrient loads differs substantially from the WTP loads. The Yarra carries an excess of Si over N, so that Si limitation does not occur locally in the Yarra region. The Yarra input is much more irregular, occurring primarily in large, but relatively brief, flood events, as opposed to Werribee's smoothly varying seasonal input. The runoff volume from the Yarra also affects density gradients and circulation in the Bay to a much greater degree than WTP runoff.

These differences mean that the blooms in the Yarra region are much more deterministic. The correlation of predicted and observed chlorophyll in the Yarra region is 0.64. The blooms are predicted in most model versions, although some parameter sets (eg. those with very high diatom sinking rates) fail to predict the blooms. If macroalgal competition is increased, the blooms tend to terminate early. There is a general tendency for the bloom to increase too quickly (although of course the temporal resolution of the observations is quite limited). The model currently does not allow adequately for the increased turbidity and stratification associated with Yarra runoff, and this may lead to over-prediction of bloom growth rates. High ammonia concentrations are predicted to persist in the Yarra region after observed concentrations have declined. This reflects the strong local trapping of nitrogen through phytoplankton uptake and settling, and subsequent remineralization from the sediment. Slower bloom initiation would lead to wider dispersal of the DIN load, consistent with the increase in Bay centre ammonia, which is observed to occur earlier than predicted. Modelled silicate concentrations are too low, again suggesting that local removal is too effective, or that silicate loads are under-estimated.

7.5.4 Limit cycle oscillations

The phytoplankton-zooplankton interactions represented in the model can, under certain circumstances, produce limit cycle solutions, which manifest as regular oscillations at

fixed frequencies. These are spontaneously driven, and should not be confused with the irregular oscillations due to fluctuations in solar forcing, transport and wind-driven resuspension that occur in other versions of the model. Limit cycles tend to occur when phytoplankton are not nutrient-limited, especially in model versions using the linear mortality formulation for zooplankton mortality. Parameter combinations that led to low phytoplankton biomass and high phytoplankton growth rates also tend to produce limit cycle solutions eg. Fig. 7.14. There are no observations that we consider to support the existence of limit cycle behaviour in the Bay. For this reason, we have dropped the linear zooplankton mortality formulation from standard analyses.

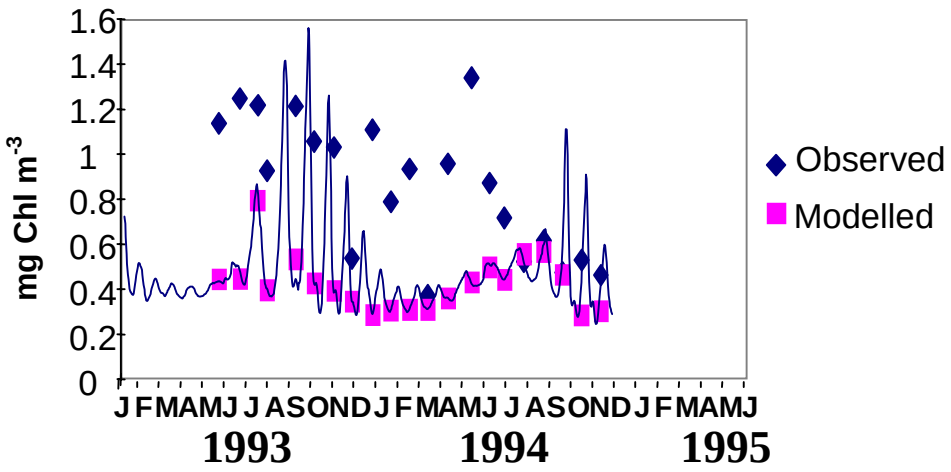

Figure 7.14 Predicted and observed Bay-wide mean chlorophyll for run 34, showing limit cycle oscillations in predicted chlorophyll.

7.6 Sensitivity Analysis

Numerical sensitivity analysis is a useful tool for examining the local dependence of model behaviour on specific parameters. The analysis is undertaken by varying all parameters one at a time by a specified (small) relative amount (in this case 20%) and observing changes in model output. In this case, we have focused on annual Bay-wide and regional pools and fluxes. The analysis provides additional insight into the model dependence on parameters, and helps to identify those parameters that potentially contribute most to uncertainty in model predictions.

There are two related drawbacks to sensitivity analysis (apart from the large computational costs): we cannot analyse synergistic effects, and we are restricted to examining local variation about a single point in parameter space. Sensitivity analysis essentially describes the local linear approximation to the non-linear relationship between predictions and parameters. Synergistic effects occur when parameters interact in a nonlinear way. We can examine interactions in particular cases, if we have *a priori* reason to suspect they are important, but the explosion of combinations makes it impossible to examine even pair-wise interactions in a comprehensive way. Because the model involves highly non-linear interactions, model sensitivity to an individual

parameter may change drastically, depending on the starting value of that parameter, other parameters and even the external forcing. We have indicated in previous sections examples where we expect sensitivity to parameters to change substantially between current loads and high loads.

The starting point for this analysis is the standard run si142. The specific model outputs examined are Bay-wide annual-average water-column pools and fluxes. The pools include DON, large phytoplankton, small phytoplankton, total chlorophyll, nitrate, ammonia, phosphate, and macroalgae; in other words, the principal nutrient and primary producer pools. The principal fluxes include primary production, recycling in the water-column, recycling from the sediment, recycling by filter-feeders, sediment respiration, microphytobenthos production, and denitrification. We also examine sensitivity to parameter changes of regional chlorophyll pools, and the interannual variation in fluxes between 1993 and 1994.

For each output variable and each parameter p, we have calculated the output value with p increased by 20%, minus the output value with p decreased by 20%, normalised to the original output value, and divided by 0.4. That is, for each output variable V and parameter p:

$$\text{Sensitivity} = (V(1.2p) - V(0.8p))/(0.4\, V(p)).$$

The output values V are averaged over the 1993-94 period of model output, and represent volume-weighted Bay-wide or regional means.

This normalised relative sensitivity is approximately equal to $\Delta(\ln V)/\Delta(\ln p)$. If the sensitivity is close to 1, V is proportional to p. If the sensitivity is close to 2, V is proportional to p^2. We have used a centred difference of p, and could in principle estimate the partial second derivative with respect to p, but we have not pursued this here.

The analysis includes 4 parameters, which are prescribed in the transport model, namely the settling velocities of large phytoplankton, labile and refractory detritus, and biogenic silica. As we have discussed in previous sections, nutrient cycling can be highly sensitive to these sinking rates. We have also examined the sensitivity of the model output to changes in the tolerance (maximum relative change per time step, 'tol' in the tables) used in the adaptive integration scheme, to assess the effects of numerical integration error. Normalised sensitivity to tol is always <0.01, and the effect of integration errors on model predictions appears to be small.

There are a few points in the selection of parameters that should be explained before proceeding. Experience in model calibration showed that the light saturation parameters for the phytoplankton fractions (KI_PL and KI_PS) do not play an important role, since much of the time nutrients, not light, are limiting to phytoplankton. KI_PL and KS_PL were therefore varied together. The mortality rate of small phytoplankton, mL_PS, applies only in the sediment and, since these phytoplankton do not sink, has negligible effect and so was not included in the analysis. The proportions of living material and labile detritus ingested by benthic filter feeders which are converted to detritus are prescribed separately, but were varied together. In the current formulation of light attenuation, k_IS and k_w are interchangeable, and they were varied together,

equivalent to a change in total background attenuation. The Redfield P:N and C:N ratios were not altered. The O:N ratio was not altered since it has no effect on any variable apart from oxygen. These economies were made because the full sensitivity analysis is very computationally intensive, the complete series of runs taking about a week to complete.

7.6.1 Sensitivity of annual, Bay-wide pools

Table 7.11 shows the sensitivity of the major model pools to variation in parameters as described above. These pools are dissolved organic matter (DON), large phytoplankton (PL), small phytoplankton (PS), chlorophyll (Chl = all phytoplankton), nitrate (NO_X), ammonia (NH_4), phosphate (PO_4), and macroalgae (MA).

Table 7.11 Sensitivity of Bay-wide annual pools to model parameters.

	DON	PL	PS	Chl	NO_X	NH_4	PO_4	MA
mum_PL	0.048	0.901	-0.549	0.448	-1.055	-0.850	-0.012	-1.770
mum_PS	-0.014	-0.323	1.084	0.116	-0.276	-0.075	0.002	-0.275
mum_MB	0.597	0.244	0.075	0.191	0.003	0.131	-0.074	-0.205
mum_MA	0.007	-0.513	-0.193	-0.413	-0.477	-0.303	0.008	1.674
mum_SG	-0.036	-0.031	-0.012	-0.025	0.005	-0.023	0.008	-0.037
KI_PL,KI_PS	-0.001	-0.009	-0.008	-0.009	0.036	0.039	0.000	0.023
KI_MB	-0.142	-0.016	-0.007	-0.013	-0.001	-0.013	0.012	0.017
KI_MA	-0.002	0.092	0.030	0.073	0.058	0.049	-0.002	-0.309
KI_SG	0.048	0.033	0.013	0.027	-0.001	0.024	-0.013	0.055
KN_PL	-0.022	-0.498	0.409	-0.215	0.491	0.617	0.005	0.871
KN_PS	0.002	0.174	-0.542	-0.050	0.030	0.049	0.000	0.102
KNMB	-0.037	-0.018	-0.006	-0.014	-0.004	-0.009	0.005	0.010
KN_MA	0.012	0.335	0.131	0.272	0.187	0.198	-0.006	-1.042
KN_SG	0.001	0.002	0.001	0.001	-0.002	0.001	0.000	0.001
KS_PL	-0.001	-0.006	0.000	-0.004	0.007	0.001	0.000	0.015
KS_MB	0.000	0.000	0.000	0.000	0.000	0.000	0.000	0.001
MAmax	0.026	-0.029	-0.013	-0.024	-0.110	-0.029	-0.003	0.274
SGmax	-0.001	-0.001	0.000	0.000	0.000	-0.001	0.000	-0.001
C_ZL	-0.002	-0.831	0.426	-0.439	0.468	0.665	-0.002	0.896
C_ZS	0.029	0.353	-2.107	-0.416	0.239	0.075	-0.002	0.252
C_BF	0.014	-0.240	0.277	-0.079	0.069	0.116	0.016	0.495
mum_ZL	0.002	-0.437	0.187	-0.242	0.197	0.298	-0.002	0.527
mum_ZS	0.007	0.045	-0.301	-0.063	0.044	0.011	-0.001	0.058
mum_BF	0.002	-0.087	0.075	-0.036	0.020	0.034	0.006	0.245
E_ZL	-0.006	-0.218	0.111	-0.115	0.119	0.169	-0.005	0.199
E_ZS	0.011	0.147	-0.967	-0.201	0.111	0.033	-0.001	0.134
E_BF	0.009	-0.063	0.116	-0.007	0.002	0.057	0.009	0.191
ml_PL	0.000	-0.150	0.009	-0.100	0.079	0.017	0.001	0.095
ml_MA	0.018	0.397	0.154	0.321	0.246	0.226	-0.007	-2.123
ml_SG	0.017	0.012	0.005	0.009	-0.004	0.009	-0.004	0.013

Table 7.11 Sensitivity of Bay-wide annual pools to model parameters (cont.)

	DON	PL	PS	Chl	NO_X	NH_4	PO_4	MA
mQ_MB	-0.303	-0.129	-0.041	-0.102	-0.002	-0.071	0.038	0.093
mQ_ZL	0.007	0.635	-0.294	0.345	-0.333	-0.470	0.006	-0.713
mQ_ZS	-0.014	-0.152	0.961	0.196	-0.107	-0.034	0.002	-0.128
mQ_BF	0.003	0.178	-0.168	0.070	-0.054	-0.066	0.002	-0.352
ms_MA	-0.002	0.086	0.031	0.069	0.095	0.047	-0.003	-0.374
ms_SG	0.021	0.014	0.006	0.012	-0.004	0.011	-0.005	0.020
FDG_ZL	0.006	-0.089	-0.022	-0.068	0.024	-0.035	0.000	-0.057
FDM_ZL	0.006	-0.090	-0.023	-0.069	0.025	-0.036	0.000	-0.060
FDG_ZS	0.002	-0.060	-0.016	-0.046	0.022	-0.027	0.001	-0.054
FDM_ZS	0.002	-0.051	-0.014	-0.039	0.018	-0.022	0.000	-0.041
FDG_BF+ FDG_DL	0.009	-0.114	-0.031	-0.088	0.037	-0.053	0.002	-0.213
FDM_BF	0.002	-0.038	-0.011	-0.029	0.015	-0.018	0.001	-0.058
r_DL	0.081	0.027	-0.005	0.017	0.002	0.022	-0.004	0.156
r_DR	0.074	-0.035	-0.008	-0.026	-0.032	-0.018	0.022	0.195
r_DSi	0.006	0.060	0.006	0.043	-0.037	-0.004	-0.002	-0.169
r_DON	-0.316	0.052	0.015	0.040	-0.024	0.023	0.020	-0.533
FDR_DL	-0.164	0.074	0.016	0.056	0.039	0.015	-0.020	-0.160
FDON_D	0.896	-0.019	-0.004	-0.014	0.022	-0.013	-0.059	-0.311
R_0	-0.156	-0.332	-0.088	-0.256	0.038	-0.196	0.025	0.053
R_D	0.035	0.058	0.018	0.046	0.103	0.020	-0.005	-0.746
Dmax	-0.474	-1.210	-0.318	-0.931	0.290	-0.632	0.078	0.000
X_CHL_N	0.000	0.000	0.000	1.000	0.000	0.000	0.000	0.343
X_SiN	-0.003	-0.122	-0.004	-0.085	0.108	0.019	0.002	-0.130
k_PN	-0.053	0.026	0.007	0.020	0.018	0.015	0.004	-0.087
k_DON	-0.069	0.035	0.012	0.028	0.016	0.025	0.003	-0.111
k_DL	-0.118	0.145	0.040	0.112	0.125	0.084	0.005	-0.457
k_w	-0.245	0.065	0.020	0.051	0.049	0.050	0.017	-0.239
Q10	0.012	0.043	0.035	0.040	0.225	0.048	-0.001	-0.088
tol	-0.002	0.000	0.001	0.000	-0.006	-0.007	0.000	0.009
w_PL	0.003	-0.953	0.055	-0.638	0.457	0.108	0.013	0.500
w_DR	0.062	-0.058	-0.017	-0.045	-0.015	-0.029	0.013	0.168
w_DL	0.077	-0.186	-0.076	-0.152	0.085	-0.025	0.004	0.073
w_DSi	0.030	0.052	0.006	0.038	-0.038	-0.001	-0.005	-0.121

The concentration of DON is controlled by a balance between DON production, which is a fixed proportion of detrital production, DON losses due to breakdown, which are proportional to the DON concentration, and export to Bass Strait. The DON pool is most sensitive to the parameter FDON_D, which controls the proportion of detritus converted to DON. It is less sensitive to the breakdown rate r_DON because export to Bass Strait is also an important loss term. It is also sensitive to other parameters that control the rate of production of detritus. As we discussed earlier, the net sediment respiration rate is controlled by the external load, and the denitrification efficiency. Thus, the parameter Dmax, and to a lesser extent R_0, have strong effects on DON through their control of denitrification. However, because DON is also produced in breaking down microphytobenthic production, its concentration is strongly dependent on microphytobenthic growth and mortality parameters, and on the background light attenuation. Parameters such as settling velocities, which affect the proportion of

detritus, which reaches the sediment, have weaker effects on DON, whose production in the model is dominated by production in the sediments.

If we wish to alter the DON concentration and thereby N export to Bass Strait, the easiest parameter to change is FDON_D, as the DON pool is almost proportional to FDON_D. The DON pool also depends strongly on r_DON, but we do not have observations to independently calibrate these two parameters. As we noted in Chapter 3, r_DON is an almost arbitrary parameter that implicitly defines the semi-labile character of the model DON pool. It is undesirable to adjust DON concentrations by altering the parameters that control detritus production, since these have stronger effects on other model components. However, when these parameters, particularly Dmax or MPB parameters, are altered for other reasons, DON levels must be checked and readjusted as necessary.

The phytoplankton size fractions compete for nitrogen and so changes in parameters affecting one fraction tend to produce compensatory changes in the other. In some cases this can result in small changes in total chlorophyll, while the relative contribution of the two fractions changes substantially. In general, total chlorophyll is far more sensitive to parameters affecting large phytoplankton, and even macroalgae, than it is to those that affect small phytoplankton. In part this is because small phytoplankton are the minority component and so their relative variation has little impact on total chlorophyll, even in the absence of compensation by large phytoplankton. For starting parameter sets in which small phytoplankton were more dominant, these conclusions would obviously change. Macroalgae compete with both phytoplankton size fractions, and thus changes which favour macroalgae reduce total phytoplankton, although their relative effect is greater on large phytoplankton.

The principal factors controlling biomass of large phytoplankton are their maximum growth rate mum_PL and nitrogen half-saturation constant KN_PL, sinking rate w_PL, grazing by large zooplankton (C_ZL, mum_ZL, mQ_ZL), competition with macroalgae (mum_MA, KN_MA, ml_MA), and denitrification efficiency (Dmax, R_0) that determines overall primary production. Large phytoplankton are relatively insensitive to small size fraction parameters, with the exception of the small zooplankton clearance rate C_ZS. Small phytoplankton are affected by the equivalent growth and grazing processes and by competition with large phytoplankton. The most influential parameters on PS are mum_PL, mum_PS, KN_PL, KN_PS, C_ZL, C_ZS, E_ZS and mQ_ZS. Small phytoplankton are more sensitive to competition by large phytoplankton than vice versa, which is not surprising as they represent the minority of the biomass. They are also less sensitive to competition by macroalgae and to denitrification. Total chlorophyll is generally less sensitive to parameter variation than are the component fractions, and is affected primarily by those parameters which strongly affect PL (mum_ZL, mum_MA, C_ZL, C_ZS, Dmax, and w_PL), and by the chlorophyll:nitrogen ratio, X_Chl_N. With the exception of the latter, all parameters which significantly affect total chlorophyll also strongly affect the individual fractions.

In Table 7.11, phytoplankton biomass appears insensitive to some parameters that can be important under other circumstances. Phytoplankton production and biomass is sensitive to the water column recycling efficiency, but is not very sensitive to the FDG and FDM parameters individually, because they each control only part of the water

column recycling flux (see the discussion of water column recycling below). Bay-wide biomass is not very sensitive to the detrital and DON parameters, but r_DSi will later be shown to have a moderate regional significance. Light saturation intensities and attenuation parameters are not particularly important, but would be expected to have a crucial role at higher loadings. In the current state, increased attenuation increases phytoplankton biomass by suppressing benthic competitors. Increases in k_DL are particularly effective, because detritus appears to be an important contributor to attenuation (Chapter 4), and tends to be high in regions near inputs where macroalgae are concentrated.

Si parameters do not play much of a role in determining Bay-wide biomass of large phytoplankton, because Si limitation is restricted spatially and temporarily. The half-saturation constant for Si-limited growth is much less important than the Si:N ratio. The Q10 value for all rate parameters has little effect on Bay-wide average biomass, but some effect on the spatial and temporal distribution. The seagrass parameters have little effect because seagrass plays only a minor role in the model nutrient budget.

A casual glance at Table 7.11 shows that the Bay-wide phosphate pool is extremely insensitive to model parameters. The predicted phosphate distribution has also shown little change throughout the model calibration process. This is because phosphate is present in such excess that it behaves virtually as a passive tracer in the model.

Nitrate and ammonia show similar patterns of sensitivity, but differences between the two are significant. These patterns of sensitivity tend to reflect those of phytoplankton, although the sign is sometimes reversed. Concentrations of ammonia and nitrate are determined by phytoplankton growth rates relative to maximum growth rates. Phytoplankton growth rates are in turn determined by overall primary production and biomass, discussed above. Parameters that directly increase primary production also increase phytoplankton biomass, phytoplankton relative growth rates and DIN. Parameters that directly increase phytoplankton biomass without changing primary production decrease relative growth rates and DIN.

The principal parameters controlling nitrate are mum_PL, mum_MA, KN_PL, C_ZL and w_PL, while mum_PS, mQ_ZL and Dmax have less effect. Ammonia is also strongly influenced by mum_PL, KN_PL, C_ZL, mQ_ZL and Dmax. The dominance of parameters affecting large phytoplankton biomass presumably again reflects the dominance of this size fraction in run si142. The ammonia pool is largely uninfluenced by w_PL and less strongly by mum_MA than is nitrate, presumably because ammonia is more evenly distributed through the Bay than nitrate and so is less influenced by coastal processes. It is of interest that neither nitrate nor ammonia is significantly influenced by KN_PS, although PS is sensitive to this parameter (but chlorophyll is not, since PL compensates for PS decline).

Another notable difference between nitrate and ammonia is that they have opposite responses to Dmax. This is because Dmax scales both nitrification and denitrification efficiency in the sediment model, so increases in Dmax lead directly to decreased ammonia release and greater nitrate release from the sediment.

Although the Si pool is not presented in the sensitivity analysis it is notable that Si-related parameters appear to have little effect on any Bay-wide pool. This does not mean they are locally unimportant in space or time.

Macroalgae are strongly affected by competition for nutrients with large phytoplankton, and macroalgal biomass is very sensitive to macroalgal growth and mortality parameters, as well as PL and ZL parameters. The extreme (approximately quadratic) sensitivity to mum_PL, mum_MA and ml_MA is explained by the fact that the macroalgal depth distribution is delicately balanced between light limited growth rates and loss rates, so that small changes in these parameters affect not only the local biomass density, but also the area occupied. As expected for phytobenthos, light limitation plays a significant role and both KI_MA and attenuation parameters are important.

7.6.2 Sensitivity of annual Bay-wide fluxes

Calculations for fluxes were carried out in the same way as described above for pools. The fluxes examined are primary production by phytoplankton (PP), release of DIN by recycling in the water-column (WRc), release of DIN from the sediment (SRc), release of DIN by benthic filter-feeders (FRc), net sediment respiration (ie. excluding consumption of MPB production) (SResp), MPB production (MPBP) and denitrification (Den) (Table 7.12).

Table 7.12 Sensitivity of model Bay-wide annual fluxes to model parameters

	PP	WRc	SRc	FRc	SResp	MPBP	Den
mum_PL	0.455	0.134	0.053	0.280	0.030	0.152	0.010
mum_PS	0.432	0.476	0.015	0.458	0.008	-0.050	0.002
mum_MB	0.246	0.275	-0.027	0.226	-0.085	1.470	-0.137
mum_MA	-0.547	-0.351	0.192	-0.360	0.109	-0.162	0.036
mum_SG	-0.034	-0.037	0.037	-0.032	0.027	-0.091	0.017
KI_PL,KI_PS	-0.012	-0.010	-0.006	-0.006	-0.004	0.002	-0.002
KI_MB	-0.014	-0.023	0.033	-0.016	0.030	-0.385	0.027
KI_MA	0.100	0.064	-0.034	0.064	-0.019	0.026	-0.005
KI_SG	0.036	0.040	-0.024	0.035	-0.022	0.110	-0.020
KN_PL	-0.189	-0.023	-0.037	-0.097	-0.027	-0.060	-0.018
KN_PS	-0.201	-0.230	-0.006	-0.199	-0.004	0.020	-0.001
KN_MB	-0.019	-0.023	0.006	-0.021	0.008	-0.091	0.010
KN_MA	0.361	0.240	-0.048	0.245	-0.031	0.087	-0.017
KN_SG	0.002	0.002	-0.006	0.001	-0.003	0.005	-0.001
KS_PL	-0.008	-0.003	-0.004	-0.009	-0.002	0.000	0.000
KS_MB	0.000	0.000	0.001	-0.001	0.000	-0.001	0.000
MAmax	-0.029	-0.007	0.144	0.000	0.073	-0.038	0.008
SGmax	-0.001	-0.001	0.001	-0.001	0.000	-0.002	0.000
C_ZL	0.072	0.418	-0.061	-0.237	-0.047	-0.046	-0.035
C_ZS	-0.406	-0.405	-0.011	-0.660	-0.006	0.079	-0.002
C_BF	-0.001	-0.168	0.022	1.328	0.027	0.070	0.032

Table 7.12 Sensitivity of model Bay-wide annual fluxes to model parameters (cont.)

	PP	WRc	SRc	FRc	SResp	MPBP	Den
mum_ZL	0.019	0.217	-0.040	-0.163	-0.026	-0.016	-0.014
mum_ZS	-0.069	-0.064	-0.008	-0.116	-0.004	0.016	-0.001
mum_BF	-0.015	-0.059	0.007	0.464	0.011	0.016	0.014
E_ZL	0.009	0.076	-0.027	-0.049	-0.024	-0.009	-0.022
E_ZS	-0.197	-0.230	-0.009	-0.188	-0.005	0.041	-0.003
E_BF	0.028	-0.042	0.009	0.594	0.016	0.031	0.021
ml_PL	-0.074	-0.066	0.009	-0.096	0.003	-0.007	-0.003
ml_MA	0.421	0.280	-0.023	0.282	-0.024	0.091	-0.024
ml_SG	0.013	0.014	-0.019	0.012	-0.012	0.038	-0.005
mQ_MB	-0.132	-0.151	0.012	-0.125	0.041	-0.739	0.067
mQ_ZL	-0.016	-0.268	0.058	0.204	0.046	0.033	0.035
mQ_ZS	0.190	0.215	0.013	0.209	0.008	-0.045	0.003
mQ_BF	0.026	0.128	0.004	-0.843	0.000	-0.043	-0.004
ms_MA	0.097	0.063	-0.023	0.074	-0.013	0.020	-0.004
ms_SG	0.016	0.017	-0.019	0.016	-0.013	0.049	-0.008
FDG_ZL	-0.085	-0.139	0.007	-0.041	0.004	-0.007	0.002
FDM_ZL	-0.087	-0.141	0.006	-0.042	0.004	-0.006	0.002
FDG_ZS	-0.056	-0.095	0.008	-0.027	0.005	-0.007	0.002
FDM_ZS	-0.047	-0.078	0.007	-0.023	0.004	-0.006	0.001
FDG_BF+ FDG_DL	-0.117	-0.097	0.047	-0.693	0.025	0.004	0.006
FDM_BF	-0.038	-0.033	0.007	-0.194	0.005	0.005	0.003
r_DL	0.011	0.088	0.051	-0.188	0.015	0.046	-0.018
r_DR	-0.030	-0.002	0.021	0.008	0.024	0.115	0.027
r_DSi	0.060	0.028	0.011	0.070	0.003	0.008	-0.004
r_DON	0.050	0.070	0.094	0.046	0.000	0.068	0.044
FDR_DL	0.067	-0.009	-0.085	-0.047	-0.039	-0.203	0.003
FDON_D	-0.018	-0.009	-0.172	-0.037	-0.150	-0.202	-0.129
R_0	-0.346	-0.316	-0.665	-0.325	-0.318	0.043	-0.008
R_D	0.056	0.053	0.113	0.052	0.047	0.019	-0.012
Dmax	-1.193	-1.086	-2.153	-1.012	-0.965	0.057	0.103
X_CHL_N	0.000	0.000	0.000	0.000	0.000	0.000	0.000
X_SiN	-0.113	-0.045	-0.035	-0.120	-0.014	0.013	0.005
k_PN	0.028	0.015	-0.011	0.015	-0.003	-0.123	0.004
k_DON	0.041	0.025	-0.010	0.024	0.000	-0.182	0.009
k_DL	0.158	0.087	-0.030	0.095	-0.011	-0.251	0.007
k_w	0.074	0.033	0.002	0.041	0.022	-0.654	0.041
Q10	0.142	0.151	0.052	0.148	0.026	0.062	0.002
tol	-0.007	-0.006	0.002	-0.008	0.001	-0.005	0.001
w_PL	-0.466	-0.471	0.063	-0.571	0.040	-0.020	0.020
w_DR	-0.058	-0.048	0.041	-0.027	0.030	0.130	0.020
w_DL	-0.191	-0.303	0.545	-0.530	0.265	0.109	0.013
w_DSi	0.053	0.032	-0.005	0.060	-0.005	0.062	-0.005

The annual denitrification flux essentially equals the external load minus export to Bass Strait through flushing. Because the latter is relatively small, the denitrification flux is only weakly sensitive to all model parameters. It is slightly sensitive to parameters,

which affect the pool of DON, which is the principal form of export to Bass Strait (see discussion of DON above).

For a given denitrification flux, the net sediment respiration rate is determined by the sediment denitrification efficiency. It is sensitive only to the denitrification parameters (Dmax, R_0, R_D), detrital sinking rates and, to a lesser extent, the proportion of detritus converted to DON. The latter two indirectly affect the denitrification efficiency and/or the denitrification loss.

The release of DIN from the sediment (SRc) is also almost entirely determined by the external load and the denitrification efficiency, and is relatively insensitive to parameters other than the denitrification parameters. The quadratic dependence on Dmax is expected: Dmax affects both the denitrification efficiency and the net sediment respiration rate. The release of DIN is weakly dependent on w_DL and some macroalgal parameters. These affect the trapping of detritus near inputs, and consequently the area over which net sediment respiration rates suppress denitrification.

The water-column recycling flux WRc is determined by the external load, the denitrification efficiency and the water column recycling efficiency. The latter is influenced by three way competition among PL, PS and MA. All PS production is grazed and so much of its production is recycled in the water column, whereas all macoalgal production is detrital and thus most ends up on the bottom. Thus increases in mum_PS increase water-column recycling while increased mum_MA suppresses it, and mum_PL has little effect. An increase in C_ZL strongly increases water-column recycling by depressing diatom biomass and sedimentation, while an increase in C_ZS decreases it by suppressing PS and increasing diatom sedimentation. Increases in either w_PL or w_DL increase sedimentation rates and reduce water-column recycling rates. The FDG and FDM parameters have a secondary effect and r_DL is also of secondary importance. Collectively the FDG and FDM parameters are important, but since recycling is divided among three grazers and six components, a change in one only affects a fraction of the total recycling flux.

Bay-wide water column primary production is also determined by the external load, sediment denitrification efficiency, and water column recycling efficiency. This total primary production is then split between phytoplankton and macroalgae, according to the outcome of competition among PL, PS and MA. This competition also affects water column recycling efficiency, and hence total primary production. We expect to see dependencies on denitrification parameters, and on the key growth and loss parameters affecting the outcome of competition between phytoplankton and macroalgae (mum_PL, mum_PS, mum_MA, KN_MA, KN_PL, KN_PS, ml_MA and w_PL). Phytoplankton production is influenced by C_ZS and to some extent E_ZS but virtually unaffected by other zooplankton or benthic filter feeder parameters. Given their strong effect on large phytoplankton biomass and macroalgal biomass, the weak effect of large zooplankton parameters on phytoplankton primary production is puzzling.

Benthic filter-feeder production is influenced significantly by most parameters, because filter-feeders depend on phytoplankton biomass (and to a lesser extent suspended labile detritus) which in turn are sensitive to many factors. Benthic filter-feeders are also sensitive to their own maximum growth rate, clearance rate and mortality coefficient. The most influential parameters are mum_PS, C_ZS, C_BF, mum_BF, E_BF, mQ_BF,

FDG, Dmax, w_PL and w_DL. Benthic filter-feeders are not very important to overall model function at the levels predicted in this model version, but certainly play a significant local role, in shallow waters, in determining phytoplankton biomass.

Microphytobenthos production is sensitive to the MPB maximum growth rate, mortality, light saturation intensity and background attenuation parameters. Background attenuation is more important for MPB, whereas k_DL is more important for macroalgae, because MPB are found deeper, where attenuation is less affected by high levels of suspended detritus.

7.6.3 Spatial variation in sensitivity of chlorophyll

Because different processes are important in different parts of the Bay, regional patterns of sensitivity differ among the parameters. For example, the settling velocity of PL has most effect in shallow regions. We have therefore examined the results of the sensitivity analysis at the level of the regions or coarse boxes. We focus on chlorophyll because it is the most important model output variable, and a key calibration variable (Table 7.13).

The spatial patterns of sensitivity mostly fit one of four general patterns: no large effect anywhere; similar effects Bay-wide; most effect in the coastal zone near inputs; and, more rarely, most effect in the Bay centre. The coastal zone response can be biased toward Werribee, Corio Bay or, occasionally, Hobsons Bay. In general, even where the effect is similar Bay-wide, the outer Sands (box 1) is only slightly affected because it is strongly moderated by exchange across the Bass Strait boundary.

Table 7.13 Sensitivity of chlorophyll regional means to model parameters

	Sands I	Sands II	East	Hobsons	NW	WTP	Corio	Centre
mum_PL	0.194	0.343	0.675	0.922	0.962	1.197	0.969	0.318
mum_PS	0.077	0.151	0.126	0.253	0.296	0.427	0.436	0.062
mum_MB	0.025	0.118	0.157	0.044	0.058	0.019	0.154	0.239
mum_MA	-0.045	-0.280	-0.590	-0.681	-0.722	-0.893	-1.159	-0.327
mum_SG	-0.013	-0.030	-0.013	-0.003	-0.008	-0.017	-0.058	-0.028
KI_PL+KI_PS	0.002	0.005	0.004	-0.017	-0.010	-0.019	-0.015	-0.010
KI_MB	-0.004	-0.012	-0.012	0.002	-0.004	0.001	-0.004	-0.017
KI_MA	0.008	0.053	0.062	0.122	0.141	0.170	0.190	0.061
KI_SG	0.013	0.030	0.013	0.003	0.012	0.022	0.074	0.029
KN_PL	-0.120	-0.196	-0.290	-0.392	-0.431	-0.520	-0.561	-0.156
KN_PS	-0.037	-0.078	-0.052	-0.076	-0.096	-0.108	-0.221	-0.033
KN_MB	0.001	-0.004	-0.011	-0.006	-0.009	-0.007	-0.010	-0.018
KN_MA	0.029	0.195	0.366	0.395	0.478	0.536	0.757	0.223
KN_SG	0.001	0.002	0.001	0.000	0.000	0.000	0.001	0.002
KS_PL	-0.003	-0.002	-0.002	-0.006	-0.020	-0.032	-0.007	-0.001
KS_MB	0.000	0.000	0.000	0.000	0.000	-0.001	-0.001	0.000
MAmax	-0.002	-0.013	-0.030	-0.055	-0.019	-0.184	-0.135	-0.008
SGmax	0.000	-0.001	0.000	0.000	0.000	0.000	-0.001	-0.001

Table 7.13 Sensitivity of chlorophyll regional means to model parameters (cont.)

	Sands I	Sands II	East	Hobsons	NW	WTP	Corio	Centre
C_ZL	-0.165	-0.371	-0.478	-0.515	-0.617	-0.633	-0.617	-0.421
C_ZS	-0.203	-0.468	-0.417	-0.448	-0.582	-0.703	-0.940	-0.368
C_BF	-0.038	-0.075	-0.093	-0.230	-0.224	-0.252	-0.136	-0.050
mum_ZL	-0.067	-0.155	-0.286	-0.481	-0.452	-0.449	-0.366	-0.212
mum_ZS	-0.031	-0.063	-0.064	-0.097	-0.142	-0.193	-0.161	-0.045
mum_BF	-0.009	-0.019	-0.039	-0.162	-0.117	-0.150	-0.062	-0.020
E_ZL	-0.017	-0.091	-0.109	-0.055	-0.118	-0.130	-0.147	-0.124
E_ZS	-0.078	-0.215	-0.207	-0.226	-0.290	-0.355	-0.462	-0.177
E_BF	-0.010	-0.015	-0.007	-0.014	-0.048	-0.044	-0.039	0.000
ml_PL	-0.061	-0.118	-0.135	-0.264	-0.251	-0.249	-0.191	-0.067
ml_MA	0.036	0.230	0.437	0.413	0.528	0.548	0.879	0.274
ml_SG	0.006	0.012	0.005	0.000	0.003	0.007	0.026	0.010
mQ_MB	-0.015	-0.065	-0.086	-0.023	-0.030	-0.007	-0.078	-0.127
mQ_ZL	0.093	0.260	0.374	0.478	0.523	0.524	0.485	0.329
mQ_ZS	0.082	0.214	0.191	0.198	0.261	0.311	0.424	0.179
mQ_BF	0.028	0.056	0.076	0.206	0.176	0.205	0.100	0.050
ms_MA	0.007	0.037	0.108	0.216	0.193	0.123	0.093	0.053
ms_SG	0.007	0.014	0.006	0.001	0.004	0.010	0.034	0.012
FDG_ZL	-0.026	-0.063	-0.066	-0.020	-0.027	-0.010	-0.012	-0.083
FDM_ZL	-0.028	-0.067	-0.065	-0.019	-0.025	-0.008	-0.010	-0.084
FDG_ZS	-0.021	-0.048	-0.044	-0.015	-0.018	-0.009	-0.011	-0.055
FDM_ZS	0.020	0.044	0.040	0.013	0.016	0.008	0.010	0.051
FDG_BF	0.023	0.057	0.071	0.055	0.048	0.041	0.038	0.069
FDM_BF	0.020	0.052	0.072	0.061	0.048	0.047	0.042	0.063
r_DL	0.017	0.034	0.028	-0.028	-0.014	0.035	0.013	0.016
r_DR	0.000	-0.010	-0.012	-0.025	-0.042	-0.041	-0.073	-0.027
r_DSi	0.002	0.015	0.037	0.202	0.193	0.182	0.115	0.020
r_DON	0.011	0.030	0.039	0.011	0.013	-0.005	-0.009	0.051
FDR_DL	-0.007	0.014	0.013	0.058	0.085	0.019	0.084	0.068
FDON_D	0.003	0.009	-0.018	-0.006	-0.014	0.001	0.031	-0.021
R_0	-0.034	-0.149	-0.205	-0.145	-0.236	-0.276	-0.236	-0.290
R_D	0.012	0.038	0.051	0.025	0.024	0.018	0.029	0.052
Dmax	-0.147	-0.594	-0.814	-0.441	-0.588	-0.456	-0.475	-1.116
X_Chl_N	1.000	1.000	1.000	1.000	1.000	1.000	1.000	1.000
X_SiN	-0.003	-0.022	-0.084	-0.509	-0.382	-0.395	-0.265	-0.029
k_PN	0.004	0.017	0.019	0.047	0.037	0.044	0.046	0.016
k_DON	0.006	0.030	0.015	0.026	0.039	0.066	0.092	0.024
k_DL	0.011	0.065	0.105	0.270	0.295	0.310	0.347	0.080
k_w	0.010	0.053	0.041	0.072	0.086	0.128	0.169	0.040
Q10	0.010	0.039	0.024	-0.015	0.003	0.038	0.102	0.046
tol	0.000	-0.001	0.000	-0.003	-0.003	-0.007	-0.004	0.002
w_PL	-0.177	-0.537	-0.690	-0.901	-1.026	-1.198	-0.965	-0.580
w_DR	-0.010	-0.043	-0.031	-0.021	-0.028	-0.067	-0.135	-0.045
w_DL	-0.041	-0.127	-0.163	-0.083	-0.047	0.099	-0.071	-0.189
w_DSi	0.003	0.013	0.022	0.133	0.177	0.155	0.088	0.021

Changes in the maximum plant growth rates produce three different spatial patterns. Increases in mum_PL strongly (proportionately) increase chlorophyll in most coastal boxes, with maximum effect off Werribee. Increases in mum_PS have much weaker effects, with maximum effect off Werribee and in Corio Bay, while increases in mum_MA produce strong (almost proportional) decreases in chlorophyll in Werribee and Corio Bay regions. Increases in mum_MB produce small increases in chlorophyll in the Bay centre. Increases in mum_SG have little effect, with a weak maximum effect in Corio Bay.

The light saturation intensities have little effect on phytoplankton, except for KI_MA, which has some effect in Corio Bay. (Of course, KI_MA, KI_SG and KI_MB have very large impacts on the distributions of the respective benthic plant biomass.) The nutrient half-saturation constants KN_PL, KN_MA and, to a lesser extent, KN_PS have moderate effect in coastal boxes with maximum effect in Corio Bay, reflecting competition for nutrients between phytoplankton and macroalgae. The zooplankton clearance rates C_ZL and C_ZS have moderate effects throughout the Bay, although C_ZS has an exaggerated effect in Corio Bay. The benthic filter-feeder clearance rate, C_BF, has a weaker effect, with maximum impact in the shallow Werribee region. The maximum large zooplankton growth rate, mum_ZL, has a moderate effect throughout the Bay, whereas mum_ZS and mum_BF have only weak effects, biased toward Werribee and Hobsons Bay. E_ZS has a moderate effect in the coastal region.

Only four parameters cause chlorophyll changes of different sign in different parts of the Bay. Increases in Q10 have a negative effect on chlorophyll in Hobsons Bay, and positive effects elsewhere. The sinking rate w_DL has a positive effect off Werribee and negative effects elsewhere. The detritus remineralization rate r_DL causes a negative response in Hobsons Bay and off the northeast coast and positive responses elsewhere. In all cases, it seems likely that these changes in parameters affect the degree of local nutrient trapping near inputs.

We can make some sweeping generalisations about regional patterns of sensitivity. Parameters related to MPB and denitrification efficiency, and the FDM and FDG parameters controlling water column recycling efficiencies, affect the Bay centre most. The large phytoplankton parameters have strong effects in coastal regions, with maximum impact off Werribee, while small phytoplankton and macroalgal parameters have maximum effect in Corio Bay. Large zooplankton parameters have more even Bay-wide impacts. Parameters related to Si cycling and the Si:N ratio have most effect in Hobsons Bay. (This is surprising, as the Yarra is the key source of silicate, and we would have expected the Werribee region to show most Si limitation.)

These general patterns are consistent with the view that recycling efficiency, whether in the water-column or sediment, most affects the Bay centre, while the transient responses of primary producers to nutrients, and grazers to phytoplankton, affects coastal areas. Competition for nutrient between phytoplankton and macrophytes is most important in Corio Bay, while off Werribee the maximum growth rate of PL helps determine the size of local blooms.

7.6.4 Sensitivity of interannual variation

We discussed earlier the change in load between 1993 and 1994, and the observed changes in pools of chlorophyll and nitrogen. The model has difficulty in reproducing the observed interannual changes in chlorophyll and DIN in the Bay centre. In an effort to gain further insight into the processes controlling interannual variation in the model, we computed an index of sensitivity to model parameters of interannual variation in key fluxes and pools. However, this analysis did not point to any parameters as providing particular leverage to increase interannual variation in model predictions.

7.7 Summary

The model is sufficiently complex that formal and rigorous parameter estimation procedures are not practical. We do not claim that the "standard" version that has emerged from this calibration run is "optimal" or a best fit to observations. It is consistent with our *a priori* understanding of processes and parameter constraints, and reproduces most of the key spatial and temporal patterns in the observations. Because we have not applied formal parameter estimation techniques, the understanding of the model behaviour and its dependence on parameter values, which has emerged from both analysis of simple approximate models (Chapter 6) and numerical experiments (Chapter 7), assumes particular importance. This understanding is not only of scientific interest, but is critical to the assessment of uncertainty involved in using the model to generate scenarios for management support (Chapter 8). We summarise below the key conclusions from Chapters 6 and 7.

In thinking about the nitrogen cycle in Port Phillip Bay, we can conceptually treat the sediment and the water column as two distinct systems, coupled by the sedimentation of detritus from the water column to the sediment, and the release of DIN from the sediment. This separation is possible because the long flushing time results in a small nitrogen loss to Bass Strait, so that denitrification approximately balances the external load. The (empirical) relationship between denitrification efficiency and net sediment respiration rate then determines both the net sediment respiration rate (input of detritus from the water column) and the flux of DIN from the sediment to the water column. To first order, the relationship between denitrification efficiency and sediment respiration rate therefore encapsulates the role of the sediments in the nitrogen cycle, and determines the total load of DIN to the water column. This can be varied by adjusting the denitrification parameters.

In a system where flushing makes a major contribution to nutrient losses, both water column and sediment fluxes will depend strongly on water column concentrations and the controls on sediment and water column fluxes would be more difficult to disentangle.

This simple model of the sediments also dominates the predicted response of the Bay to changes in nitrogen load. As the load increases, the sedimentation rate increases, but the denitrification efficiency decreases. At some point, the decrease in denitrification efficiency balances the increase in respiration rate, setting a maximum denitrification capacity for the Bay. Loads exceeding this capacity can only be balanced by export of

nitrogen from the Bay, which, because of the low flushing rate, requires a very steep increase in water column total nitrogen, resulting in rapid eutrophication.

Given the critical importance of the empirical relationship between sediment respiration rate and denitrification efficiency, it is worth reminding ourselves of some of the uncertainties in this relationship. It is based on sediment chamber measurements of respiration rate and DIN release at a relatively small number of sites and occasions in the Bay. Most of the contrast in the observations defining the empirical relationship is due to spatial variation across the Bay. We do not have good data defining the time scales on which denitrification efficiency responds to changes in local sediment respiration. Correlation is not necessarily causation: some of the observed spatial contrast in denitrification efficiency may reflect other sediment properties that co-vary with respiration rate. Process models of the underlying sediment biogeochemistry provide only qualitative support for the form of the empirical relationship. We do not understand for example why maximum denitrification efficiencies in Port Phillip Bay are so high. It seems possible that these are linked to the high observed levels of bioirrigation and bioturbation, but this association has yet to be established and quantified. The simple empirical sediment model does not allow for burial of organic N at high loads. Current burial rates of organic N in Port Phillip Bay are poorly understood. It is highly desirable that scientific research be targeted at all these issues.

Given the external load and the flux of DIN from the sediment, primary production in the water column is determined by the water-column recycling efficiency. This is rather more difficult to predict, as it depends on the balance of competition among different phytoplankton fractions and benthic macroalgae, and consequently on a large number of parameters affecting growth, light limitation, nutrient limitation, grazing and sinking rates of these components. The measured rates of Bay-wide primary production essentially fix the effective average water column recycling efficiency during the Study, but do not allow us to fix the parameters controlling changes in this efficiency with changes in load. The observed spatial and temporal patterns in water column pools and fluxes provide additional constraints on these parameters.

It is worth noting that the preceding analysis assumes that nitrogen is the principal limiting nutrient in Port Phillip Bay. Both observations and modelling suggest that this is true throughout most of the Bay most of the time. Phosphate is present in great excess, and consequently behaves approximately as a passive tracer. Diatoms are the dominant phytoplankton, and silicate appears to limit diatom production in particular regions at particular times. The role of silicate limitation in the observed interannual variation in Bay-wide chlorophyll, in response to changes in riverine loads, is still ambiguous, because of uncertainty about Si loads and recycling of biogenic Si.

The standard model version includes two phytoplankton size fractions: large cells which are fast growing, and subject to weak grazing control, and small cells which are slower growing, but strong competitors for nutrient, and subject to strong grazing control. The large cells represent bloom species, and in the standard model which incorporates Si cycling, the large cells require Si (ie. are diatoms). It is desirable that non-diatom bloom species (dinoflagellates) also be included in the standard model in future.

The balance between small and large phytoplankton depends strongly on a considerable number of parameters, some of which are poorly constrained *a priori*. These parameter

values must be refined by calibrating the model against the Bay-wide annual mean observations, and spatial and temporal patterns at a range of scales. After calibration, the small and large phytoplankton in the standard model version generally behave according to both observations and expectations. The bloom species dominate near inputs, or in response to transient loads. The small phytoplankton tend to form a persistent but less responsive background population. In this region of parameter space, the biomass of large phytoplankton is also generally more sensitive to small changes in most parameters, and these responses tend to be reflected in the parameter sensitivity of total chlorophyll.

The DIN concentration throughout much of the Bay is low. The DIN pool turns over very rapidly, and is strongly regulated by phytoplankton growth rates and half-saturation constants for growth. There are exceptions where DIN accumulates temporarily near inputs. Reproducing these observations has been a challenge and incorporating Si limitation appears to be critical to explaining patterns of ammonia utilisation in the Werribee region. There are arguments for greater model spatial resolution near inputs and this is a potential area for future model development.

The model explicitly represents both ammonia and nitrate, but does not predict nitrate concentrations well. Observed nitrate concentrations are low compared with ammonia, but are underestimated by the model. Observations suggest this is due to overestimation of uptake, and the model representation of ammonia and nitrate uptake by phytoplankton, which includes ammonia inhibition, may well be inadequate. Nitrate was included primarily as a diagnostic variable but, without additional information on phytoplankton uptake kinetics (eg. from ^{15}N uptake experiments), it could be argued that it has not proved particularly useful, and that use of a combined DIN variable in the model would have been acceptable.

Phosphate is present in great excess and generally behaves like a passive tracer, with a concentration gradient around sources and another across the Sands. The spatial distribution predicted by the model generally agrees well with observations. Values in the model are a little high despite the fact that the 59 box transport model slightly over-estimates flushing rates (Walker 1997b). This may indicate that there is net burial of P in the sediments, which is not included in the model. Small errors in the Bass Strait boundary condition may also contribute to this discrepancy. The large excess of P over N in Port Phillip Bay is primarily due to denitrification. Under conditions where denitrification is suppressed, P is exported along with N as organic matter, and phosphate concentrations in the Bay are reduced, although given the overall N:P concentrations in inputs, N is still likely to be limiting.

Silica has a high degree of variability at time scales of months to seasons, associated with Yarra Si inputs and WTP N loads. It is an important limit on spring blooms off Werribee. The model predictions agree reasonably well with observations, particularly in the immediate vicinity of Werribee, but inadequacies in the Si loads or Si dynamics may partly explain the model's difficulty in representing interannual changes in Bay centre chlorophyll.

DON is the principle form of N that is exported from the Bay, but we have very few observations to directly constrain internal DON cycling within the Bay. The current model treats the excess DON in Port Phillip Bay as semi-labile, subject to both

significant production (mostly in the sediment) and remineralization. The observations are ambiguous: the sediment cores showed high concentrations of DON in pore water, but the sediment chambers did not measure high rates of release of DON to the water column. The excess DON in the Bay could alternatively be modelled as a very refractory pool, which enters the Bay in runoff and acts as a passive tracer. In the current model version, production and export of DON reduces the overall cycling of nitrogen in the Bay, and changes in parameters which increase DON concentrations decrease primary production accordingly. Under increased loads, export of total N is predicted to become increasingly important relative to denitrification, but the relative contribution of DON export will diminish as concentrations of DIN and phytoplankton N in the water column increase.

Microphytobenthos biomass and production in Port Phillip Bay are both large. In the model, MPB are generally not nutrient limited, as they have access to pore water DIN. They are severely light-limited in the deeper parts of the Bay. Their biomass and production are primarily determined by growth rate and density-dependent mortality. MPB can potentially enhance denitrification efficiencies by trapping DIN that would otherwise escape to the water column. However, in the current model version, MPB have very little direct effect on sediment biogeochemistry, which is controlled by the net sediment respiration rate. We have chosen this formulation because high denitrification efficiencies are observed in the Bay centre in the absence of MPB production.

Macroalgae and seagrass distributions are both restricted in depth distribution by light limitation. Seagrass have a higher light requirement than macroalgae, and are found shallower than 5 m, while macroalgae are found to 10 m depth or more. In the model, macroalgae require high water column nutrient concentrations, and are concentrated in regions where DIN accumulates. In order to obtain a distribution of macroalgae matching observations, the model must include an additional loss term for macroalgae in shallow water, which we associate with bottom stress. Seagrass in the model are assumed to be directly adversely affected by high water column nutrient concentrations, and their distribution is biased towards low nutrient areas close to the entrance. They are both sensitive to changing nutrient loads. Corio Bay in particular may be dominated by macroalgae at high input loadings, and seagrass dominated at low input loadings. As levels of eutrophication increase and light attenuation increases accordingly, the maximum depth occupied by both macroalgae and seagrass decreases, but macroalgae can compensate by colonising a wider range of shallow habitats.

Benthic filter-feeders in the model have been adjusted to match the patchy and mostly historical or literature estimates of biomass and clearance rates. They do have a minor role in the standard version of the model, but uncertainty about their real biomass and ecology is such that their effect could be underestimated. In the model, filter-feeders are generally predicted to occur at highest concentrations in the north-western part of Port Phillip Bay. This corresponds to the observed distribution of the introduced fan-worm *Sabella spallanzanii*. The effects of a large increase in benthic filter-feeder biomass are considered as a "Sabella scenario" in Chapter 8.

Much of the qualitative understanding of Bay-wide fluxes and pools, and their response to nutrient loads, was derived from simplified one-box models discussed in Chapter 6. The numerical analysis of the spatially-resolved model presented in this chapter has

allowed us to address two broad issues. The first issue concerns the extent to which spatial and temporal variation within the Bay scales up (through non-linear interactions) to significantly modify conclusions from one-box steady-state models about Bay-wide fluxes and pools. At current loadings, inclusion of spatial and temporal variation does not appear to modify significantly the qualitative conclusions from simple models. Much of the understanding derived from one-box models is entirely consistent with the outcome of simulation experiments and sensitivity analyses measured at the Bay-wide scale. The effects of spatial variation on Bay-wide fluxes are more important at high loadings. For example, in a spatially-resolved model, the onset of eutrophication occurs at lower loadings, but more gradually, than in one-box models.

The spatially-resolved model also allows us to address local and transient phenomena which cannot be addressed by one-box models. This capability becomes more important given current management attitudes and plans. If there were serious prospects of major increases in loads, then the Bay-wide assimilation capacity would be the critical management issue. However, current plans are to slowly reduce nutrient loads to the Bay. At current loads, the key environmental issues are local or regional rather than Bay-wide, and understanding and predicting local responses to specific changes in loads from particular sources will be the key requirement for management decision support. This is a more challenging task for the model, but we believe the results described in this chapter are encouraging.

8 MANAGEMENT SCENARIOS

8.1 Use of the model as a management support tool.

The purpose of the Port Phillip Bay study was to provide managers with an improved scientific basis for managing the Bay. The integrated model has been developed both as an aid to scientific synthesis and understanding, and as a management support tool. In the latter role, the model can be used to predict the response of the Bay to changes in nutrient loads (eg. what would happen if nitrogen loads from a particular source were halved or doubled), to changes in forcing (eg. what would happen if the Bay experienced several unusually wet or unusually dry years in a row), or to changes in ecological function (eg. what would happen if benthic filter feeders became much more abundant, or if denitrification efficiency decreased).

Assessing the reliability of complex model predictions is always difficult. In Chapter 7, we used the level of agreement between model predictions and observations during the PPBES as a performance measure. However, when a model is used to make predictions about responses to actions outside the historical or documented experience, the accuracy or reliability of predictions depends to a large degree on the extent to which the model captures the key processes and feedbacks which control these responses. The qualitative analysis of Chapter 6 and the numerical experiments described in Chapter 7 are important because they contribute to our understanding of the robustness of model predictions and their dependence on model formulation and parameter values.

In managing complex ecological systems, we should recognise the uncertainty in predictions, and allow for it by adopting an adaptive management approach (Holling 1978). An adaptive approach recognises that understanding and predictive capability will improve with time. While choosing current management actions on the basis of best current knowledge and understanding, an adaptive management strategy monitors the response of the system to these actions, and includes explicit procedures to refine system understanding and predictive models, and review management actions, in the light of the results. A key lesson from experience in adaptive management of ecological systems is the importance of avoiding "option foreclosure" (management actions whose consequences are difficult to reverse if they turn out to be unfavourable). Management actions can be difficult to reverse either on economic grounds, or because of non-linear responses of the managed system. The potential hysteresis in response to nitrogen loads discussed in Chapter 6 provides a good example of the latter.

The Victorian agencies responsible for managing Port Phillip Bay have already adopted a conservative approach to the PPBES findings, undertaking to reduce current nitrogen loads by 1000 tonnes N y^{-1} in the short-term. This decision was partly based on early model results, and in particular the concept of a denitrification-based assimilative capacity described in the PPBES Final Report (Harris *et al*. 1996) and in Chapter 6 of this report. The agencies are in the process of establishing a structure for ongoing scientific management, incorporating the key elements (monitoring and model review) of the adaptive approach.

The use of the model for management purposes is just beginning. The model has been used to address a variety of scenarios requested by management agencies, ranging in scale from major changes in loads or ecological function, to minor changes in local inputs. In this chapter, we present a selection of these scenarios and the corresponding model predictions. This selection is intended to provide a picture of the potential uses of the model, and of the response of the Port Phillip Bay ecosystem, according to the model, to a variety of perturbations.

We begin by revisting the response of the Bay to large changes in total nutrient load. We then deal with changes in the secondary inputs: Patterson River and Mordialloc Creek, and the minor inputs from Werribee River and Kororoit Creek. We follow this with a discussion of the model sensitivity to changes in temperature. The mechanism that produces the very efficient denitrification observed in the Bay is not fully understood, and could potentially change for unforeseen reasons. We therefore carry out an investigation of the effects of reduction in denitrification efficiency. Finally, we address briefly the potential impact of introduced species such as the fan worm *Sabella spallenzani*, on the nitrogen cycle and water quality in the Bay.

8.2 The effect of increased loading to Port Phillip Bay.

The effects on the model of increased nutrient loading to the Bay were discussed in detail in Harris *et al*. (1996). However, the model has been modified significantly through subsequent development and calibration, and we present here the results obtained using the current standard version (si142). This version uses a conservative value of 200 mg N m^{-2} d^{-1} for R_0, the critical parameter controlling denitrification capacity. This value is close to the lower end of the 95% confidence interval (see Chapter 7).

Nutrient inputs (N, P and Si) from the four principle sources (WTP, Yarra, Patterson and Mordialloc) have been scaled by factors of 0.5, 1, 1.5, 2, 2.5, 3, 3.5 and 4 from the current values (Chapter 5). Figures 8.1 and 8.2 show the response of phytoplankton in terms of chlorophyll and primary production. In both cases, for loadings between 0.5 and 2 times the current load, there is a gradual response, chlorophyll approximately trebling over this 4 fold increase in loads. However, between 2 and 3 times the current load, phytoplankton biomass increases 4 fold and primary production trebles. With further increases in load, chlorophyll and production continue to increase, although at a slower rate. Almost all of this increase in biomass is made up of large phytoplankton; indeed small phytoplankton increase by a factor of only about 3 between 0.5 and 3 times loading, and thereafter decline slightly. This behaviour is consistent with the qualitative analysis and simulation results reported in the PPBES Final Report (Harris *et al*. 1996) and in Chapter 6 of this report. It suggests that the denitrification or assimilative capacity of the model is between two and three times current loads.

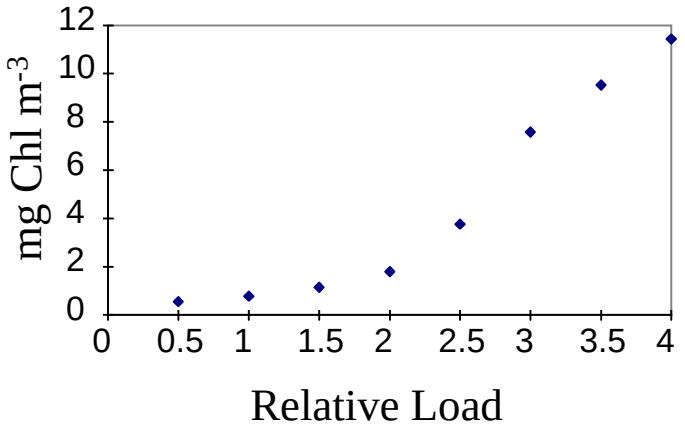

Figure 8.1 Mean Bay-wide annual chlorophyll concentration versus nitrogen load relative to current load.

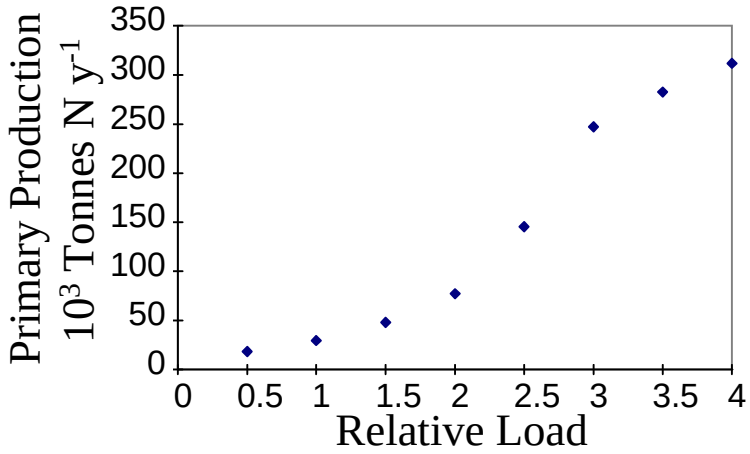

Figure 8.2 Phytoplankton primary production versus nitrogen load relative to current load.

Denitrification reaches a maximum of ca 15000 tonnes N y^{-1} at about 2.5 times the current nitrogen load, or ca 17000 tonnes N y^{-1} (Figure 8.3). This capacity is lower than the estimate from simple one-box models, which for these parameters, would be 22000 tonnes N y^{-1}. The difference in denitrification capacity is attributable to the spatial and temporal structure in sediment respiration rates in the simulation model. Note that the denitrification loss increases almost in proportion to external load up to the maximum, and export from the Bay amounts to only about 2000 tonnes N y^{-1} at the maximum. Denitrification losses decrease rapidly once the assimilation capacity is exceeded, and export quickly becomes the dominant loss term. Note however that the full simulation model does not reproduce the "catastrophic" response predicted by the one-box model, where denitrification fails completely once the denitrification capacity is exceeded. Some denitrification is maintained (in less productive areas of the Bay) after the assimilative capacity is exceeded.

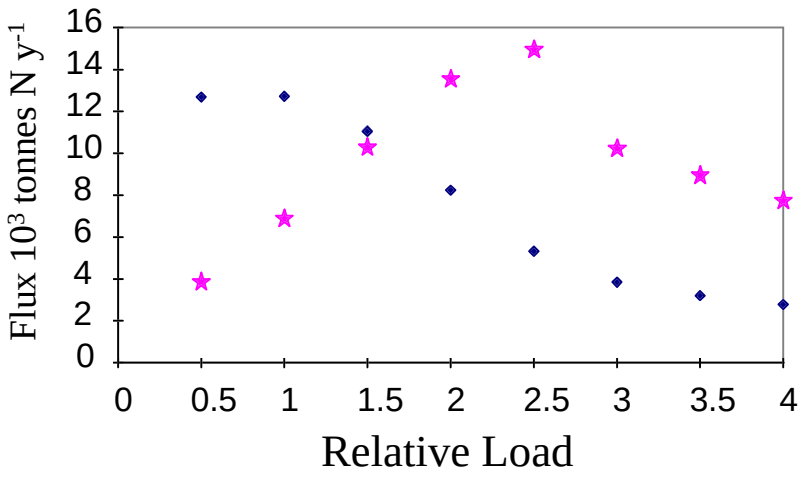

Figure 8.3 Denitrification flux (stars) and MPB production (diamonds) vs nitrogen load relative to current load.

Microphytobenthos production starts to decline if loads are increased even moderately above current levels (Figure 8.3), due to increased biomass and suspended detritus, increased light attenuation and decreased bottom light. In this model version, this decrease in MPB production does not lead to a direct decline in denitrification efficiency.

Over this range of external loads, the contribution of water-column recycling to total recycling of DIN decreases from 70% to 40%, while sediment release increases from 15 to 45%. This change reflects both the increased dominance of large phytoplankton and the reduced denitrification efficiency at high loads. Benthic filter-feeders contribute about 15% of the recycled DIN throughout this range of loads.

Bay-wide macroalgal production shows a complicated pattern of response to changes in external load (Fig. 8.4), reflecting the interactive effects of nutrient limitation and light limitation, and spatial variation within the Bay. Up to 1.5 times current load, macroalgae are nutrient limited and respond everywhere to increases in nutrient concentrations, with maximum contributions from the northern and western regions affected by the major inputs. As loads exceed 1.5 times, biomass starts to decline in these regions due to increasing light attenuation. However, biomass in Corio Bay continues to increase from 1.5 to 3.5 times current loads, and between 2.5 and 3.5 times, the increase in Corio Bay is sufficient to reverse the declining trend in Bay-wide biomass. Biomass in the Sands, which are shallow and nutrient-limited, is predicted to continue to increase up to 4 times current loads.

As one would expect, macroalgal biomass becomes concentrated at shallow depths as nutrient loads increase. The mean depth of macroalgal biomass in the Bay decreases from nearly 7 m at current loads to less than 4.5 m at 4 times (Fig 8.5). Model predictions may be partly affected by the limited resolution of bottom depth afforded by the 59-box transport model. Thus, the narrow east coast boxes have large mean depths and support little biomass at any loads. Only 2 model boxes are less than 4 m deep. Macroalgal production is about a sixth of planktonic primary production at inputs of less than 2 times current loading, and less than 5% of phytoplankton production for inputs in

excess of 3 times current loading. However, locally off Werribee and in Corio Bay, macroalgal production can exceed phytoplankton production. Given the effective transfer of primary production to the Bay bed by macroalgae, this local production has a strong influence on local nutrient cycling and trapping.

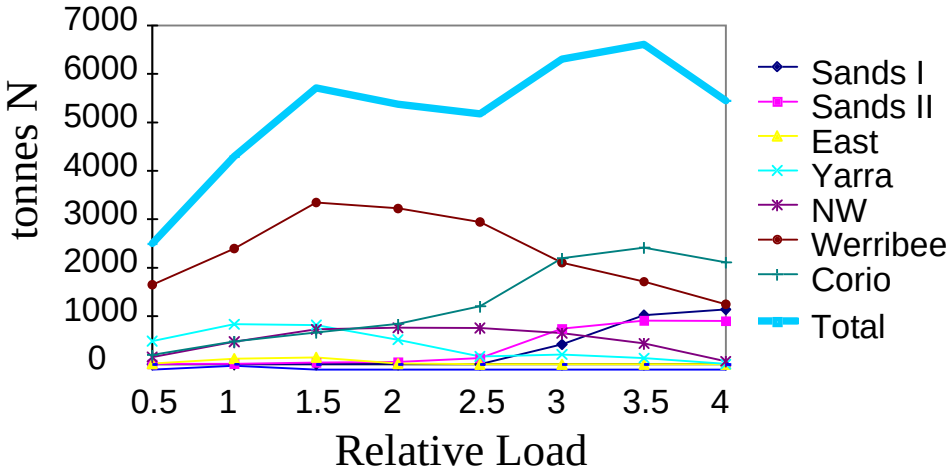

Figure 8.4 Macroalgal biomass by region vs nitrogen load relative to current load

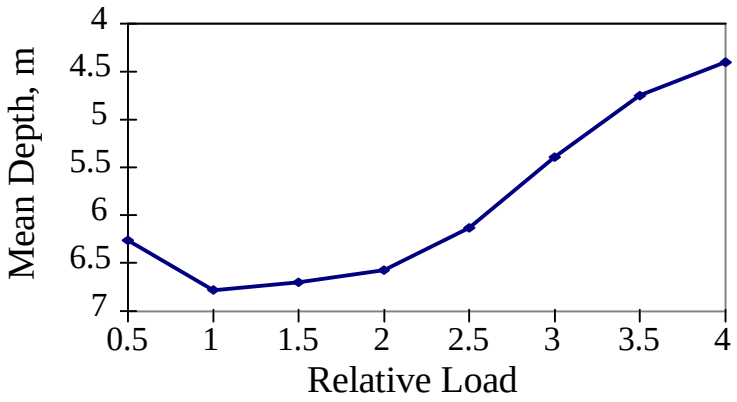

Figure 8.5 Mean depth of macroalgal biomass vs nitrogen load relative to current load.

Seagrasses decline as loads increase. At very low loads, seagrasses are broadly distributed in shallow regions in the southern Bay and in Corio Bay. Loads in excess of current loads causes the seagrass beds to disappear in Corio Bay, and at 2 to 2.5 times current loads, seagrasses have largely disappeared from the Bay, except in Swan Bay. Dense seagrass beds are predicted to occur in this very shallow nutrient-limited region at 2-2.5 times current loads. However, it is unclear whether the model correctly predicts exchange of organic matter between Swan Bay and the rest of the Bay. Again, the current model structure provides limited resolution of bottom depth, and finer spatial and bottom depth resolution is needed to address impacts on seagrass in more detail.

8.3 The role of secondary sources

Changes to total loads of the kind discussed in the preceding section could only be produced by changes to the major sources (Yarra and WTP). We consider here the local and Bay-wide impacts of changes in four minor sources. The Patterson River and Mordialloc Creek are together responsible for a DIN load comparable to that of the Yarra River, although they provide much less organic nitrogen than the Yarra. We consider the impact of changes in this load, focusing on the region near the input sites. The Werribee River and Kororoit Creek typically have very low runoff and nutrient loads. There is evidence (discussed in Chapter 5) that these creeks were responsible for very high runoff and loads during a brief runoff event in September 1993. The load associated with this event is uncertain, and we have considered the transient local effect of a three-fold variation in this load.

The effect of varying the inputs of the two minor creeks (Werribee River and Kororoit Creek) is, at the Bay wide average scale, trivial. Increasing daily loads from these sources to three times the estimated (standard) input changed Bay-wide production and chlorophyll by only 3%. The Patterson-Mordialloc system is more important, and a change from zero to two times loading caused a 20% increase in chlorophyll and a 26% increase in Bay-wide production. As the difference between zero and two times normal inputs for these rivers amounts to about 30% of total input to the Bay, these figures represent a somewhat less than proportional increase in biomass with load. About half these changes occur between zero and current loads, so that the complete elimination of Patterson-Mordialloc inputs would only lead to about a 10% drop in chlorophyll Bay-wide.

Local effects of increased loading via minor rivers can be significant. In Figures 8.6-8.8 we present chlorophyll concentrations for boxes 49, 47 and 44 which form a coast-offshore transect between the Werribee River and Kororoit Creek on the north west coast of Port Phillip Bay. Even the coastal box (49) is largely unaffected by current inputs from the minor creeks. When these inputs are trebled, there is a large bloom in the coastal box following the September 1993 runoff event, with chlorophyll levels 6-10 times background levels (Fig. 8.6). A significant enhancement in chlorophyll persists for about 3 months, particularly when the standard model predicts blooms. Moving offshore to box 47, we see that there is still some effect of enhanced loading, with a doubling of the initial bloom and minor enhancement for two months (Fig. 8.7). Finally, fine box 44, which is part of the Bay-centre region, shows negligible response to trebled inputs (Fig. 8.8). The bloom in September 1993 in fine box 44 is driven by the concurrent runoff from the Yarra River. Thus, the effects of the input from Werribee River and Kororoit Creek are restricted to nearby coastal areas.

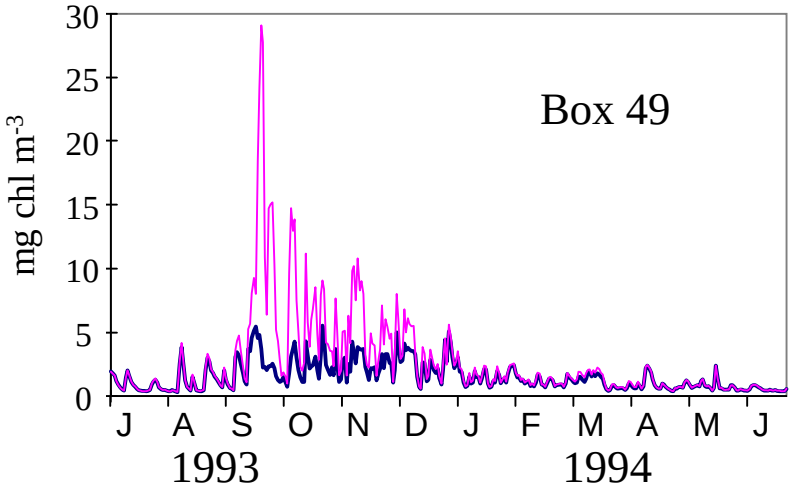

Figure 8.6 Effect of nutrient inputs from Werribee River and Kororoit Creek on chlorophyll in box 49 (inshore) at standard (thick line) and trebled (thin line) loads.

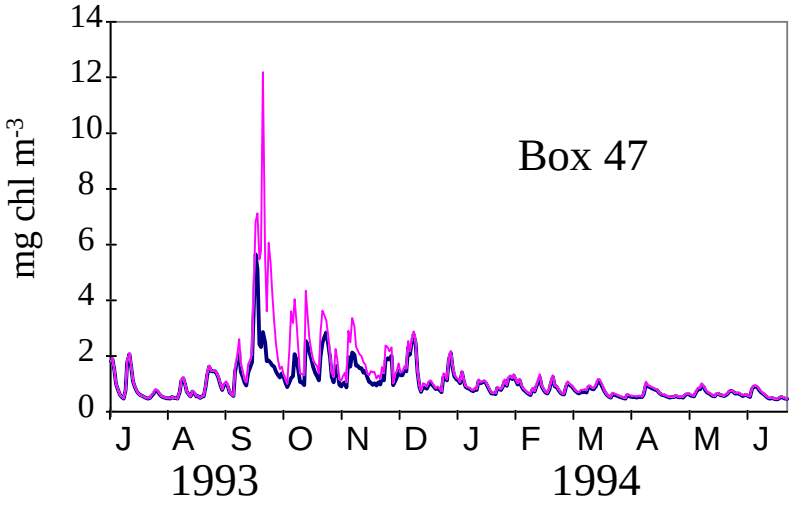

Figure 8.7 Effect of nutrient inputs from Werribee River and Kororoit Creek on chlorophyll in box 47 (offshore) at standard (thick line) and trebled (thin line) loads.

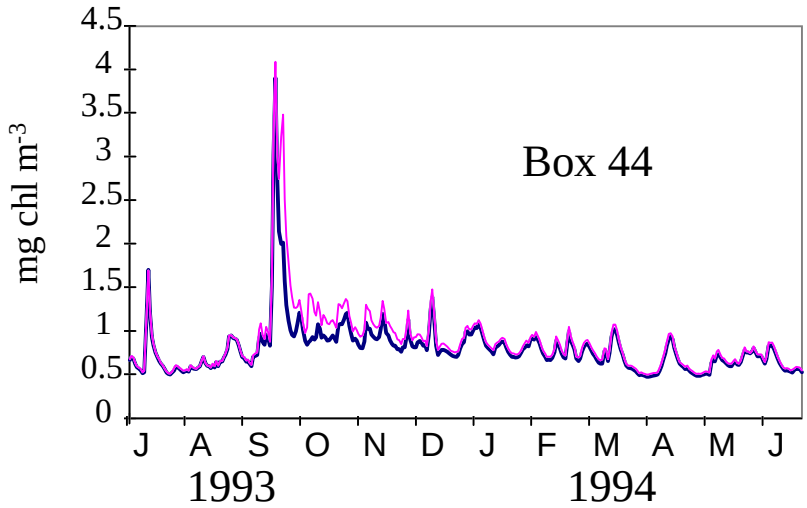

Figure 8.8 Effect of nutrient inputs from Werribee River and Kororoit Creek on chlorophyll in box 44 (Bay centre) at standard (thick line) and trebled (thin line) loads.

Because there is no single dominating flood comparable to that observed in the Werribee River, the effect of changing the loads of the Patterson Mordialloc (P-M) system from zero to twice current levels is locally less spectacular than the minor creeks. This is more than made up for in the persistence and wide-spread nature of the effects. In the absence of P-M loads, the entire east coast region behaves similarly to the Bay centre, with low and fairly constant biomass, except that the coastal region responds more to the Yarra input event of the spring of 1993 than does the Bay centre. Doubled inputs from the P-M system produce large blooms in coastal waters along the east coast (Fig. 8.9). These blooms, particularly from spring 93 to summer 94, propagate even into the neighbouring Bay centre (Fig. 8.10). Background chlorophyll levels are persistently increased throughout the Bay centre, and to a lesser extent throughout the Bay (Fig. 8.11, Table 8.1).

Table 8.1. Percentage change in annual average chlorophyll when the Patterson Mordialloc load is increased from 0 to 2 × current load, for runs based on si142

	Sands I	Sands II	East	Hobsons	NW	WTP	Corio	Centre
si142	3.4	16.1	79.9	34.9	25.6	20.7	14.7	30.5

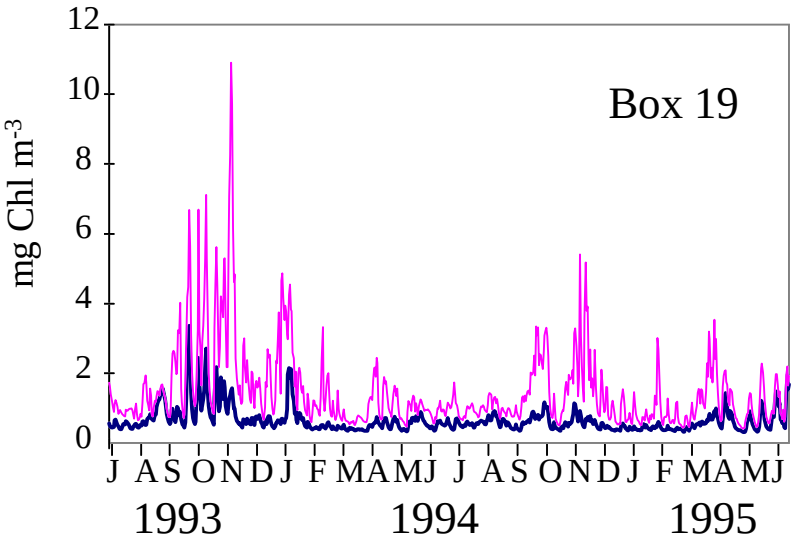

Figure 8.9 Chlorophyll concentrations in coastal box 19 with 0 × (thick line) and 2 × (thin line) nutrient inputs from the Patterson-Mordialloc Rivers.

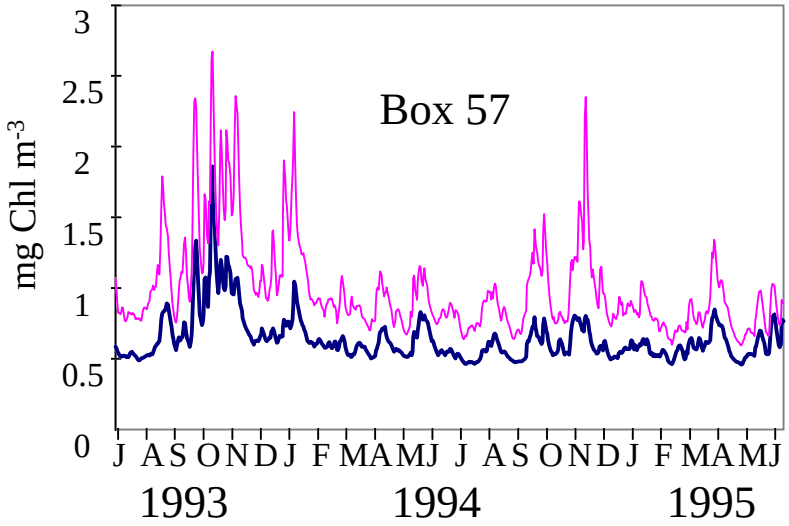

Figure 8.10 Chlorophyll concentrations in eastern Bay-centre box 57 with 0 × (thick line) and 2 × (thin line) nutrient inputs from the Patterson-Mordialloc Rivers.

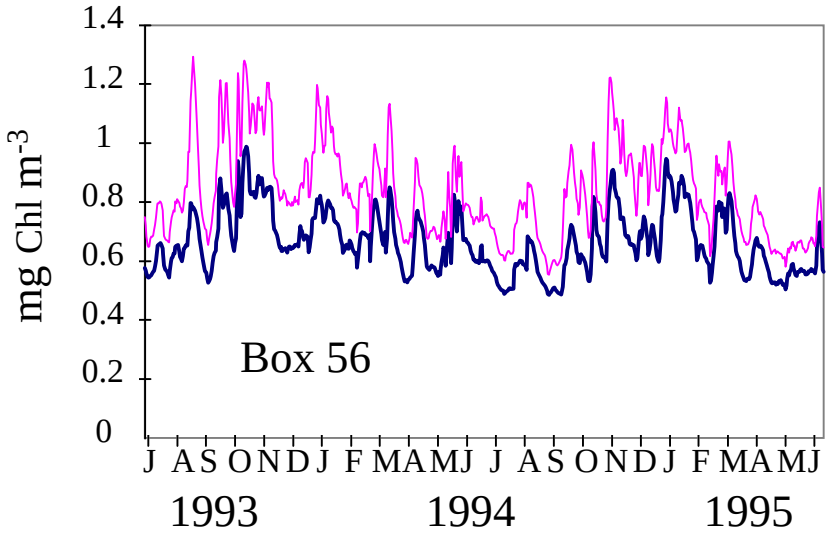

Figure 8.11 Chlorophyll concentrations in mid Bay-centre box 56 with 0 × (thick line) and 2 × (thin line) nutrient inputs from the Patterson-Mordialloc Rivers.

8.4 Changes in temperature

The seasonal cycle of temperature in Port Phillip Bay was increased by 3 ^{o}C throughout the year as a "global warming" scenario. In fact, changes in rainfall, catchments and runoff resulting from climate change are likely to have more important impacts on the Bay than changes in mean temperature. In addition, the model can only represent effects of temperature change through the Q10 effect on rate processes, whereas impacts of temperature on community composition are likely to be of more significance to Bay ecosystems.

At a Q10 of 2, a 3 ^{o}C temperature increase represents a 23% increase in model rate parameters. However, certain key model fluxes, such as denitrification losses and

sediment respiration rates, are strongly constrained by the nutrient loads, and are insensitive to changes in temperature. The largest percentage change is in the flux of DIN recycled in the water column, which is least constrained by the input load. In general, the changes in fluxes due to increased temperature are comparable to, or smaller than, the interannual variation in fluxes predicted to result from changes in runoff and loads between 1993 and 1994 (Table 8.2).

Table 8.2 The percentage effect of a 3 ^{o}C warming (Run si100) on model fluxes in Port Phillip Bay, compared with the predicted interannual percentage change in fluxes in 1993-95 (Run si42)

	PP	WRc	SRc	FRc	SResp	MPB Pr	Den
3 ^{o}C warming	9.56	12.58	2.00	12.62	1.67	16.04	1.41
Interannual	14.34	10.77	18.08	8.97	18.65	4.63	19.12

Pool sizes are generally reduced by the increase in temperature, although DON and PO_4 concentrations are marginally increased (Table 8.3). For DIN and phytoplankton, interannual variation in load and the temperature increase have effects of comparable magnitude, although temperature effects are relatively more important in the case of nitrate and small phytoplankton, which are minor constituents.

Table 8.3 The percentage effect of a 3 ^{o}C warming (Run si100) on model pools in Port Phillip Bay, compared with the predicted interannual percentage change in pools in 1993-95 (Run si42)

	DON	PL	PS	NO_X	NH_4	PO_4
3 ^{o}C warming	0.89	-6.16	-6.86	-17.74	-6.38	0.71
Interannual	12.12	16.83	3.11	4.00	11.58	8.42

These results support the conclusion that, in developing climate change scenarios for the Bay (and for other coastal systems), managers should be as much or more concerned with potential changes in runoff and loads as with direct effects of temperature changes on rate processes.

8.5 Changes in denitrification efficiency

Identification of the critical role of denitrification in maintaining the Port Phillip Bay ecosystem is one of the principle outcomes of the Port Phillip Bay Study. However, the processes and factors that maintain the unusually high denitrification efficiencies in Bay sediments are not understood in detail. It is possible, at least in principle that changes in the benthic ecosystem in the Bay, independent of changes in external loads, could result in decreases in denitrification efficiency to levels more commonly observed in other systems. We have investigated the effects of changes in the denitrification parameters on model behaviour and predicted water quality. Specifically, we have varied Dmax

through the range 0.1, 0.3, 0.5, 0.7, and 0.9, where 0.7 is the standard value. (This experiment was conducted with a model version (si42) in which macroalgae have lower biomass and production. However, this is not expected to affect the conclusions for most model fluxes and variables.)

For each value of Dmax, we have calculated the ratio of the principal Bay-wide annual fluxes to the corresponding flux at Dmax = 0.7 (Table 8.4). The predicted responses of Bay fluxes to changes in Dmax are consistent with our understanding of the fundamental links among water column and sediment recycling efficiencies, external load and primary production (Chapters 6 and 7). As Dmax decreases, an increased proportion of DIN produced by sediment respiration is released to the overlying water column. This increased DIN release (SRc) drives increased primary production (PP). Net sediment respiration (SResp), water column recycling (WRc), and filter-feeder recycling (FRc) are all driven by primary production, and it is not too surprising that these all increase roughly in proportion as Dmax decreases. DIN release from sediments increases more quickly because it is driven by both an increase in net sediment respiration, and a decrease in denitrification efficiency.

Table 8.4 Absolute values of model fluxes in the standard run si42 (Dmax = 0.7), and model fluxes for different Dmax values relative to fluxes for Dmax = 0.7.

	PP	WRc	SRc	FRc	SResp	MPBP	Den
si42	28416	15354	5889	3319	12975	10910	7086
Dmax							
0.1	3.98	3.62	8.29	3.71	3.98	0.54	0.40
0.3	2.25	2.03	3.86	2.05	2.22	0.69	0.86
0.5	1.37	1.32	1.83	1.31	1.36	0.89	0.97
0.7	1	1	1	1	1	1	1
0.9	0.80	0.83	0.56	0.83	0.81	1.03	1.01

As Dmax decreases, the values of all these fluxes are determined by the establishment of a new balance between loss to denitrification and export to Bass Strait as sinks for the nitrogen load to the Bay. Denitrification is the dominant sink in the standard run. In fact, the total denitrification loss decreases only slightly, and therefore remains the dominant sink, down to Dmax = 0.3. To this point, decreases in denitrification efficiency are almost compensated by increases in sediment respiration. However, the denitrification flux decreases substantially at Dmax = 0.1, and the majority of the N load is then exported to Bass Strait. At Dmax = 0.1, DIN release from sediments has increased to a point where it rivals water-column recycling as a source of DIN to the water column.

The increased export to Bass Strait is of course driven by increased concentrations of dissolved and particulate nitrogen pools in the water column. As Table 8.5 shows, the mean concentrations of all pools increase, but the dominant contributors to the total nitrogen in the water column are DON and ammonia. Ammonia undergoes a large relative increase, and at Dmax = 0.1 begins to rival DON as a nitrogen export medium. Large phytoplankton biomass increases much more than small phytoplankton biomass in relative and absolute terms. The decrease in phosphate reflects an increase in the export

of organic P. Nitrate concentrations initially decrease due to the decrease in nitrification, but then increase due to ammonia inhibition of nitrate uptake.

The predicted large increase in ammonia at Dmax = 0.1 is rather surprising, given that water column light levels are still high. One might expect bloom phytoplankton to take advantage of these favourable conditions for growth. In the model, this does not occur because silicate is severely depleted Bay-wide, and the large phytoplankton in the model require silicate. Small phytoplankton increase in relative terms between Dmax = 0.3 and Dmax = 0.1, as silicate limitation becomes severe, but grazing control prevents their utilising the available ammonia. In the real world, one might expect this ammonia to be used, at least episodically, by other bloom species such as dinoflagellates. If the predicted ammonia concentrations were converted to phytoplankton biomass, the annual mean Bay-wide biomass would be about 60 mg N m^{-3}, or 9 mg Chl a m^{-3} at our assumed Chl:N ratio.

Table 8.5 Mean annual Bay-wide concentrations (mg N m^{-3}, mg P m^{-3}) vs Dmax.

Dmax	DON	PL	PS	NO_X	NH_4	PO_4
0.1	79.37	13.35	3.44	2.90	43.10	55.13
0.3	51.31	8.44	2.10	1.00	11.04	65.56
0.5	38.99	4.93	1.90	1.10	8.29	69.79
0.7	33.74	3.57	1.75	1.24	6.74	71.50
0.9	30.51	2.86	1.63	1.37	5.70	72.53

As one might expect, there are significant regional differences in the response to changes in Dmax. Effects on water column fluxes are weaker in the Yarra and Werribee regions, where sediment respiration rates and DIN release rates are already high. For Dmax = 0.7, chlorophyll levels in the Yarra and Werribee regions are about twice those in the central Bay, but for Dmax = 0.1, chlorophyll in the Bay centre is only marginally lower than in the Yarra region, and is higher than off Werribee. These patterns also reflect the increasing importance of silicate limitation for Dmax = 0.1.

Bay-wide microphytobenthos production falls as Dmax decreases due to increased attenuation and decreased bottom light. Effects of increased light attenuation on MPB and macrophytes are of course most severe in deeper boxes. Seagrass is widely distributed in shallower parts of the Sands region (coarse boxes 1 and 2) for Dmax = 0.7, but for Dmax = 0.5 it is restricted to a region of Swan Bay and nearby waters, and is absent at Dmax = 0.1. By contrast, macroalgae thrive in the high DIN environment predicted under silicate limitation, at least in the shallower coastal regions of the Bay. With Dmax = 0.7, macroalgae are primarily restricted to the Yarra and Werribee regions near inputs. As Dmax decreases, this range expands to include other western and northern regions, then the east coast, and finally the Sands.

Although the quantitative prediction of macroalgal biomass differs between run si42 and the standard model version (si142), the qualitative conclusion that macroalgal biomass will increase and seagrass decrease in shallow areas as Dmax decreases is likely to be

robust. Increased macroalgal biomass is likely in turn to result in increased problems of drift algae on beaches.

8.6 Increase in benthic filter-feeders

Recently there has been considerable concern about the effects of introduced species in Australian coastal ecosystems. One species that has recently appeared in Port Phillip Bay is *Sabella spallenzani*, a fan-worm that has also become extremely abundant in Cockburn Sound in West Australia. Concerns have been raised about the potential impacts of *Sabella* on nutrient cycling and water quality in Port Phillip Bay. We have conducted a series of model experiments to investigate the effects of large increases in benthic filter-feeder biomass on the model.

We should note that this is a preliminary investigation. The interactions between *Sabella* and other benthic fauna are unknown. These interactions could have indirect effects on sediment biogeochemistry and denitrification efficiencies that we have not taken into account. We have simply assumed that *Sabella* represent an unusually high biomass of benthic filter feeders which are otherwise similar in their ecological role to our generic filter feeders. Thus, they intercept suspended particulate organic matter, release DIN into the water column, and release detritus to the sediment surface. Because *Sabella* do not appear to have exceptional clearance or growth rates, we have assumed that their high biomass reflects low mortality rates. We have accordingly multiplied the quadratic mortality coefficient for benthic-filter feeders (mQ_BF) in the model by factors of 1, 0.5, 0.25, and 0.1. (We understand that *Sabella* biomass in Port Phillip Bay has declined in the last year. This could reflect an increase over time in mortality rate, a common feature of the population dynamics of introduced species.)

It has been hypothesized that filter-feeders could intercept organic material before it reached the bed and thus prevent it being denitrified, leading to eutrophication. In fact, increased filter-feeder biomass in the model has the opposite effect. As mQ_BF falls to one tenth of its original value, and ingestion and resultant recycling of DIN by filter feeders (FRc) increase by a factor of three, primary production drops by nearly 30% (Fig. 8.12). The release of DIN from the sediment is little affected. This is unsurprising since, as stated often before, the net sediment respiration rate and sediment release of DIN Bay-wide are determined only by the denitrification efficiency, and the need for denitrification losses to balance external load. Increased filter-feeder biomass can affect sediment respiration rates and therefore denitrification efficiencies locally, by concentrating organic loads to the sediment in coastal waters, but this has only a marginal effect on Bay-wide denitrification efficiency.

The Bay takes on a more oligotrophic character as filter-feeder biomass increases. Primary production drops, primarily because of a decrease in recycling efficiency in the water column. DIN release in the water column, WRc, is cut by more than a factor of two at the lowest value of mQ_BF (Fig. 8.12), because of the efficient direct transfer of detritus to the sediment by benthic filter feeders.

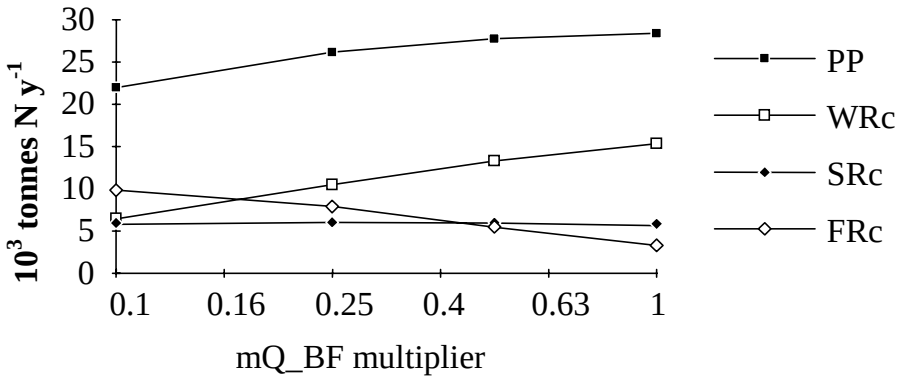

Figure 8.12. Model fluxes when filter-feeder mortality (mQ_BF) is multiplied by factors of 1, 0.5, 0.25, 0.1.

The total phytoplankton (PL+PS) pool, like primary production, also decreases by about 30% as filter-feeder biomass increases (Fig. 8.13). This is largely because PL falls to about a third of its normal biomass, and PS actually rises substantially. Filter feeders have the same clearance rates for large and small phytoplankton, and the contrasting response of PL and PS reflects two indirect effects. Benthic filter-feeders graze small zooplankton as well as phytoplankton, so that small phytoplankton experience reduced overall grazing pressure, at least for intermediate filter-feeder densities. There is also a contribution from spatial effects: large phytoplankton have high biomass in shallow areas near inputs, and the water column clearance rate imposed by a given density (per unit area) of benthic filter feeders increases in inverse proportion to depth. In the Werribee and Corio Bay regions, at the maximum filter feeder biomass (minimum mQ_BF), the combination of high sinking rates and filter-feeder grazing is almost sufficient to eliminate diatoms from shallow coastal waters (Table 8.6). This effect is less important in the Bay centre, where the effect of removal of small zooplankton is arguably more important in driving the shift from large to small phytoplankton.

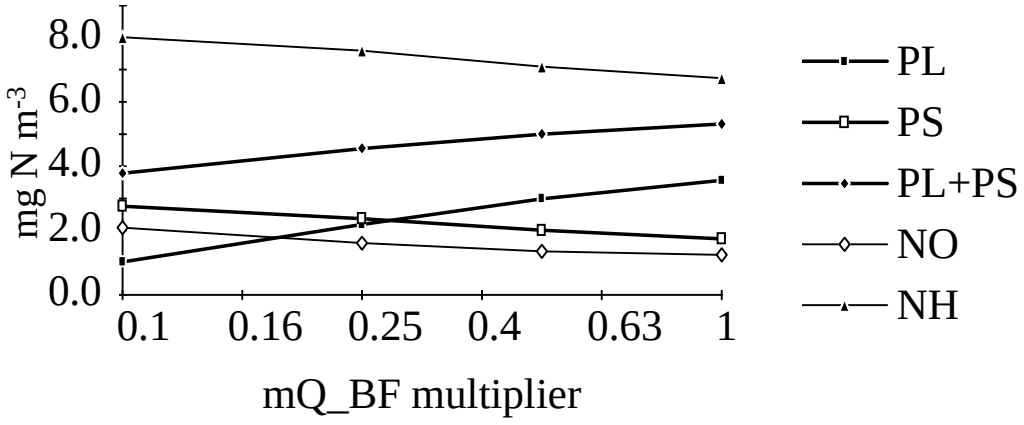

Figure 8.13. Phytoplankton and DIN concentrations when filter-feeder mortality (mQ_BF) is multiplied by factors of 1, 0.5, 0.25, 0.1.

Table 8.6. Predicted biomass (mg N m^{-3}) of large and small phytoplankton vs relative values of mQ_BF, for three Bay regions.

Multiplication Factor	Werribee		Bay Centre		Corio Bay	
	PL	PS	PL	PS	PL	PS
1	5.71	2.97	3.12	1.38	3.49	2.51
0.5	4.10	3.59	2.70	1.59	2.71	3.13
0.25	2.10	4.01	2.07	1.90	1.58	4.14
0.1	0.29	3.0	1.00	2.42	0.24	4.84

Both ammonia and nitrate levels rise slightly as filter-feeders increase (Fig. 8.13). Again, this increase is concentrated in shallow areas near inputs, where filter-feeders can severely reduce the concentrations of large diatoms. There is a possibility that dinoflagellates might be selected for in these areas if, by maintaining a position high in the water column during calm periods, they were able to avoid grazing by benthic filter feeders. (On the other hand, dinoflagellates are presumably grazed by benthic filter-feeders, given that accumulation of toxins or unpleasant taste by shellfish is one of the principal impacts of red tides.)

A reduction in plankton biomass following the introduction of filter-feeders is not unusual. It has been well documented following the introduction of zebra mussels to North American Great Lakes (Mellina *et al*. 1995). That introduction also led to a decrease in phytoplankton cell size, similar to that predicted for Port Phillip Bay. However concentrations of the limiting nutrient in the Great Lakes, (P rather than N), also decreased, whereas our model predicts an increase.

Sabella spallenzani has stripped most phytoplankton out of waters in Cockburn Sound (Clapham 1996). This effect of reduced phytoplankton biomass has been modelled in French coastal waters overstocked with cultured oysters (Raillard and Ménesguen 1994). By reducing phytoplankton abundance, *Sabella spallenzani* compete with other filter-feeders and reduce their productivity. This might affect the shellfish industry in Port Phillip Bay and could indirectly affect commercial and recreational fish stocks. On the other hand, high biomass benthic communities are good at buffering ecosystems against fluctuations (Ott and Fedra 1977). Our model predicts beneficial effects of increased filter-feeder biomass on benthic macrophytes. The increased DIN levels aid growth of macroalgae, while seagrasses also benefit from decreased light attenuation.

9 CONCLUSIONS

In the preceding chapters we have described the formulation, calibration and analysis of an integrated (physical-biogeochemical-ecological) model of nutrient cycling in Port Phillip Bay. We believe that the model incorporates and in several respects extends the "state-of-the-art" in estuarine modelling. The model is unusual in its recognition of the importance of coupling between water column and benthic processes, and in its ability to treat the roles of different planktonic and benthic functional groups in this coupling. The model allows for interactions among planktonic and benthic primary producers, and the role of both bloom and non-bloom phytoplankton. It recognises the importance of benthic microalgal production in shallow coastal systems, as well as the more obvious or traditional benthic macrophytes. The model allows for interactions among different limiting nutrients, and for the effect of multiple water column constituents on light attenuation and light limitation. This representation of ecological and biogeochemical processes is set within the framework of an efficient and well-calibrated physical transport model.

The model has the benefit of being calibrated against a set of field observations, which is virtually unprecedented in terms of spatial and temporal coverage and diversity. The model owes a large debt to the scientists who designed and managed the PPBES field program, and carried out the individual field tasks. Without a data set of this scope, it would be difficult to justify the development of a model with this level of complexity or sophistication. Several of the key novel processes incorporated in the model have been directly suggested by field results.

The success of the model calibration has also depended on the approach adopted in the physical modelling task P8 (Walker 1997 a, b), which succeeded in providing a transport model with realistic physical exchanges at intermediate spatial resolution and long time steps. Without this approach, the integrated model calibration, which involved hundreds of simulations over 20 year periods, would simply not have been feasible. The model calibration and application would also not have been possible without the catchment load models developed by Sokolov (1996).

In developing the integrated model, we have deliberately adopted a strategy of combining numerical simulation with qualitative and semi-quantitative analyses based on model simplification and approximation and analysis of steady-state solutions. This strategy has also proved invaluable in understanding the behaviour of the full model, both at current nutrient loads and under a variety of management scenarios. Without this understanding, model calibration via numerical simulation alone would have been much more difficult, if not impossible. This understanding underlies our assessment of the robustness of model predictions in scenarios to uncertainty in model formulation and parameter values.

The qualitative analysis has yielded new scientific concepts and insights that we believe will find further application in coastal zone management. We have extended the concepts of nutrient export and recycling efficiencies developed for pelagic ecosystems to coupled pelagic-benthic ecosystems, and used these to relate external loads directly to primary production and eutrophication. We have linked changes in recycling efficiencies

to switches in dominance between planktonic and benthic primary producers. We have shown that the interaction between sediment respiration and denitrication efficiency can set an upper limit to the denitrification capacity. For systems such as Port Phillip Bay with long flushing times, nitrogen loads exceeding this capacity are likely to lead rapidly to severe eutrophication. This insight is exciting because it offers a scientific basis for defining an assimilative capacity for these systems.

While the Port Phillip Bay Environmental Study represents a major advance in our understanding of nitrogen cycling in Port Phillip Bay, we do not regard that understanding or the associated model development as "complete", and we have identified a number of priorities for futher field research and model development or analysis.

Given its importance, sediment biogeochemistry in general and denitrification efficiency in particular are an obvious focus for further field studies. It is highly desirable that we understand the processes that support the high denitrification efficiencies observed in Port Phillip Bay. While further measurements of water column-sediment fluxes under a wider range of conditions will help, we also need innovative field or laboratory studies designed to identify the physical location and microenvironments associated with these reactions within the sediment, and their responses to a variety of perturbations. It is also desirable that we understand better the composition and source of the large pool of apparently refractory organic N in Port Phillip Bay sediments, and the circumstances under which this material accumulates and is remineralised.

Given its importance in regulating the intensity and composition of phytoplankton blooms, a better knowledge and understanding of silicate loads and cycling within Port Phillip Bay is also highly desirable. The model suggests that the Bay is vulnerable to dinoflagellate blooms at times of silicate limitation, reinforcing the (widely-recognised) need for improved understanding of the processes controlling dinoflagellate blooms.

Further process studies of benthic macrophytes, especially filamentous macroalgae, are also desirable. Primary production by benthic macrophytes is one of the least constrained significant fluxes in our current budgets and models, and is likely to be most significant in coastal areas near inputs.

We have a number of priorities for further model development. A Lagrangian particle-tracking technique was used to couple the hydrodynamic and transport models, to allow us to run the transport model with long time steps (Walker, 1997a). This works well for dissolved constituents and neutrally buoyant particles, but has some drawbacks for sinking particulates, particularly under stratified conditions. We are working on techniques to overcome these, to allow better treatment of suspended inorganic particles. We are particularly interested in improving treatment of the effects of turbidity and stratification in the Yarra plume, referred to in Chapter 7, in modelling oxygen drawdown in bottom water under stratified conditions, and in treating drift algae.

Future management use of the model is likely to focus increasingly on local impacts near point sources, and will require finer horizontal resolution near inputs. This can be achieved using the existing hydrodynamic model resolution.

In terms of ecological processes, there are minor issues associated with effects of sediment instability on seagrass distribution, and with nitrate dynamics and uptake, which emerged during model calibration. Perhaps more important is further experimentation with the incorporation of dinoflagellates as a third phytoplankton group.

There is a great deal of scope for further development of process models of sediment biogeochemistry. More use can be made of the existing sediment profile and flux data, as well as the results of new process experiments discussed above. Sediment biogeochemistry requires (and deserves) a major strategic research program.

Collecting a data set as comprehensive as the PPBES data set may be prohibitively expensive for most estuarine or coastal systems. From a management perspective, this raises two obvious and related questions. How much can we simplify models and still obtain useful management predictions? What kinds of data are essential and cost-effective in calibrating simpler models? The PPBES data set provides an ideal test bed for addressing these questions.

As discussed in Chapter 8, the principal management agencies may use the model for ongoing management purposes in Port Phillip Bay. We have identified elsewhere (Newell and Harris, 1997) the data needs for ongoing operation and assessment of the model as a management tool. In brief, these consist of time series of forcing data, including both physical forcing and catchment runoff and loads; time series of water quality measurements at fixed sites; and occasional monitoring of sediment pools and fluxes, water column fluxes, and benthic flora and fauna. Further targeted monitoring may be required to assess the impact of particular management decisions.

10 ACKNOWLEDGEMENTS

Many people and organisations contributed to the development of the model and data sets described in this report. The development of the model has been possible because of the successful design and management of the study by the PPBES Technical Group led by Graham Harris. Members of the Technical Group, and the scientists involved in individual nutrient and ecology tasks, contributed to valuable discussions about processes in the Bay and the interpretation of field data. The integrated model has relied heavily on the physical transport model developed by Stephen Walker and the interface tools developed by Jason Waring. Ken Ouyang was responsible for programming the ecological model code. Brian Newell, Colin Arrowsmith, Doug Hall and Robert Molloy provided valuable support throughout the study.

Funding was provided by Melbourne Water through the Port Phillip Bay Environmental Study.

11 REFERENCES

Aksnes, D. L., Ulvestad, K. B., Baliño, B. M., Berntsen, J. Egge, J. K. and Svendsen, E. (1995) Ecological modelling in coastal waters: towards predictive physical-chemical-biological simulation models. *Ophelia* **41**, 5-36

Aller, R. C (1980) Quantifying solute distribution in the bioturbated zone of marine sediments by defining an average microenvironment. *Geochim. Cosmochim. Acta* **44,** 1955-1965

Aller, R. C. (1984) The importance of relict burrow structures and burrow irrigation in controlling sedimentary distributions. *Geochim. Cosmochim. Acta* **48,** 1929-1934

Andersen, V. and Nival, P. (1988) A pelagic ecosystem model simulating production and sedimentation of biogenic particles: the role of salps and copepods. *Mar. Ecol. Prog. Ser*. **44**, 37-50

Bach, H. K. (1993) A dynamic model describing the seasonal variations in growth and the distribution of eelgrass (*Zostera marina* L.) I. Model theory. *Ecol. Modell.* **65**, 31-50

Banse, K. (1976) On the interpretation of data for the carbon-nitrogen ratio of phytoplankton. *Limnol. Oceaonogr*. **19**, 695-699

Banse, K. (1982) cell volumes, maximal growth rates of unicellular algae and ciliates and the role of ciliates in the marine pelagial. *Limnol. Oceanogr*. **27**, 1059-1071

Bathman, V., Noji, T. T. and Peinert, R. (1987) Copepod faecal pellets: abundance, sedimentation and content at a permanent station in the Norwegian Sea in May June 1986. *Mar. Ecol. Prog. Ser*. **38**, 45-51

Beardall, J. and Light, B. (1994) *Biomass, productivity and nutrient requirements of microphytobenthos.* CSIRO Port Phillip Bay Environment Study Technical Report no. 16, Melbourne

Beardall, J. and Light, B. (1997) *Microphytobenthos in Port Phillip Bay, Victoria: Distribution and primary productivity*. CSIRO Port Phillip Bay Environment Study Technical Report no. 30, Melbourne

Beardall, J., Roberts, S. and Royle, R. (1996) *Phytoplankton in Port Phillip Bay: Spatial and seasonal trends in biomass and primary productivity*. CSIRO Port Phillip Bay Environment Study Technical Report no. 35, Melbourne

Beattie, G., Redden, A. M. and Royle, R. (1996) *Microzooplankton grazing on phytoplankton in Port Phillip Bay, Victoria.* CSIRO Port Phillip Bay Environment Study Technical Report no. 31, Melbourne

Beer, T. (1983) Australian estuaries and estuarine modelling. *Search* **14,** 136-140

Beer, T., Carnovale, F., Carvalho, C and Cope, M. E. (1992*) Literature review of physical and chemical inputs to Port Phillip Bay*. CSIRO Division of Atmospheric Research, Report SB/3/7

Blackburn, N. D. and Blackburn, H. T. (1993) A reaction diffusion model on C-N-S-O species in a stratified sediment. *FEMS Microbiol. Ecol*. **102,** 207-215

Brown, V. B. (1980) Report: macrophytes of west Corio Bay. pp 233-238 In: V. B. Brown, K. S. Rowand and S. C. Ducker (eds.*) The effect of sewage effluent on the macrophytes off Werribee, Port Phillip Bay*. Ministry of Conservation of Victoria, Environmental Studies program, Task Report no 273

Bulthuis, D. A. and Woelkerling, Wm. J. (1983) Seasonal variation in standing crop, density and leaf growth rate of the seagrass *Heterozostera tasmanica*, in Western Port and Port Phillip Bay, Victoria, Australia. *Aquat. Bot*. **6**: 111-136

Bulthuis, D. A., Axelrad, D. M. and Mickelson, M. J. (1992) Growth of the seagrass *Heterozostera tasmanica* limited by nitrogen in Port Phillip Bay, Australia*. Mar. Ecol. Prog. Ser*. **89**, 269-275

Burke, C. M. (1995) *Microprofiles of oxygen concentration in Port Phillip Bay*. Report, Department of Aquaculture, University of Tasmania at Launceston, Tasmania, Australia

Campbell, S. (1995) *The role of macroalgae and seagrasses in productivity and nutrient cycling in Port Phillip Bay*. Unpublished report to CSIRO Port Phillip Bay Environment Study.

Chapelle, A., Lazure, P. and Ménesguen, A. (1994) Modelling eutrophication events in a coastal marine ecosystem. Sensitivity analysis. *Estuar. Coast. Shelf Sci*. **39**, 529-548

Chidgey, S. S. and Edmunds, M. J. (1997) *Standing crop and nutrient content of macrophytes in Port Phillip Bay*. CSIRO Port Phillip Bay Environment Study Technical Report no. 32 Melbourne.

Clapham, G. (1996) The filtration rate, oxygen consumption and biomass of the introduced polychaete *Sabella spallenzanii* Gmelin within Cockburn Sound: Can it control phytoplankton levels and is it an efficient filter feeder? BSc. Thesis Edith Cowan University, Western Australia

Conover, R. J. (1968) Zooplankton - life in a nutritionally dilute environment. *Am. Zool*. **8**, 107-118

Conover, R. J. (1979) Secondary production as an ecological phenomenon. In *Zoogeography and diversity in plankton*. (Eds. S van der Spoel and A. C. Pierot-Bults)

CSIRO 1992 *Port Phillip Bay Environment Study: Project Design*. A report to Melbourne Water by CSIRO INRE Project Office, CSIRO Australia

DeBoer, J. A. (1981) Nutrients pp355-392 in *The biology of seaweeds*. Eds. C. S. Lobban and M. J. Wynne, Blackwell Scientific Publications, Oxford

Doering, P. H., Oviatt, C. A., Beatty, L. L., Branzon, V. F., Rice, R., Kelly, S. P., Sullivan, B. K. and Frithsen, J. B. (1989) Structure and function in a model coastal ecosystem: silicon, the benthos and eutrophication. *Mar. Ecol. Prog. Ser*. **52**, 287-299

Doney, S. C., Naijar, R. G. and Stewart, S. (1995) Photochemistry, mixing and diurnal cycles in the upper ocean. *J. Mar. Res*. **53**, 341-369

Droop, M. R. (1968) Vitamin B12 and marine ecology IV. The kinetics of uptake, growth and inhibition in *Monochrysis lutheri*. *J. Mar. Biol. Ass. U.K*. **48**, 689-733

Droop, M. R. (1983) Twenty-five years of algal growth kinetics. A personal view. *Bot. Mar*. **26**, 99-112

Druffel, E. R. M., Williams, P. M., Bauer, J. E. and Ertel, J. R. (1992) Cycling of dissolved and particulate organic matter in the open ocean. *J. Geophys. Res*. **97**, 15639-15659

Duarte, C. M. (1989) Temporal biomass variability and production/biomass relationships of seagrass communities. *Mar. Ecol. Prog. Ser.* **51**, 269-276

Duarte, C. M. and Cebrián, J. (1996) The fate of marine autotrophic production. *Limnol. Oceanogr*. **41**, 1591-1609.

Ducklow, H. W. (1991) The passage of carbon through microbial foodwebs: results from flow network models. *Mar. Microb. Food Webs* **5**, 129-144

Ecological Modelling Centre (1993) MIKE 21 EU Eutrophication Module a short description, DHI/VK Hørsholm, Denmark

Eppley, R. W. (1972) Temperature and phytoplankton growth in the sea. *Fish. Bull*. **70**, 1063-1085

Eppley, R. W., Rogers, J. N., and McCarthy, J. J. (1969) Half-saturation constants for the uptake of nitrate and ammonia by marine phytoplankton. *Limnol. Oceanogr*. **14**, 912-920

Evans, G. T. and Garcon, V. C. (1997) *One dimensional models of water column biogeochemistry*. Joint Global Ocean Flux Study Report No. 23, JGOFS Bergen, Norway.

Evans, G. T. and Parslow, J. S. (1985) A model of phytoplankton annual cycles. *Biol. Oceanogr*. **3**, 327-347

Fasham, M. J. R. Ducklow, H. W. and McKelvie, S. M. (1990) A nitrogen based model of plankton dynamics in the oceanic mixed layer. *J. Mar. Res*. **48**, 591-639

Fasham, M. J. R., Holligan, P. M. and Pugh, P. R. (1983) The spatial and temporal development of the spring phytoplankton bloom in the Celtic Sea, April 1979. *Prog. Oceanogr*. **12**, 87-145

Fenchel, T. 1987 *Ecology of protozoa*. Springer-Verlag, Berlin

Fennel, W. (1995) A model of the yearly cycle of nutrients and plankton in the Baltic Sea. *J. Mar. Syst*. **6**, 313-329

Flood, P. R., Deible, D. and Morris, C. C. (1992) Filtration of colloidal melanin from sea water by planktonic tunicates. *Nature* **355**, 630-632

Fong, P., and Harwell M. A. (1994). Modeling seagrass communities in tropical and subtropical Bays and estuaries: a mathematical model synthesis of current hypotheses. *Bull. Mar. Sci*. **54**, 757-781

Fong, P., Donohoe, R. M. and Zedler, J. B. (1993) Competition with macroalgae and benthic cyanobacterial mats limits phytoplankton abundance in experimental microcosms. *Mar. Ecol. Prog. Ser.* **100,** 97-102

Fortier, L., Le Fèvre, J. and Legendre, L. (1994) Export of biogenic carbon to fish and to the deep ocean: the role of large planktonic microphages. *J. Plankton Res.* **7**, 809-839

Frost, B. W. (1972) Effects of size and concentration of food particles on the feeding behaviour of the marine copepod Calanus pacificus. *Limnol. Oceanogr*. **17**, 805-815

Frost, B. W. (1975) A threshold feeding behaviour in *Calanus pacificus Limnol. Oceanogr.* **20**, 263-266

Frost, B. W. (1987) Grazing control of phytoplankton stock in the open subarctic Pacific Ocean: a model assesing the role of mesozooplankton, particularly the large calanoid copepods *Neocalanus* spp. *Mar. Ecol. Prog. Ser.* **39**, 49-68

Fuhrman, J A. (1987) Close coupling between release and uptake of dissolved free amino acids in seawater studies by an isotope dilution method. *Mar. Ecol. Prog. Ser*. **37**, 45-52

Furnas, M. J. and Mitchel A. W. (1988) Photosynthetic characteristics of Coral Sea picoplankton (<2μm size fraction). *Biol. Oceanogr*. **5**, 163-182

Geider, R. J., MacIntyre, H, L. and Kana, T. M. (1996) A dynamic model of photoadaption in phytoplankton. *Limnol. Oceanogr*. **41**, 1-15

Gerritsen, J., Holland, A. F. and Irvine, D. E. (1994) Suspension-feeding bivalves and the fate of primary production: an estuarine model applied to Chesapeake Bay. *Estuaries* **17**, 403-416

GESAMP (1991) *Reports and studies no. 43 Coastal Modelling*. International Atomic Energy Agency, Vienna

Gibbs, C. F., Tomczak, M. jr. And Longmore, A. R. (1986) The nutrient regime of Bass Strait. *Aust. J. Mar. Freshwater Res*. **37**, 451-466

Gilpin, M. E. (1973) Do hares eat lynx? *Amer. Nat*. **107**, 727-730

Goldman, J. C. and Gilbert, P. M. (1983) Kinetics of inorganic nitrogen uptake by phytoplankton pp 233-274 in E J Carpenter and D. G. Capone (eds.*) Nitrogen in the marine environment*. Academic Press.

Hall, D. N. (1994) *The Port Phillip Bay Environmental Study: Status Review*. CSIRO Port Phillip Bay Environment Study Technical Report no. 9, Melbourne.

Harris, G. P.(1986) *Phytoplankton ecology*. Chapman and Hall, London.

Harris, G., Batley, G., Fox, D., Hall, D., Jernakoff, P., Molloy, R., Murray, A., Newell, B., Parslow, J., Skyring, G. and Walker, S. (1996*) Port Phillip Bay Environmental Study Final Report*, CSIRO, Canberra, Australia.

Harris, R. P. and Paffenhofer, G. A. (1976) The effect of food concentration on cumulative ingestion and growth efficiency of two small marine planktonic copepods. *J. Mar. Biol. Ass. U.K.* **56**, 875-888

Hedges, J. I. (1992) Global biogochemical cycles: progress and problems. *Mar. Chem*. **39**, 67-93

Hedgpeth, J. W. (1977) Models and muddles some philosophical observations. *Helgoländer Wiss. Meeresunters*. **30**, 92-104

Hein, M., Pedersen, M. F. and Sand-Jensen, K. (1995) Size-dependent nitrogen uptake in micro- and macroalgae. *Mar. Ecol. Prog. Ser*. **118,** 247-253

Hillman, K., Walker, D. I., Larkum, A. W. D and McComb, A. J. (1989) Productivity and nutrient limitation. pp635-685 in *Biology of Seagrasses* (eds. A. W. D. Larkum, A. J. McComb and S. A. Shepherd) Aquatic Plant Studies 2, Elsevier

Hodgkin, E. P, and Birch, R. E. (1982) Eutrophication of a Western Australian estuary. *Oceanologica Acta*, Proceedings International Symposium on Coastal Lagoons. Bordeaux, France 1981. 313-318

Hodgkin, E. P., Birch, P. B., Black, R. E. and Humphries, R. B. (1980) *The Peel-Harvey estuarine system study (1976-1980),* Report no. 9 Department of Conservation and Environment, Perth, WA

Holibaugh, J. T. and Azam, F. (1983) Microbial degradation of dissolved proteins in seawater. *Limnol. Oceanogr*. **28**, 1104-1116

Holling, C. S. (1966) The functional response of invertebrate predators to prey density. *Mem Entmol. Soc. Canada* **48:** 1-87

Holling, C. S. (1978) *Adaptive Environmental Assessment and Management*. John Wiley and Son, New York.

Holloway, M. and Jenkins, G. (1993) *The role of zooplankton feeding in nitrogen and carbon cycling in Port Phillip Bay*. CSIRO Port Phillip Bay Environment Study Technical Report no. 11, Melbourne

Huntley, M. E. and Lopez, M. D. G. (1992) Temperature-dependent production of marine copepods: a global synthesis. *Am. Nat*. **140**, 201-242

Hutchinson, G. E. (1961) The paradox of the plankton. *Am. Nat*. **95**, 137-145

Hydrotechnology (1993) *Groundwater nutrient and toxicant inputs to Port Phillip Bay*. CSIRO Port Phillip Bay Environment Study Technical Report no. 13, Melbourne

Ikeda, T. (1974) Nutritional Ecology of Marine Zooplankton. *Mem. Fac. Fish. Hokkaido Univ*. **22**, 1-97

Jackson, G. A. (1990) A model of the formation of marine algal flocs by physical coaggulation processes. *Deep-Sea Res*. **37**, 1197-1211

Jackson, G. A. and Eldridge, P. M. (1992) Food web analysis of a planktonic system of Southern California. *Prog. Oceanog.* **30,** 223-251

Jones, R. I. (1994) Mixotrophy in planktonic protists as a spectrum of nutritional strategies. *Mar. Microb. Food Webs* **8**, 87-96

Jørgensen, S. E. (1993) *Fundamentals of ecological modelling, 2nd Edition*, Elsevier, Amsterdam.

Jumars, P. A., Pendry, D. L., Baross, J. A., Perry, M. J. and Frost, B. W. (1990) Closing the microbial loop: dissolved carbon pathway to heterotrophic bacteria from incomplete ingestion, digestion and adsorption in animals. *Deep-Sea Res*. **36**, 483-495

Kemp, W. M., Sampou, P., Caffrey, J., Mayer, M., Henriksen, K. and Boynton, W. R. (1990) Ammonium recycling versus denitrification in Chesapeake Bay sediments. *Limnol. Oceanogr*. **35**, 1545-1563

Kimmerer, W. J. and McKinnon, A. D. (1985) A comparative study of zooplankton in two adjacent emBayments, Port Phillip and Westernport Bays, Australia*. Est. Coast. Shelf Sci*. **21,** 145-159

Kimmerer, W. J. and McKinnon, A. D. (1987) Growth, mortality, and secondary production of the copepod *Acartia tranteri* in Westernport Bay, Australia*. Limnol. Oceanogr*. **32**, 14-28

Kimmerer, W. J., Smith, S. V. and Hollibaugh, J. T. (1993) A simple heuristic model of nutrient cycling in an estuary. *Est. Coast. Shelf Sci*. **37**, 145-159

Kiørboe, T and Sabatini, M. (1995) Scaling of fecundity, growth and development in marine planktonic copepods. *Mar. Ecol. Prog. Ser*. **120**, 285-298

Kirk, J. T. O. (1983) *Light and photosynthesis in aquatic ecosystems*. Cambridge University Press. Cambridge.

Klepper, O. (1995) Modelling the oceanic food web using a quasi steady-state approach *Ecol. Modell.* **77**, 33-41

Klumpp, D. W., Howard, R. K. and Pollard, D. A. (1989) Trophodynamics and nutritional ecology of seagrass communities pp394-457 in *Biology of Seagrasses* (eds. A. W. D. Larkum, A. J. McComb and S. A. Shepherd) Aquatic Plant Studies 2, Elsevier

Kraemer, G. P. and Mazzella, L. (1996) Nitrogen assimilation and growth dynamics of the Mediterranean seagrasses *Posidonia oceanica, Cymodocea nodosa*, and *Zostera nolti*. In J. Kuo, R. C. Philips, D. I. Walker and H. Kirkman (Eds.) *Seagrass biology: proceedings of a international workshop.* Rottnest Island, Western Australia

Kremer, J. N. and Nixon, S. W. (1978) *A coastal marine ecosystem simulation and analysis*. Ecological Studies 24, Springer-Verlag, Berlin

Langdon, C. (1988) on the causes of interspecific differences in the growth-irradiance relationship for phytoplankton. *J. Plankton Res*. **10**, 129-1312

Larsson, U. and Hagstrom, Å. (1982) Fractionated primary production, exudate release and bacterial production in a Baltic eutrophication gradient. *Mar. Biol*. **67**, 55-70

Leakey, R. J. G., Burkill, P. H. and Sleigh, M. A. (1992) Planktonic ciliates in Southampton Water: abundance, biomass, production, and role in pelagic carbon flow. *Mar. Biol*. **114**, 67-83

Lederman, T. C. and Tett, P. (1981) Problems in modelling the photosynthesis-light relationship for phytoplankton. *Bot. Mar*. **24,** 125-134

Light, B. R., and Woelkerling, W. J. (1992*) Literature and information review of the benthic flora of Port Phillip Bay, Victoria, Australia*. CSIRO Port Phillip Bay Environment Study Technical Report no. 12, Melbourne.

Logan, B. E. and Aldredge, A. L. (1989) Potential for increased nutrient uptake by flocculating diatoms. *Mar. Biol*. **101**, 443-450

Longmore, A. R., Cowdell, R. A., and Flint, R. (1996*) Nutrient status of the water in Port Phillip Bay*. CSIRO Port Phillip Bay Environment Study Technical Report no. 24, Melbourne.

Lord, D. A. (1994) Coastal eutrophication: prevention is better than cure the Perth coastal water study. *Water* **February 1994**, 22-27

Lord, D. A. and Hillman, K. (1995) *Perth coastal waters study summary report*. Water authority of Western Australia Leederville, WA.

Lucas, M. I., Probyn, T. A. and Painting, P. A. (1987) An experimental study of microflagellate bacterivory: further evidence for the importance and complexity of microplanktonic interactions. *S. Afr. J. Mar. Sci*. **5**, 791-808

Lüning, K. (1981) Light pp 326-354 in *The biology of seaweeds*. Eds. C. S. Lobban and M. J. Wynne, Blackwell Scientific Publications, Oxford.

Madden, C. J. and Kemp, W. M. (1996) Ecosystem model of an estuarine submersed plant community: calibration and simulation of eutrophication responses. *Estuaries* **19**, 457-474

Magro, K. L., Arnott, G. H. and Hill, D. R. A. (1996*) Algal blooms in Port Phillip Bay from March 1990 to February 1995: Temporal and spatial distribution and dominant species*. CSIRO Port Phillip Bay Environment Study Technical Report no. 27, Melbourne.

Mann, K. H. (1982) *Ecology of coastal waters, a systematic approach.* Blackwell Scientific Publications, Oxford.

Mantoura, R. F. C. and Woodward, E. M. S. (1982) Conservative behaviour of riverine dissolved organic carbon in the Severn Estuary, chemical and geochemical implications. *Geochim. Cosmochim. Acta* **47**, 1293-1309

Marshall, S. M. (1973) Respiration and feeding in copepods *Adv. Mar. Biol*. **11**, 57-120

Martens, J. H. and Krause, M. (1990) The fate of faecal pellets in the North Sea. *Helgoländ. Meeres*. **44**, 9-19

Martin, J. H., Gordon, R. M. and Fitzwater, S. E. (1990) Iron in Antarctic waters. *Nature* **345**, 341-343

May, R. M. (1981) *Theoretical Ecology principles and applications 2nd Edition*, Blackwell Scientific Publications, Oxford

McCauley, E. and Murdoch, W. W. (1987) Cyclical and stable populations: plankton as paradigm. *Am. Nat*.**129**, 97-121

McGlade, J. M. and Price, A. R. G. (1993) Multi-disciplinary modelling: an overview and practical implications for the governance of the gulf. *Mar. Polut. Bull*. **27**, 361-377

Mellina, E., Rasmussen, J. B. and Mils, E. L. (1995) Impact of zebra mussel (*Dreissena polymorpha*) on phosphorous cycling and chlorophyll in lakes. *Can. J. Fish. Aquat. Sci*. **52**, 2553-2573

Mickleson, M. J. (1990) *Dissolved oxygen in bottom waters of Port Philip Bay. Volume 1* - Report. MMBW Environmental Services Series No. 90/010 Melbourne and Metropolitan Board of Works, Victoria

MMBW/FWD, (1973) *Environmental Study of Port Phillip Bay: Report on Phase One 1968-1971*. Melbourne and Metropolitan Board of Works and Fisheries and Wildlife Department of Victoria. Melbourne.

Moloney, C. L. and Field, J. G. (1989) General allometric equations for rates of nutrient uptake, ingestion and respiration in planktonic organisms. *Limnol. Oceanogr*. **34**, 1290-1299

Moloney, C. L. and Field, J. G. (1991) The size based dynamics of plankton food webs. I. A simulation model of carbon and nitrogen flows. *J. Plankton Res*. **13**, 1003-1038

Moloney, C. L., Bergh, M. O., Field, J. G. and Newell, R. C. (1986) The effect of sedimentation and microbial nitrogen regeneration in a plankton community: a simulation investigation. *J. Plankton Res*. **8,** 427-444

Moloney, C. L., Field, J. G. and Lucas, M. I. (1991) The size based dynamics of plankton food webs. II. Simulations of three contrasting southern Benguela food webs. *J. Plankton Res*. **13,** 1039-1092

Monbet, Y. (1992) Control of phytoplankton biomass in esturaies: a comparative analysis of microtidal and macrotidal estuaries. *Estuaries* **15,** 563-571

Montagna, P. A., Blanchaurd, G. F. and Dinet, A. (1995) Effect of production and biomass of intertidal microphytobenthos on meiofaunal grazing rates. *J. Exp. Mar. Biol. Ecol*. **185**, 149-165

Montagnes, D. J. S., Lynn, D. H., Roff, J. C. and Taylor, W. D. (1988) The annual cycle of heterotrophic planktonic ciliates in the waters surrounding the Isle of Shoals, Gulf of Maine: an assessment of their trophic role. *Mar. Biol*. **99**, 21-30

Morris, C. C. and Diebel D. (1993) Flow rate and particle concentration within the house of the pelagic tunicate *Oikopleura vanhofeffeni*. *Mar. Biol*. **115**, 445-452

Munk, W. H. and Riley, G. A. (1952) Adsorption of nutrients by aquatic plants. *J. Mar. Res*. **11**, 215-240

Murray, A. G. (1994) *Western Treatment Plant Outputs to Port Phillip Bay*. CSIRO Port Phillip Bay Environment Study Technical Report no. 15, Melbourne.

Murray, A. G. and Eldridge, P. M. (1994) Marine viral ecology: incorporation of bacteriophage into the microbial planktonic food web paradigm. *J. Plankton Res*. **16**, 627-641

Murray, A. G. and Parslow, J. S. (in prep) The response of a semi-enclosed Bay to increased nutrient loading: a dynamical model and its analytical solution.

Murray, J. D. (1993) *Mathematical biology, 2nd Edition*. Springer-Verlag, Berlin

Newell, B. S. (1990) *An appraisal of the effects of the Werribee treatment complex discharge on the ecology of Port Philip Bay*. MMBW Environmental Services Series No. 90/007 Melbourne and Metropolitan Board of Works, Victoria.

Newell, B. and Harris, G. (1997) *Recommended monitoring programs for Port Phillip Bay*. CSIRO Port Phillip Bay Environmental Study Technical Report no 43, Melbourne

Nicholson, G. J., Longmore, A. R., and Cowdell, R. A. (1996*) Nutrient status of the sediments of Port Phillip Bay*. CSIRO Port Phillip Bay Environment Study Technical Report no. 26, Melbourne

Nielsen, S. L. and Sand-Jensen, K. (1990) Allometric scaling of maximal photosynthetic growth rates to surface/volume ratio. *Limnol. Oceanogr*. **35**, 177-180

Nielsen, T. G., and Richardson, K. (1989) Food chain structure of the North Sea plankton communities: seasonal variations of the role of the microbial loop. *Mar. Ecol. Prog. Ser*. **56**, 75-87

Norro, A. and Frankignoulle, M. (1995) Biogeochemical box modelling at small scale application to the inorganic carbon cycle in the Bay of Calvi. *Ecol. Modelling* **88**, 101-112

Norwicki, B. L. (1994) The effect of temperature, oxygen, salinity, and nutrient enrichment on estuarine denitrification rates measured with a modified nitrogen gas flux technique. *Estuar. Coast Shelf Sci.* **38,** 137-156

NSR Environmental Consultants Pty. Ltd. (1993*) Surface inputs into Port Phillip Bay (excluding the Yarra river and WTC).* CSIRO Port Phillip Bay Environment Study Technical Report no. 12, Melbourne

Odate, T, and Maita, Y. (1988) Regional variation in the size composition of phytoplankton communities in the western North Pacific Ocean. *Biol. Oceanogr*. **6,** 65-78

Officer, C. B., Biggs, R. B., Taft, J. L., Cronin, L. E., Tyler, M. A. and Boynton, W. R. (1984) Chesapeake Bay anoxia:origin, development and significance. *Science*, **223,** 22-27

O'Leary, T, Leeming, R. Nichols, P. D. and Volkman, J. K. (1994) *The distribution and concentrations of biomarkers for sewage, primary producers and bacteria in the major sediment types of Port Phillip Bay.* CSIRO Port Phillip Bay Environment Study Technical Report no. 17, Melbourne.

Omori, K., Hirano, T and Takeoka, H, (1994) The limitations to organic loading on a bottom of a coastal ecosystem. *Mar. Poll. Bull*. **28**, 73-80

Orr, J., Hunt, D. T. E., and Lack, T. J. (1990) Waste disposal and the estuarine environment. In *Estuarine water quality management.* Ed. W. Michaelis, Coastal and Estuarine Studies 36. Springer-Verlag, Berlin.

Ott, J. and Fedra, K. (1977) Stabilisizing properties of a high-biomass benthic community in a fluctuating environment. *Helgol. wiss Meeresunters.* **30**, 485-494

Pace, M. L., Glasser, J. E. and Pomeroy, L. R. (1984) Simulation analysis of continental shelf food webs. *Mar. Biol.* **82,** 47-63

Paffenhofer, G. A. (1976) Feeding, growth and food conversion of the marine planktonic copepod *Calnus helgolandicus*. *Limnol. Oceanogr*. **21**, 39-50

Park, K., Kuo, A. Y. and Neilson, B. J. (1996) A numerical model of hypoxia in the tidal Rappahannock River of Chesapeake Bay. *Est. Coast. Shelf Sci*. **42**, 563-581

Parker, R. A. (1993) Dynamic models for ammonium inhibition of nitrate uptake by phytoplankton. *Ecol. Modelling*, **66,** 113-120

Parsons, T. R. and Kesseler (1983) Computer model analysis of pelagic systems in estuarine waters 161-194 in *The role of freshwater outflow in coastal marine ecosystems*. Ed. S. Skreslet. Springer-Verlag, Berlin

Parsons, T. R., Takahashi, M. and Hargrave, B. (1984*) Biological oceanographic processes, 3rd Edition*. Pergamon Press, Oxford

Pett, R. J. (1989) Kinetics of microbial mineralisation of organic carbon from detrital Skeletonema costatum cells. *Mar. Ecol. Prog. Ser*. **52**, 123-128

Pickney, J. L. and Zingmark, R. G. (1993) Modeling the annual production of intertidal benthic microalgae in estuarine ecosystems. *J. Phycol*. **29**, 396-407

Platt, T., Subba Rao, D. V. and Irwin, B. (1983) Photosynthesis of picoplankton in the oligotrophic ocean. *Nature*, **301,** 702-704

Platt, T., Denman, K. L. and Jasby, A. D. (1977) Modelling the production of phytoplankton. *The Sea* **6**, 805-855

Platt, T., Mann, K. H. and Ulanowicz R. E. (eds.) (1981*) Mathematical models in biological oceanography*. The UNESCO Press, Paris

Poore, G. (1992) *Soft-bottom macrobenthos of Port Phillip Bay: a literature review*. CSIRO Port Phillip Bay Environment Study Technical Report no. 2, Melbourne

Prézelin, B. B. and Matlick, H. A. (1980) Nutrient-dependent low light adaption in the dinoflagellate *Gonyaulax polyedra*. *Mar, Biol*. **74**, 141:150

Prézelin, B. B., Putt, M. and Glover, M. E. (1986) Diurnal patterns in photosynthetic capacity and depth dependent photosynthesis-irradiance relationships in *Synechococcus* spp. and larger phytoplankton in three water masses in the Northwest Atlantic Ocean. *Mar. Biol*. **91**, 205-217

Prieur, L. and Sathyendranath, S. (1981) An optical classification of coastal and oceanic waters based on the specific spectral adsorption curves of phytoplankton pigments, dissolved organic matter, and other particulate materials. *Limnol. Oceanogr*. **26**, 671-689

Radach, G. and Lenhart, H. J. (1995) Nutrient dynamics in the North Sea: fluxes and budgets in the water column derived from ERSEM. *Neth. J. Sea Res*. **33**, 301-335

Radach, G. and Moll, A. (1993) Estimation of the variability of production by simulating annual cycles of phytoplankton in the central North Sea. *Prog. Oceanogr*. **31**, 339-349

Radford, P. J. (1993) *The modules of the European Regional Seas Ecosystem Model.* Plymouth Marine Laboratory

Raillard, O. and Ménesguen, A. (1994) An ecosystem box model for estimating the carrying capacity of a macrotidal shellfish system. *Mar. Ecol. Prog. Ser*. **115,** 117-130

Raymont, J. E. G. (1980*) Plankton and productivity in the oceans. Volume I Phytoplankton 2nd Edition*. Pergamon Press, Oxford

Raymont, J. E. G. (1983*) Plankton and productivity in the ocean. Volume 2 Zooplankton 2nd Edition*. Pergamon Press, Oxford

Redfield, A. C. (1934) On the proportions of organic derivatives in seawater and their reationship to the composition of phytoplankton. *James Johnstone memorial volumes*, Liverpool

Redfield, A. C., Ketchum, B. H. and Richards, F. A. (1963) The influence of organisms on the composition of seawater. pp26-77 in *The Sea Volume 2*. Ed. M. N. Hill, Wiley-Interscience, New York.

Rhyther, J. H. (1956) Photosynthesis in the ocean as a function of light intensity. *Limnol. Oceanogr*. **1**, 61-70

Riisgard, H. U. and Larsen, P. S. (1995) Filter-feeding in marine macro-invertebrates: pump characteristics, modelling and energy costs. *Biol. Rev*. **70**, 67-106

Riley, G. A., Stommel, H. and Bumpus, B. A. (1949) Quantitative ecology of the plankton of the western North Atlantic. *Bull. Bing. Oceanogr. Coll*. **12,** 1-169

Robbins, J. A. (1986) A model for particle-selective transport of tracers in sediments with conveyer belt deposit feeders. *J. Geophys. Res*. **91 C7**, 8542-8558

Round, F. E. (1981) *The ecology of algae*, Cambridge University Press, Cambridge

Rosenzweig, M. L. (1971) Paradox of enrichment: destabilization of exploitation in ecological time. *Science* **171**, 385-387

Ruardij, P. and Van Raaphorst, W. (1995) Benthic nutrient regeneration in the ERSEM ecosystem model of the North Sea. *Neth. J. Sea Res*. **33**, 453-483

Rubenstein, D. I. And Koehl, M. A. R. (1977) The mechanisms of filter feeding: some theoretical considerations. *Am. Nat*. **111**, 981-994

Seitzinger, S. P. (1987) Nitrogen biogeochemistry in an unpolluted estuary: The importance of benthic denitrification. *Mar. Ecol. Prog. Ser*. **37**, 65-73

Seitzinger, S. P. (1988) Denitrification in freshwater and coastal marine ecosystems: Ecological and geochemical significance. *Limnol. Oceanogr*. **33**, 702-724

Shapiro, M. A. (1975) *A preliminary report on the Westernport Bay study*. Ministry for Conservation, Victoria, Melbourne

Sheldon, R. W., Prakash, A. and Sutcliffe, W. H. jr. (1972) The size distribution of particles in the ocean. *Limnol. Oceanogr*. **17**, 327-340

Sherr, E. B. and Sherr, B. F. (1987) High rates of consumption of bacteria by pelagic ciliates. *Nature*, **325,** 710-711

Short, F. T., Burdick, D. M. and Kaldy, J, E, III (1995) Mesocosm experiments quantifying the effects of eutrophication on eelgrass, *Zostera marina*. *Limnol. Oceanogr*. **40**, 740-749

Silver, M. W. and Bruland K. W. (1981) Differential feeding and faecal pellet composition of salps and pteropods, and the possible origin of the deep water flora and olive green 'cells'. *Mar. Biol*. **62**, 263-273

Skyring, G. W., Longmore, A. R., Chiffings, A. W. and Crossland, C. J. (1992) Nutrients. pp29-79 in *Port Phillip Bay Environmental Study: Status Review*. (ed. D. N. Hall) Port Phillip Bay Environment Study Technical Report no. 9, Melbourne

Sloth, N. P., Blackburn, H., Hansen, L. S., Risgaard-Petersen, N. and Lomstein B. A. (1995) Nitrogen cycling in sediments with different organic loading. *Mar. Ecol. Prog. Ser*. **116**, 163-170

Smayda, T. J. (1970) The suspension and sinking of phytoplankton in the sea. *Oceanogr. Mar. Biol. Ann. Rev*. **8,** 353-414

Sokolov, S. (1996) *Inputs from the Yarra River and Patterson River/Mordialloc Main Drain into Port Phillip Bay*. CSIRO Port Phillip Bay Environment Study Technical Report no. 33, Melbourne

Solidoro, C., Dejak, C., Franco, D., Pastres, P. and Pecenik, G. (1995) A model for macroalgae and phytoplankton growth in the Venice Lagoon. *Environm. Internat*. **21**, 619-626

Sommer, U. (1989) Maximal growth rates of Antarctic phytoplankton: only weak dependence on cell size. *Limnol. Oceanogr*. **345**, 109-1116

Sprung, M. (1993) Estimating macrobenthic secondary production from body weight and biomass: a field test in an non-boreal intertidal habitat. *Mar. Ecol. Prog. Ser*. **100**, 103-109

Steele, J. H. and Henderson, E. W. (1981) A simple plankton model. *Am. Nat.* **17**, 676-691

Steele, J. H. and Henderson, E. W. (1992) The role of predation in plankton models. *J. Plankton Res*. **14,** 157-172

Stigebrandt, T. R. and Wulf, F. (1987) A model for the dynamics of nutrients and oxygen in the Baltic proper. *J. Mar. Res*. **45**, 729-759

Talling, J.F. (1955) The relative growth rate of three plankton diatoms in relation to underwater radiation and temperature. *Ann. Bot. New Ser*. **19**, 329-341

Tamsalu, R. and Ennet, P. (1995) Ecosystem modelling in the Gulf of Finland. II. The aquatic ecosystem model FINEST. *Est. Coast. Shelf Sci*. **41**, 429-458

Taylor, A. H. and Joint, I. (1990) A steady state analysis of the 'microbial loop' in stratified systems. *Mar. Ecol. Prog. Ser*. **59**, 1-17

Tett, P. (1987) The ecophysiology of exceptional blooms. *Rapp. P.-v. Réun. Const. Explor. Mer*, **187,** 47-60

Tett, P. (1990) The photic zone. pp59-87 in *Light and Life in the Sea* (eds. P. J. Herring, A. K. Cambell, M. Whitfield and L. Maddock) Cambridge

Tett, P., Edwards, A. and Jones, J. (1986) A model for the growth of shelf-sea phytoplankton in summer. *Estuar. Coast. Shelf Sci*. **23**, 641-672

Theil, H., Pfannkuche, O., Schriever, G., Lochte, K., Gooday, A. J., Hemleben, Ch. Mantoura, R. F. G., Turley, C. M., Patching, J. M. and Rieman, F. (1988) Phytodetritus on the deep sea floor in a central oceanic region of the northeast Atlantic. *Biol. Oceanogr*. **6**, 203-239

Thompson, W. R. (1937) *Science and common sense: an Aristotalian excursion*. Longmans, London.

Tong, G D. and Cathers, B. (1991) *Sydney deepwater outfalls environmental monitoring program pre-commissioning phase. Volume 4 - Numerical modelling* Report 90/01 Australian Water and Coastal Studies PTY.

Tumbio, M. L. and Downing, J. A. (1994) An empirical model for the prediction of secondary production in marine benthic invertebrate populations. *Mar. Ecol. Prog. Ser.* **114**, 165-174

van Raaphorst, W., Kloostehuis, H. T., Cramer, A. and Bakker, K. J. M.. (1990). Nutrient early diagenesis in the sandy sediments of the Dogger Bank area, North Sea: pore water results. *Neth. J. Sea Res.* **26**, 25-52

Vedel, A. and Riisgård, H. U. (1993) Filter-feeding in the *polychaete Nereis diversicolor*: growth and bioenergetics. *Mar. Ecol. Prog. Ser.* **100**, 145-152

Verity, P. (1985) Grazing, respiration, excretion and growth rates of tintinnids. *Limnol. Oceanogr*. **30**, 1268-1282

Vezina, A. F. and Platt, T. (1987) Small scale variability of new production and particulate fluxes in the ocean. *Can. J. Fish. Aquat. Sci*., **44,** 198-205

Vollenweider, R. A. (1975) Input-output models with special reference to the phosphorous loading concept in limnology. *Schweiz. Z. fur Hydrologie* **37**, 53-82

Voltera, V. (1926) Fluctuations in the abundance of species considered mathematically. *Nature* **118,** 198-205

Walker, S. J. (1997a) *Hydrodynamic models of Port Phillip Bay*. CSIRO Port Phillip Bay Environment Study Technical Report no. 38, Melbourne

Walker, S. J. (1997b) *A transport model of Port Phillip Bay*. CSIRO Port Phillip Bay Environment Study Technical Report no. 39, Melbourne

Weinbauer, M. G. and Peduzzi, P. (1995) Effect of virus-rich high molecular weight concentrates of seawater on the dynamics of dissolved amino acids and carbohydrates. *Mar. Ecol. Prog. Ser.* **127,** 245-253

Williams, P J LeB. (1975) Biological and chemical aspects of dissolved organic materials in seawater. p301-363 in *Chemical Oceanography* (Eds. J P Riley and G Skirrow)

Williams, P J LeB. (1995) Evidence for the seasonal accumulation of carbon-rich dissolved organic matter, its scale in comparison with changes in particulate material and its consequential effect on net C/N assimilation ratios. *Mar. Chem*. **51**, 17-29

Williams, B.J. (1978) Mathematical modelling for the management of waste water systems. Ph. D. Thesis, University of Melbourne, Melbourne, Vic.

Wilson, R. S., Cohen, B. F. and Poore, G. C. B. (1993) *The role of suspension-feeding and deposit-feeding benthic macroinvertabrates in nutrient cycling in Port Phillip Bay*. CSIRO Port Phillip Bay Environment Study Technical Report no. 10, Melbourne

Woods, J. D. and Onken, R. (1982) Diurnal variation and primary production in the ocean - preliminary results of a Lagrangian ensemble model. *J. Plankton Res*. **4**, 735-756

Yangi, T., Yamamoto, T., Koizum, Y., Keda, T., Kamizono, M., Tamori, H. (1995) A numerical simulation of red tide formation. *J. Mar. Syst*. **6**, 269-285

You, Z., Greilach, P. R., Turnbull, J. F., Hatton, D. N. and Black, K. P. (1996) *Field measurements of suspended sediment concentrations in Port Phillip Bay*. CSIRO Port Phillip Bay Environment Study Technical Report no. 28, Melbourne

Zimmerman, R. C., Cabello-Pasini, A. and Alberte, R. S. (1994) Modeling daily production of aquatic macrophytes from irradiance measurements: a comparative analysis *Mar. Ecol. Prog. Ser*. **114**, 185-196